UNIVERSITY OF NAIROBI
COLLEGE OF BIOLOGICAL AND PHYSICAL SCIENCES
DEPARTMENT OF CHEMISTRY

ANTIPLASMODIAL AND ANTICANCER PRINCIPLES FROM *MILLETTIA DURA*, *MILLETTIA LEUCANTHA* AND *MILLETTIA LASIANTHA*

BY

DANIEL BUYINZA

I80/96687/2014

A Thesis Submitted in Fulfilment of the Requirements for the Award of the Degree of Doctor of Philosophy (PhD) in Chemistry of the University of Nairobi

2020

DECLARATION

I declare that this thesis is my original work and has not been submitted elsewhere for examination, publication or award of a degree. Where other people's work or my own work has been used, this has properly been acknowledged and referenced in accordance with the University of Nairobi's requirements.

Signature:  Date: 14th September, 2020

Daniel Buyinza
I80/96687/2014
Department of Chemistry

This thesis is submitted with our approval as research supervisors:

	Signature	Date
Dr. Solomon Derese Department of Chemistry University of Nairobi sderese@uonbi.ac.ke		14th September, 2020
Dr. Albert Ndakala Department of Chemistry University of Nairobi andakala@uonbi.ac.ke		14th September, 2020

DEDICATION

This work is dedicated to the Buyinza family.

ACKNOWLEDGEMENTS

I acknowledge the University of Nairobi for admitting me to the doctoral studies. I am sincerely indebted to my academic supervisors, Dr. Solomon Derese and Dr. Albert Ndakala for their persistent patience with me in all the stages of the doctoral study. They mentored and played the critical role of a parent, offering me academic and emotional support. I was privileged to have been guided by Prof. Abiy Yenesew. The academic guidance of this great scholar including securing me a grant to the University of Potsdam, laid the unshakable foundations that culminated into the successful completion of my PhD. Gratitude to Prof. Leonidah Kerubo Omosa, Dr. John Onam Onyatta and Dr. John Wanjohi for the encouragements at my low moments in Chiromo. Thank you "DAAD", the German Academic Exchange Services for financing my study through the Natural Products Research Network for Eastern and Central Africa (NAPRECA). I appreciate the financial support from the University of Potsdam through Prof. Heiko Moller and Dr. Matthias Heydenreich, thank you Matthias for being my host supervisor as well. Angela Krtitschka is thanked for taking the NMR measurements. Appreciation to both the Analytical and Organic Chemistry groups of the Institute of Chemistry University of Potsdam for the harmonious working relationship during my time at the Institute. George Kwesiga, I remember our time in Nairobi but more so in Potsdam as we rushed out every morning to catch a train to Golm. My gratitude to Prof. Vincent Kam Wai Wong and Paolo Coghi of the State Key Laboratory of Quality Research in Chinese Medicine, Macau University of Science and Technology, for the Cytotoxicity assays and to Dr. John Waweru for the antiplasmodial tests. I thank Mr. Patrick Chalo Mutiso of the School of Biological Science University of Nairobi for the identification and collection of the plants studied. Special recognition to Dr. Ivan Gumula, Dr. Grace Bakyayita Kizito and Mr. Peter Wefafa of Kyambogo University for the continuous guidance right from my undergraduate to date. Thanks to my fellow postgraduate students at the Chemistry Department University of Nairobi: Dr. J. Atilaw, Dr. A. Fozia, Dr. S. Yahuba, R. Owori, M. Andima, V. A. Nchiozem-Ngnitedem, C. Carolyn, Ibrahim, Vincent, Brenda, Hilda and Martin for the shared moments. Special appreciation to my beloved wife and children for the perseverance and constant prayers during my studies. My dearest parents, your inspiration to educate me amidst your poverty has born a new legacy, bravo papa and bravo mama. Glory to my creator, the Almighty God who lifts the poor from the refuse and sit them among the princes.

ABSTRACT

Despite all the undertakings to fight malaria and cancer, the infections occurrencies per year is still high or even rising as the case for cancer, making them the leading causes of fatality in the world. The *Plasmodium* resistance and varied side effects of the conventional cancer drugs is a major hitch in the treatment of malaria and cancer, hence posing a big challenge to the global health care. Phytochemicals from higher plants have produced safe antimalarials and anticancers and still offer hope for new drugs. The aim of this study therefore was to search for anticancer and antimalarial principles from *Millettia dura, Millettia leucantha* and *Millettia lasiantha* from Kenya. The compounds were isolated using column chromatography over silica gel 60 (60-120 mesh) plus Sephadex LH-20. Purification was done on a Chromatotron (7924T, 24V, 200 rpm). Compounds were characterized basing on NMR, MS, UV and IR spectral data. A total of 51 compounds were isolated and characterized. The first phytochemical study on the flowers of *M. dura* yielded nine compounds, this being the first report of 4,2′-dihydroxy-4′-methoxychalcone (**228**) from the genus. Seven compounds were isolated from the pods while thirteen compounds were gotten from the stem bark. The presence of deguelin (**170**) and tephrosin (**171**) in the stem bark of *M. dura* was a unique finding. This is also the first report of the four flavonoids, chrysin (**229**), apigenin (**230**), chrysin 7-*O*-*β*-*D*-glucoside (**231**) and genkwanin (**232**) from the genus isolated from *M. leucantha* (leaves), meanwhile, the root bark yielded six compounds. This is the primary phytochemical study on *M. lasiantha* which gave four flavones from its leaves, four compounds from the stem bark, while out ot the four compounds isolated from the roots, 3,8-dihydroxy-7,9-dimethoxycoumestan (**241**) and 7,5′-dihydroxy-6′,4′-dimethoxycoumaronochromone (**242**) are novel compounds. Out of the samples screened againest W2 and D6 strains of *P. falcipalum*, the stem bark extract had the highest activity of 31.9±8.6 and 23.1±4.5 µg/ml againest W2 and D6 respectively, while the most active compound was milletone (**172**) with respective IC_{50}'s of 33.1±3.7 and 27.4±3.1 µM againest W2 and D6. Out of the fifteen flavonoids tested for cytotoxicity, tephrosin (**171**) and durmillone (**99**) were the most active with respective strong IC_{50}'s of 3.14 and 6.6 ±1.2 µM against A549 cancer cell line. Chemotaxonomic review of *M. dura* and its morphologically related *M. ferruginea* showed both taxa to elaborate mainly isoflavones (33 reported) out of which 23 have C-8 prenyl group or its modification as 2,2-dimethylchromene moety at C-7/C-8 and 91% of the isoflavones are 5-deoxygenated. Oxygenation at C-8 has been reported only in *M. dura*. Millettone

(**172**) and millettosine (**173**) only identified in the seedpods of *M. dura* could be responsible for the morphological difference observed in the seed pods of the two taxa and serves to distinguish *M. dura* from *M. ferruginea*.

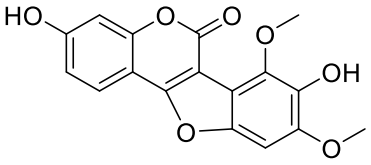

241

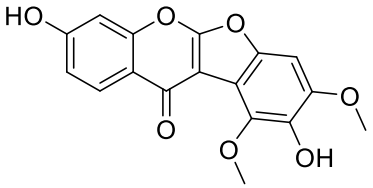

242

TABLE OF CONTENTS

Contents

LIST OF TABLES

LIST OF FIGURES

APPENDICES

ABBREVIATIONS AND SYMBOLS

DAAD	Deutscher Akademischer Austauschdienst (German Academic Exchange Services)
NAPRECA	Natural Product Research Network for East and Central Africa
NMR	Nuclear Magnetic Resonance
MS	Mass Spectrometry
UV	Ultra Violet
IR	Infra-Red
P. falcipalum	Plasmodium falciparum malaria parasite
µg/ml	Microgram per milliliter
µM	Micro molar
IC_{50}	Inhibition concentration
D6	D.Walliker-6 (chloroquine-sensitive (Indochina) clones of *P. falciparum*)
W2	Walliker-2 (chloroquine-resistant (Indochina) clones of *P. falciparum*)
DNA	Deoxyribonucleic acid
WHO	World Health Organization
ACTs	Artemisinin Combination Therapies
MDA-MB-231	M.D. Anderson Metastasis Breast cancer cell line
NCI-H460	Lung cancer cell line
CSCs	Cancer stem cells
A549	Adenocarcinomic human alveolar basal epithelial cells
EBV	Epstein-Barr virus
MTT	3-(4,5-dimethylthiazol-2-yl)-2,5-diphenyltetrazolium bromide
LV	Leaves
FL	Flowers
SD	Seeds
SP	Seed pods
SB	Stem bark
ST	Stems
RB	Root bark
TB	Timber
RT	Roots
FT	Fruit
MTP	Mitochondrial transmembrane potential
TLC	Thin Layer Chromatography
HRESIMS	High resolution electro spray ionization mass spectrometry
EtOAC	Ethyl acetate
MeOH	Methanol
CH_2Cl_2	Dichloromethane
PE	Petroleum ether
DMSO	Dimethylsulphoxide
µL	Micro liter
µCi	Micro curie
rpm	Revolutions per minute
MCF-7	Michigan Cancer Foundation-7
ABCA4	ATP Binding Cassette Subfamily A Member 4
ABCA12	ATP Binding Cassette Subfamily A Member 12

CHAPTER ONE
INTRODUCTION

1.1 Background of the study

Malaria (WHO, 2018a) and cancer (WHO, 2018b) are global health challenges causing loss of many lives (WHO, 2018a, 2018b; Siegel *et al*., 2019). Low income and developing economies carry the biggest burden of these diseases. For example, 93% of the global malaria cases occur in Africa, and Uganda alone accounts for 4% of the worlds' malaria cases (Commonwealth, 2019). Out of the 17 million cancer cases diagnosed and the 9.5 million cancer deaths registered in 2018, the low-medium income countries contributed 20% (American Cancer Society, 2019). In the management of these diseases, nature has offered the most potent malaria (Willcox *et al*., 2004; Woon-Chien *et al*., 2016) and cancer (Iqbal *et al*., 2017; Amaral *et al*., 2019) drugs and it still serves as a source for new and safe lead molecules.

Quinine (**1**) from *Cinchona succiruba* (Foley and Tilley, 1998) plus the subsequent synthetic derivative chloroquine (**2**) (Biagini *et al*., 2005; Mushtaque *et al*., 2015; Vandekerckhove and Matthias, 2015) have been used effectively in the management of malaria. However, the parasite developed resistance to these drugs (Foley and Tilley, 1998). The discovery of the antimalarial drug artemisinin (**3**) from *Artemisia annua* (Wright 2005; Blazquez *et al*. 2013) came in handy to manage the multidrug resistant malaria (Woodrow, 2005). However, resistance has been reported against artemisinin and artemisinin combination therapies (ACTs) in Southeast Asia (Cooper *et al*., 2018; WHO, 2018a). Resistance to ACTs has also been reported in Equatorial Guinea (Cooper *et al*., 2018), bringing the resistance to Africa as well. The emergence of resistance is threatening the gains made in the fight against malaria, necessitating the search for new antimalarial drugs.

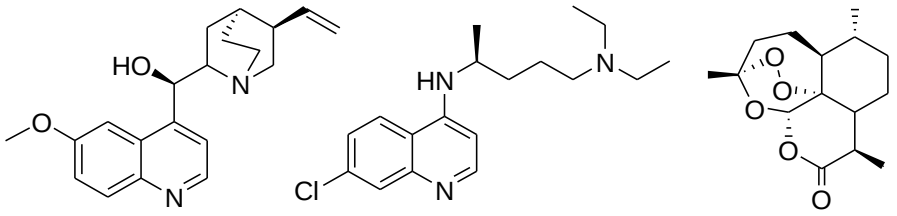

Plants have also offered a good number of drugs and lead molecules in the treatment of cancer. Some of these include vincristine (**4**) and vinblastine (**5**) from *Catharanthus roseus* (Noble, 1990;

Kumar *et al*., 2013; Ashoka *et al*., 2017) which have been used against breast, liver, leukemia, testes and lung cancer and paclitaxel (**6**) from *Taxus brevifolia* (Wani *et al*., 1971; Stierle *et al*., 1993; Haque *et al*., 2016) for the management of ovarian, breast and lung cancer (Maurie, 1991).

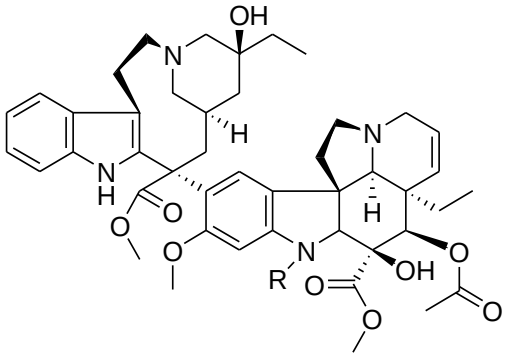

	4	5
R	CHO	CH_3

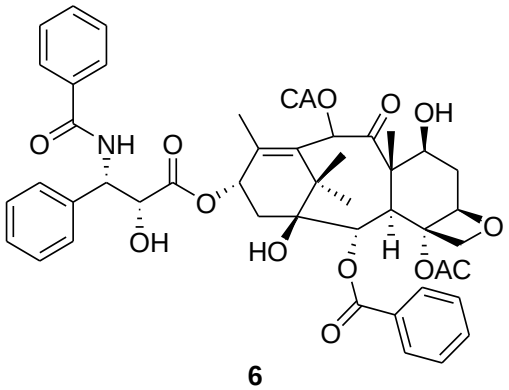

6

There are reported cases of cancer resistance attributed to inherent and or acquired resistance (WHO, 2018b). The realization that most of the common cancer drugs are toxic with adverse effects (Ojima *et al*., 2016) brings to question their safety profiles. It is therefore important, to discover and develop anticancer agents to overcome resistance and toxicity. In this respect, three *Millettia* species namely: *M. dura, M. leucantha* and *M. lasiantha* have been investigated for possible antiplasmodial and anticancer principles.

1.2 Statement of the problem

Malaria and cancer are major challenges to public health care. They are the global leading causes of mortality (WHO, 2018b; Siegel *et al*., 2019). The global malaria deaths stood at 435,000 and Africa contributed 93% of this total in 2018 (WHO, 2018a; Commonwealth, 2019). While the global cancer related deaths was 9.6 million in 2018 (American Cancer Society 2019; Bray *et al*. 2018). The malaria parasites have developed resistance against conventional drugs such as quinine (**1**), chloroquine (**2**) and artemisinin (**3**) and artemisinin combination therapy (Cooper *et al*., 2018). In the case of anticancer agents, the problem is not only resistance (WHO, 2018b) but also toxicities and unbearable side effects (Ojima *et al*., 2016). There is need to continue the search for efficacious and safer drugs. Secondary metabolites from nature have been used in the management of malaria and cancer, producing antimalarial drugs such as quinine (**1**) (Foley and Tilley, 1998) and artemisinin (**3**) (Wright, 2005; Blazquez *et al*. 2013) which are a backbone to many malaria

drugs. Nature has also provided several anticancer drugs including vincristine (**4**), vinblastine (**5**) (Noble, 1990; Kumar *et al*., 2013; Ashoka *et al*., 2017) and paclitaxel (**6**) (Wani *et al*., 1971; Stierle *et al*., 1993; Haque *et al*., 2016) from which more potent and or safer drugs have been synthesized. On this basis, it was important to revisit nature, the in- exhaustible source of chemotherapy in the quest for antimalarials and anticancers, by studying *M. dura, M. leucantha* and *M. lasiantha.*

1.3 Objectives

1.3.1 General objective

The general objective of this study was to identify antimalarial and anticancer principles from *Millettia* species.

1.3.2 Specific objectives

The definite intents of the study were to:

i. Separate and characterize secondary metabolites from *Millettia dura, Millettia leucantha* and *Millettia lasiantha*.
ii. Evaluate *in vitro* antiplasmodial action of extracts plus compounds.
iii. Evaluate the anticancer activities of extracts and compounds.
iv. Establish the chemotaxonomic markers that differentiate *M. dura* from *M. ferruginea*

1.4 Justification

The genus *Millettia* (Leguminosae) is rich in flavonoids (Chatsumpun, 2010) which have exhibited a range of biological and pharmacological activities (Yankep *et al*., 2003). An earlier study on *M. dura* showed moderate antiplasmodial activities of 13 - 53μM for the pure compounds and 10 - 12μg/ml for the crude extracts (Derese *et al*., 2014a). The CH_2Cl_2-MeOH (1:1,V/V) extract from *M. oblata* ssp. *teitensis* (stem bark) showed moderate antiplasmodial activities with IC_{50} values of 10 - 12μg/ml for chloroquine senstive and resistant strains of *falciparum* (Derese *et al*., 2014a). On this basis, it was important to further study *M. dura* and other *Millettia* species for more potent antiplasmodial metabolites.

Extracts and pure isolates from a number of *Millettia* have also been tested for their anticancer activities. The dichloromethane : methanol (1:1v/v) crude extract from *M. usaramensis* ssp.

usaramensis (root bark) had a moderate activity of IC_{50} 11.63µg/ml for the human breast cancer cell line (MDB-MB-231) while the rotenoids isolated from it, showed moderate cytotoxicities between IC_{50} 25.7 - 207.2µM (Deyou *et al*., 2015b). The chloroform extract of *M. pervilleana* (root bark) has IC_{50} values of 0.047 - 0.12µg/ml on KB cells (Palazzino *et al*., 2003). Pure compounds isolated from *M. dura* show weak IC_{50} values of 153.5 - 174.1µM for the MDB-MB-231 (Marco *et al*., 2017a). The compounds from *M. oblata* ssp. *teitensis*, had moderate activity of IC_{50} 33.3 - 93.8µM against the humanoid breast cancer cell line (Deyou *et al*., 2017b). Phytochemicals from *M. leucantha* had moderate toxicities ranging from 3.69 to 7.36µg/ml against NCI-H460 lung cancer cell line (Phrutivorapongkul *et al*., 2003). These promising anticancer results necessitated investigations on *M. dura*, *M. leucantha* and *M. lasiantha* for active anticancer agents.

Given the health challenges from malaria and cancer, the effect of resistance and toxicities downplaying the current drugs and the fact that nature is a good source of antimalarial and anticancer drugs, it was important to undertake this study in anticipation for new efficacious and safer antimalaria and anticancer agents from the studied plants.

CHAPTER TWO

LITERATURE REVIEW

2.1 Malaria

Malaria is a protozoal infection (Nogueira and Lopes, 2011; Mushtaque, 2015) triggered in human by *Plasmodium* parasites like *falciparum*, *vivax*, *malariae*, *ovale* plus *knowelsi* (Amir *et al*., 2018). Among these, *P. falciparum* is the most devastating in Africa that accounted for 99.7% of all the malaria deaths in 2017 (WHO, 2018a). The parasites are transmited by mosquitoes which thrive well in tropical regions of the world.

Malaria has far reaching effects globaly with fatalities varying across economies. In 2017, there was a global recount of two hundred ninteen million malaria incidences with 435,000 fatalities (Table 2.1) (WHO, 2018a). Children under 5 years were the most affected accounting for 61% of all the deaths due to malaria worldwide (WHO, 2018a). Africa accounted for 92% of the total malaria burden in 2017 (WHO, 2018a). According to the world malaria report 2018, 350 million people were at high risk of malaria in the East African region with 45.6 million confirmed cases and 103,600 deaths due to malaria in 2017 (WHO, 2018a). In Table 2.2, Uganda accounted for 4%, Tanzania 3%, Rwanda 3% and Kenya had a 3% prevalence of the global malaria cases in 2017, figure 2.1 (WHO, 2018a).

Table 2.1: Estimated malaria burden by WHO region in 2017

WHO Region	Malaria Cases	Malaria Deaths
Africa	200,000,000	403,000
South-East Asia	11,300,000	19,700
East Mediterranean	4,400,000	8,300
Western Pacific	1,900,000	3,620
America	976,000	630
World	219,000,000	435,000

Source of data: World malaria report 2018

Table 2.2: African country malaria share 2017 (WHO estimates)

Country	%ge	Country	%ge
Nigeria	25	Mali	3
Democratic Republic of Congo	11	Tanzania	3
Mozambique	5	Rwanda	3
India	4	Angola	2
Uganda	4	Malawi	2
Burkina Faso	4	Guinea	2
Ghana	4	Benin	2
Nigia	4	Others	19
Cameroon	3	Total	100

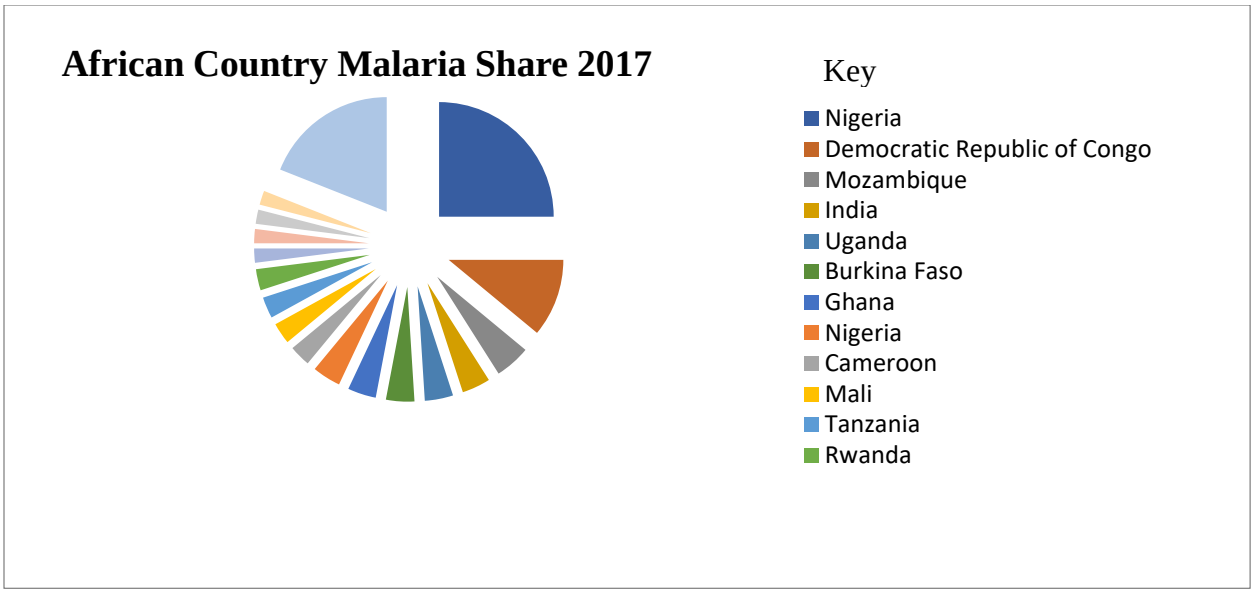

Figure 2.1: Pie chart showing African Country Malaria Share 2017 (WHO Estimates)

The global malaria infection of 219 million people in 2017, was a rise from the previous year's of 217 million people but, in terms of fatalities, there was a marginal decrease in fatalities from 451,000 to 435,000 (WHO, 2018a). A typical example is the 48% increase in malaria incidences in Brazil in 2017 (PAHOWHO, 2018). The upward infection rate is attributed to relaxation in the survellance and control measures while the decrease in motarity is attributed to early diagnosis and treatment (PAHOWHO, 2018). This is a clear call to intensify survellance and control as well as immediate treatment on diagnosis to avert the scourge. The poor in less developed countries are the most affected (Kebede *et al*., 2010; Caussy *et al*., 2015). In terms of resource commitment, an estimated $3.1billion was spent in 2017 on malaria intervention globally which was a shortfall from the budgeted $4.4billion (WHO, 2018a). The biggest share of $2.2billion was committed to WHO African region. Malaria endemic governments contibuted 28% ($0.9billion) of the $3.1billion from their resources to this cause (WHO, 2018a).

2.1.1 Antimalarial from nature

Antimalarial from nature or their derivatives have been at the forefront in the fight against malaria. The most prominent of these include quinine (**1**), chloroquine (**2**), artemisinin (**3**), primaquine (**7**), mefloquine (**8**) and their combinations (Bruce *et al.*, 1950; Baird, 2005; Woodrow, 2005; Kumar *et al.*, 2014, Vandekerckhove and Hooghe, 2015). The aminoquinoline antimalarial drug quinine (**1**) was isolated from *Cinchona succiruba* (Rubiaceae) in 1812 and it became the cornerstone for

development of modern antimalarial. An era of organic synthesis followed triggering the manufacture of aminoquinoline-based antimalarials; chloroquine (**2**), primaquine (**7**), mefloquine (**8**), amodiaquine (**9**) and quinidine (**10**) using quinine (**1**) as a template (Willcox *et al*., 2004). In 1946, a quinazolin alkaloid, febrifugine (**11**) said to be 100-times more active than quinine was isolated from *Dichroa febrifuga* (Willcox *et al*., 2004). However, its development into antimalarial has been limited by its side effects (Willcox *et al*., 2004). In 1971, another important antimalarial, a sesquiterpene lactone, artemisinin (**3**) was isolated from *Artemisia annua* (Woodrow, 2005). More effective artemisinin based semisynthetic antimalarial such as artemether (**12**), arteether (**13**) and sodium artesunate (**14**) have been developed (Willcox *et al*., 2004). The search for antimalarial from nature is still an active research.

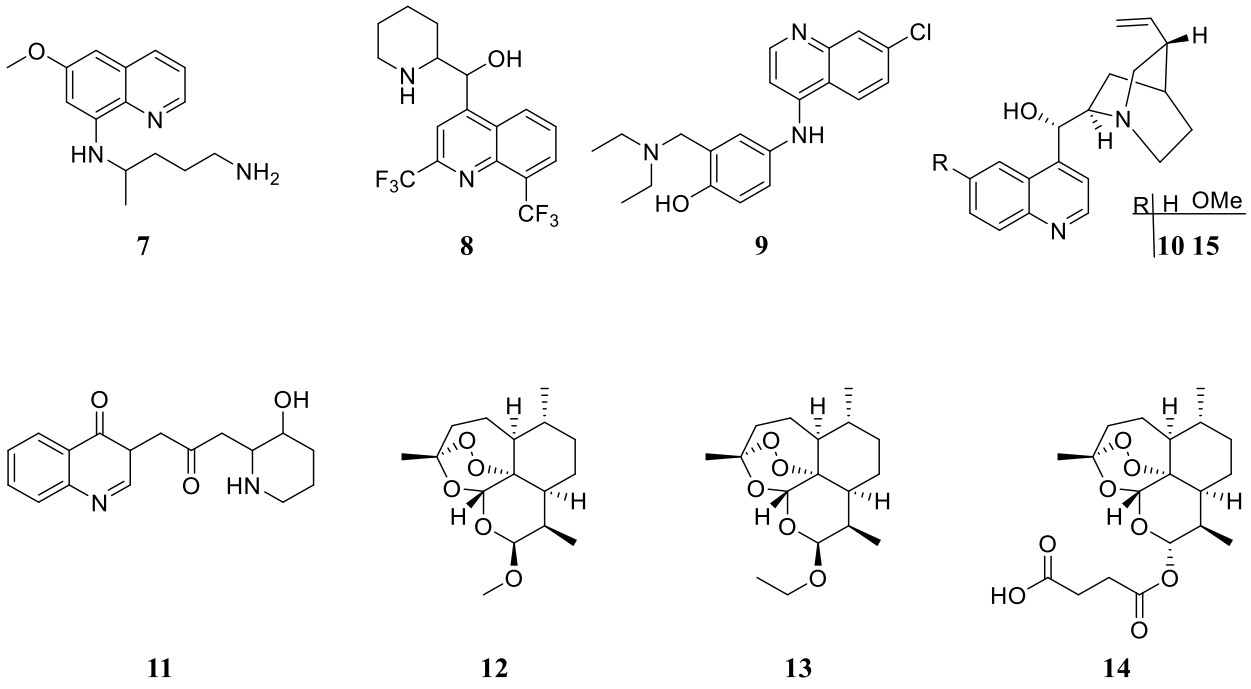

Figure 2.2: Antimalarials from nature

2.1.2 Resistance to antimalarial

The success in the management and / or elimination of malaria was hindered by the early emergence of drug resistant *Plasmodium* strains. *Plasmodium* resistance to drugs has been growing at a rate much higher than the development of new antimalarial. Antimalarial drug resistance has been reported for *P. malariae, vivax,* besides *falciparum* (White *et al*., 2014; Gunjan *et al*., 2017). In Table 2.3, a brief overview of the time of the likely onsets of resistance to some conventional antimalarial is given.

Table 2.3: Time of resistance onsets to some antimalarial (data from Gunjan *et al*., 2017)

Antimalarial	Time introduced	First report of resistance	Place of first occurrence
Quinine	1820	1925	S. America
Chloroquine	1947	1957	Thai-Cambodia boarder
Fansidar	1979	1980	
Mefloquine	1974	1987	
Artemisin	1972	2008	

Owing to mutation and travel patterns, the problem of *Plasmodium* resistance to first line antimalarial and their combination therapies has since then spread to other malaria endemic regions including Africa (Cooper *et al*., 2018). A search therefore for new antimalarial with a different mode of action is an immediate necessity.

2.2 Cancer

Cancer is the fast growth and splitting up of abnormal cells in a body part (American Cancer Society, 2016). Cancer cells outlive normal cells and are able to invade other body parts or organs (Haque *et al*., 2016) causing over 100 cancer types (Iqbal *et al*. 2017). The risk factors associated with various cancers include genetics, behavior (use of tobacco and alcohol, or dietary factors plus physical inactivity), infections, environment, carcinogens as well as radiation (Bloom *et al*., 2011). 31% of the cancers in Sub-Saharan Africa are caused by infections, a figure above the world's average of 15% (American Cancer Society, 2018).

Cancer is a menace to world public well-being (WHO, 2018b; Siegel *et al*., 2019), being the principal backer of fatality in highly established nations but also the succeeding contributor to fatality on the African continent after cardiovascular disease (American Cancer Society, 2018). Cancer causes 1 out of 6 deaths worldwide, which is more than malaria, AIDS, and tuberculosis combined (American Cancer Society, 2018). The elderly people (≥50 years) are the most affected

accruing to 80% of the cancer prevalences globally (American Cancer Society, 2018). The worldwide cancer burden in 2018 was about eighteen million incidences alongside the over nine million bereavements (International Agency for Research on Cancer, 2018), and this was anticipated to reach ≈ 30 million cancer occurrences with approx. sixteen million related demises as it clocks 2040 (WHO, 2018c), Table 2.4.

Table 2.4: Global Cancer Estimates and Projections (in millions)

	Cancer State	Growth rate	Cancer Projections
Year	2018		2040
Cases	18.1	1.63	29.5
Deaths	9.6	1.71	16.4

East Africa is estimated to have had 7.7% fresh cancer numbers resulting in 5.3% related lives lost in 2018 (Globocan, 2018) Table 2.5. This is a threat amidst the poor health care systems in this region. From Table 2.5, the female population is most affected by cancer in Eastern Africa. This calls for regular screening of the common cancers among women to ensure early detection and treatment.

Table 2.5: Cancer prevalence in Eastern Africa in 2018 (Globocan 2018)

	Population	Cancer cases	Cancer deaths
Male	215,198,311	129,476	94,731
Female	218,444,860	202,701	136,237
Totals	433,643,171	332,177	230,968
Percentage (%)		7.65	5.32

In 2017, the global estimated expenditure on cancer medicines and related supportive care reached US$ 133 billion (WHO, 2018c). Premature mortality from cancer in developing countries (including Africa) caused an estimated cost of lost productivity totalling to $46.3 billion in 2017 (Bray *et al*., 2018). This reveals the economic threat by the burden of disease in poor countries.

2.2.1 Anticancer drugs from nature

The role of natural products in the control of disease is irrefutable. It is reported that between 1980 and 2019, 174 new anticancer drugs have been approved worldwide for sell either as cancer drugs or remedy (Amaral *et al*., 2019). Out of this total, 53% are natural products or their derivatives (Amaral *et al*., 2019). One class of such anticancer phytochemicals are Vinca alkaloids isolated in

1957 by Collip and group (Haque *et al*., 2016) from *Catharanthus roseus* G. Don. (Apocynaceae). The very first of the vinca alkaloids were vincristine (**4**) and vinblastine (**5**) which are tubulin heterodimers that disrupt microtubules' functions or arrest cell metaphase. These vinca alkaloids are used as therapies against several cancers including breast, liver, leukemia, prostate and lung cancers (Iqbal *et al*., 2017). Semisynthetic derivatives of vinca alkaloids on market include vinorelbine (**16**), vindesine (**17**) and vinflunine (**18**) (Iqbal *et al*. 2017; Madhushree, 2016). Taxanes are another important class of anticancer agents which bind to microtubules praying a centrol role in cell division. Paclitaxel (**6**) and docetaxel (**19**) were the first-generation taxanes to be isolated (Wani *et al*., 1971; Ojima *et al*., 2016) from *Taxus* brevifolia Nutt, *T. baccata*, *T. canadensis* and *Corylus avellana* (bark and leaf) (Iqbal *et al*., 2017). They are strong anticancer agents against ovarian, breast and lung cancers among others. The synthetic analogs of paclitaxel (**6**) that followed in 1990 (Amaral *et al*., 2019) include Cabazitaxel (**20**) larotaxel (**21**), milataxel (**22**), ortataxel (**23**) and tesetaxel (**24**) which are therapies for, pancreatic, lung, breast and urethral bladder cancers (Iqbal *et al*., 2017).

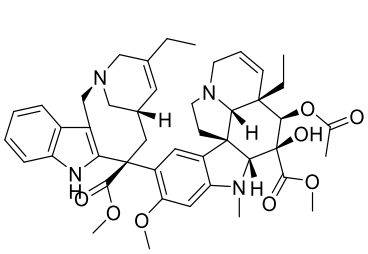

16

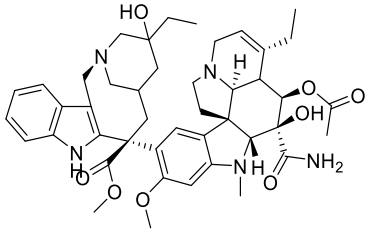

17

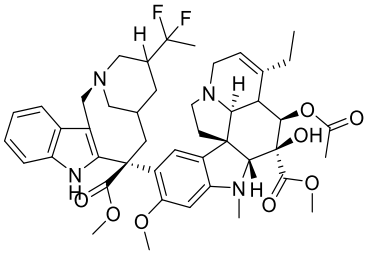

18

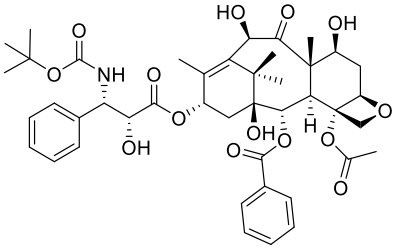

19

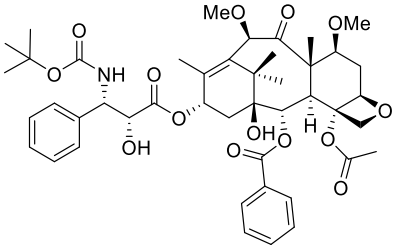

20

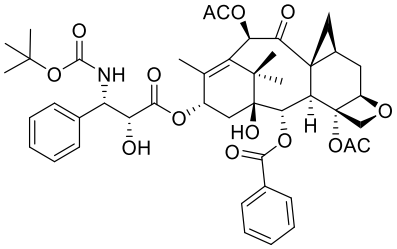

21

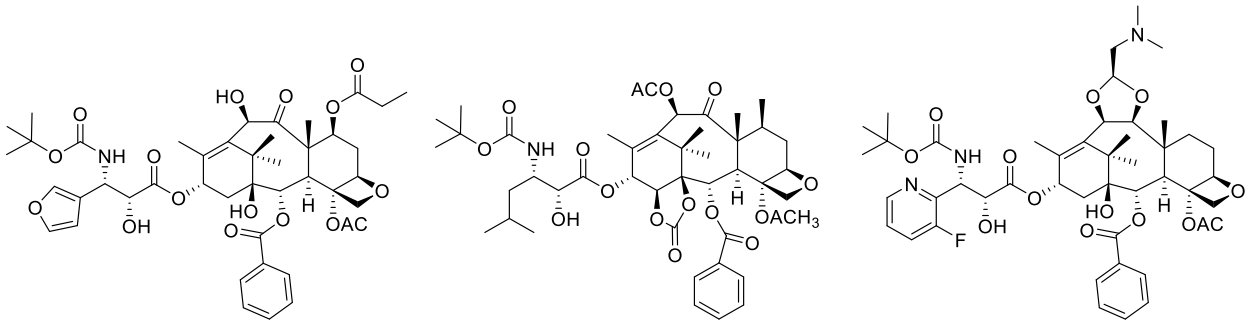

22 23 24

Figure 2.3: Anticancer drugs from nature

2.2.2 Treatment of cancer and related side effects

The conventional methods used in the management of cancer include immunotherapy, vaccination, chemotherapy, surgery, radiotherapy, photodynamic therapy, stem cell transformation, hormone therapy, 'targeted' therapy or a combination of these (Iqbal *et al*., 2017; Upadhyay *et al*., 2017). However, these have been met with limitations such as severe side effects, bioavailability, toxicity, non-specificity, fast clearance and restriction in metastasis in addition to being expensive (Iqbal *et al*., 2017; WHO, 2018b). In particular, platinum alkylating anticancer drugs are highly toxic to multiple organs (Ojima *et al*., 2016; Iqbal *et al*., 2017). The rapidly dividing normal cells in our bodies under usual physiological circumstances like those of hair gland, bone core and digestive tract among others, can be targeted by these anticancer drugs. As a result, the patient suffers decreased blood production, gastrointestinal area inflammation, hair damage, immunosuppression, heart ailments and nervous complaints (Iqbal *et al*., 2017). In this regard, chemotherapeutics sought from nature may be less toxic and are likely to offer the desired therapeutic effect owing to their functional similarity to the compounds in our bodies.

2.2.3 Resistance in cancer treatment

Drug-resistant human pathogens have led to diseases harder to treat. The extreme use of medications, inadequate medications, self-medications, wrongly prescribed medications etc. are prime in promoting drug resilient strains of human pathogens (Gunjan *et al*., 2017; Upadhyay *et al*., 2017). An approximated 80% to 90% death in cancer patients are being attributed to drug resistance (Amaral *et al*., 2019). The increased signal transduction (transfer of signal across cell membrane) and growth factor activities of cancer cells supersede proliferation and promotes

aptosis failing the body system to control these processes, and as such, resistant cancerous cells set in (Boik, 2001). Through mutation, the cancer cells develop drug resistant genes (Aung *et al*., 2017) that render the treatment ineffective. Also onset of cancer drug resistance is being ascribed to emergence of comparatively unusual but vastly drug resistant and gradually multiplying tumour-triggering building blocks termed, "cancer stem cells" (CSCs) (Ojima *et al*., 2016). Cancer resistance to drug can be intrinsic (inherent with in cell even before therapy) or acquired (in response to treatment) (Gunjan *et al*., 2017). Drug resistance in cancer follows different mechanisms like efflux of drugs (pumping the drug out of the cell faster than can diffuse in), inactivation of drugs, modification of drug targets, inhibition of cell death, induction of epithelial–mesenchymal transition (loss of cell differentiation features), and enhanced DNA damage repair activity (Upadhyay *et al*., 2017). In this respect, anticancer drugs with a superior mode of action are urgently needed to avert the problem of resistance to the current drugs.

2.2.4 Relationship between malaria and cancer

There are several antimalarials that have shown good activity against cancer. For example, an antimalarial febrifugine (**11**) from *D. febrifuga* and cinconine (**15**) from *Cinchona nicrantha* show anticancer properties (Willcox *et al*., 2004). The well-known antimalarial artemisinin (**3**) and its analogues have shown potent anticancer activity inhibiting proliferation, metastasis, as well as angiogenesis in primary cancer cell lines and cultures (Aftab *et al*., 2017). Also, it is imperative recording that, *Plasmodium falciparum*-derived proteins have been linked to the activation of Epstein-Barr virus (EBV) in acute malaria infection which accelerates the development of Burkitt lymphoma in children (Frimpong-Boateng, 2010). This therefore gives a direct link between malaria and cancer, a reason for which this study focused on both malaria and cancer.

2.3 Botany of the genus *Millettia*

The genus *Millettia* belongs to the family of Leguminosae (Fabaceae) and subfamily Papilionoideae (Beentje, 1994). This genus has about 260 species widely distributed over the tropical regions of Africa, Australia, Asia and America (Dagne and Bekele, 1990; Chatsumpun *et al*., 2010; Havyarimana *et al*., 2012; Kamto *et al*., 2012; Ren *et al*., 2016). About 139 *Millettia* species are reported to be endemic to Sub-Saharan Africa, Figure 2.4 (Banzouzi *et al*., 2008). Plants of this genus are either trees, climbers/lianas or shrubs (Beentje, 1994). Among the six

Millettia species (*M. dura, M. leucantha, M. lasiantha*, *M. usaramensis* ssp. *usaramensis*, *M. oblata*, and *M. tanaensis*) found in Kenya (Maundu and Tengnäs, 2005), *M. dura* is the most widely distributed and is also found in Tanzania, Uganda, Zimbabwe, Burundi, Rwanda, and DRC (Beentje, 1994). In this study *M. dura*, *M. leucantha* and *M. lasiantha* were investigated.

Figure 2.4: Distribution of *Millettia* in Africa (Banzouzi et al., 2008)

2.3.1 *Millettia dura*

Millettia dura Dunn (Figure 2.5) is a shrub or tree. Its bark is light grey and scaly (Beentje, 1994). It carries 15-19 elliptic or ovate leaflets on each leaf with blue-purplish flowers and a 14-20 cm oblong fruit (Beentje, 1994). It is a shade or ornamental tree with a tough wood having close resemblance to *M. ferruginea* (Dagne *et al*., 1991). It is found at the periphery of moist forest (1200-2000m above sea level) but also cultivated in Mwanga, Muhatia and Muvanga in Kenya (Beentje, 1994).

Figure 2.5: M. dura (taken by Buyinza 2015)

2.3.2 *Millettia leucantha*

Millettia leucantha Vatke is a sacandent shrub, tree (1-12 m high), or liana (Beentje, 1994). It has pinnate leaves with 5-7 leaflets and white or blue-violet flowers (Phrutivorapongkul *et al*., 2003). Mostly common on rockey hills (600-1500m above sea level) within the secondary bushlands or semi-deciduous forests of the Kamba land (Beentje, 1994).

2.3.3 *Millettia lasiantha*

Millettia lasiantha is a liana. It has 7-9 elliptical leaflets on each leaf, mauve flowers and densily hairly oblong fruits with the beak turned down (Beentje, 1994). Endemic to the evergreen coastal forests of Dzombo, Boni, Mdogo, Mwele, Mangea and Mombasa (1-500m above sea level) in Kenya (Beentje, 1994).

2.4 Ethnomedicinal uses of *Millettia* species

Millettia dura seeds are traditionally an important fish toxin within Kenya (Kokwaro, 1994) and Ethopia (Dagne *et al*, 1989) and the roots of *Millettia lasiantha* are used as an aphrodisiac in Kenya (Kokwaro, 1994). *Millettia* species have several therapeutic values in Sub-Saharan Africa including treatment of malaria, fevers, inflamations, headaches, colds, wounds, swellings among others (Banzouzi *et al*., 2008). Table 2.6 highlights some of the traditional uses of some *Millettia* species.

Table 2.6: Traditional Uses of some *Millettia* Species (adopted from Banzouzi *et al*., 2008)

Species	Part used	Disease/condition
M. aromatic, Dunn	Trunk	Headaches
M. barteri, Dunn	Bark	Feverish aches
M. congolensis, Dur	Seeds and leaves	Viral diseases and fevers
M. dura, Dunn	Roots and leaves	Hernias, diarrheas and painful menstruations, hunt/fish poison
M. elongatistyla, Gillet	Leaves or roots	Malaria and schistosomiasis
M. ferruginea, Baillet	Leaves	Bacterial
M. lasianthia, Dunn	Roots	Aphrodisiac
M. oblata, Dunn	Roots	Swelling and bladder problems
M. oboensis, Baker	Leaves	Colds /headaches
M. pervilleana, Vigular	Not specified	Malaria
M. usaramensis, Taubert	Roots	Convulsion and aphrodisiac

2.5 Biological evaluation of *Millettia* species for malaria and cancer

The crude extracts of *Millettia* species have been evaluated to determine their efficacy against various ailments (Banzouzi *et al*., 2008). Herein the antiplasmodial and anticancer activities of the crude extracts of Kenyan *Millettia* species is highlighted. The crude extracts of three of the Kenyan *Millettia* species namely: *M. dura*, *M. oblata* ssp. *teitensis* and *M. usaramensis* ssp. *usaramensis* were evaluated for their antiplasmodial action towards D6 plus W2 species of *P. falciparum* as in Table 2.7. In vitro antiplasmodial activity for a pure compound is considered to be excellent with IC_{50} less than 1µM, good if IC_{50} is between 1 and 20µM, moderate for IC_{50} between 20 and 100µM, low when IC_{50} lies between 100 and 200µM and not active for IC_{50} is more than 200µM. Meanwhile, for the crude extract, good activity is for IC_{50} below 10µg/ml, moderate for IC_{50} ranging from 10 to 50µg/ml, low when IC_{50} is between 50 and 100µg/ml while not active if IC_{50} is greater than 100µg/ml (Batista *et al*., 2009; Namukobe *et al*. 2015).

Table 2.7: Antiplasmodial activities of crude extracts of Kenyan *Millettia* species

Plant/part*	IC_{50} in µg/ml		Reference
	D6	W2	
M. dura (SB)	21.4±2.9	23.6±4.1	Derese *et al*., 2014b
M. dura (SP)	18.5±2.6	18.8±2.5	
M. dura (SD)	254±1.9	22.5±0.9	
M. oblata ssp. *teitensis* (SB)	10.0±2.3	12.0±1.2	
M. usaramensis ssp. *usaramensis* (SB)	21.1	28.0	Yenesew *et al*., 2003

* SB: Stem bark; SP: Seed pods: SD: Seeds

In an anticancer evaluation, the crude extract of *M. usaramensis* ssp. *usaramensis* (root bark) showed a moderate activity of IC_{50} equaling 11.63µg/ml towards ER-negative MDA-MB-231 (Deyou *et al*., 2015b). While the root bark extract from *M. dura* showed cytotoxicity, IC_{50} of 31.7µg/ml against the same humanoid breast cancer cell line (Marco *et al*., 2017a). In vitro anticancer activity for a pure compound is considered to be strong with IC_{50} below 10µM, good if IC_{50} is between 10 and 50µM, moderate if IC_{50} from 50 to100µM, low if IC_{50} ranges between 100 and 250µM and not active for IC_{50} more than 250µM. Meanwhile, for the crude extract, strong activity for IC_{50} lower than 20µg/ml, good activity if IC_{50} is between 20 and 50µg/ml, moderate for IC_{50} from 50 to 100µg/ml, low if IC_{50} runing from 100 to 200µg/ml and not active for IC_{50} beyond 200µg/ml (Kuete and Effert, 2015).

In view of the traditional uses of the different species of this genus and the ethno-medical evaluations against malaria and cancer, it was important that the active principles in the crude extracts be isolated and bioassayed. Section 2.6 below highlights the phytochemicals isolated from the *Millettia* species from Kenya and those elsewhere between 2014 and 2019.

2.6 Phytochemistry of the genus *Millettia*

Phytochemical studies have shown that, the genus *Millettia* is rich in flavonoids *sensu lato* as shown in Tables 2.8 – 2.14. The flavonoid sub-classes: chalconoids (Table 2.8), flavanones (Table 2.9), flavans (**44** and **45**) (Dat *et al*., 2019), isoflavanones (Table 2.10), flavones (Table 2.11), isoflavones (Table 2.12), pterocarpans (Table 2.13) and rotenoids (Table 2.14) are elaborated in the genus. Most of these flavonoids are prenylated, Tables 2.8 – 2.14. The genus also produces other classes of secondary metabolites: alkaloids (Table 2.15) (Zhenyu *et al*., 2017; Zingue *et al*., 2019), terpenoids (Zhenyu *et al*., 2017) (Table 2.16), steroids (Zhenyu *et al*., 2017), and coumarins (Yunyao *et al*., 2017; Harrison *et al*., 2019).

There are several reviews on the phytochemistry of the genus prior to this study (Derese, 2004; Musyoki, 2008; Barasa, 2011; Gumula, 2014; Marco, 2015; Tsegaye, 2015). The phytochemical review in this study focused on the secondary metabolites isolated from *Millettia* species from Kenya and those isolated elsewhere between 2014 and 2019.

2.6.1 Chalconoids from *Millettia* species

This is a sub-class of flavonoids having a structural backbone of C_6-C_3-C_6. The uniqueness of this sub-class is absence of ring C and the modified numbering that starts with ring B as shown in Figure 2.6. They commonly occur in plants as yellow pigments (Buckingham *et al*., 2015).

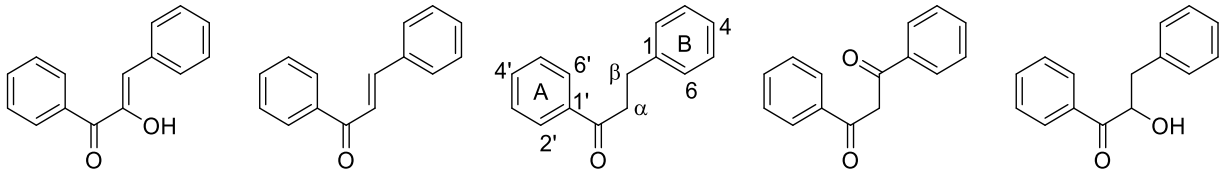

Figure 2.6: Basic structure of chalconoids

Biogenetically chalconoids are commonly oxygenated at positions 4′ and 6′/2′ as for the reported examples in Table 2.8. They are α, β dehydrogenated apart for **29** as well as being *O*-geranylated as for **26**, **27** and **29**. Almost all of these chalconoids have either a furan ring or a pyran ring attached to ring B through the oxygenation at C-4′ except for **16** that has an oxoprenyl instead. Ring A is unsubstituted apart for **40**, **41** and **42** for which C-4 has either a methoxyl or a hydroxyl group. Oxo-substitution at C-2′ is a common feature to these chalconoids. Table 2.8 gives an overview of the observation.

Table 2.8: Chalconoids from *Millettia* species from Kenya and those isolated elsewhere between 2014 and 2019

Compound	Source	Reference
Isoliquiritigenin (**25**)	*M. usaramensis* ssp *usaramensis* (SB)	Yenesew *et al*., 1998
4′- *O*-geranyl oxyisoliquiritigenin (**26**)	*M. usaramensis* ssp *usaramensis* (SB)	Yenesew *et al*., 2003b, 1998; Deyou *et al*., 2015
4- *O*-geranyl Oxyisoliquiritigenin (**27**)	*M. usaramensis* ssp *usaramensis* (RB)	Deyou *et al*., 2015
Butein (**28**)	*M. dura* (RB)	Marco *et al*., 2017
4′- Geranyloxy-α,4,2′-trihydroxydihydrochalcone (**29**)	*M. usaramensis* ssp *usaramensis* (SB)	Yenesew *et al*., 1998
Ovalitenin A (**30**)	*M. pulchra* (ST)	Xiaowei *et al*., 2015
Ovalitenin B (**31**)		
Pongamol (**32**)	*M. pinnata* (SD)	Perumalsamy *et al*., 2015
2′,6′-Dimethoxyfurano-[2″,3″:4′,3′]-*β*-hydroxydihydrochalcone (**33**)	*M. brandisiana* (RT)	Pailee *et al*., 2019
2′-Methoxyfurano-[2″,3″:4′,3′]-dihydrochalcone (**34**)		
Brandisianone E (**35**)		
Lonchocarpine (**36**)		
2′-Hydroxy-6″,6″-dimethylchromeno-[2″,3″:4′,3′]-*β*-hydroxychalcone(**37**)		
2′-Methoxy-6″,6″-dimethylchromeno-[2″,3″:4′,3′]-*β*-hydroxychalcone (**38**)		

Compound	Source	Reference
Praecansone B (**39**)		
4-Methoxylonchocarpin (**40**)	*M. pachycarpa* (SD)	Yanbei *et al*., 2019
Isobavachromene (**41**)		
3,2'-Dihydroxy-4-methoxy-4'-prenyloxychalcone (**42**)	*M. leucantha* (FT)	Uraiwan *et al*., 2018
4-Hydroxyderricin (**43**)	*M. oblate* (RT)	Deyou thesis, 2015

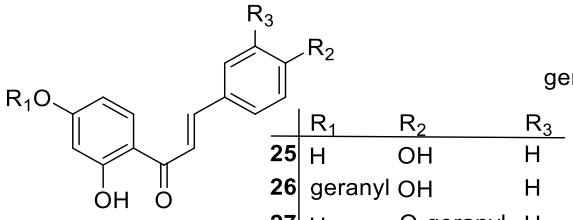

	R_1	R_2	R_3
25	H	OH	H
26	geranyl	OH	H
27	H	O-geranyl	H
28	H	H	OH

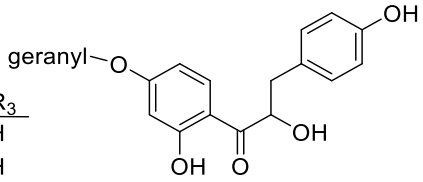

29

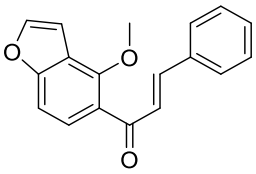

30

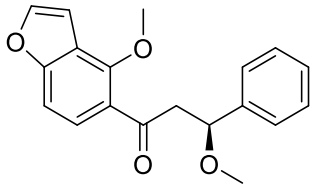

31

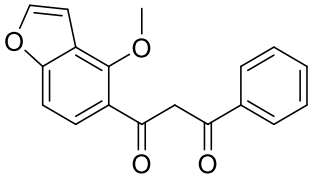

32

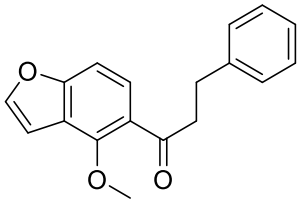

33

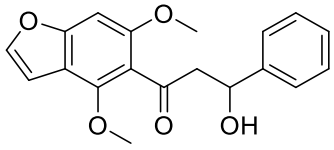

34

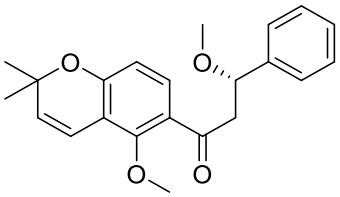

35

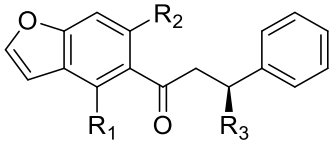

	R_1	R_2	R_3
36	OH	H	H
37	OH	H	OH
38	OMe	H	OH
39	OMe	OMe	OH

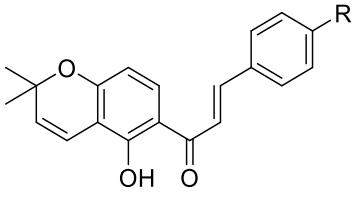

R	OMe	OH
	40	**41**

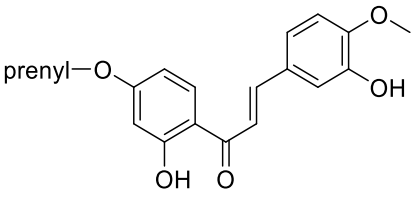

42

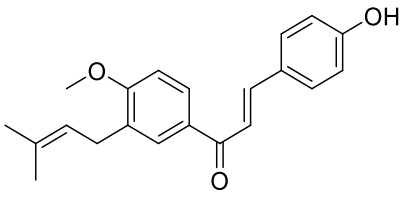

43

2.6.2 Flavan and isoflavans from *Millettia* species

Reduction of flavanones give rise to flavans with flavan-3-ol as intermediates. Flavans occur mostly as leaf surface constituents, having low natural abundance (Buckingham *et al*., 2015). There is one flavan, Tupichinol C (**44**) and one isoflavan (3s)-vestitol (**45**) reported from *M. dielsiana* (Dat *et al*., 2019) within the review period.

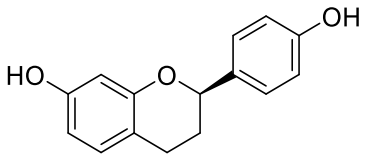

44

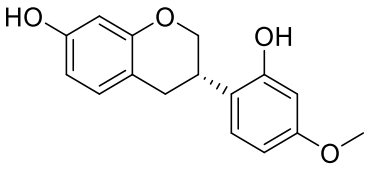

45

2.6.3 Flavanones from *Millettia* species

This sub-class is the C_2-C_3 saturated flavone by addition of hydrogen to the double bond. Figure 2.7 gives the basic skeleton with the usual numbering.

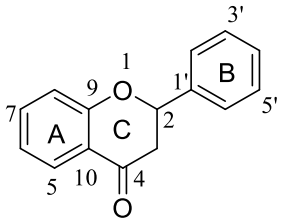

Figure 2.7: Basic structure of flavanones

Three of the reported flavanones (Table 2.9) carry an oxogeranyl substituent at C-7 (**46** and **47**) or C-4′ (**48**). Five of the flavanones (**49**, **50**, **53**, **54** and **55**) have a cyclized oxopyran ring between C-7 and C-8 apart from **53** which cyclizes through C-6. Flavanones **51** and **52** carry an uncyclized prenyl at C-8 and an oxoprenyl at C-7.

Table 2.9: Flavanones from *Millettia* species from Kenya and those isolated elsewhere between 2014 and 2019

Compound	Source	Reference
(*S*)-4′-*O*-geranyl-7-hydroxyflavanone (**46**)	*M. usaramensis* ssp. *Usaramensis* (RB)	Deyou *et al*., 2015
(2R,3R)-4′-*O*-geranyl-7-hydroxydihydroflavonol (**47**)		
7-*O*-geranyl-5-hydroxyflavanone (**48**)		
4′-Hydroxyisolonchocarpin (**49**)	*M. pachycarpa* Benth (SD)	Yanbei Tu *et al*., 2019
Dorspoinsettifolin (**50**)		
Brandisianones C (**51**)	*M. brandisiana* (RT)	Pailee *et al*., 2019

Compound	Source	Reference
7-*O*-8-bis-(3,3-dimethylallyl)-5-hydroxyflavanone (**52**)		
Brandisianones D (**53**)		
(−)-Isolonchocarpin (**54**)		
Obovatin (**55**)		

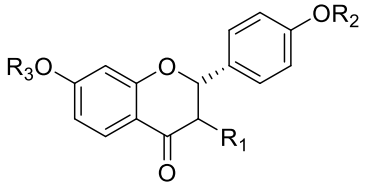

	R_1	R_2	R_3
46	H	-geranyl	H
47	OH	-geranyl	H
48	H	H	-geranyl

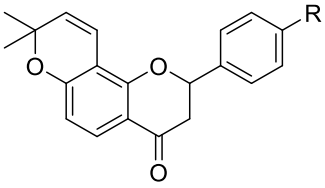

R	OH	OMe
	49	**50**

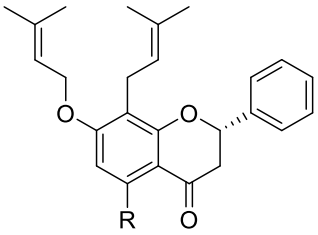

R	H	OH
	51	**52**

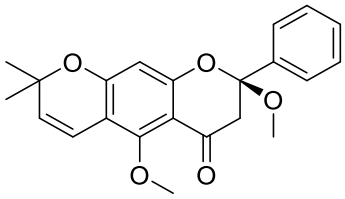

53

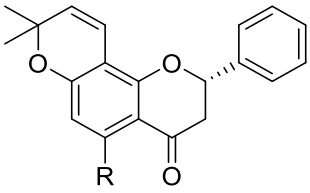

R	H	OH
	54	**55**

2.6.4 Isoflavanones from *Millettia* species

This subclass has the flavanone skeleton but with ring B attached to C-3 instead of C-2. This leads to a 3-phenylchroman scaffold arising from an aryl migration in the corresponding flavanone. Figure 2.8 shows the basic structure.

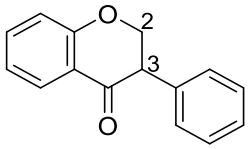

Figure 2.8: Basic structure of Isoflavanone

Few isoflavanones (Table 2.10) have been reported for this genus within the review period. Among these, the kenusanone F 7-methyl ether (**56**) from the seeds of *M. pachycarpa* Benth (Yanbei *et al*., 2019), in addition to having a cyclized oxopyran ring between C-7 and C-8, it is uniquely oxidized to an extra carbonyl at C-4′. Also millexatin K (**57**) and millexatin L (**58**) from the roots of *M. extensa* (Benth.) (Raksat *et al*., 2019) cyclises through the oxygenation of C-2 to C-2' in addition to oxo-prenylation of C-4'. Millettilone A (**59**), 3R-Claussequinone (**60**) and Pendulone (**61**) from timber of *M. pendula* (Aye *et al*., 2019).

Table 2.10: Isoflavanones from *Millettia* species from Kenya and those isolated elsewhere between 2014 and 2019

Compound	**Source**	**Reference**
Kenusanone F 7-methyl ether (**56**)	*M. pachycarpa* (SD)	Yanbei Tu *et al*., 2019
Millexatin K (**57**)	*M. extensa* (RT)	Raksat et al., 2019
Millexatin L (**58**)		
Millettilone A (**59**)	*M. pendula* timbe(TB)	Aye *et al*., 2019
3R-Claussequinone (**60**)		
Pendulone (**61**)		

*TB timber

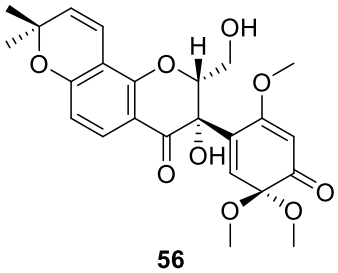

56

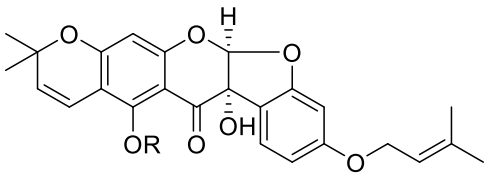

R	Me	H
	57	**58**

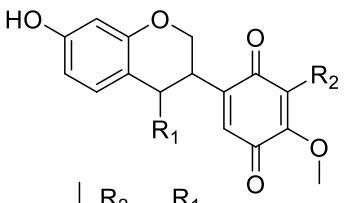

	R_2	R_1
59	OMe	H
60	H	H
61	H	OMe

2.6.5 Flavones from *Millettia* species

The chemical structure of flavones consists of two phenyl groups interconnected by three carbon atoms forming oxygenated heterocycles (González-Vallinas *et al*. 2013). They have a basic skeleton of C_6-C_3-C_6 constituting three cyclic rings A-C-B with ring B attaching through C-2 and a double bond at C-2, Figure 2.9. Flavones like other flavonoids are numbered starting with the heteroatom as in Figure 5. The known flavonoids are biogenetically oxygenated at C-7 through a

free hydroxyl, methoxyl, oxoprenyl or cyclized prenyl. The known flavones are prenylated except for **72**, **75**, **76**, **77** and **80**. The oxygenation at C-7 for flavones **62-67**, **74**, **78**, **79**, **82-85** cyclizes through C-8 into a furan ring. Flavone **81** has a unique furan ring to C-6, while compound **75** forms a new furan ring by the oxygenation at C-5 through C-6. Table 2.11 gives the flavones reported within the review period.

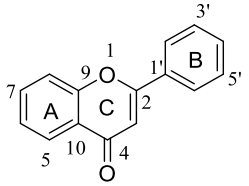

Figure 2.9: Basic structure of flavones

Table 2.11: Flavones from *Millettia* species from Kenya and those isolated elsewhere between 2014 and 2019

Compound	Source (Part)	Reference
Pubinerone (**62**)	*M. pubinervis* (TG)	Na *et al*., 2014
Karanjin (**63**)		
Kanjone (**64**)		
3,6-Dimethoxy-[2",3":7,8]-furanoflavone(**65**)		
Pongaglabrone (**66**)		
Pongapin (**67**)		
Pongaflavone (**68**)		
3,6-Dimethoxy-6",6"-dimethylchromeno-[2",3":7,8]-flavone (**69**)		
Pongachromene (**70**)		
3,6-Dimethoxy-3',4'-methylenedioxy-6",6"-dimethylchromeno-[2",3":7,8]-flavone (**71**)		
Demethoxykanugin (**72**)		
2″,2″-Dimethylpyrano-[5″,6″;7,8]-flavone (**73**)	*M. pulchra* (ST)	Xiaowei *et al*., 2015
2,2-Dimethylpyrano-[5,6,:7,8]-flavone (**74**)		
7-(4-Methoxyphenyl)-9H-furo-[2, 3-f]-chromen-9-one (**75**)	*M. ovalifolia* (SB)	Taj *et al*., 2015
3,7-Dihydroxy-2-phenyl-4H-chromen-4-one (**76**)		
4',7-Dihydroxy-3',6-dimethoxyflavonol 7-*O*-*β*-D-glucopyranoside (**77**)	*M. pachycarpa* (SD)	Yunyao *et al*., 2017
3,3'-Dimethoxyfurano-[2",3":7,8]-flavone (**78**)	*M. leucantha* (FT)	Uraiwan *et al*., 2018
Pongapinnol C (**79**)		
3,7-Dimethoxyflavone (**80**)		
Pinnatin (**81**)	*M. brandisiana* (RT)	Pailee *et al*., 2019
Brandisianones A (**82**)		
Brandisianones B (**83**)		
Lanceolatin B (**84**)		
Pongaglabol (**85**)		
6″,6″-Dimethylchromeno-[2″,3″:7,8]-flavone (**86**)		
Candidine (**87**)		
5-Methoxy-6″,6″-dimethylchromeno-[2″,3″:7,8]-flavone (**88**)		
5-Hydroxy-6″,6″-dimethylchromeno-[2″,3″:7,6]-flavone (**89**)		
5-Methoxy-6″,6″-dimethylchromeno-[2″,3″:7,6]-flavone (**90**)		

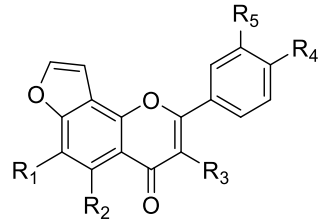

	R_1	R_2	R_3	R_4	R_5
62	H	OH	OMe	H	H
63	H	H	OMe	H	H
64	OMe	H	H	H	H
65	OMe	H	OMe	H	H
66	H	H	H	-OCH_2O-	
67	H	H	OMe	-OCH_2O-	
74	H	H	H	H	H
78	H	H	H	H	OMe
79	H	H	OMe	H	OH

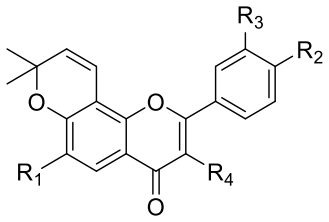

	R_1	R_2	R_3	R_4
68	H	H	H	OMe
69	OMe	H	H	OMe
70	H	-OCH_2O-		OMe
71	OMe	-OCH_2O-		OMe
73	H	H	H	H

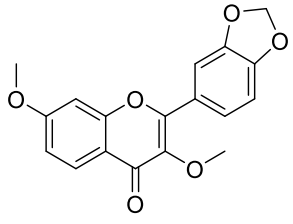

72

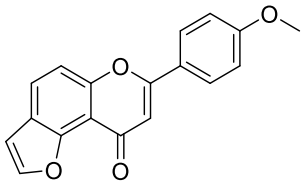

75

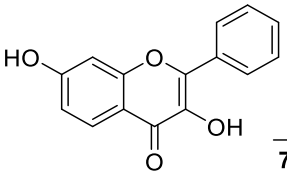

	R_1	R_2
76	OH	OH
80	OMe	OMe

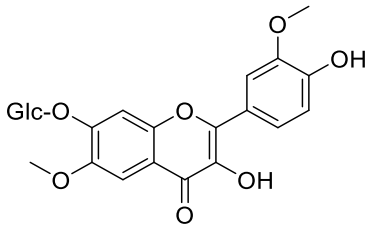

77

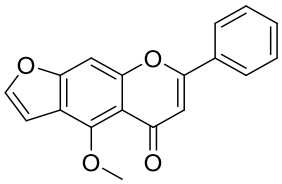

81

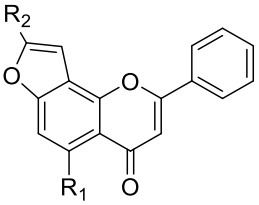

	R_1	R_2
82	OH	$C(CH_3)_2OH$
83	H	$C(CH_3)_2OH$
84	H	H
85	OH	H

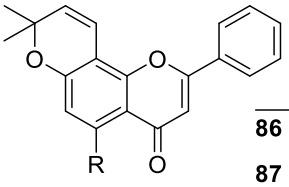

	R
86	H
87	OH
88	OMe

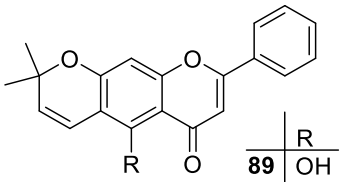

	R
89	OH
90	OMe

2.6.6 Isoflavones from *Millettia* species

Isoflavones have the basic flavone skeleton with ring B attaching through C-3, Figure 2.10. Biogenetically, they arise from flavanones by an aryl migration. They are mainly restricted to papilionoideae subfamily in leguminosae (Buckingham *et al*., 2015). This is the largest subclass of flavonoids in *Millettia* species.

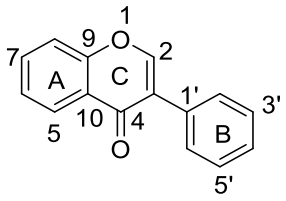

Figure 2.10: Basic structure of isoflavones

An oxocyclopyran ring between C-8 and C-9 is a common feature taking 50% of the reported isoflavones. Carbon C-4′ of isoflavones is substituted with either a methoxy or methylenedioxy or an oxoprenyl, Table 2.12. The other isoflavanoids show the usual biogenetic oxygenation on C-7 aslo at C-4′. About 80% of the isoflavanoids occur in the stem bark of the studied plants.

Table 2.12: Isoflavonoids from *Millettia* species from Kenya and those isolated elsewhere between 2014 and 2019

Compound	Source	Reference
Formononetin (**91**)	*M dura* (SP)	Yenesew *et al*., 1997a
Maximaisoflavone D (**92**)	*M dura* (SB)	Yenesew *et al*., 1996
7,2′-Dimethoxy-4′, 5′-methylenedioxyisoflavone (**93**)	*M dura* (RB)	Marco *et al*., 2017
Maximaisoflavone B (**94**)	*M oblata* ssp. *teitensis* (SB)	Deyou *et al*., 2017
7,3′-Dimethoxy-4′,5′-methylenedioxyisoflavone (**95**)	*M dura* (SB)	Derese *et al*., 2003
Erythrin-A (**96**)	*M dura* (SB)	Yenesew *et al.*, 1996.
Calopogoniumisoflavone A (**97**)		
Jamaicin (**98**)	*M. usaramensis* ssp *usaramensis* (SB)	Yenesew *et al.,* 1998
Durmillone (**99**)	*M dura* (SP)	Yenesew *et al*., 1996
	(RB)	Marco *et al*., 2017
Durallone (**100**)	*M dura* (SP)	Yenesew *et al*., 1996
6-Methoxycalopogonium isoflavone (**101**)	*M dura* (SP)	Yenesew, *et al.*, 1997b
Isoerythrin-A-4′-(3-methylbut-2-enyl)ether (**102**)	*M dura* (SP)	Yenesew *et al*., 1996
	M dura (SB)	Derese *et al*., 2003
	M dura (RB)	Marco *et al*., 2017
6-Demethyldurallone (**103**)	*M dura* (SP)	Yenesew *et al*., 1996
Calopogonium isoflavone B (**104**)	*M dura* (RB)	Marco *et al*., 2017
Isojamaicin (**105**)	*M. usaramensis* ssp *usaramensis* (SB)	Yenesew *et al.,* 1998
Maximaisoflavone-H (**106**)	*M dura* (SB)	Yenesew *et al*., 1996
Predurallone (**107**)	*M dura* (SP)	Yenesew *et al*., 1996
7-Hydroxy-8,3′,4′-trimethoxylisoflavone (**108**)	*M dura* (RB)	Marco *et al*., 2017
Nordurlettone (**109**)	*M dura* (SB)	Derese *et al*., 2003
8-*O*-methylretusin (**110**)	*M oblata* ssp. *teitensis* (SB)	Derese *et al*., 2014
7-hydroxy-8,3′,4′-trimethoxyisoflavone (**111**)	*M. usaramensis* ssp *usaramensis* (RB)	Deyou *et al*., 2015
Maximaisoflavone J (**112**)	*M oblata* ssp. *teitensis* (SB)	Derese *et al*., 2014
4′-prenyloxyderrone (**113**)		

Compound	Source	Reference
Barbigerone (**114**)	*M. usaramensis* ssp *usaramensis* (SB)	Yenesew *et al*., 2003b
Maximaisoflavone G (**115**)	*M. usaramensis* ssp *usaramensis* (SB)	Yenesew *et al*., 1998
Mildurone (**116**)	*M oblata* ssp. *teitensis* (SB)	Derese *et al*., 2014
Wistin (**117**)	*M. leucantha* (RB)	Derese *et al*., 1994
Ferrugone (**118**)	*M. dura* (SP)	Yenesew *et al*., 1997
Norisojamaicin (**119**)	*M. usaramensis* ssp *usaramensis* (SB)	Yenesew *et al*., 1998, Carren *et al*., 2014
7,2′,5′-Trimethoxy-3′,4′-methylenedioxyisoflavone (**120**)	*M. oblata* ssp. *teitensis* (LV)	Deyou *et al*., 2017
8-Prenylmilldurone (**121**		
Millesianin C (**122**)	*M. dielsiana* (ST)	Ye *et al*., 2014
Ichthynone (**123**)		
Hydroxy-6-methoxy-3-4-methylenedioxy-8-3-3-dimethylallyl-isoflavone (**124**)		
Millesianin H(**125**)		
Millesianin D (**126**)		
Millesianin I (**127**)		
Alpinumisoflavone (**128**)	*M. thonningii* (SD)	Ayine *et al*., 2016; Harrison *et al*., 2019
O,O-dimethylalpinumisoflavone (**129**)		
4′-*O*-methylalpinumisoflavone (**130**)		
5-*O*, methyl-4-*O*-(3-methylbut-2-en-1-yl)alpinumisoflavone (**131)**	*M. thonningii* (SD)	Harrison *et al*., 2019
Pachyloisoflavone B (**132**)	*M. pachyloba* (ST and LV)	Na *et al*., 2017
Milletenol A (**133**)	*M. pachycarpa* (SD).	Yan *et al*., 2019
Cis-3′′,4′′-dihydro-3′′,4′′-dihydroxylonchocarpusone (**134**)		
7-Hydroxy-2′,4′,5′-trimethoxyisoflavone (**135**)		
Derrisisoflavone G (**136**)	*M. aboensis* (RT)	Ajaegbu *et al*., 2018
Derrisisoflavone L (**137**)		
Derrisisoflavone M (**138**)		
Mildiside A (**139**)	*M.dielsiana* (ST)	Dat *et al*., 2019
Ononin (**140**)		
Millexatin G (**141**)	*M. extensa* (LV and RT)	Raksat *et al*., 2019
Millexatin H (**142**)		
Isoauriculasin (**143**)		
2′-Deoxyisoauriculatin (**144**)		
Isoauriculatin (**145**)		
Millexatin B (**146**)		
Millexatin I (**147**)		
Millexatin D (**148**)		
Auriculasin (**149**)		
Auriculatin (**150**)		
Scandenone (**151**)		
Millipurone (**152**)		
Millexatin A (**153**)		
6,7-Dimethoxy-3′,4′-methylenedioxy-8-(3,3-dimethylallyl)isoflavones (**154**)	*M. ferruginea* (SD)	Deyou and Jang, 2018

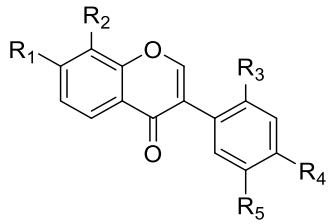

	R_1	R_2	R_3	R_4	R_5
91	OH	OMe	OMe	OMe	H
92	-OCH_2O-		H	OMe	OMe

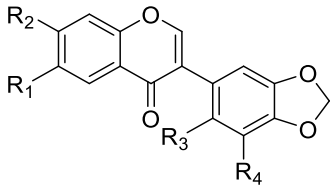

	R_1	R_2	R_3	R_4
93	H	OMe	OMe	H
94	H	prenyl	H	H
95	H	OMe	H	OMe

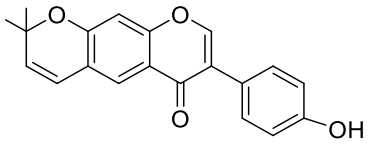

96

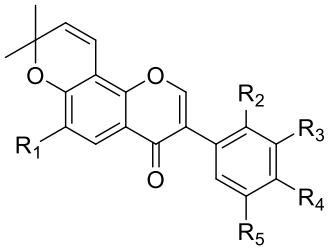

	R_1	R_2	R_3	R_4	R_5
97	H	H	H	OMe	H
98	H	OMe	H	-OCH_2-	
99	OMe	H	H	-OCH_2-	
100	OMe	H	H	OMe	OMe
101	OMe	H	H	OMe	H
102	H	H	H	O-prenyl	H
103	OH	H	H	OMe	OMe
104	H	H	-OCH_2-		H
105	H	H	-OCH_2-		OMe

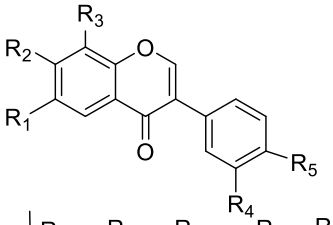

	R_1	R_2	R_3	R_4	R_5
106	H	-OCH_2O-		H	OMe
107	OMe	OH	prenyl	OMe	OMe
108	H	OH	OMe	OMe	OMe
109	H	H	OH	H	O-prenyl

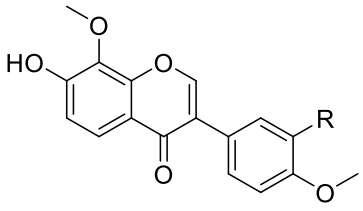

	110	**111**
R	H	OMe

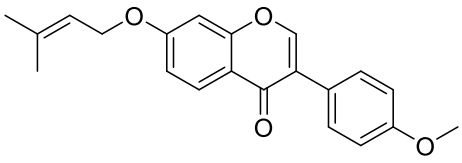

112

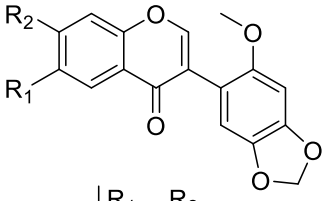

	R_1	R_2
115	H	OH
116	OMe	OMe

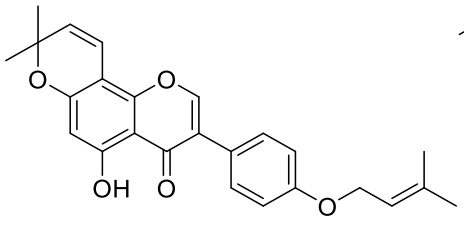

113

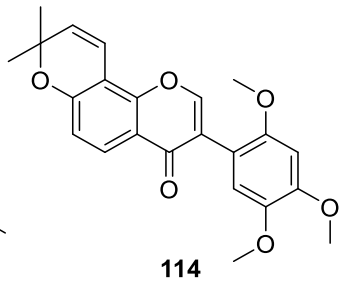

114

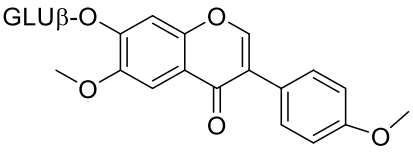

117

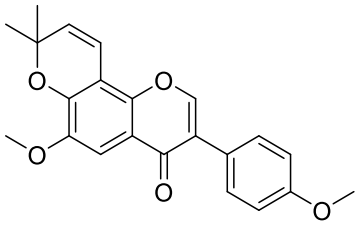

118

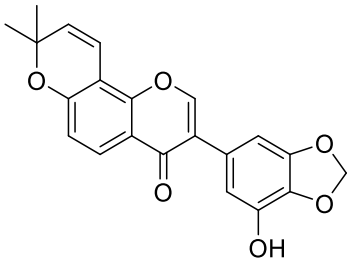

119

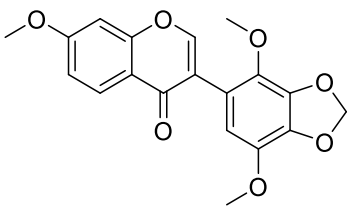

120

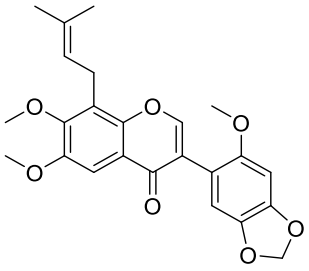

121

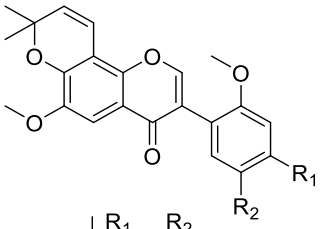

	R_1	R_2
122	OMe	OMe
123	-OCH_2O-	

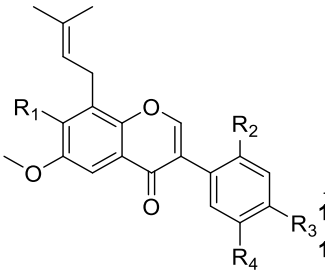

	R_1	R_2	R_3	R_4
124	OH	H	-OCH_2O-	
125	OH	H	OMe	H
126	OH	OMe	-OCH_2O-	
127	OH	OMe	OMe	OMe

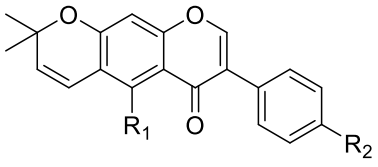

	R_1	R_2
128	OH	OH
129	OMe	OMe
130	OH	OMe
131	OMe	O-prenyl

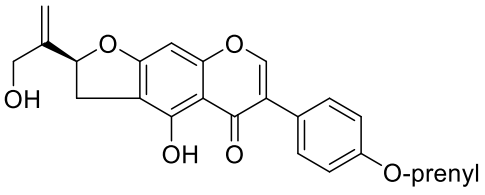

132

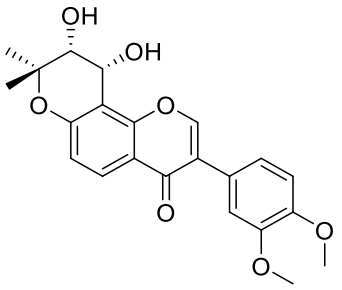

133

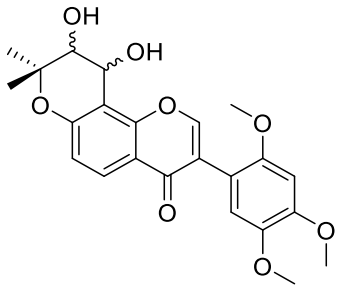

134

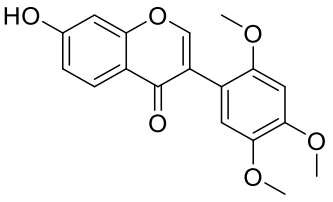

135

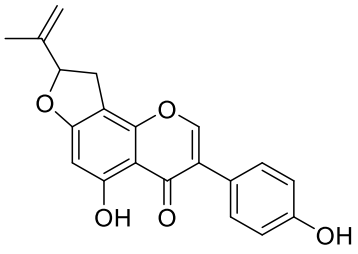

136

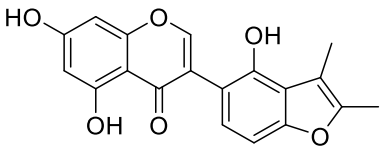

137

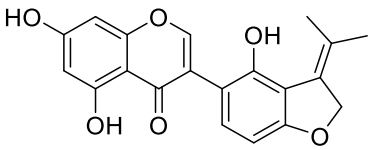

138

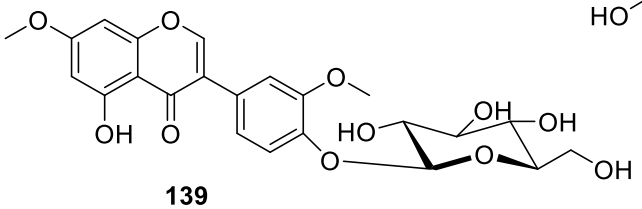

139

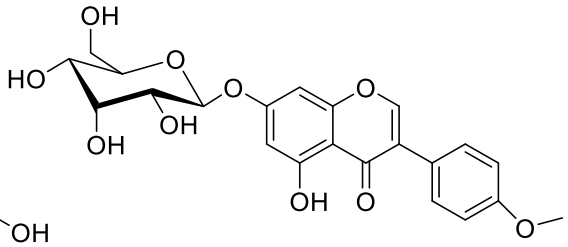

140

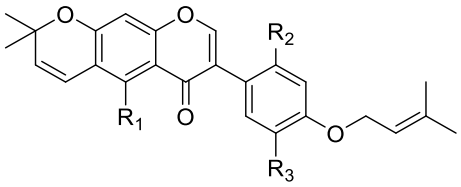

	R_1	R_2	R_3
141	OH	OMe	OMe
142	OMe	H	OH
143	OH	H	OH
144	OH	H	H
145	OH	OH	H
146	OMe	OH	H

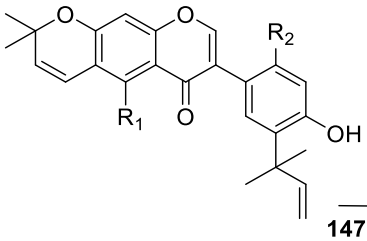

	R_1	R_2
147	OH	H
148	OMe	OH

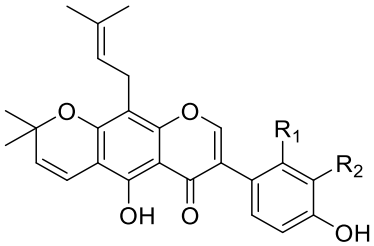

	R_1	R_2
149	H	OH
150	OH	H
151	H	H

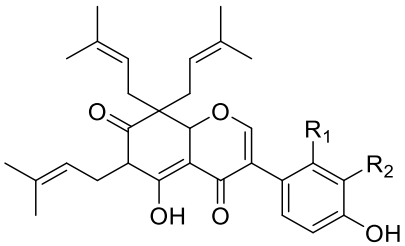

	R_1	R_2
152	H	OH
153	OH	H

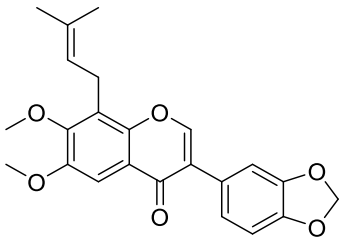

154

2.6.7 Pterocapanoids from *Millettia* species

The pterocarpans are modified 4-hydroxy isoflavans which cyclise to give an additional ring C. It arises from the ether linkage between 4- and 2'- positions of the corresponding isoflavan. The basic structure, Figure 2.11 displays the cyclisation alongside common numbering scheme used.

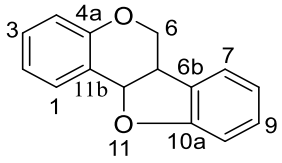

Figure 2.11: Basic structure of pterocarpans

There are two pterocarpans **166** and **167** reported from *M. dura* (RB) and *M. micans* (Marco *et al*., 2017) respectively, Table 2.13. Six pterocapans are reported between 2014-2019, Table 2.13. They have comparable substitution pattern in ring A and D except for **157** which is unsubstituted at C-8. Oxygenation at C-3 is either through a hydroxyl or a methoxyl substituent where as a heterocyclic substitution at C-8 and C-9 is a common feature in these compounds.

Table 2.13: Pterocarpans from *Millettia* species from Kenya and those isolated elsewhere between 2014 and 2019

Compound	Source	Reference
Perocarpine (**155**)	*M. speciose* (RT)	(Zhao *et al*., 2017)
Medicarpin (**156**)		
Homopterocarpin (**157**)		
3-*O*-Prenylmaackiain (**166**).	*M. dura* (RB)	Marco *et al*., 2017
Micanspterocarpan (**167**).		
Pisatin (**168**)	*M. pachycarpa* Benth (SD)	Yunyao *et al*., 2017
Pachylobin A (**169**)	*M. pachyloba* (ST & LV)	Na *et al*., 2017
9-Hydro-3,8- dimethoxyl pterocarpan (**170**)	*M. aboensis* (RT)	Ajaegbu *et al*., 2018
Maackiain (**171**)		
(−)-Medicarpin (**172**)	*M. brandisiana* (RT)	Pailee *et al*., 2019
(−)-Maackiain (**173**)		
Secundiflorol I (**174**)	*M. pendula* (TB)	Aye *et al*., 2019
3,8-Dihydroxy-9-methoxypterocarpan (**175**)		
3,10-Dihydroxy-7,9-dimethoxypterocarpan (**176**)		
Erycristagallin (**177**)	*M. extensa* (RT)	Raksat *et al*., 2019

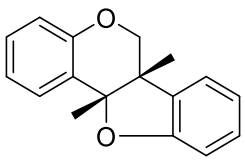

155

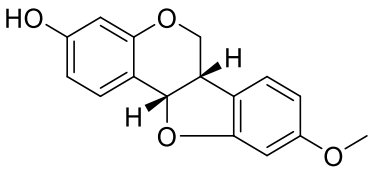

156

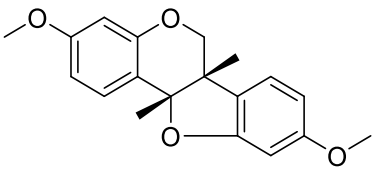

157

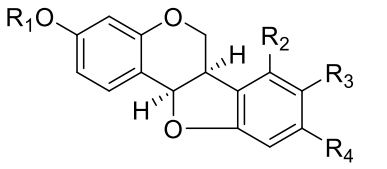

	R_1	R_2	R_3	R_4
158	prenyl	H	-OCH_2O-	
159	H	OMe	OMe	OMe

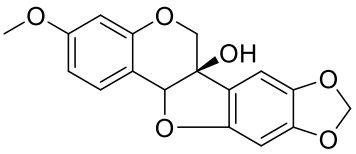

160

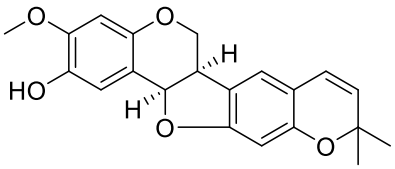

161

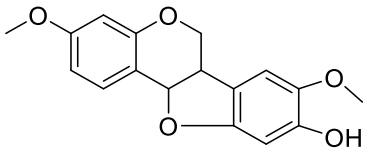

162

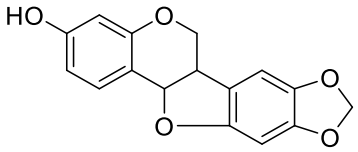

163

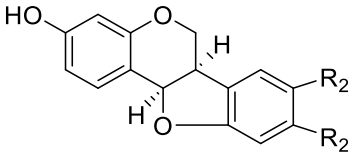

	R_1	R_2
164	H	OMe
165	-CH_2O-	

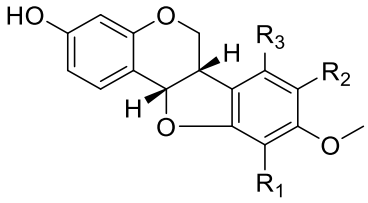

	R_1	R_2	R_3
166	H	OMe	H
167	H	OH	H
168	OH	H	OMe

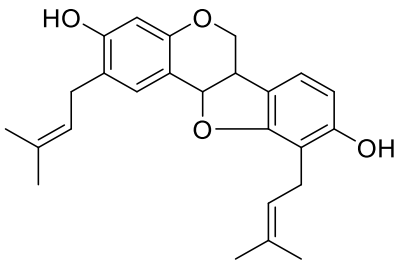

169

2.6.8 Rotenoids from *Millettia* species

This constitutes the second largest class of flavonoids from this genus. In addition to the skeleton of isoflavonoids, these compounds have an extra carbon in their structure which gives rise to an extra ring D. The basic structure is therefore tetracyclic arising from oxidative cyclization of 2'-methoxyisoflavone. The numbering is modified from the known heterocylic numbering system that starts with the heteroatom as shown in Figure 2.12.

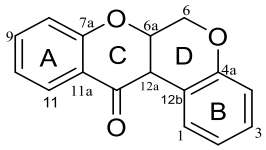

Figure 2.12: Basic structure of rotenoid

Most of the rotenoids reported from *Millettia* species are C-11 deoxygenated, Table 2.14. They all have a methylenedioxy substituent to ring B except for compounds **170**, **171**, **174**, and **181-183** as well as being hydroxylated at C-12a except for **174**, **175**, **183, 186, 188, 192, 195, 196, 198, 199, 205,** and **206**. A methylenedioxy substituent between C-2 and C-3 is common as well to these rotenoids.

Table 2.14: Rotenoids from *Millettia* species from Kenya and those isolated elsewhere between 2014 and 2019

Compound	**Source**	**Reference**
(±)-Deguelin (**170**)	*M. dura* (SD)	Yenesew *et al*., 1997b
Tephrosin(**171**)		
Millettone (**172**)		
(-)-Millettosin (**173**)		
(±)-Rotenone (**174**)		
6a,12a-Dehydromillettone (**175**)	*M. usaramensis* ssp *usaramensis* (SB)	Yenesew *et al*., 2003b; 1998
(+)-Usararotenoid-A (**176**)		
(+)-Usararotenoid-B (**177**)		
Usararotenoid-C (**178**)		
12α-Hydroxy-12-dihydro-(+)-usararotenoid-A (**179**)		
(+)-12a-Epimillettosin (**180**)		
12a-Hydroxymunduserone (**181)**	*M. oblata* ssp. *teitensis* (LV)	Deyou *et al*., 2017
Munduserone (**182**)		
6a,12a-Dehydrodeguelin (**183**)		
Oblarotenoid A (**184**)		
Oblarotenoid B (**185**)		
Oblarotenoid C (**186**)		
Oblarotenoid D (**187**)		
Caeruleanone A (**188**)	*M. caerulea* (LV)	Bueno *et al*., 2014
Caeruleanone B (**189**)		
Caeruleanone C (**190**)		
12a-Hydroxyisomillettone (**191**)		
11-Hydroxy-6a,12a-dehydrodeguelin(**192**)		
11-Hydroxytephrosin (**193**)	*M. caerulea* (FT)	Bueno *et al*., 2014
Cis-(6aβ,12aβ)-hydroxy- rotenone (**194**)		
Pongarotene (**195**)	*M. pinnata* (SD)	Perumalsamy *et al*., 2015
Erythynone (**196**)	*M. caerulea* (FT)	Bueno *et al*., 2014
12a-Hydroxyerythynone (**197**)		
12a-Deoxyusarotenoid-A (**198**)	*M. usaramensis* ssp *usaramensis* (SB)	Bosire *et al*., 2014
6a,12a-Dehydrousarotenoid-A (**199**)		
(−)-Villosinol (**200**)	*M. brandisiana* (RT)	Pailee *et al*., 2019
2-*O*-demethyltephrosin (**201**)	*M. pachycarpa* (SD)	Yunyao *et al*., 2017
(−)-12α-Hydroxyrotenone (**202**)	*M. brandisiana* (RT)	Pailee *et al*., 2019
Trans-4′,5′-dihydro-4′,5′ dihydroxytephrosin (**203**)	*M. pachycarpa* (SD)	Yan *et al*., 2019
Cis-4′,5′-dihydro-4′,5′-dihydroxytephrosin (**204**)		
Millettiaosas A (**205**)	*M. speciose* (RT)	Zhao *et al*., 2017
Millettiaosas B (**206**)		

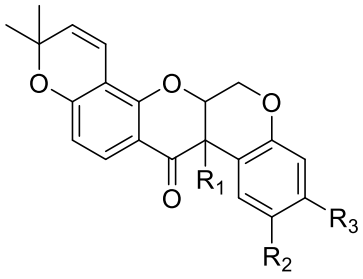

	R_1	R_2	R_3
170	H	OMe	OMe
171	OH	OMe	OMe
172	H	-OCH_2O-	
173	OH	-OCH_2O-	

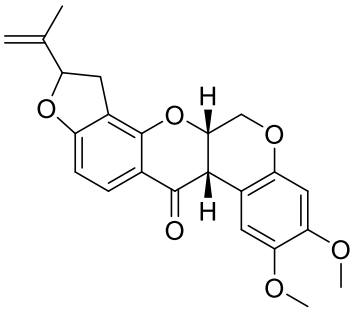

174

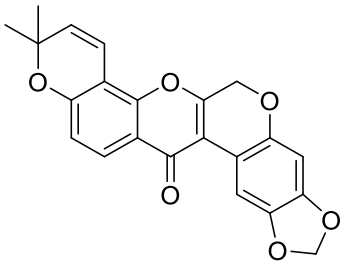

175

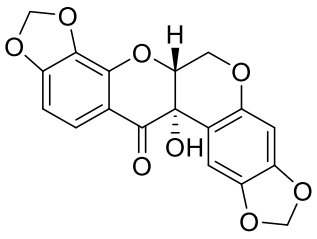

176

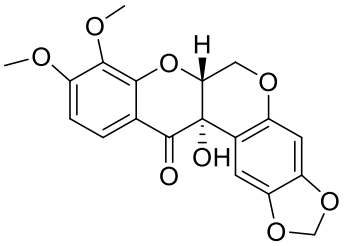

177

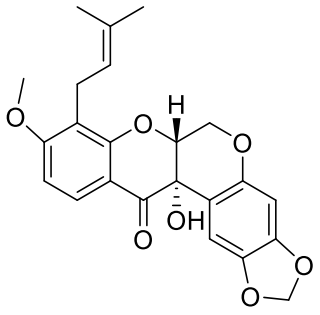

178

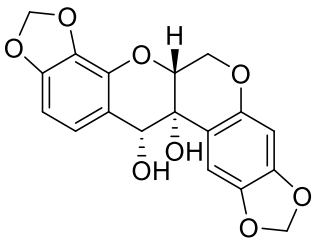

179

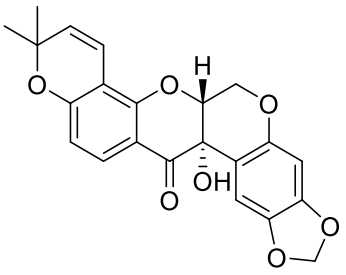

180

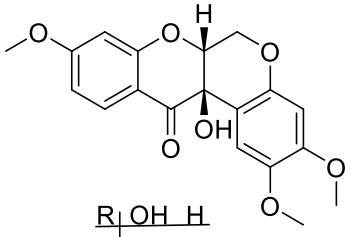

R OH H

181 182

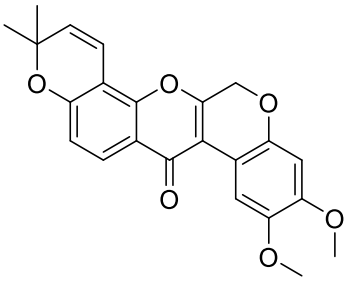

183

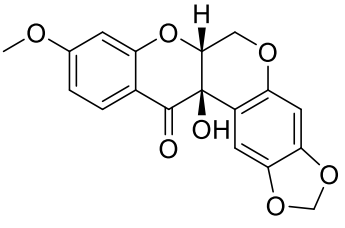

184

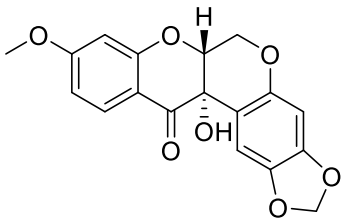

185

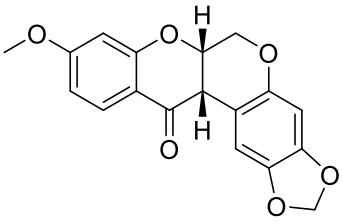

186

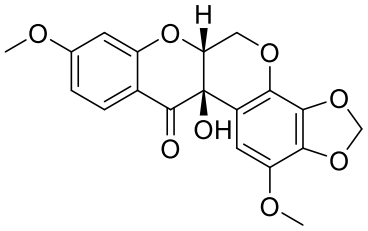

187

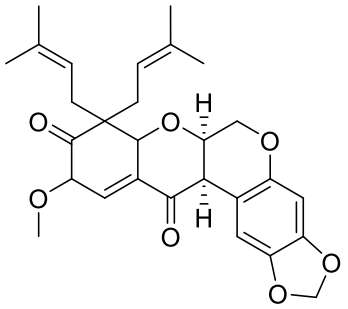

188

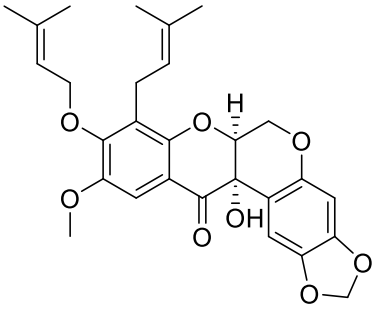

189

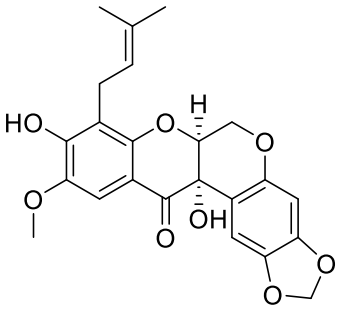

190

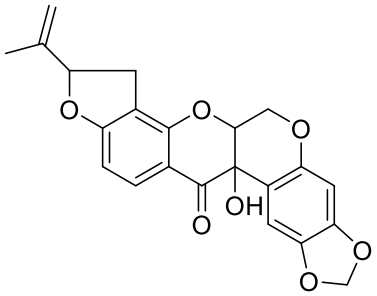

191

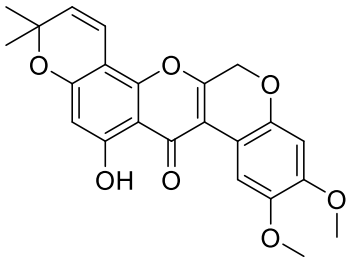

192

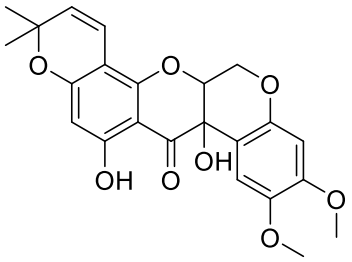

R	OMe	H
	193	**200**

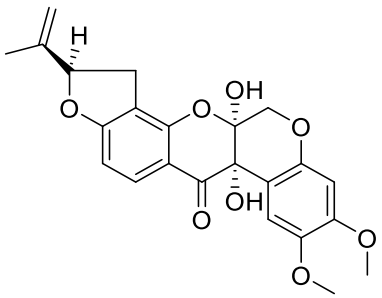

194

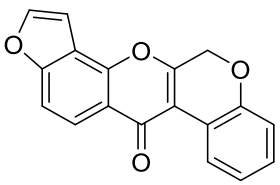

195

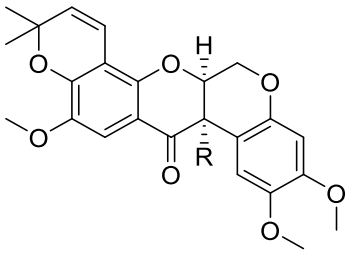

R	H	OH
	196	**197**

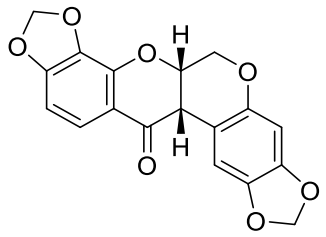

198

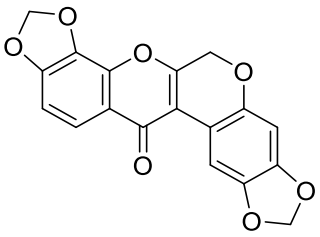

199

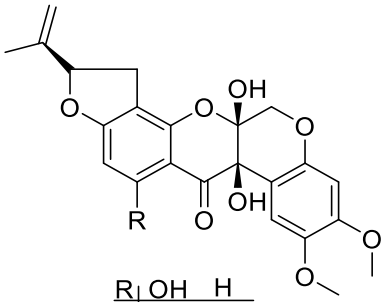

R	OH	H
	201	**202**

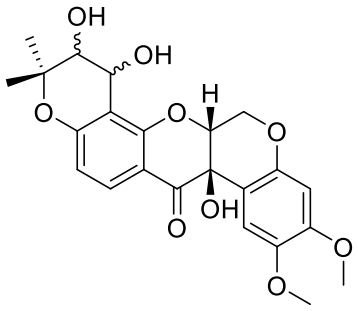

	trans	*cis*
	203	**204**

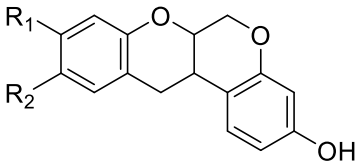

	R_1	R_2
205	OCH_2O	
206	OMe	H

2.6.9 Terpenoids from *Millettia* species

There are 16 terpenoids reported within the review period from *M. usaramensis* ssp *usaramensis*, *M. speciose* and *M. macrophylla*, Table 2.15. Eight of these are penta-cyclic, seven are tetra-cyclic and the other one is tri-cyclic. Compounds **209**, **213**, **215** and **216** are glycosilated. All of these terpenoids have either a ketonic or a free hydroxyl group.

Table 2.15: Terpenoids from *Millettia* species from Kenya and those isolated elsewhere between 2014 and 2019

Compound	Source	Reference
Lupeol (**207**)	*M. usaramensis* ssp *usaramensis* (SB)	Yenesew *et al*., 1998
Shionone (**208**)	*M. speciose* (RT)	Zhao *et al*., 2017
Stigmasterol 3-*O*-*β*-*D*-glucoside (**209**)		
7-carbonyl-*β*-sitosterol (**210**)		
7-*β*-hydroxylathyrol (**211**)		
Stigmasterol (**212**)		
β-daucosterol (**213**)		
Lupeolcaffeate (**214**)		
Pedunculoside (**215**)		
Glycyrrhizic acid (**216**)		
Pyracrenic acid (**217**)		

Compound	Source	Reference
Rotundicacid (**218**) *β*-sitosterol acetate (**219**) Lupenone (**220**) Lupeol (**221**) Stigmaastenon (**222**)e	*M. macrophylla* (SB)	Zingue *et al*., 2019

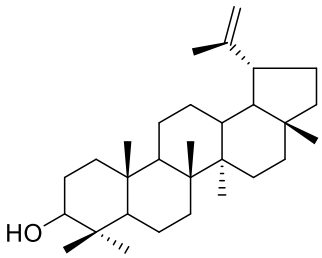

207

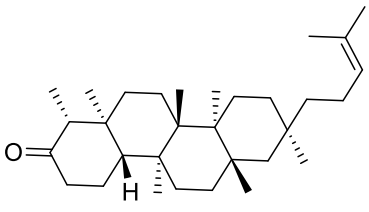

208

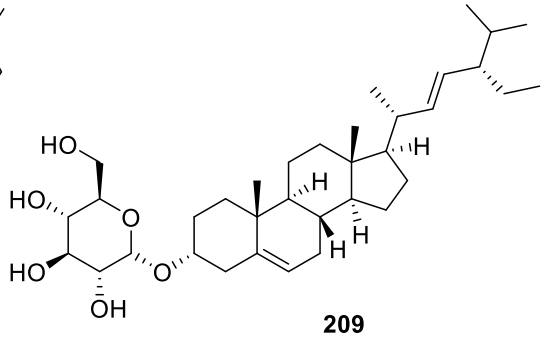

209

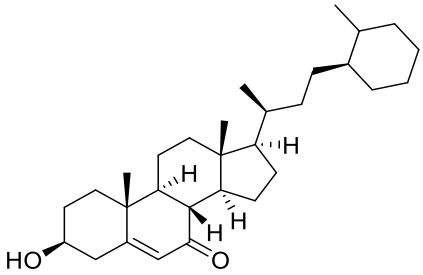

210

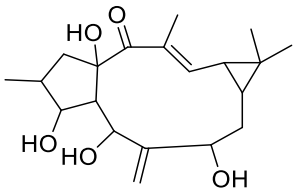

211

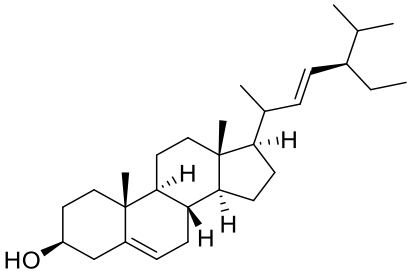

212

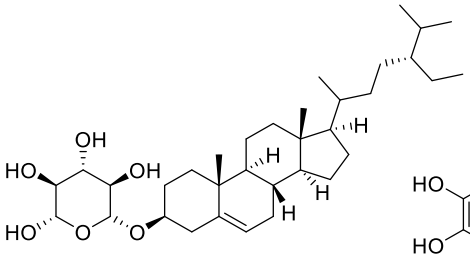

213

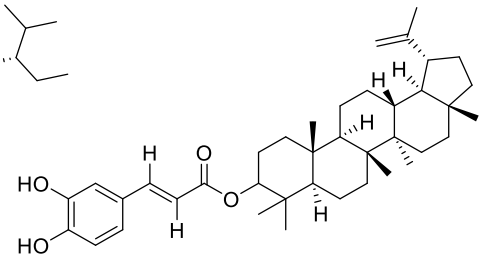

214

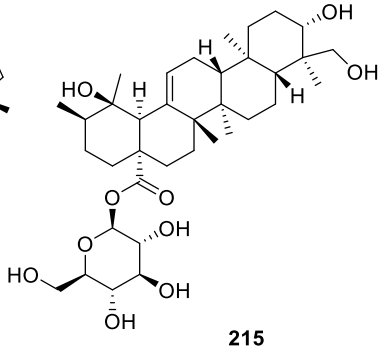

215

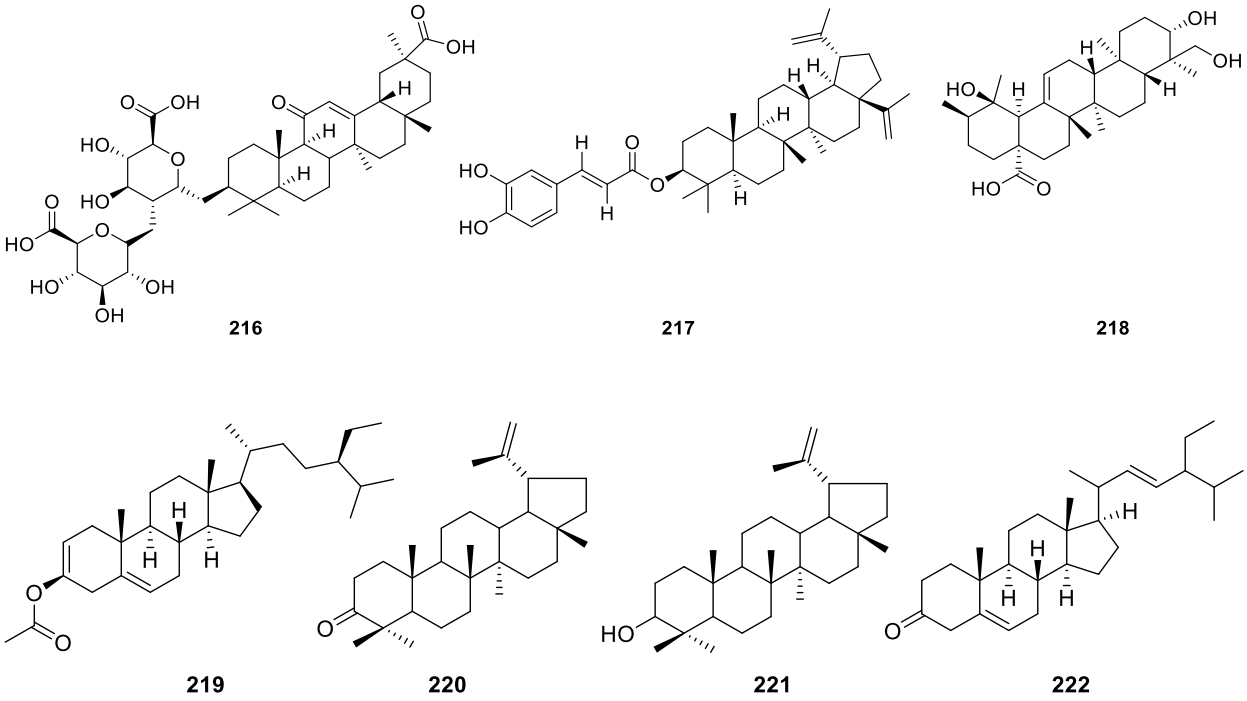

2.6.10 Alkaloids from *Millettia* species

There are few alkaloids from this genus. Table 2.16 shows those reported in the review period. Two of these **223** and **225** are benzophenantharidine alkaloids while **224** and **226** are simple alkaloids.

Table 2.16: Alkaloids from *Millettia* species from Kenya and those isolated elsewhere between 2014 and 2019

Compound	Source	Reference
Berberine (**223**)	*M. pachycarpa* (SD)	Yunyao *et al*., 2017
N-methylcytisine (**224**)	*M. speciose* (RT)	Zhao *et al*., 2017
Sanguinarine (**225**)		
Erythroidine (**226**)		

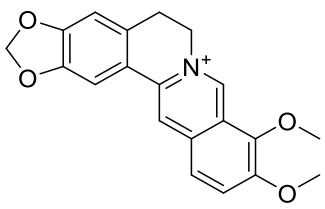

223

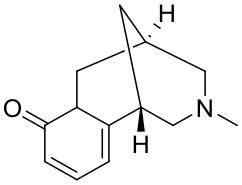

224

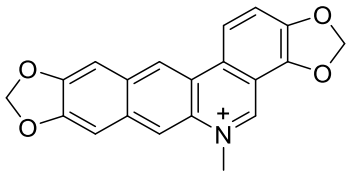

225

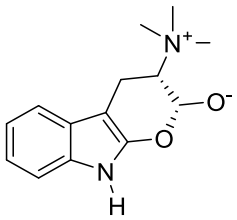

226

2.7 Pharmacological activities of *Millettia*

The medicinal importance of *Millettia* is due to the presence of numerous compounds majority of which are flavonoids (Rahman *et al*., 2015). The wide biological application including larvicidal, insecticidal, antifungal, antibacterial, antiviral, anti-inflammatory, antioxidant, antiplasmodial and anticancer is based on the structural diversity of compounds this genus offers.

2.7.1 Antiplasmodial activity

Antiplasmodial studies of most compounds isolated from the *Millettia* species from Kenya have been done exclusively by Abiy *et al*., 2003 and Derese *et al*., 2014 as in Table 2.17 below. Out of all the tested compounds, 4′-*O* –geranyloxyisoliquiritigenin **(27)** had the highest activity of **IC_{50}**, 8.7 and 10.6 µM against D6 and W2 *plasmodium* strains respectively.

Table 2.17: Anti-plasmodial activities of flavonoids from Kenyan *Millettia* species

Flavonoids	**IC_{50} in (µM)**		**Reference**
	D6	**W2**	
Maximaisoflavone H **(3)**	38.7±0.6	45.6±0.1	Derese *et al*., 2004
Maximaisoflavone B **(6**)	58.9±1.5	33.3±1.7	
Jamaicin **(13)**	45.6±2.3	46.6±1.2	
7,2′-Dimethoxy-4′,5′-methylenedioxyisoflavone **(14)**	49.4±0.2	51.5±0.7	
Mildurone **(15)**	40.7±2.2	50.4±0.8	
Calopogoniumisoflavone A**(16)**	51.5±5.7	45.8±3.2	
Durmillone**(1)**	25.1±1.6	37.3±1.8	
Isoerythrin A 4′-(3-methyl-2-butenyl)ether(**17)**	21.8±0.55	24.7±0.8	
Isojamaicin **(18)**	39.0±0.8	48.7±1.1	
Nordurlettone**(19)**	51.4±1.7	20.8±1.5	
7,3′-Dimethoxy-4′,5′-methylendioxyisoflavone **(20)**	56.3±0.8	42.8±0.6	
Durallone **(21)**	49.9±2.4	32.7±0.4	
6-Methoxycalopogonium isoflavone A**(22)**	35.4±1.9	53.3±1.7	
Deguelin **(23)**	21.1	13.8±4.5	

Millettone **(24)**	64.1	48.9±12.9	
Usararotenoid-A **(25)**	66.6	60.7	Yenesew *et al*, 2003
12a-Epimillettosin **(26)**	22.2	19.4	
4′-*O* –Geranyloxyisoliquiritigenin **(27)**	8.7	10.6	
Barbigerone **(88)**	27.0	27.3	
Usararotenoid C **(29)**	25.8	70.1	
6a,12a-Dehydromillettone **(30)**	33.3	39.1	
Chloroquine **(11)**	0.094	0.009	
Quinine **(9)**	0.209	0.044	

2.7.2 Anticaner activity

Apigenin (**21**) a known flavonoid exhibits significant anti-tumor activity in numerous cancer cells like breast, colon, lung (Chen *et al*. 2016), prostate and pancreatic cancers, and being hepatocarcinogenesis (Shan et al. 2017). Pubinerone (**25**) from the twigs of *M. pubinervis* shows toxicity of IC_{50} > 40μM towards human leukemia, hepatoma, lung carcinoma, breast adenocarcinoma and colon adenocarcinoma cell lines (Na *et al*., 2014). The *cis*-(6aβ,12aβ)-hydroxyrotenone (**137**) plus rotenone (**117**) isolated in fruits of *M. caerulea* (Bueno *et al*., 2014) demonstrated strong cytotoxicities of IC_{50}, 0.1 and 0.3μM against HT-29 human colon cancer cells respectively (Bueno *et al*., 2014). Caeruleanone C (**133**) exhibited potent mitochondrial transmembrane potential (MTP) inhibition with IC_{50}, 0.07μM. While caeruleanones B (**132**) and C (**133**) prospectively triggered quinone reductase with inhibition values equaling 0.9 and 1μM with respective minimal host cell toxicities of IC_{50} ≈35 and 28μM (Lynette *et al*., 2014). *Millettia pulchra* flavonoids are potentially protective ingredients in myocardial ischemia owing to their negative effects on inotrope, hence lessening myocardial oxidative harm and variation of gene expression linked with apoptosis (Huang *et al*., 2015). Deyou *et al*., 2015 reported cytotoxic activities of compounds isolated from *M. usaramensis* ssp. *usaramensis* (RB) against MDB-MB-231 cells as usararotenoid A (**119**) 87.3μM, millettosin (**46**) 61.7μM, 12a-epimillettosin (**123**) 100.7μM, usararotenoid C (**121**) 25.7μM and 4′-*O*-geranylisoliquiritigenin (**149**) 125.5μM (Deyou *et al*., 2015b).

Compounds isolated from fruits of *M. leucantha* Kurz, 3,2'-dihydroxy-4-methoxy-4'-prenyloxychalcone (**165)** exhibited moderate cytotoxicity of IC_{50} value 51μM towards MCF-7 cell line and no toxicity for the Vero cells, pongamol (**155**) presented toxicity for both KB NCI-H187 as well as Vero cell with respective IC_{50}'s of 63.6, 114.4 and 28.4μM, while 3,6-dimethoxyfurano-

[2",3":7,8]-flavone (2**8**) was only cytotoxic against KB cell line, IC_{50} of 110.2 μM (Uraiwan *et al*., 2018). Obovatin (**63**) isolated from *M. brandisiana* (roots) showed toxicity against MOLT-3 of 69.7 ± 28.9, HepG-2 of 100.4 ± 7.2μM, A549 of 113.4 ± 15.4μM, HuCCA-1 of 122.7 ± 24.2μM and HeLa of 123.3 ± 0.02μM (Pailee *et al.*, 2019).

Literature has demonstrated the potential of compounds from *Millettia* as anticancer agents and illustrates the continued research on the genus for both antimalarial and anticancer agents. On this basis, it was important to study *M. dura, M. leucantha* and *M. lasiantha* in anticipation for an effective antimalarial and or anticancer. Nature harboring the threatening pathogens, still offers the solution to eliminate them.

2.8 Chemotaxonomic relationship between *M. dura* and *ferruginea*

It was noted that *M. dura* is taxonomically related to the *M. ferruginea* endemic to Ethiopia (Dagne *et al*., 1991). with two subspecies, *darassana* and *ferruginea* (Dagne *et al*.,1989). On this basis, Dagne *et al*., 1991 undertook a comparative phytochemical survey to distinguish these two taxa. It was found that *M. ferruginea* was richer in isoflavanoids than *M. dura.* The distribution of the flavonoids in the stem and roots of the two taxa varied remarkably (Table 2.15). *M. ferruginea* elaborates C-5 oxygenated flavanoids a feature which was absent in *M. dura*. On the other hand, *M. dura* showed some C-8 oxygenation, a feature not observed in *M. ferruginea.* At that point, a differentiating conclusion was drawn basing on the fact that C-8 oxygenated isoflavones, like maximaisoflavone H (**106**) was only found in *M. dura* and while C-5 oxygenated isoflavones, including 5-hydroxydurmillone (**231**), pre-5-methoxydurmillone (**233**) and 7-hydroxy-5,6-dimethoxy-3′,4′-methylenedioxyisoflavone (**230**) only occurred in *M. ferruginea.*

This study having looked at the flowers, leaves and stem bark of *M. dura*, it was important to make a detailed survey on the literature of the two plants and make a more informed chemotaxonomic conclusion. Table 2.18 below gives an overview from the previous study.

Table 2.18: Distribution of flavonoids in different parts of *M. dura*, *M. ferruginea* ssp. *darassana* and *M. ferruginea*.

Compound	Rereference	*M. dura*	*M. ferruginea*	
			ssp. *darassana*	ssp. *ferruginea*
Chalcones				
4′-*O*-Geranylisoliquiritigenin (**1**)	Dagne, et al., 1991		+ (RB)	
4-Hydroxylonchocarpin (**227**)		+ (SB)		+ (SB)
4-Hydroxyderricin (**43**)		+ (SB)		
Flavanone				
4′-Hydroxyisolonchocarpin (**49**)	Dagne *et al*., 1991			+ (SB)
Isoflavones				
Barbigerone (**114**)	Dagne *et al*., 1991			+ (SD)
Calopogoniumisoflavone A (**97**)			+ (SD)	+ (SD)
Calopogoniumisoflavone B (**104**)				+ (SB)
7,2′-Dimethoxy-4′, 5′-methylenedioxyisoflavone (**93**)		+ (RB)		
Durlettone (**228**)	Ollis *et al*., 1967; Dagne *et al*., 1991	+ (SD)		
Durmillone (**99**)		+ (SD)	+ (SD)	+ (SD)
Ferrugone (**118**)			+ (SB, SD)	+ (SB, SD)
7-*O*-Geranylformononetin (**229**)	Dagne *et al*., 1991		+ (RB)	
7-Hydroxy-5,6-dimethoxy-3′,4′-methylenedioxisoflavone (**230**)	Dagne *et al*., 1989		+ (SB)	
Ichthynone (**123**)	Ollis *et al*., 1967	+(SB)	+ (SB)	
Isojamaicin (**105**)	Dagne *et al*., 1991	+ (SB)		+ (SB)
Jamaicin (**98**)	Dagne *et al*., 1989			+ (SB)
Maximaisoflavone B (**94**)	Dagne *et al*., 1991	+ (SB)		
Maximaisoflavone H (**106**)		+ (SB)		
5-Methoxydurmillone (**231**)			+ (SB)	+ (SB)
Milldurone (**116**)	Ollis *et al*., 1967	+ (SD)		
Nordurlettone (**109**)	Dagne *et al*., 1991	+ (SB)	+ (SB)	
Prebarbigerone (**232**)				+ (SD)
Predurmillone (**233**)			+ (SB)	
Preferrugone (**234**)			+ (SD)	
Rotenoids				
Deguelin (**170**)	Ollis *et al*, 1967	+ (SD)		+ (SD)
6a,12a-Dehydrodeguelin (**183**)		+ (SD)		
12-Hydroxy millettone (**235**)	Dagne *et al*., 1991			
12a-Hydroxyrotenone (**236**)			+ (SD)	
Millettone (**172**)	Ollis *et al*, 1967; Dagne *et al*., 1991	+(SD)		
Millettosin (**173**)		+ (SD)		
Rotenone (**174**)		+ (SD)		+ (SD)
Tephrosin (**171**)		+ (SD)	+ (SD)	+ (SD)
Pterocarpene				
Flemichapparin B (**237**)	Dagne *et al*., 1989		+ (SB)	

From Table 2.18, it could clearly be seen that, the following; millettone (**172**), 12-hydroxymillettone (**235**), durlettone (**228**), 6a,12a-dehydrodeguelin (**170**), millettosin (**173**), milldurone (**116**) only occurred in the seeds of *M. dura* while 4-hydroxyderricin (**43**), maximaisoflavone B (**94**), maximaisoflavone H (**106**) as well as 7,2′-dimethoxy-4′, 5′-methylenedioxyisoflavone (**93**) were found in its bark only. From the seeds of *M. darrasana*; were; preferrugone (**234**), predurmillone (**233**) and nordurlettone (**109**), and in the bark was found; ichthynone (**123**), 7-hydroxy-5,6-dimethoxy-3′,4′-methylenedioxisoflavone (**230**), flemichapparin B (**237**), 4′-*O*-geranylisoliquiritigenin (**1**) and 7-*O*-geranylformononetin (**229**). In the bark of *M. Ferruginea*; calopogoniumisoflavone B (**104**), 4-hydroxylonchocarpin (**227**), 4′-hydroxyisolonchocarpin (**49**) and isojamaicin (**105**) were found yet prebarbigerone (**232**) only found in the seeds of this sub species. This categorization, supports the reported chemotaxonomic difference between the three taxa. Basing on the subsequent studies on these species, an elaborated chemotaxonomic review will be discussed in chapter four.

From Table 2.18, there are flavonoids that have not been covered in Tables 2.14-2.16. These additional flavonoids arising from the distribution table of flavonoids are outside those covered within the literature review period. These are shown in figure 2.13.

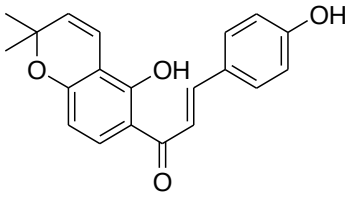

227

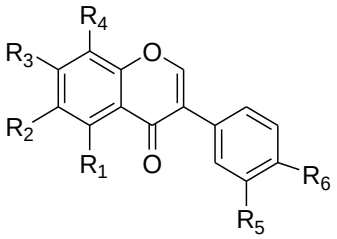

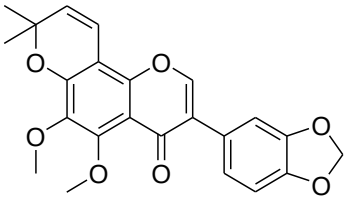

231

	R_1	R_2	R_3	R_4	R_5	R_6
228	H	H	OMe	H	H	O-Prenyl
229	H	H	O-Geranyl	H	H	OMe
230	OMe	OMe	OH	H	OCH_2O	

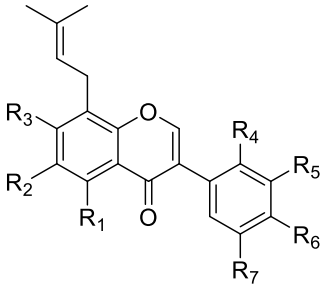

	R_1	R_2	R_3	R_4	R_5	R_6	R_7
232	H	H	Me	OMe	H	OMe	OMe
233	H	OMe	H	H	OCH_2O		H
234	H	H	H	OMe	OCH_2O		OMe

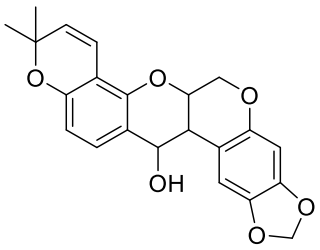

235

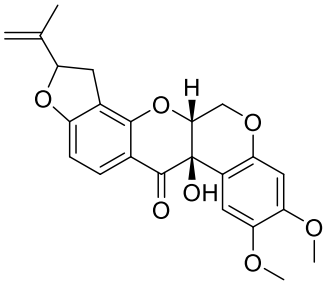

236

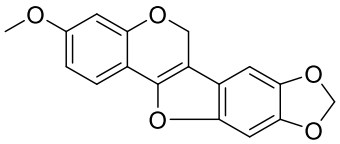

237

Figure 2.13: Additional compounds from *M. dura* and *M. ferruginea* (outside review period)

CHAPTER THREE
MATERIALS AND METHODS

3.1 General experimentation

All solvents used for chromatography were purified by fractional distillation over a glass distillation column. Extracts and eluents were concentrated under vacuum on an IKA RV10 digital rotary evaporator (5-280 rpm) with a digital heating water bath (IKA HB10, 20 - 180°C). Wet column chromatography was done using silica gel 60 (60-120 mesh, India). Investigative shrill coat chromatography was done over silica gel 60 F_{254} (Merck, Germany) prior-coated aluminium sheets. The TLC spots were viewed under UVGL 58 handheld UV-lamp (254-365nm). Gel percolation being executed over Sephadex LH-20. Purification was done using preparative rotors coated with silica gel 60 G/F254 loaded on a Chromatotron (7924T, 24V, 200 rpm, USA), with an initial purge of 250-1000ml/min and then reducing to 10-15ml/min. Nuclear magnetic resonance spectrometry was used to analyze the samples using a Varian Avance (AV500) and Brucker spectrometers, referencing with the residual solvent signal. The spectra were processed using Topspin (3.5pl 7) and MestRenova (11.04) software. Infra Red spectral measurements were taken from Bruker Tensor-27 FT-IR spectrometer (Cricket, Harrick Scientific). Meanwhile, HRESIMS peaks were recorded using an LTQ orbitrap spectrometer (Thermo Scientific, USA).

3.2 Plant material

Millettia leucantha was collected from Mua hills in Machakos in September 2016. *Millettia dura* was collected from the grounds of Chiromo campus, University of Nairobi (UoN) in January 2017. While *Millettia lasiantha* was collected in February 2018 from Mombasa. The identification and collection of all the plant material was done by the guidance of Mr. Patrick Chalo Mutiso, a plant specialist from the herbarium at the School of Biological Sciences, UoN.

3.3 Extraction and purifications

Powdered plant material of the diferent parts of the three *Millettia* species studied were extracted and chromatographed as described in the preeding subsections.

3.3.1 Extraction and purification of compounds from the flowers of *M.* dura

Air dried and pulverized flowers of *M. dura* (1.8kg) were extracted (4 x 24hrs) by cold percolation using six litres of dichloromethane/methanol (1:1 v/v). A total of 209.38g (11.6% yield) of the crude sample extract was obtained after concentration. Fractionation of the crude (150g) was done by wet chromatography over 600g of silica gel in a glass column and eluted gradiently using hexane/ethyl acetate. The portions that eluted at 5% ethyl acetate in hexane were combined and passed through Sephadex LH - 20 (dichloromethane/methanol (1:1)) obtaining compounds **97** (285mg) and **98** (57mg). The fractions that eluted with 10% ethyl acetate in hexane yielded compounds **99** (54.1 mg) and **228** (26.3mg) after passing it over Sephadex LH - 20 (dichloromethane/methanol (1:1)). Crystallization (CH_2Cl_2/MeOH) of the fractions eluting with 15% of ethyl acetate in hexane yielded compound **100** (177mg), the mother liquor was loaded on Sephadex LH - 20 (dichloromethane/methanol (1:1)) yielding 79.6mg of **123** plus **101** (52.6mg). The fractions eluting with 20% ethyl acetate in hexane gave **227** (21.9mg) by recrystallization in dichloromethane/methanol. Compound **91** (29.6mg) was obtained using Chromatotron (Hexane: EtOAC: MeOH, 6:3:1) from fraction that eluted with 30% ethyl acetate in hexane.

3.3.2 Extraction and purification of compounds from the seeds of *M.* dura

The air dried and ground seed pods of *M. dura* (2.5kg) were exhaustively extracted by cold percolation using eight liters of dichloromethane/methanol (1:1v/v). This gave 238.13g (9.5% yield) of dark brown extract when concentrated on a rotary evaporator. A portion (200g) of the extract was fractionated by chromatography over silica gel using hexane in increasing percentages of ethyl acetate. The fractions that came out with 3% EtOAC in hexane, loaded on a Chromatotron (Hexane: EtOAC, 6:4) afforded compounds **172** (19.7mg), **173** (10.5mg) and more of Compound **97** (2.6mg). Compound **171** (16.4mg) and more of **98** (2.5mg) were gotten from those fractions that came out with 5% EtOAC in hexane. The fractions that eluted at 15% were subjected to size exclusion chromatographic separation using Sephadex LH - 20 (dichloromethane/methanol (1:1)) producing more of compounds **101** (8.7mg) and **100** (5.2mg).

3.3.3 Extraction and purification of compounds from the stem bark of *M.* dura

Four kilograms (4kg) of the dry and ground bark of the stems of *M. dura* were extracted by cold percolation (6x24hrs) using 12 liters of dichloromethane/methanol (1:1v/v). This gave 410.98g

(10.3% yield) of a brown extrude after concentration. A fraction (300g) of this extrude was fractionated by column chromatography on silica gel using hexane in growing percentages of ethyl acetate. Fractions that eluted at 3% EtOAC in hexane were run through Sephadex LH - 20 (dichloromethane/methanol (1:1)) providing **102** (123.1mg) which was recrystallized in (CH_2Cl_2/MeOH). The last fractions from the Sephadex LH - 20 column were combined and loaded onto Chromatotron (Hexane: EtOAC: MeOH, 6:3:1) yielding compound **112** (91.4mg) and more of compound **97** (159.7mg). The early fractions that eluted at 5% solidified and was filtered; the residue was run over a Chromatotron (Hexane: EtOAC: MeOH, 6:3:1) to give more of compounds **101** (88.4mg) and **98** (39.0mg). The filtrate was loaded on Sephadex LH - 20 (dichloromethane/methanol (1:1)) offering 166.4mg of compounds **114** and more of compound **99** (61.5mg). The later fractions that eluted at 5% were loaded onto the Chromatotron (Hexane: EtOAC: MeOH, 6:3:1) and yielded compound **170** (344.5mg) and more of **171** (363.7mg). From the fractions that eluted at 7% EtOAC in hexane, compounds **118** (194.1mg) was obtained after running it on the Chromatotron (Hexane: EtOAC: MeOH, 6:3:1). Fractions that eluted at 15% EtOAC in hexane yielded compound **92** (12.7mg) after passing it through Sephadex LH - 20 (dichloromethane/methanol (1:1)). Compound **115** (62.0mg) was obtained from fractions that eluted at 20-25% EtOAC after purification over Sephadex LH - 20 (dichloromethane/methanol (1:1)).

3.3.4 Extraction and purification of compounds from the leaves of *M. leucantha*

Dry and pulverized leaves of *M. leucantha* (400g) were extracted (4x12hrs) with one litre of methanol in each extraction. A brown crude extract, 70.3g (17.6% yield) was obtained after concentration. A fraction, 63.8g of the extract was purified by column chromatography using 600g of silica gel and eluted using dichloromethane in increasing percentage of methanol. The fractions that eluted with 10% MeOH in CH_2Cl_2, gave a yellow powder of **229** (65mg). The fractions that eluted with 50% MeOH in CH_2Cl_2 gave a yellowish solid (90mg). A portion of 80mg was purified over sephadex LH-20 using MeOH/CH_2Cl_2 (1:1v/v) to give 34.2mg of **230** and more of **229** (21mg). The fraction that eluted with 70% MeOH in CH_2Cl_2 gave 38mg of a dirt white solid. This was loaded over sephadex LH-20 running with MeOH/CH_2Cl_2 (1:1v/v) to afford 16.2mg of compound **231** and 18.1mg of compound **232** as white solids.

3.3.5 Extraction and purification of compounds from the roots of *M. leucantha*

The air dried and ground roots (3.0kg) of *M. leucantha* were extracted (8x12 hours) with six litres of CH_2Cl_2: MeOH to afford 308.31g of a brown extract (10.3% yield) after concentration. 150g of the extract was adsorbed on 200g of silca gel (60-230 mesh merck-Germany grade) and loaded in column containing 800g silca gel slurry. Gradient elution started with 100% hexane in increasing percentage of ethylacetate. Fractions eluting with 5% EtOAC in hexane gave 5.7mg of compound **237** as a white solid. The eluent at 7% EtOAC in hexane yielded a yellowish powder (43.6mg) of compound **233** on solidification. The fractions that eluted with 10% EtOAC in hexane produced yellow solids of compound **234** (33.6mg) on solidification in methanol. The fractions that eluted with 15% ethylacetate in hexane, purification over sephadex LH-20 to yield compounds **235** (19.7mg) and **236** (25mg) as yellowish solids.

3.3.6 Extraction and purification of compounds from the leaves of *M. lasiantha*

Dry and ground leaves (0.62kg) of *M. lasiantha* were extracted with three litres of CH_2Cl_2: MeOH and gave a dark green extract (99.28g = 16.0% yield). 90g of the extract were adsorbed on 100g of silica gel (60-230 mesh merck-Germany grade) and loaded over 500g slurry of silca gel in a glass column. Fractionation started with 100% hexane in increasing amounts of ethylacetate. Combined portions eluting between 20-40% EtOAC in hexane were purified on sephadex, flashing with CH_2Cl_2: MeOH (1:1 v/v). 30mg of this portion was loaded on a chromatotron (6:3:1 H: E: M) to give a yellow solid of compounds **229** (17.2mg) and **230** (10.2mg). Fractions that eluted with 60-80% EtOAC in hexane after passing it over sephadex gave light yellow powder of **238** (75mg) and the fractions at 90% after sephadex gave white solid of compound **231** (12mg).

3.3.7 Extraction and purification of compounds from the stems of *M. lasiantha*

1.68kg of dry powdered stems of *M. lasiantha* were extracted using five liters of CH_2Cl_2: MeOH (1:1 v/v) and gave 121.3g (7.2% yield) of a dark brown extract. Loaded 100g of the extract adsorbed on 100g of silica gel onto 500g slurry of silica in a column. Elution started with 100% ethyl acetate. The fractions that eluted with 20% EtOAC in hexane gave a mixture of compounds **239** and **240** (6mg) and white solids of **235** (7mg). The fractions that eluted with 30% EtOAC in hexane after sephadex was loaded on a chromatotron (6:3:1 Hexane: EtOAC: MeOH) to give white solids of **91** (9mg).

3.3.8 Extraction and purification of compounds from the roots of *M. lasiantha*

Dry and ground powdered roots (300g) of *M. lasiantha* were extracted with ethyl acetate (1 litre) and gave a dark brown extract (15g). A fraction of this extract (10g) was fractionated on silica gel (70-230mesh, 63-200μm) using petroleum ether (PE) in increasing concentrations of ethyl acetate. The fractions that eluted with 15% EtOAC in PE gave white fluffy crystals of **91** (2.7mg). The early fractions that eluted at 30% EtOAC in PE on crystalization in CH_2Cl_2 gave white fluffy crystals of **241** (3.1mg) and the later fractions gave white crystals of **242** (2.3mg). While a white powder of **243** (5.3mg) solidified from fractions that eluted with 20% EtOAC in PE.

3.4 Biological tests

Crude extracts and pure compounds were subjected to antiplasmodial and cytotoxicity assays as described in the subsequent subsections.

3.4.1 *In vitro* antiplasmodial activity

A semi-automated micro-dilution test technique (Desjardins *et al*. 1979) which determines the compounds capability to constrain assimilating [G-3H] hypoxanthine by malaria parasite was employed (O'Neill *et al*., 1985). The parasites were cultured by a method earlier described by (Trager and Jensen 1976). Both chloroquine sensitive and resistant plasmodium species were used. Parasites were cultured in closed thermoses at 37°C, 3% O_2, 5% CO_2 and 92% N_2 environment having a pH of 7.4 (Ayuko *et al*. 2009), with enhanced heat deactivated 10% humanoid serum and erythrocytes to attain a 3% haematocrit. On attainment of ring stage, parasites were synchronized with 5% sorbitol and tested at 0.4% parasitemia passage into 96-well plates. Stock solutions of compounds were prepared at 1mg/ml in DMSO adulterated by RPM1640 to attain 0.2% DMSO and tested in triplicate as done by (Desjardins *et al*. 1979). Equivalent amounts of DMSO were taken to be negative controls while 1.1μM artemisinin served as positive control. The cultures were then incubated for 48 hours at 37°C. Thereafter, individual wells were pulsed with 25 μL of cultured medium having 0.5 μCi [G-3H]-hypoxanthine (Ayuko *et al*. 2009) and the plates were then incubated for another 18 hours. Contents of every plate were reaped onto glass fibre filters,

washing carefully using distilled water and then after drying, measuring radioactivity by scintillation counter.

3.4.2 Cytotoxicity assay

DMSO was used as the solvent for all tested compounds which was prior kept at −20°C. Cell viability was measured using a 3-(4,5-dimethylthiazol-2-yl)-2,5-diphenyltetrazolium bromide (MTT) assay. A 96-well microtiter plate with 4×10^3 cells was seeded before drug application. After culturing overnight, different amounts (0.039–100µmol/l) of the compounds to be tested were then added to the cells and then incubating for 72 hours. Negative controls were drug-free cells. Thereafter, adding 10µl of MTT solution (5mg/ml) to the individual wells which were nurtured to 37 °C for another 4 hours. 100µl of a solubilization buffer (10% SDS in 0.01mol/l HCl) was added and then allowed to incubate overnight. Cell viability was determined in each well the following day. Absorbance at A_{570nm} was measured to evaluate the cellular enzymes reduction of tetrazolium salt into an insoluble formazan dye. The percentage of viable cells was computed from the formular:

$$\% \text{ of viable cells} = \frac{A_{Treated}}{A_{Control}} \text{ x } 100$$

Obtaining data from three independent experiments enabled calculation of standard deviation (Atilaw *et al*., 2017).

3.5 Spectroscopic data of the compounds

Formononetin **(91)**

Obtained as dirt white needlelike crystals. NMR data found in Table 4.8, Appendix 1.

Maximaisoflavone-D (**92)**

Obtained as white crystals. NMR data found in Table 4.17, Appendix 2.

Maximaisoflavone-B (**94**)

Obtained as colorless crystals. NMR data in Table 4.14, Appendix 3.

Calopogoniumisoflavone A (**97**)

Obtained as white UV active (254 and 365 nm) solid. NMR data Table 4.1, Appendix 4.

Jamaicin (**98**)

Obtained as white crystals and its NMR data given in Table 4.2, Appendix 5

Durmillone (**99**)

Obtained as a white solid. NMR data in Table 4.3, Appendix 6.

Dullarone (**100**)

Obtained as white needlelike crystals. NMR data Table 4.4, Appendix 7.

6-Methoxycalopogonium isoflavone A (**101**)

Obtained as white fluffy like solid. NMR data, Table 4.9, Appendix 8.

Isoerythrin-A-4′-(3-methylbut-2-enyl)ether (**102**)

Obtained as a light weight white powder. NMR data Table 4.13, Appendix 9.

Barbigerone (**114**)

Obtained as white needle crystals. NMR data, Table 4.16, Appendix 10.

Maximaisoflavone G (**115**)

Obtained as dirt white solid. See NMR data in Table 4.18, Appendix 11.

Ferrugone (**118**)

Obtained as need-like crystals. NMR data Table 4.15, Appendix 12.

Ichthynone (**123**)

Obtained as white crystals. NMR data, Table 4.7, Appendix 13.

Kaempferol (**227**)

Obtained as yellow needle crystals. NMR data Table 4.5, Appendix 18.

4, 2′-Dihydroxy-4′-methoxy chalcone (**228**):

Obtained as a light brown gum. NMR data, Table 4.6, Appendix 19.

Deguelin (**170**)

Compound (**170**) was isolated as a white solid. NMR data found in Table 4.19, Appendix 14.

Tephrosin (**171**)

Obtained as a brown oily compound. NMR Table 4.12, Appendix 15.

Milletone (**172**)

Obtained as colorless needle like crystals. NMR table 4.10, Appendix 16.

Milletosin (**173**)

Obtained as colorless needle like crystals. NMR data, Table 4.11, Appendix 17.

Chrysin (**229**)

Obtained as a yellowish solid. NMR data given in Table 4.20, Appendix 20.

Apigenin (**230**)

Obtained as a yellowish solid. NMR data listed in Table 4.21, Appendix 21.

Chrysin-*7-O-β-D*-glucoside (**231**)

Obtained as a yellowish solid. NMR data tabulated in Table 4.22, Appendix 22.

Genkwanin (**232**)

Obtained as a yellowish solid. NMR data found in Table 4.23, Appendix 23.

6,7,4'-Trimethoxyflavone (**233**)

Obtained as a yellowish solid. NMR data as given in Table 4.24, Appendix 24.

Taxasin (**234**)

Obtained as a yellowish solid. NMR data recorded in Table 4.25, Appendix 25.

6,7,4'-Trimethoxyisoflavone (**235**)

Obtained as a yellowish solid. NMR data record in Table 4.26, Appendix 26.

Paraben acid (**236**)

Obtained as a yellowish solid. NMR data values given in Table 4.27, Appendix 27.

Maackiain (**237**)

Obtained as a yellowish solid. NMR data Table 4.28, Appendix 28.

Luteolin (**238**)

Obtained as white crystals. NMR data Table 4.29, Appendix 29.

Geneistein (**239**)

Genistein was obtained as white solid. The NMR data tabulated in Table 4.30, Appendix 30.

Isoliquiritigenin (**240**)

Light brown gum. NMR data found in Table 4.31, Appendix 31.

8,3-dihydroxy-7,9-dimethoxycoumestan (Trivial name Lascoumestan) (**241**)

White solid UV λmax(MeOH) = 254, 304 and 346nm, IR (neat) υ max 3367, 2988, 2360, 1718, and 1625/cm. ESI-HRMS molecular ion, $[M+H]^+$ at m/z = 329.0654 (cal. 329.0656), for molecular formula $C_{17}H_{12}O_7$. NMR data found in Table 4.32, Appendix 32.

7,5′-dihydroxy-6′,4′-dimethoxycoumaronochromone (**242**)

This compound was gotten as white non-crystalline solid. The HRESIMS spectrum showed $[M+H]^+$ at *m/z* = 328.0587 (calcd 328.0583) corresponding to $C_{17}H_{12}O_7$. NMR data recorded in Table 4.33, Appendix 33.

Genistein-7-*O*-glucoside (or Genistin) (**243**)

White solid UVλmax 242, 246, 326nm, ESIRMS $[M+H]^+$ m/z 433.1 for $C_{21}H_{20}O_{10}$. NMR data as given in Table 4.34, Appendix 34.

CHAPTER FOUR
RESULT AND DISCUSSION

4.1 General

In this study, secondary metabolites from *Millettia dura* (flowers, seeds and stem bark), *Millettia leucantha* (leaves and root bark) and *Millettia lasiantha* (leaves, stem and roots) were isolated and characterized. Chromatographic techniques were used in the isolation of the compounds and characterization was based on NMR, MS, IR and UV spectroscopic techniques. A total of 51 compounds mainly flavonoids were identified in this study. Biological evaluation of some of the compounds and extracts was done for antiplasmodial activities and cytotoxicity for anticancer properties. The discussions in the following subsections give a detailed account of the study and results obtained.

4.2 Compounds isolated and characterized from *Millettia dura*

Majoriy of the secondary metabolites isolated from this species were isoflavones chacterized if the preceeding subsections.

4.2.1 Characterization of compounds from the flowers of *Millettia dura*

The flowers of *M. dura* gave nine metabolites consisting of one flavonol, one chalcone and seven prenylated isoflavones were isolated and characterized. These included calopogoniumisoflavone-A (**97**), jamaicin (**98**), durmillone (**99**), dullarone (**100**), kaempferol (**227**), 4,2′-dihydroxy-4′-methoxychalcone (**228**), ichthynone (**123**), formononetin (**91**) and 6-methoxycalopogoniumisoflavone-A (**101**). Thi is the primary report of the flavonol, kaempferol (**227**) plus chalcone 4,2′-dihydroxy-4′-methoxychalcone (**228**) from *Millettia* (Buyinza *et al*., 2019) and it's the first report of the other compounds from the flowers of *M. dura*.

4.2.1.1 Calopogonium isoflavone-A (97)

Compound **97** was obtained as a white solid. The presence of an oxyolefinic methine proton δ_H 7.90 (*s*, 1H, H-2,) and carbon signal δ_C 151.9 (in range 150.6-155.4 ppm), the olefinic quaternary carbon δ_C 124.6 (in the range 122.0-126.1 ppm) and the carbonyl carbon δ_C 176.0 (in the range

174.2-181.2 ppm) in the ^{13}C NMR were characteristic of a heterocyclic ring C of an isoflavone (Agrawal, 1989).

The NMR spectra gave characteristic peaks for two substituents. That is, the overlapping methyl protons at δ_H 1.46 (*s*, 6H) in the ^1H NMR and the pair of *ortho* interacting alkenyl protons δ_H 5.67 (H-3″), 6.76 (H-4″, *d*, 1H, *J* = 10.0Hz) meant presence of a 2″, 2″-dimethylcyclopyran ring as the first substituent. The singlet δ_H 3.78 (*s*, 3H, δ_C 55.2) in the NMR spectra was suggestive of a methoxy group as the other substituent.

The proton signal δ_H 8.02 (*d*, 1H, *J* = 8.8Hz) appeared deshielded by the peri effect of the carbonyl, so it was assigned to H-5 and its coupling pattern δ_H 6.82 (*d*, 1H, *J*= 8.8Hz) was assigned to H-6 allowing for the oxygenation at C-7. The ^1H NMR displayed an AA′BB′ aromatic protons δ_H 6.91, 7.44 (*d*, 2H, *J* = 2.2, 7.4Hz) which was attached to a para substituted ring B. This permited placement of $–OCH_3$ attachment to C-4′. The only remaining way the pyran ring could be accommodated in the structure was fixing it at C-8 through the biogenetically expected oxygenation at C-7.

From all the HMBC correlations (Table 4.1), this compound was characterized to be 4′-methoxy-[7,8]-(2″, 2″-dimethylpyrano)isoflavone. This was a known metabolite previously reported as calopogoniumisoflavone-A isolated from the stem bark of *M. dura* (Yenesew *et al*., 1996), *M. oblata* ssp *teitensis* (stems) (Derese *et al*., 2014), and from the stem of *M. dielsiana* Harms (Ye *et al*., 2014).

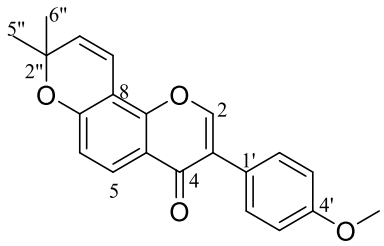

97

Table 4.1: NMR data of calopogoniumisoflavone-A (97)

Position.	δ_C	δ_H, *m*, (*J* in Hz)	HMBC (H → C)
2	151.9	7.90, *s*	C-1′, C-4, C-9
3	124.6		
4	176.0		
5	127.1	8.02, *d*, (8.8)	C-4, C-7, C-8, C-9
6	115.3	6.82, *d* (8.8)	C-7, C-8, C-10

Position.	δ_C	δ_H, *m*, (*J* in Hz)	HMBC (H → C)
7	157.3		
8	109.1		
9	152.4		
10	118.2		
1′	124.1		
2′/6′	130.2	7.44, *d*, (7.4)	C-2′/6′, C-3′/5′, C-3, C-4′
3′/5′	113.9	6.91, *d*, (7.4)	C-1′, C-3′/5′, C-4′
4′	159.5		
2″	77.7		
3″	130.1	5.67, *d*, (10.0)	C-2″, C-4″, C-8, C-5″/6″
4″	114.9	6.76, *d*, (10.0)	C-2″, C-5″/6″, C-7, C-8, C-9
5″/6″	28.1	1.46, *s*	C-2″, C-3″, C-5″/6″
OCH_3	55.2	3.78, *s*	C-4′

4.2.1.2 Jamaicin (98)

Compound (**98**) was obtained as white crystals from methanol. The characteristic peaks for an isoflavone were seen at δ_H 7.90 (*s*,1H) for the oxyolefinic methine proton (H-2) in the ^{1}H NMR together with its carbon signal at δ_C 153.9 (C-2), 112.9 for the olefinic quaternary carbon (C-3) and 175.8 for the carbonyl carbon (C-4) in the ^{13}C NMR (Agrawal, 1989).

The NMR spectra gave substituent peaks for $-OCH_3$ as δ_H 3.72 (*s*, 3H, δ_C 57.0), for a methylenedioxy at δ_H 5.94 (*s*, 2H), δ_C 101.5 and for a 2″, 2″-dimethylpyran given by overlapping methyl protons δ_H 1.49 (*s*, 6H) plus the pair of *ortho* coupled olefinic protons δ_H 5.70, 6.80 (*d*, 1H, *J* = 10.0Hz) in the ^{1}H NMR.

The AX coupled aromatic protons δ_H 6.84 and δ_H 8.03 (*d*, 1H, *J* = 8.8Hz) were assignable to H-6 and H-5 respectively, H-5, being highly deshielded by the peri effect of the carbonyl. The remaining pair of singlets in the aromatic region at δ_H 6.61 and δ_H 6.82 (*s*, 1H) could only be possible in ring B. The correlation of the methylenedioxy protons with carbons δ_C 141.3 and 148.5 and also the singlet protons δ_H 6.82 (*s*) with δ_C 141.3 and δ_H 6.61 (*s*) with δ_C 148.5 enabled fixing of the $-OCH_2O-$ group through C-4′ and C-5′. The $-OCH_3$ group was then fixed at C-2′.

The final structure of compound (**98**) was confirmed from the HMBC correlations (Table 4.2) and the compound was identified as 2′-methoxy-[4′,5′]-methylenedioxy-[7,8]-(2″,2″-dimethylcyclopyrano)isoflavone which had earlier been reported as jamaicin gotten from seeds of *M. ferruginea* (Highet and Highet, 1967), stem bark of *M.dura* (Yenesew *et al*., 1998), *M. oblata* ssp *teitensis*, stems (Derese *et al*., 2014), and the grains of *M. pachyloba* (Mai *et al*., 2010).

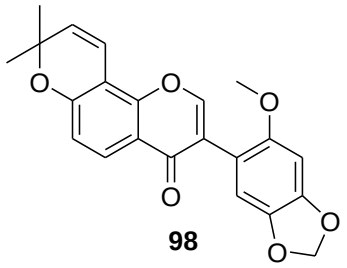

98

Table 4.2: NMR data of jamaicin (98)

Position.	δ_C	δ_H, *m*, (*J* in Hz)	HMBC (H → C)
2	153.9	7.90,*s*	C-1′, C-3, C-4, C-9
3	112.9		
4	175.8		
5	126.8	8.03, *d*, (8.8)	C-4, C-7, C-8, C-9
6	115.1	6.84, *d*, (8.8)	C-7, C-8, C-10
7	157.3		
8	109.4		
9	152.5		
10	118.5		
1′	122.0		
2′	153.0		
3′	115.2	6.82, *s*	C-1′, C-2′, C-4′, C-5′
4′	148.5		
5′	141.3		
6′	95.5	6.61, *s*	C-1′, C-2′, C-3, C-4′, C-5′
2″	77.7		
3″	130.3	5.70, *d*, (10.0)	C-2″, C-8, C-5″/6″
4″	111.3	6.80, *d*, (10.0)	C-2″, C-5″/6″, C-7, C-8, C-9
5″/6″	28.2	1.49, *s*	C-2″, C-3″, C-5″/6″
OCH_3	57.0	3.72, *s*	C-2′
OCH_2O	101.5	5.94, *s*	C-4′, C-5′

4.2.1.3 Durmillone (99)

Compound **99** was obtained as a white solid. The NMR data of this compound was similar to that of compound **98** having the same substituent. The difference was that the deshielded peri proton δ_H 7.55 (*s*, 1H) was a singlet. This meant that C-6 was substituted with the only methoxy group δ_H 3.96, (*s*, 3H).

Instead of an AX spin system as in compound **99**, this compound had an ABX proton system at δ_H 6.87 (*d*, 1H, *J* = 8.8Hz, H-5′), δ_H 6.97 (*dd*, 1H, *J* = 8.8, 1.7Hz, H-6′) and δ_H 7.10 (*d*, 1H, *J* = 1.7Hz, H-2′). The ABX protons δ_H 7.10 and 6.87 correlated with the same carbons δ_C 147.7, δ_C 147.8 as the methylene protons δ_H 5.99 (*s*, 2H). Therefore, -OCH_2O- group was in ring B at C-3′, C-4′ and then, the 2″,2″-dimethypyran ring was in ring A at C-7, C-8.

Through HMBC correlations (Table 4.3), the final structure was affirmed and was characterized as [3′,4′]-methylenedioxy-6-methoxy-[7,8]-(2″,2″-dimethylpyrano)isoflavone. This compound was earlier reported as durmillone from *M. ferruginea* ssp *ferruginea* (seeds) (Highet and Highet, 1967), from the vine stems of *M. dielsiana* Harms (Ye *et al*., 2014) and grains of *M. pachyloba* (Mai *et al*., 2010).

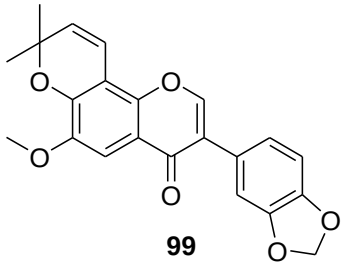

99

Table 4.3: NMR data of durmillone (99)

Position.	**δ_C**	**δ_H, *m*, (*J* in Hz)**	**HMBC (H → C)**
2	151.9	7.93,*s*	C-3, C-4, C-9
3	124.5		
4	175.6		
5	105.3	7.55, *s*	C-4, C-7, C-8, C-9, C-10
6	147.3		
7	147.4		
8	110.3		
9	147.5		
10	117.7		
1′	126.1		
2′	109.9	7.10, *d*, (1.7)	C-3, C-4′, C-6′
3′	147.8		
4′	147.7		
5′	108.5	6.87, *d*, (8.8)	C-1′, C-2′, C-5′
6′	122.5	6.97, *dd*, (1.7, 8.8)	C-2′, C-3, C-4′
2″	78.3		
3″	130.5	5.74, *d*, (10.0)	C-2″, C-5″/6″, C-8
4″	115.3	6.81, *d*, (10.0)	C-2″, C-5″/6″, C-7, C-8, C-9
5″/6″	28.1	1.55, *s*	C-2″, C-3″, C-4″, C-5″/6″
OCH_3	56.5	3.96, *s*	C-6
OCH_2O	101.3	5.99, *s*	C-4′, C-5′

4.2.1.4 Dullarone (100)

This was obtained as white needlelike crystals from methanol. This compound had the characteristic spectral data for an isoflavone as in compound **97**. Compound **100** had similar substituents as compound **99**, however, with additional two methoxy peaks δ_H 3.89 (*s*, 3H), and δ_H 3.91 (*s*, 3H) instead of the methylenedioxy peak at δ_H 5.99.

Having the same ABX proton pattern of δ_H 6.91 (*d*, 1H, *J* = 8.3Hz), δ_H 7.02 (*dd*, 1H, *J* = 8.3Hz, 2.0Hz), and δ_H 7.23 (*d*, 1H, *J* = 2.0Hz), meant that the additional methoxy substituents were attached to C-3 and C-4. The actual position of the substituent was fixed based on the biogenesis which calls for oxygenation at C-7, C-4′ and the HMBC correlations (Table 4.4).

The compound was identified as 3′,4′,6-trimethoxy-[7,8]-(2″,2″-dimethylpyrano)isoflavone earlier reported as dullarone from *M. dura* (SB) (Yenesew *et al*., 1996), the stem of *M. oblata* ssp *teitensis* (Derese *et al*., 2014) and the stem of *M. dielsiana* Harms (Ye *et al*., 2014).

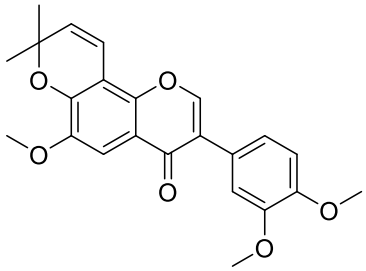

100

Table 4.4: NMR data of durallone (100)

Position.	**δ_C**	**δ_H, *m*, (*J* in Hz)**	**HMBC (H → C)**
2	151.9	7.97,*s*	C-3, C-4, C-9
3	124.2		
4	175.7		
5	105.1	7.75, *s*	C-4, C-7, C-8, C-9, C-10
6	147.26		
7	147.4		
8	110.3		
9	147.33		
10	117.7		
1′	124.9		
2′	112.6	7.23, *d*, (2.0)	C-3, C-4′, C-6′
3′	148.8		
4′	149.1		
5′	111.2	6.91, *d*, (8.3)	C-1′, C-3′, C-6′
6′	121.0	7.02, *dd*, (2.0, 8.3)	C-2′, C-3, C-4′
2″	78.3		
3″	130.5	5.73, *d*, (10.0)	C-2″, C-5″/6″, C-8
4″	115.2	6.79, *d*, (10.0)	C-2″, C-5″/6″, C-7, C-8, C-9
5″/6″	28.1	1.54, *s*	C-2″, C-3″, C-4″, C-5″/6″
3′-OCH_3	56.0	3.91, *s*	C-3′
4′-OCH_3	56.0	3.89, *s*	C-4′
6-OCH3	56.4	3.94	C-6

4.2.1.5 Kaempferol (227)

Compound **227** was obtained as yellow crystals from methanol. The ^{13}C NMR showed signals δ_C 148.0, (C-2, in range 140.0-151.2ppm), 137.1, (C-3, in range 133.5-140.0ppm) and 177.3 (C-4)

characteristic for a 5-hydroxyflavonol (Agrawal, 1989). The proton singlet δ_H 12.92 (*s*) highly deshielded by the peri-effect of the carbonyl δ_C 177.3, confirmed that C-5 had a hydroxyl substituent. There was no other substituent peak in the NMR spectra.

The ^{1}H NMR showed a set of *meta* interacting protons δ_H 6.35 (H-6), 6.14 ((H-8), *d*, 1H, *J* = 1.9Hz,) for a penta substituted ring A. Another pair of AA′BB′ aromatic protons δ_H 6.87 and 8.05 (*d*, 2H, *J* = 10.0Hz) respectively assignable to H-3′/5′ and H-2′/6′ for *para* substitution in ring B. Hence substitution at C-3 (δ_C 137.1), C-4′ (δ_C 160.5) and C-7 (δ_C 165.7) was by hydroxyl groups.

The HMBC correlations (Table 4.5) confirmed the assignments, and compound **227** was therefore characterized to be 3,5,7,4′-tetrahydroxyflavone which was reported as kaempferol, a known flavonol isolated from the aerial parts of *Lespedeza virgata* (Yan *et al*., 2008) and also from the twigs of *M. leptobotrya* Dunn (Zhi Na *et al*., 2013). This is the first report of kaempferol from *M. dura*.

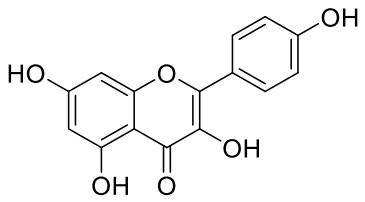

227

Table 4.5: NMR data of kaempferol (227)

Position.	**δ_C**	**δ_H, *m*, (*J* in Hz)**	**HMBC (H → C)**
2	148.0		
3	137.1		
4	177.3		
5	162.5		
6	94.56	6.35, *d*, (1.9)	C-4, C-7, C-8, C-9, C-10
7	165.7		
8	99.3	6.14, *d*, (1.9)	C-5, C-6, C-7, C-10
9	158.3		
10	104.3		
1′	123.7		
2′/6′	130.7	8.05, *d*, (10.0)	C-1′, C-3, C-2′/6′, C-3′/5′, C-4′
3′/5′	116.3	6.87, *d*, (10.0)	C-1′, C-3′/5′, C-2′/ 6′C-4′
4′	160.5		
5-OH		12.92, *s*	

4.2.1.6 4, 2′-Dihydroxy-4′-methoxychalcone (228)

Compound **228** was isolated as orange gum. The ^{1}H NMR showed a pair of *trans* olefinic doublet protons δ_H 7.46 (*d*, 1H, *J* = 15.3Hz, Hα) and δ_H 7.85 (*d*, 1H, *J* = 15.3Hz, Hβ) typical of a chalcone (Deyou *et al*., 2015b; Dominguez *et al*., 1989; Yenesew *et al*., 1998). The chalcone skeleton was further confirmed from the ^{13}C-NMR spectra showing peaks δ_C 118.0 for C-α (in the range 116.6-128.1ppm), 144.4 for C-β (in the range 136.9-145.4ppm) and a conjugated carbonyl peak 192.1 (in the range 188.8-194.6ppm) as reported by (Pelter *et al*., 1976). The highly de-shielded proton δ_H 13.55 (2-OH) showed this compound was a 2′-hydroxychalcone (Adesanwo *et al*., 2009).

The ^{1}H NMR spectra showed one substituent δ_H 3.86 (*s*, 3H) for a methoxyl group. The presence of an AA′XX′ spin system δ_H 6.89 (*d*, 2H, *J* = 8.6Hz, H-3/5) and 7.57 (*d*, 2H, *J* = 8.6Hz, H-2/6) together with a correlating quaternary δC 158.2 (C-4) suggested *para*- oxygenation at C-4 in ring B. The ABX spin system δ_H 6.48 (*d*, 1H, *J* = 3.2, H-3′), 6.50 (*dd*, 1H, *J* = 3.2, 8.5, H-5′) and 7.84 (*d*, 1H, *J* = 8.5, H-6′) revealed tri-substitution in ring A. The location of the methoxy at C-4′ was based on its HMBC correlations with δ_C 166.2 (Table 4.6) and C-4 had an –OH substituent.

Hence compound **228** was identified to be 4, 2′-dihydroxy-4′-methoxychalcone reported from the roots of *Codonopsis cordifolioidea* (Qiao-li *et al*., 2011; Meng *et al*., 2013). This is the primary report of this compound in this genus *Millettia*.

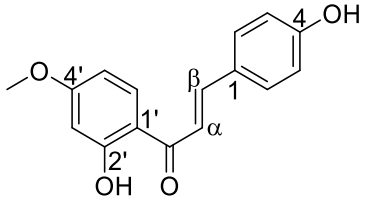

228

Table 4.6: NMR data of 4, 2′-dihydroxy-4′-methoxychalcone (228)

Position.	δ_C	δ_H, *m*, (*J* in Hz)	HMBC (H → C)
1	127.8		
2/6	130.7	7.57, *d*, (8.6)	C-β, C-2/6, C-4
3/5	116.2	6.89, *d*, (8.6)	C-1, C3/5, C-4
4	158.2		
1′	114.3		
2′	166.8		
3′	101.2	6.48, *d*, (3.2)	C-1′, C-2′, C-5′
4′	166.2		
5′	101.2	6.50, *dd*, (3.2, 8.5)	C-1′, C-3′, C-4′

Position.	δ_C	δ_H, *m*, (*J* in Hz)	HMBC (H → C)
6′	131.8	7.84,*d*, (8.5)	C-2′, C-4′, C=O
4′-OCH_3	55.8	3.86,*s*	C-4′
C-α	118.0	7.47, *d*, (15.3)	C-β, C-1, C=O
C-β	144.4	7.86, *d*, (15.3)	C-α, C-2/6, C=O
C=O	191.2		
2′-OH		13.55, *s*	

4.2.1.7 Ichthynone (123)

Compound **123** was obtained as white amorphous solid. It had the same spectral features of an isoflavone as compound **98**. The ^{1}H NMR of compound **123** showed δ_H 3.94 (*s*, 3H) for an extra methoxyl in addition to a 2″,2″-dimethylpyran ring given by δ_H 5.73 (*d*, 1H, *J* = 10.0Hz, H-3″), 6.79 (*d*, 1H, *J* = 10.0Hz, H-4″) and 1.54 (*s*, 6H), a methylenedioxy δ_H 5.95 (*s*, 2H) and a methoxyl δ_H 3.72 (*s*, 3H) substituents in compound **98**.

The peri deshielded proton δ_H 7.54 (*s*, 1H, H-5) was a singlet meaning that C-6 was substituted. Hence, the additional methoxy was fixed at the oxygenated quaternary carbon δ_C 147.2 (C-6). The final structure was confirmed on the basis of HMBC correlations (Table 4.7).

This compound was found to be 2′,6-dimethoxy-[4′,5′]-methylenedioxo-[7,8]-(2″,2″-dimethylpyrano)isoflavone. Compound **123** had been reported earlier as ichthynone from seeds of *M. ferruginea* (Highet and Highet, 1967), from the fruits of *M. caerulea* (Ren *et al*., 2016), stems of *M. dielsiana* Harms (Ye *et al*., 2014) and from the grains of *M. pachyloba* (Mai *et al*., 2010).

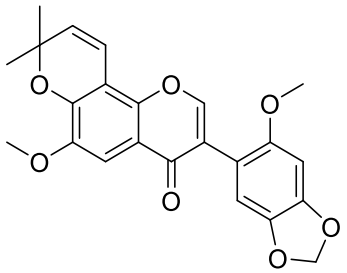

123

Table 4.7: NMR data of ichthynone (123)

Position.	δ_C	δ_H, *m*, (*J* in Hz)	HMBC (H → C)
2	153.7	7.90, *s*	C-1′, C-3, C-4, C-9
3	113.1		
4	175.5		
5	105.3	7.54, *s*	C-4, C-7, C-8, C-9, C-10
6	147.2		
7	147.5		
8	110.4		
9	147.1		
10	117.7		
1′	121.6		
2′	153.1		
3′	111.3	6.81, *s*	C-1′, C-2′, C-4′, C-5′
4′	141.3		
5′	148.5		
6′	95.6	6.61, *s*	C-1′, C-2′, C-3, C-4′, C-5′
2″	78.2		
3″	130.4	5.73, *d*, 10.0	C-2″, C-5″/6″, C-8, C-9
4″	115.4	6.79, *d*, 10.0	C-2″, C-5″/6″, C-7, C-8, C-9
5″/6″	28.1	1.54, *s*	C-2″, C-3″, C-4″, C-5″/6″
2′-OCH_3	57.0	3.72, *s*	C-2′
6-OCH_3	56.4	3.94,*s*	C-6
OCH_2O	101.5	5.95, *s*	C-4′, C-5′

4.2.1.8 Formononetin (91)

It was obtained as white needlelike crystals in methanol. This compound had an isoflavone ring skeleton based on an oxyolefinic methine proton δ_H 8.33 (*s*, 1H, H-2,) and δ_C 153.2 (C-2), the olefinic quaternary carbon δ_C 124.2 (C-3) and the carbonyl δ_C 174.6 (C-4) (Agrawal, 1989). From the ^{1}H NMR, the compound showed only one substituent δ_H 3.73 (s, 3H) for a methoxy.

The presence of proton signals having an AA′BB′ spin system δ_H 6.99 (*dd*, 2H, *J* = 2.0, 8.5Hz) and δ_H 7.51 (*dd*, 2H, *J* = 2.0, 8.5Hz), meant that ring B was para substituted at C-4′ likely through oxygenation as biogenetically expected. The ^{1}H NMR further showed three mutually coupled aromatic protons at δ_H 7.97 (*d*, 1H, *J* = 8.8Hz,), 6.94 (*dd*, 1H, *J* = 8.8, 2.3Hz) and 6.87 (d, *J* = 2.3Hz) assigning them to H-5, H-6 then H-8 in that order. The down shifted chemical shift of C-7 (162.6ppm) revealed that it was oxygenated as expected by biogenetic considerations. The methoxyl cluster was fixed at (C-4′) basing on the correlation (Table 4.8) of its protons with δ_C 159.0 (C-4′) instead of δ_C 162.6 (C-7).

The NMR data (Table 4.8) compares well with that reported in literature for 7-hydroxy-4′-methoxyisoflavone reported as formononetin, a compound previously isolated from *M. dura* seed pods (Yensew *et al*., 1997), from the stem bark of *Plattycelphium voense* (Gumula *et al*., 2012). This is its first reported from the flowers of *M. dura*.

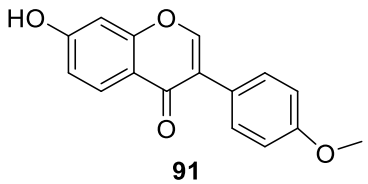

91

Table 4.8: NMR data of formononetin (91)

Position.	**δ_C**	**δ_H, *m*, (*J* in Hz)**	**HMBC (H → C)**
2	153.2	8.33,*s*	C-1′, C-4, C-9
3	124.2		
4	175.6		
5	127.3	7.97, *d*, (8.8)	C-4, C-6, C-7, C-9
6	115.2	6.94, *dd*, (2.3, 8.8)	C-7, C-8, C-10
7	162.6		
8	102.1	6.87, *d*, (2.3)	C-7, C-9, C-10
9	157.4		
10	116.6		
1′	123.2		
2′/6′	113.6	6.99, *dd* (2.0, 8.4)	C-2′/6′, C-3, C-4′,
3′/5′	130.1	7.51, *dd* (2.0, 8.4)	C-1′, C-2′, C-3′/5′, C-4′
4′	159.0		
4′-OCH_3	55.2	3.78, *s*	C-4′

4.2.1.9 6-Methoxycalopogonium isoflavones-A (101)

This compound was gotten as white fluffy crystals from ethyl acetate. The compound had spectral resemblance to compound **97**, having an isoflavone skeleton. In addition to the substituent of compound **97**, the ^{1}H NMR spectra showed presence of an additional methoxy group δ_H 3.95 (*s*, 3H). The singlet proton δ_H 7.55 (*s*, 1H, H-5) deshielded by the peri-effect of the carbonyl (δ_C 175.7, C-4) was suggestive that C-6 was substituted. The additional methoxy group was therefore fixed at C-6.

Basing on this and by relating the NMR data (Table 4.9) with that in literature, compound **101** was characterized as 6-methoxycalopogoniumisoflavone A previously isolated from the seed pods of *M. dura* (Yenesew *et al*., 1997), stem of *M. dielsiana* Harms (Ye *et al*., 2014) and *M. oblata* ssp *teitensis* stem vains (Derese *et al*., 2014).

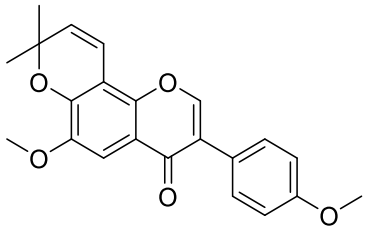

101

Table 4.9: NMR data of 6-methoxycalopogoniumisoflavone-A (101)

Position.	δ_C	δ_H, *m*, (*J* in Hz)	HMBC (H → C)
2	151.7	7.94, *s*	C-1′,C-4, C-9
3	124.5		
4	175.7		
5	105.2	7.55, *s*	C-4, C-7, C-9, C-10
6	147.2		
7	147.3		
8	110.3		
9	147.5		
10	117.7		
1′	124.3		
2′/6′	114.0	6.96, *d*, (8.8)	C-2′/6′, C-3, C-4′
3′/5′	130.2	7.49, *d*, (8.8)	C-1′, C-2′, C-3′/5′, C-4′
4′	159.6		
2″	78.3		
3″	130.4	5.73, *d*, (10.0)	C-2″, C-4″, C-8, C-5″/6″
4″	115.3	6.80, *d*, (10.0)	C-2″, C-7, C-8, C-9
5″/6″	28.1	1.55, *s*	C-2″, C-3″, C-4″, C-5″/6″
4′-OCH_3	55.4	3.83, *s*	C-4′
6-OCH_3	56.4	3.95, *s*	C-6

4.2.2 Characterization of compounds from the seed pods of *Millettia dura*

Seven compounds (three rotenoids and four isoflavones) were isolated and characterized from the SP of *Millettia dura*. All the isoflavonoids calopogoniumisoflavone A (**97**), jamaicin (**98**), durallone (**100**) and 6-methoxycalopogonium isoflavone-A (**101**) have already been discussed in section 4.1 above. Characterization of the rotenoids only is discussed in the following subsections.

4.2.2.1 Milletone (172)

It was obtained as colorless needle like crystals from methanol. From the presence of a pair of non-equivalent methylene protons at δ_H 4.07 (*dt*, 1H, *J* =1.1, 1.1, 12.1Hz), 4.53 (*dd*, 1H, *J* =3.1, 12.1Hz, H-6α, H-6β) and the oxymethine proton 4.82 (*ddd*, 1H, *J*=1.2, 3.0, 4.2Hz, H-6a) together with the methine 3.69 (*dt*, 1H, *J* =1.0, 1.0, 4.0Hz, H-12a), the compound was identified to be a rotenoid.

According to (Agrawal, 1989)), carbon peaks δ_C 66.3 (in range 65.1-66.8ppm, C-6), 72.3 (in range 71.6-72.2ppm, C-6a), 44.6 (in range 43.5-45.3ppm, C-12a) characteristic of the extra ring B and the carbonyl 188.9 (in range 183.9-194.3ppm), are typical of rotenoids.

The ^{1}H NMR spectra revealed two substituents. A methylenedioxy given by a pair of non-overlapped methylene protons δ_H 5.71, 5.76 (*d*, 1H, *J* = 1.3Hz) and the other being a pyran ring given by a pair of coupled olefinic protons δ_H 5.51 (*d*, 1H, *J* = 10.8Hz, H-3′), 6.54 (*dd*, 1H, *J* = 1.0, 10.0Hz, H-4′) together with a pair of correlating methyl protons δ_H 1.28 and 1.35 (*s*, 3H).

The ortho-copouled aromatic protons δ_H 6.33 and 7.60 (*d*, 1H, *J* = 8.7Hz) was attributed to H-10 and H-11 respectively, H-11 being deshieled by the peri effect of the carbonyl δ_C 188.9 allowing for the biogenetic oxygenation of C-9. The singlet δ_H 6.31 (*s*, 1H) was attributed to H-4, H-1 δ_H 6.61 (*d*, 1H, *J* = 1.0Hz) appeared as a doublet due to the W-correlation effect with H-12a (*J* = 1.0Hz) (Yenesew *et al*., 1997).

The low chemical shift of C-8 (δ_C 109.2) suggested that this carbon was not oxygenated, so the the prenyl group was attached to this quaternary cyclizing through the oxygen at C-9. Hence the methylenedioxy could only be in ring A attached to C-2 and C-3. Compound **172** was confirmed through HMBC correlarations (Table 4.10) to be millettone isolated from seed pods of *M. dura* (Ollis *et al*., 1967; Yenesew *et al*., 1997).

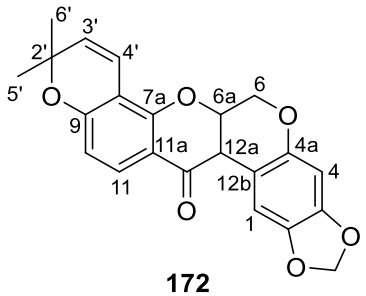

172

Table 4.10: NMR data of milletone (172)

Position.	**δ_C**	**δ_H, *m*, (*J* in Hz)**	**HMBC (H → C)**
1	106.7	6.61, *d*, (1.0)	C-4a, C-4, C-3, C-2, C-12a, C-12b
2	142.2		
3	147.8		
4	98.5	6.31, *s*	C-2, C-3, C-4a, C-12b
4a	148.4		
6	66.3	4.07, *dt*, (12.1, 1.2) 4.52, *dd*, (12.1, 3.0)	C-4a, C-6a, C-7a, C-12, C-12a, C-12b
6a	72.3	4.82, *ddd*, (4.2, 3.0, 1.2)	C-6, C-7a, C-12 ,C-12a, C-12b

Position.	δ_C	δ_H, *m*, (*J* in Hz)	HMBC (H → C)
7a	156.7		
8	109.2		
9	160.0		
10	111.3	6.33, *d*, (8.7)	C-4′, C-8, C-9, C-11a
11	128.3	7.60, *d*, (8.7)	C-7a, C-8, C-9, C-10, C-12
11a	112.7		
12	188.9		
12a	44.6	3.69, *dt*, (4.0,1.0)	C-1, C-4a, C-6, C-6a, C-11a, C-12
12b	105.9		
2′	77.7		
3′	129.0	5.51, *d*, (10.0)	C-2′, C-5′, C-6′, C-8, C-9
4′	115.4	6.54 *d*, (10.0)	C-2′, C-5′, C-6′, C-7a, C-8, C-9
5′	28.2	1.35,*s*	C-2′, C-3′, C-4′, C-6′
6′	27.8	1.28, *s*	C-2′, C-3′, C-4′, C-5′
OCH_2O	101.3	5.71, 5.76, *d*, (1.3)	C-2, C-3

4.2.2.2 Milletosin (173)

It was obtained as colorless needle like crystals in methanol. The presence of a pair of non-overlapping methylene protons δ_H 4.36, 4.53 (*dd*, 1H, *J* = 2.4, 10.2Hz, H-6α, H-6β) together with an oxymethine proton 4.48 (*dd*, 1H, *J* = 1.0, 2.4Hz, H-6a) were characteristic for a 12a-hydroxy rotenoid (Agrawal, 1989).

Two substituents were clear in the ^{1}H NMR. A methylenedioxy δ_H 5.76 (*s*, 2H) and a pyran ring due to a pair of coupled olefinic protons at 5.53 (*d*, 1H, *J* = 10.1Hz, H-3′), 6.51 (*d*, 1H, *J* = 10.1Hz, H-4′) and the pair of correlating methyl protons δ_H 1.30, 1.36 (*s*, 3H).

The pair of *ortho*-interacting phenyl protons δ_H 6.39, 7.61 (*d*, 1H, *J* = 8.2Hz) were respectively attributed to H-10 and H-11 on the basis that, H-11 was deshielded by the carbonyl (δ_C 191.0), while a pair of aromatic singlet δ_H 6.39 (*s*, 1H) and 6.43 (*s*, 1H,) was attributed to H-4 and H-1 respectively, in ring A.

Again, C-8 being shielded (δ_C 109.2), the pyran ring was at C-8 / C-9 in ring D. This leaves the methylenedioxy to be fixed at C-2 / C-3 in ring A. Furthermore, H-1 (6.43ppm) being shielded suggested a *cis*- relative configuration between the –OH group at C-12a and the H-6a (Bueno *et al*., 2014; Rastrelli *et al*., 1999; Yenesew *et al*., 1998a).

From the HMBC correlations (Table 4.11), this compound was identified to be milletosin a compound previously reported from the roots of *Dalea searlsiae* (Belofsky *et al*., 2014), stem bark

of *M. usaramensis* ssp *usaramensis* (Deyou *et al*., 2015), and *M. dura* (seeds) (Yenesew *et al*., 2003).

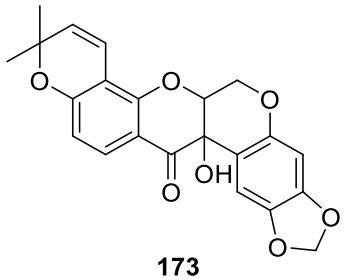

173

Table 4.11: NMR data of milletosin (173)

Position.	**δ_C**	**δ_H, *m*, (*J* in Hz)**	**HMBC (H → C)**
1	105.7	6.43, *s*	C-3, C-4a, C-12a
2	149.5		
3	142.1		
4	98.6	6.36, *s*	C-2, C-12b
4a	149.6		
6	63.8	4.36, *dd*, (10.2, 1.0) 4.53, *dd*, (10.2, 2.4)	C-4a, C-6a, C-7a, C-12 ,C-12a
6a	75.8	4.48, *dd*, (2.4, 1.0)	C-6, C-7a, C-12 ,C-12a, C-12b
7a	156.4		
8	109.2		
9	160.5		
10	111.5	6.39, *d*, (8.2)	C-8, C-9, C-11a
11	128.2	7.61, *d*, (8.2)	C-7a, C-9, C-12
11a	110.9		
12	191.0		
12a	67.3		
12b	109.8		
2′	77.8		
3′	129.0	5.53, *d*, (10.1)	C-2′, C-5′, C-6′, C-8
4′	114.7	6.51, *d*, (10.1)	C-2′, C-7a, C-9
5′	28.1	1.36, *s*	C-2′, C-3′, C-4′, C-6′
6′	27.4	1.30, *s*	C-2′, C-3′, C-4′, C-5′
OCH_2O	101.6	5.76, *s*	C-2, C-3

4.2.2.3 Tephrosin (171)

This was obtained as a brown oily compound as reported by Lou *et al*., (2016). This compound had similar spectral features as **173** apart for the two methoxy signals δ_H 3.75 (*s*, 3H) and δ_H 3.64 (*s*, 3H) and absence of methylenedioxy peaks. The pair of methoxy substituents was fixed to C-2 and C-3 in place of the methylenedioxy on the basis that δ_H 3.64 correlated with δc 143.9 while

3.75 correlated with 151.1 (Table 4.12). It had a *cis*-B/C ring configuration due to a shielded H-1 chemical shift δ_H 6.45 (*s*, 1H) (Bueno *et al*., 2014).

Basing on the NMR data (Table 4.12) and that in literature, this was a known rotenoid, tephrosin previously isolated from the seed pods of *M. dura* (Yenesew *et al*., 1997).

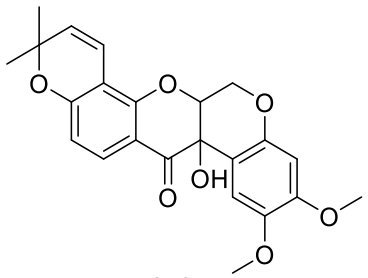

171

Table 4.12: NMR data of tephrosin (171)

Position.	**δ_C**	**δ_H, *m*, (*J* in Hz)**	**HMBC (H → C)**
1	110.0	6.45, *s*	C-2, C-3, C-4a, C-12a, C-12b
2	143.9		
3	151.1		
4	111.7	6.47, *s*	C-2, C-3, C-4a, C-12b
4a	148.3		
6	63.7	4.48, *dd*, (12.2, 1.0) 4.61, *dd*, (12.2, 2.0)	C-4a, C-6a, C-7a, C-12a
6a	76.3	4.59, *dd*, (2.0, 1.0)	C-7a, C-12 ,C-12a, C-12b
7a	156.5		
8	109.1		
9	160.5		
10	101.1	6.46, *d*, (8.8)	C-8, C-11, C-11a
11	128.4	7.70, *d*, (8.8)	C-7a, C-9, C-11a, C-12
11a	111.3		
12	191.1		
12a	67.5		
12b	108.6		
2′	78.0		
3′	129.1	5.59, *d*, (10.1)	C-2′, C-5′, C-6′, C-8
4′	115.0	6.59 *d*, (10.1)	C-2′, C-5′, C-6′, C-7a, C-9
5′	28.1	1.36,*s*	C-2′, C-3′, C-4′, C-6′
6′	27.4	1.30, *s*	C-2′, C-3′, C-4′, C-5′
2-OCH_3	56.3	3.64, *s*	C-2
3-OCH_3	55.7	3.75, *s*	C-3

4.2.3 Characterization of compounds from the stem bark of *Millettia dura*

Thirteen secondary metabolites were isolated and characterized from *Millettia dura* stem bark. Six of these calopogoniumisoflavone A (**97**), jamaicine (**98**), durmillone (**99**), durallone (**100**), 6-

methoxycalopogoniumisoflavone A (**101**), and tephrosin (**171**) have already been discussed. The other seven isoerythrin-A-4′-(3-methylbut-2-enyl)ether (**102**), maximaisoflavone J (**112**), ferrugone (**118**), barbigerone (**114**), maximaisoflavone D (**92**), maximaisoflavone G (**115**) and (±) deguelin (**170**) are discussed below.

4.2.3.1 Isoerythrin-A-4′-(3-methylbut-2-enyl)ether (102)

It was obtained in form of a white powder. The spectral data Table 4.13 was indicative that this compound was an isoflavone. From the ^{1}H NMR, there were two substituents. A 2″, 2″-dimethylpyran ring which was deduced from the correlating methyl protons δ_H 1.49 (*s*, 6H, H-5″/6″), and the *ortho* olefinic protons δ_H 5.67 (H-3″), 6.84 ((H-4″), *d*, 1H, *J* = 10.0Hz). Then an oxoprenyl group identified by the correlated methyl protons δ_H 1.76 (H-5‴), and 1.80 ((H-6‴), *s*, 3H,), a pair of methylene protons 4.56 (*d*, 2H, *J* = 6.6Hz, H-2‴) and an olefinic methine proton 5.49 (*dd*, 1H, *J* = 6.6, 13.2Hz, H-3‴).

The ^{1}H NMR showed protons in aromatic region with an AX spin system δ_H 8.00 and 6.86 (*d*, 1H, *J* = 8.4Hz) assigned to H-5 and H-6 respectively on the basis that H-5 is deshielded by the peri effect of the carbonyl. This guided the attachment of the pyran ring at C-7 / C-8. It also displayed an AA′BB′ spin aromatic protons δ_H 6.96 (H-3′/5′) and 7.47 ((H-2′/6′), *d*, 2H, *J* = 8.8Hz,) consistent with the *para* substitution in ring B. The methylene protons at δ_H 4.56 showed a strong correlation with the oxygenated carbon δc 159.4 and on this basis, the oxyprenyl substituent was fixed at C-4′. The compound was identified as isoerythrin-A-4′-(3-methylbut-2-enyl)ether which had earlier been reported from *M. dura* (SB) by Yenesew *et al*., (1996).

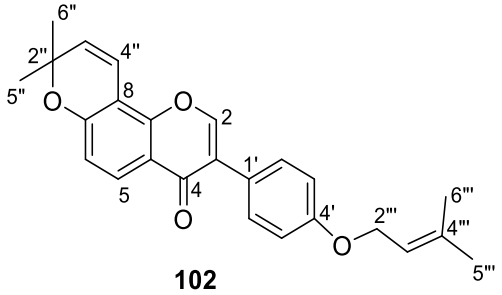

102

Table 4.13: NMR data of isoerythrin-A-4′-(3-methylbut-2-enyl)ether (102)

Position.	δ_C	δ_H, *m*, (*J* Hz)	HMBC (H → C)
2	152.4	7.98, *s*	C-1′, C-3, C-4, C-9
3	125.0		
4	176.2		

Position.	δ_C	δ_H, *m*, (*J* Hz)	HMBC (H → C)
5	126.9	8.00, *d*, (8.4)	C-4, C-7, C-9, C-10
6	115.3	6.86, *d*, (8.4)	C-7, C-8, C-10
7	157.8		
8	118.9		
9	152.9		
10	109.9		
1′	124.8		
2′/6′	130.7	7.47, *d*, (8.8)	C-2′/6′, C-3, C-3′/5′, C-4′
3′/5′	115.0	6.96, *d*, (8.8)	C-1′, C-3′/5′, C-4′
4′	159.4		
2″	78.3		
3″	131.0	5.76, *d*, (10.0)	C-2″, C-5″/6″, C-8
4″	115.6	6.84, *d*, (10.0)	C-2″, C-5″/6″, C-8, C-9
5″/6″	28.4	1.49, *s*	C-2″, C-3″, C-4″, C-5″/6″
2‴	65.4	4.56, *d*, (6.6)	C-3‴, C-4‴, C-4′
3‴	120.2	5.49, *dd*, (6.6, 13.2)	C-2‴, C-5‴, C-6‴
4‴	138.6		
5‴	26.0	1.80, *s*	C-3‴, C-4‴, C-6‴
6‴	18.0	1.76, *s*	C-3‴, C-4‴, C-5‴

4.2.3.2 Maximaisoflavone B (94)

It was obtained as a white powder. This compound was identified to have an isoflavone skeleton as in compound **102** basing on the NMR data (Table 4.14) (Agrawal, 1989). From the ^{1}H NMR, the compound had only two substituents, a methylenedioxy (δ_H 6.00, *s*, 2H) and an oxoprenyl by the correlated methyl proton δ_H 1.78 and 1.82 (*s*, 3H), a pair of methylene proton 4.62 (*d*, 2H, *J* = 6.8Hz) and an olefinic methine proton 5.50 (*t*, 1H, *J* = 6.8Hz).

The ^{1}H NMR further showed two sets of ABX spin system; δ_H 8.13 (*d*, 1H, *J* = 8.6Hz, H-5), 6.88 (*dd*, 1H, *J* = 8.6, 2.3Hz, H-6) and 6.86 (*d*, *J* = 2.3, H-8) as well as at δ_H 7.48 (*d*, 1H, *J* = 8.8Hz, H-5′), 7.08 (*dd*, 1H, *J* = 8.8, 2.3Hz, H-2′) and 6.97 (*d*, 1H, *J* = 2.3Hz, H-6′).

The methylene proton δ_H 4.62 showed a strong correlation with the oxygenated quaternary δ_C 163.9, enabling placement of the oxyprenyl at C-7. In the same way, correlation of the methylenedioxy δ_H 6.00 with δ_C 147.5 (C-3′/4′) allowed its placement between C-3′/4′. This compound was characterized as 3′,4′-methylenedioxy-7-(3″,3″-dimethyloxopyrano)isoflavone, which had earlier been reported as maximaisoflavone B isolated from the leaves (Deyou *et al*., 2017b) of *M. oblata* ssp.*teitensis*.

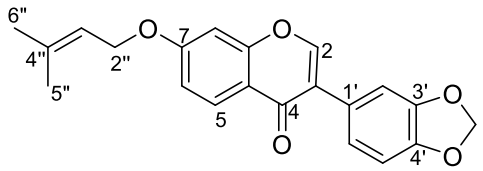

94

Table 4.14: NMR data of maximaisoflavone-J (94)

Position.	δ_C	δ_H, *m*, (*J* Hz)	HMBC (H → C)
2	152.3	7.92, *s*	C-1′, C-3, C-4, C-9
3	124.7		
4	175.3		
5	127.3	8.12, *d*, (8.6)	C-4, C-6, C-7, C-9
6	100.8	6.88, *dd*, (8.6, 2.3)	C-7, C-8, C-10
7	163.3		
8	108.1	6.86, *d*, (2.3)	C-7, C-9, C-10
9	157.8		
10	118.1		
1′	125.0		
2′	109.7	7.08, *d*, (2.3)	C-3, C-4′, C-6′
3′	147.5		
4′	147.5		
5′	130.1	7.48, *d*, (8.8)	C-1′, C-3′, C-4′
6′	122.3	6.97, *dd*, (8.8,2.3)	C-2′, C-3, C-4′
2″	65.5	4.62, *d*, (6.8)	C-3″, C-4″, C-7
3″	118.5	5.50, *dd*, (6.8)	C-5″, C-6″
4″	139.2		
5″	25.5	1.82, *s*	C-3″, C-4″, C-6″
6″	18.0	1.78, *s*	C-3″, C-4″, C-5″
O-CH_2-O	101.3	6.00, *s*	C-3′, C-4′

4.2.3.3 Ferrugone (118)

This compound was obtained as needle-like crystals in methanol. This compound was identified as an isoflavone based on its characteristic NMR signals (Table 4.15) (Agrawal, 1989). Four substituents were identified from the ^{1}H NMR spectra, the 2″, 2″-dimethylpyran ring deduced from the correlating melthylene protons (δ_H 5.71 (H-3″) and 6.82 (H-4″), *d*, 1H, *J* = 10.1Hz,)) and the methyl protons δ_H 1.50 (*s*, 6H), the methylenedioxy δ_H 6.02 (*s*, 2H) and two methoxy substituents (δ_H 3.83 and 3.87 (*s*, 3H)).

A pair of AX aromatic protons (δ_H 8.04, 6.85 (*d*, 1H, *J* = 8.8Hz)) was respectively assigned to H-5 and H-6, guided by the fact that H-5 was deshielded by the peri effect of the carbonyl δ_C 175.8. The only aromatic singlet δ_H 6.52 (*s*, 1H) attributed to ring B, was assigned to H-6′. The correlation

of δ_H 6.82 (H-3″) with C-8 and 5.71 (H-4″) with C-9 alowed the placement of the pyran ring to C-7 / C-8. While the correlation of δ_H 6.02 with δ_C 130.0 and 137.1 enabled placement of the methylenedioxy to C-3′ / C-4′.

From the NMR data Table 4.15, compound **118** was identified to be ferrugone, an isoflavone aerlier reported from Abyssinian *berbera* tree (Highet and Highet, 1967; Dagne and Bekele, 1990a) also from *M. ferruginea* (Dagne *et al*., 1990) and then from the SP of *M. dura* (Yenesew *et al*., 1996).

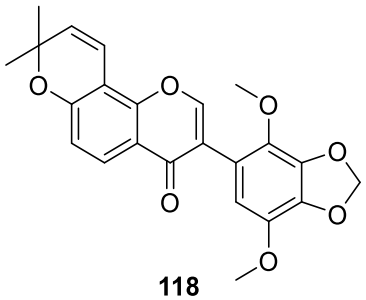

118

Table 4.15: NMR data of ferrugone (118)

Position.	**δ_C**	**δ_H, *m*, (*J* in Hz)**	**HMBC (H → C)**
2	152.4	7.92, *s*	C-1′, C-3, C-2′, C-4, C-9
3	122.0		
4	175.8		
5	126.7	8.04, *d*, (8.8)	C-4, C-6, C-7, C-8, C-9
6	115.0	6.85, *d* (8.8)	C-5, C-7, C-8, C-10
7	157.3		
8	109.3		
9	153.4		
10	118.3		
1′	117.9		
2′	136.8		
3′	139.0		
4′	137.1		
5′	139.1		
6′	110.1	6.52, *s*	C-1′, C-2′, C-3, C-4′, C-5′
2″	77.7		
3″	130.2	5.71, *d*, (10.0)	C-2″, C-4″, C-8, C-5″/6″
4″	115.1	6.82, *d*, (10.0)	C-2″, C-3″, C-5″/6″, C-7, C-8, C-9
5″/6″	28.1	1.51, *s*	C-2″, C-3″, C-5″/6″
2′-OCH_3	60.2	3.83 *s*	C-2′
5′-OCH_3	56.9	3. 87, *s*	C-5′
OCH_2O	101.9	6.02, *s*	C-3′, C-4′

4.2.3.4 Barbigerone (114)

This compound was gotten as white needle crystals from methanol and was identified as a flavonoid (Table 4.16) (Agrawal, 1989). The ^{1}H NMR spectra gave characteristic signals (δ_H 3.93, 3.78 (*s*, 3H) and 3.86 (*s*, 3H)) for three methoxyl substituents, and the methyl protons δ_H 1.52 (*s*, 6H) as well as the ortho coupled olefinic protons (5.72 (H-3″) and 6.82 (H-4″), *d*, 1H, *J* = 10.0Hz,)) confirmed a 2″, 2″-dimethylpyran ring.

The ^{1}H NMR showed a pair of AX protons δ_H 8.05 and 6.86 (*d*, 1H, *J* = 8.7Hz) assignable to H-5 and H-6 respectively. The ^{1}H NMR also presented a pair of aromatic proton singlets δ_H 6.63 and 6.95 (*s*, 1H) which could be attributed to a tetra-substituted ring B.

The pyran ring was fixed at C-7 / C-8 on the basis of the correlation of δ_H 5.72 with C-8 (δ_C 109.3) and 6.82 with C-9 (154.0). The methoxy δ_H 3.93 correlating with δ_C 149.7 was fixed to C-2′, 3.86 correlating with 143.0 was placed at C-5′, while 3.78 was attached to C-4′ having correlated with 151.9 (Table 4.16). The final structure was characterized to be barbigerone, a compound reported earlier from *M. ferruginea* ssp *darassana* (Dagne *et al*., 1990), stem of *M. dielsiana* Harms (Ye *et al*., 2014).

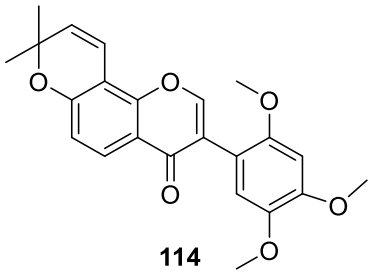

114

Table 4.16: NMR data of barbigerone (114)

Position.	δ_C	δ_H, *m*, (*J* in Hz)	HMBC (H → C)
2	152.4	7.97, *s*	C-1′, C-2′, C-3, C-4, C-9
3	112.2		
4	175.9		
5	126.7	8.05, *d*, (8.7)	C-4, C-7, C-8, C-9
6	115.1	6.85, *d* (8.7)	C-5, C-7, C-8, C-10
7	157.2		
8	109.3		
9	154.0		
10	118.4		
1′	121.5		
2′	149.7		
3′	98.3	6.63, *s*	C-1′, C-3, C-4′
4′	151.9		

Position.	δ_C	δ_H, *m*, (*J* in Hz)	HMBC (H → C)
5′	143.0		
6′	115.3	6.95, *s*	C-1′, C-2′, C-3, C-4′, C-5′
2″	77.6		
3″	130.2	5.72, *d*, (10.0)	C-2″, C-8, C-5″/6″
4″	115.1	6.82, *d*, (10.0)	C-2″, C-3″, C-5″/6″, C-7, C-8, C-9
5″/6″	28.1	1.52, *s*	C-2″, C-3″, C-5″/6″
2′-OCH_3	56.2	3.93 *s*	C-2′
4′-OCH_3	56.9	3.78, *s*	C-4′
5′-OCH_3	56.6	3.86, *s*	C-5′

4.2.3.5 Maximaisoflavone-D (92)

Compound 92 was obtained as white crystals from methanol and was identified as an isoflavone (Table 4.17). The ^{1}H NMR spectra showed three substituents, a methylenedioxy δ_H 6.22 (*s*, 2H), and two methoxy groups δ_H 3.93 and 3.92 (*s*, 3H).

The ^{1}H NMR spectra further displayed AX protons system in aromatic region at δ_H 6.99 and 7.90 (*d*, 1H, *J* = 8.5Hz) with the latter being deshielded by the carbonyl δ_C 175.7 (C-4) were assignable to H-6 and H-5 respectively, C-7 being oxygenated as biogenetically expected. The ^{1}H NMR also displayed an ABX spin system of δ_H 6.93 (*d*, 1H, *J* = 8.3Hz), 7.03 (*dd*, 1H, *J* = 2.0, 8.3Hz) and 7.18 (*d*, 1H, *J* = 2.0Hz) represented a 3, 4-disubstitution in ring B, C-4′ being oxygenated.

The methylenedioxy δ_H 6.22 correlations with the quaternary δ_C 134.7 and 152.4 seen by the AX spin system, enabled its placement to C-7 / C-8. The methoxy group δ_H 3.92 correlating with δ_C 149.7 as protons δ_H 7.18 and 7.03 guided its placement at C-4′, while the methoxy group δ_H 3.93 correlating with 148.9 as proton 6.93 was fixed to C-3′. Based on these HMBC correlations (Table 4.17) and literature (Yenesew *et al*., 1996), this metabolite was identified as 3′,4′-dimethoxy-[7,8]-methylenedioxyisoflavone which had earlier been report as maximaisoflavone-D from the seed pods of *M. dura* (Yenesew *et al*., 1996).

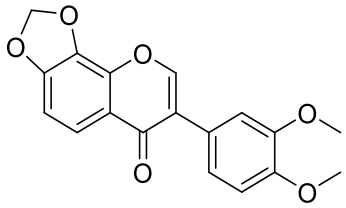

92

Table 4.17: NMR data of maximaisoflavone-D (92)

Position.	δ_C	δ_H, *m*, (*J* in Hz)	HMBC (H → C)
2	151.9	7.94,*s*	C-1′, C-3, C-4, C-9
3	124.9		
4	175.7		
5	121.1	7.90, *d*, (8.5)	C-4, C-7, C-9
6	107.5	6.99, *d*, (8.5)	C-7, C-8, C-10
7	134.7		
8	152.4		
9	141.4		
10	120.7		
1′	124.5		
2′	112.7	7.18, *d*, (2.0)	C-3, C-4′, C-6′
3′	148.9		
4′	149.4		
5′	111.3	6.93, *d*, (8.3)	C-1′,C-3′
6′	121.3	7.03, *dd*, (8.3, 2.0)	C-2′, C-3, C-4′
3′-OCH_3	56.1	3.93, *s*	C-3′
4′-OCH_3	56.1	3.92, *s*	C-4′
OCH_2O	103.5	6.22, *s*	C-7, C-8

4.2.3.6 Maximaisoflavone G (115)

This was obtained as a white solid and identified to be an isoflavone, Table 4.18 (Yenesew *et al*., 1998c). The proton peak δ_H 6.00 (*s*, 2H) for a methylenedioxy and 3.63 (*s*, 3H) for a –OCH_3 represented the only substituents for this compound.

The peri deshielded proton at δ_H 7.92 (*d*, 1H, *J* = 8.7Hz, H-5) which showed an ABX spin system with protons δ_H 6.92 (*dd*, 1H, *J* = 2.3, 8.7Hz) together with δ_H 6.86 (*d*, 1H, *J* = 2.3Hz) allowed the assignment of the later protons to H-6 and H-8 respectively. The singlet aromatic proton δ_H 6.81 and 6.86 (*s*, 1H) could only be attributed to ring B.

The proton singlet δ_H 6.85 correlating with the same carbon (δ_C 152.8, C-2′) as the methoxy δ_H 3.65, enabled placement of the later to C-2′. Meanwhile, the methylene proton δ_H 6.00 correlating with the same oxygenated quaternaries δ_C 140.3 and 147.9 as the singlet protons δ_H 6.81 and 6.85 permitted its placement to C-4′ / C-5′. To make up the ABX spin system in ring A required substitution at C-7, which could only be through an –OH. Basising on this, compound **115** was considered to be 7-hydroxy-2′-methoxy-[4′,5′]-methylenedioxyisoflavone, which had recently been reported as maximaisoflavone G from *M. oblata* ssp *teitensis* (Deyou *et al*., 2017b) and earlier on from the SB of *M. usaramensis* ssp *uramensis* (Yenesew *et al*., 1998).

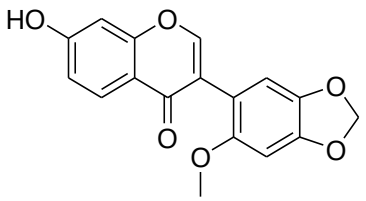

115

Table 4.18: NMR data of maximaisoflavone-G (115)

Position.	**δ_C**	**δ_H, *m*, (*J* in Hz)**	**HMBC (H → C)**
2	154.2	8.13, *s*	C-1′, C-3, C-4, C-9
3	112.9		
4	174.3		
5	127.2	7.92, *d*, (8.7)	C-4, C-6, C-7, C-9
6	115.1	6.92, *dd*, (8.7, 2.3)	C-7, C-8, C-10
7	162.5		
8	102.2	6.86, *d*, (2.3)	C-7, C-9, C-10
9	157.5		
10	116.6		
1′	121.5		
2′	152.8		
3′	111.1	6.81, *s*	C-1′, C-2′, C-4′, C-5′
4′	147.9		
5′	140.3		
6′	95.5	6.85, *s*	C-1′, C-2′, C-5′, C-3, C-4′
2′-OCH_3	56.6	3.65, *s*	C-2′
OCH_2O	101.2	6.00, *s*	C-4′, C-5′
7-OH		10.78, *s*	

4.2.3.7 (±) Deguelin (170)

Compound (**170**) was isolated as a white solid. This compound had the same characteristic features of a rotanoid as tephrosin (**171)**. It had an extra signal δ_H 3.82 (*d*, 1H, 4.2Hz) to the substituents of **171** which was assigned to H-12a.

The structure was confirmed from HMBC correlations Table (4.19) and the NMR data was consistent with that reported in literature for (±) deguelin isolated from seeds of *M. ferruginea* (Highet and Highet, 1967), from aerial parts of *Dalea ornate* (Wei *et al*., 2014; Lee *et al*., 2015; Nayak and Kim 2015; Deardorff *et al*., 2016) and seeds of *M. dura* (Yenesew *et al*., 2003).

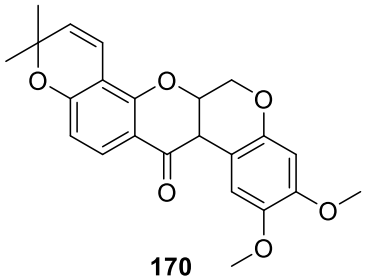

170

Table 4.19: NMR data of (±) deguelin (170)

Position.	δ_C	δ_H, *m*, (*J* Hz)	HMBC (H → C)
1	110.4	6.77, *s*	C-2, C-3, C-4a, C-12a, C-12b
2	143.8		
3	149.5		
4	111.5	6.43, *s*	C-2, C-3, C-4a, C-12a, C-12b
4a	146.7		
6	66.3	4.16, *dd*, (12.0, 1.0)	C-4a, C-6a, C-7a, C-12, C-12a
		4.61, *dd*, (12.0, 3.1)	
6a	72.3	4.89, *ddd*, (4.2, 3.1, 1.0)	C-6, C-7a, C-12 ,C-12a, C-12b
7a	157.3		
8	109.3		
9	160.1		
10	115.2	6.83, *d*, (8.7)	C-8, C-11, C-11a
11	128.6	7.72, *d*, (8.7)	C-7a, C-8,C-9, C-12
11a	112.8		
12	189.3		
12a	44.4	3.82 *d*, (4.2)	C-1, C-4a, C-11a, C-12b
12b	104.8		
2′	77.7		
3′	128.7	5.53, *d*, (10.1)	C-2′, C-5′, C-6′, C-8
4′	115.8	6.62, *d*, (10.1)	C-2′, C-7a, C-8, C-9
5′	28.5	1.42, *s*	C-2′, C-3′, C-4′, C-6′
6′	28.2	1.35, *s*	C-2′, C-3′, C-4′, C-5′
2-OCH_3	56.3	3.74, *s*	C-2
3-OCH_3	55.9	3.78, *s*	C-3

4.3 Compounds isolated and characterized from *Millettia leucantha*

The of this species produced mainly flavones while the roots yielded isoflavones as elucidated in the subsequent subsections.

4.3.1 Characterization of compounds from the leaves of *Millettia leucantha*

Four flavonoids were isolated and characterized from the leaves of *Millettia leucantha*. These included chrysin (2**29**), apigenin (2**30**), chrysin 7-*O*-*β*-*D*-glucoside (**231**), genkwanin (2**32**). This

being the first report of compounds **229**, **231** and **232** from the genus *Millettia* and the first report of **230** from *M. dura*.

4.3.1.1 Chrysin (229)

Compound **229** was obtained as a bright yellow powder. The ^{13}C NMR spectral signals at δ_C 161.8 (C-2), in range (157.4-165.8ppm), 105.5 (C-3), in range (102.3-113.7ppm) and δ_C 182.2 (C-4) in the range of (175.2-183.4ppm) together with ^{1}H NMR signal at δ_H 6.83 (H-3) allowed the characterization of this compound as a flavone (Agrawal, 1989). The presence of a highly deshielded singlet δ_H 12.68 (*s*, 1H, 5-OH) further specified this compound as a 5-hydroxyflavone.

The ^{1}H NMR did not show characteristic peaks for any substituent. The observed AB protons δ_H (6.08 (H-6) and δ_H 6.39 (H-8), *d*, 1H, *J* = 2.0Hz)) revealed substitution at C-7 to be through oxygenation by –OH as a biogenetical fulfillment. An ABX proton spin system was seen for δ_H 8.08 (*d*, 2H, *J* = 8.2Hz, H-2′/6′), 7.44 (*d*, 2H, *J* = 8.2Hz, H-3′/5′) and 7.47 (*m*, H-4′) typical of un-substituted ring B.

The structure was confirmed through HMBC correlations (Table 4.20) and it was found to be 5,7-dihydroxyflavone commonly reported as chrysin from the leaves and flowers of *Calycotome spinosa* (Larit *et al*. 2012) as well as terrestrial parts of *Scutellaria intermedia* (Karimov *et al*., 2017). This is also the first report of chrysin from this genus.

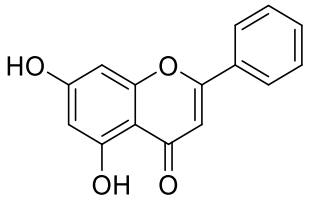

229

Table 4.20: NMR data of chrysin (229)

Position.	**δ_C**	**δ_H, *m*, (*J* in Hz)**	**HMBC (H → C)**
2	161.8		
3	105.5	6.83, *s*	C-1′, C-2, C-4, C-10
4	182.2		
5	165.0		
6	99.3	6.08, *d*, (2.0)	C-5, C-7, C-8, C-10
7	164.8		
8	94.4	6.39, *d*, (2.0)	C-6, C-7, C-9, C-10
9	157.8		
10	104.3		

Position.	δ_C	δ_H, *m*, (*J* in Hz)	HMBC (H → C)
1′	131.0		
2′/6′	126.7	7.93, *d*, (8.2)	C-2, C-2′/6′, C-4′
3′/5′	129.4	7.47, *d*, (8.2)	C-1′, C-3′/5′ C-4′
4′	132.3	7.44, *m*	C-2′/6′, C-3′/5′
5-OH		12.68, s	C-4, C-5, C-6, C-10

4.3.1.2 Apigenin (230)

Compound **230** was obtained as a yellow powder. Just like compound **229**, this compound was identified as a 5-hydroxy flavonoid, Table 4.21 (Pelter *et al*. 1976).

The *meta* coupled protons δ_H 6.29, 6.58 (*d*, 1H, *J* = 2.1Hz) were assignable respectively to H-6 and H-8, having C-7 oxygenated through a hydroxyl. The *ortho* ineracting protons δ_H 7.97, 7.06 (*d*, 2H, *J* = 8.9Hz) could only be attributed to H-2′/6′ and H-3′/5′. This is typical of an AA′BB′ spin system in ring B substituted at C-4′, in this case by a hydroxyl. While the singlet proton δ_H 6.67 (*s*, 1H) was assigned to H-3.

The HMBC correlation (Table 4.21) affirmed the assignments and the compound was found to be 4′,5,7-trihydroxyflavone which had earlier been reported as apigenin from the aerial parts of *Lespedeza virgata* (Yan *et al*., 2008), the twigs of *M. leptobotrya* Dunn (Zhi Na *et al.*, 2013) and the aerial parts of *Scutellaria intermedia* (Karimov *et al*., 2017).

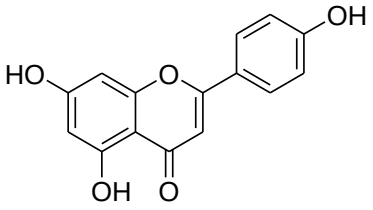

230

Table 4.21: NMR data of apigenin (230)

Position.	δ_C	δ_H, *m*, (*J* in Hz)	HMBC (H → C)
2	163.9		
3	103.4	6.67, *s*	C-1′, C-2, C-4, C-10
4	182.1		
5	157.9		
6	93.4	6.29, *d*, (2.1)	C-5, C-7, C-8, C-10
7	164.3		
8	99.7	6.58, *d*, (2.1)	C-6, C-7, C-9, C-10
9	153.4		

Position.	δ_C	δ_H, *m*, (*J* in Hz)	HMBC (H → C)
10	105.4		
1′	122.4		
2′/6′	128.4	7.97, *d* , (8.9)	C-2, C-2′/6′, C-4′
3′/5′	115.7	7.06, *d*, (8.9)	C-1′, C-3′/5′ C-4′
4′	161.2		
5-OH		13.05, *s*	C-5, C-6, C-10

4.3.1.3 Chrysin 7-*O*-*β*-*D*-glucoside (231)

This compound was obtained as light yellow powder. It had comparable characteristic peaks for a 5-hydroxyflavone as for compounds 2**29** and **230**, Table 4.22 (Agrawal, 1989). In addition to the spectral features of compounds **229** and **230**, the ^{13}C NMR of this compound showed peaks at δ_C 61.0, 69.9, 73.6, 76.9, 77.7 and 100.3 which are characteristic of a sugar moiety (Agrawal, 1989). The ^{1}H NMR also gave a peak at δ_H 5.11 (*d*, *J* = 6.7Hz, 2H) which is typical of an anomeric proton of a *β*-*D*-glucose moiety (Agrawal, 1989b; Andersen & Markham, 2006). Further still, peaks δ_H 3.73 (*d*), 3.47 (*d*), 3.33 (*d*), 3.31 (*d*) and 3.20 (*t*) in the ^{1}H NMR, are consistent with a glucose moiety. The correlation of the anomeric proton δ_H 5.11 with the oxygenated quaternary carbon δ_C 164.1 enabled the placement of the glucose moiety at C-7.

Basing on literature and the HMBC correlations (Table 4.22), compound **231** was found to be chrysin 7-*O*-*β*-*D*-glucoside isolated from the leaves of *Adenocarpus mannii* (Ndjateu *et al*., 2014), leaves and flowers of *Calycotome spinosa* (Larit *et al*., 2012) and leaves and aerial parts of *Acacia pennata* (Kim *et al*., 2015).

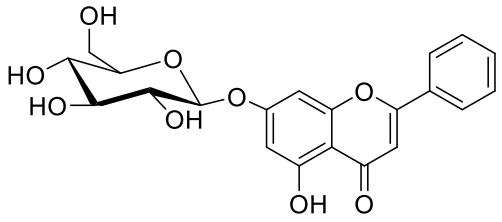

231

Table 4.22: NMR data of chrysin 7-*O*-*β*-*D*-glucoside (231)

Position.	δ_C	δ_H, *m*, (*J* in Hz)	HMBC (H → C)
2	163.7		
3	105.9	7.08, *s*	C-1′, C-2, C-4, C-10
4	182.7		
5	161.6		
6	100.2	6.49, *d*, (2.1)	C-4, C-7, C-8, C-10
7	164.1		

Position.	δ_C	δ_H, *m*, (*J* in Hz)	HMBC (H → C)
8	95.5	6.90, *d*, (2.1)	C-4, C-6, C-7, C-9, C-10
9	157.6		
10	106.1		
1′	131.1		
2′/6′	127.0	8.11, *d*, (7.6)	C-2, C-2′/6′, C-3′/5′, C-4′
3′/5′	129.7	7.63, *d*, (7.6)	C-1′, C-3′/5′
4′	132.7	7.61, *m*	C-1′, C-2′/6′
C-1″	100.3	5.11, *d*, (6.7)	C-5″, C-7
C-2″	73.6	3.33, *d*, (6.5)	
C-3″	76.9	3.31, *d*, (6.6)	
C-4″	69.9	3.20, *t*, (7.3, 6.6)	
C-5″	77.7	3.47, *d*, (7.3)	
C-6″	61.0	3.73, *d*, (9.2)	
5-OH		12.83, *s*	C-5, C-6, C-10

4.3.1.4 Genkwanin (232)

Compound **232** was a yellow powder and it had comparable spectral data to compound **229** except for a methoxy signal δ_H 4.02 (*s*, 3H)/ δ_C 55.7 in the NMR spectra. The attachment of this substituent was placed at C-7 due to the correlation of its proton δ_H 4.02 with δ_C 164.3, in conformity with the biogenetically expected oxygenation.

The complete structure was affirmed through HMBC correlations (Table 4.23) and it was found to be 5-hydoxy-7-methoxyflavone reported as genkwanin from *Enicostemma littorate* (leaves, roots and whole plant) (Sen *et al*., 2016).

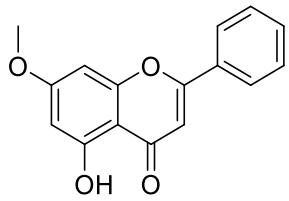

232

Table 4.23: NMR data of genkwanin (232)

Position.	δ_C	δ_H, *m*, (*J* in Hz)	HMBC (H → C)
2	163.8		
3	105.3	6.81, *s*	C-1′, C-2, C-4, C-10
4	182.3		
5	162.5		
6	99.0	6.31, *d*, (2.1)	C-5, C-7, C-8, C-10
7	164.3		

Position.	δ_C	δ_H, *m*, (*J* in Hz)	HMBC (H → C)
8	94.0	6.60, *d*, (2.1)	C-6, C-7, C-9, C-10
9	158.0		
10	100.0		
1′	131.8		
2′/6′	126.4	8.09, *d*, (8.2)	C-1′, C-2, C-2′/6′, C-4′
3′/5′	129.1	7.63, *d*, (8.2)	C-1′, C-3′/5′ C-4′
4′	131.4	7.63, *m*	C-2′/6′, C-3′/5′
7-OCH_3	55.7	4.02	C-7
5-OH		12.92, *s*	C-5

4.3.2 Characterization of compounds from the roots of *Millettia leucantha*

Six compounds were isolated and characterized from the roots of *Militia leucantha*. These are: 6, 7, 4′-trimethoxyflavone (**233**), taxasin (**234**), 6, 7, 4′-trimethoxyisoflavone (**235**), paraben acid (**236**) and maackiain (**237**).

4.3.2.1 6, 7, 4′-Trimethoxyflavone (233)

Compound **233** was obtained as a yellow powder. It was also characterized as a flavone based on the characteristic NMR signals, Table 4.24 (Agrawal, 1989). The signal δ_H 7.61 (*s*, 1H), δ_C 104.3 was indicative of C-3 unsubstituted flavone (Andersen and Markham, 2006). There were three methoxy substituents peaks, δ_H 3.83, 3.91 and 4.01 (*s*, 3H) in the ^{1}H NMR spectra.

The ^{1}H NMR further showed aromatic protons with an AA′XX′ spin state at δ_H 7.43 and δ_H 6.95 (2H, *d*, *J* = 8.7 Hz) consistent with a *para* substituted ring B. These were ascribed to H-2′/6′ and H-3′/5′ respectively, the former having correlated with δ_C 160.2 (C-2). The more deshielded aromatic singlet δ_H 7.80, was assigned to H-5 on its strong correlation with δ_C 174.9 (C-4) and δ_H 6.76 was then assigned to H-8.

The methoxy δ_H 3.83 correlating with the same carbon δ_C 159.5 as the AA′XX′ protons, was placed C-4′. While δ_H 3.91 was attached to C-7 basing on its strong correlation with δ_C 152.1, a carbon seen by the singlet at δ_H 7.80 (H-5). The remaining methoxy group δ_H 4.01 correlated with the same carbon δ_C 145.6 as the singlet δ_H 6.76 allowing its placement at C-6.

Compound **233** was identified as 6,7,4′-trimethoxyflavone based on literature and the HMBC correlations (Table 4.24). It had earlier been reported from *Gynerium sagittatum* (roots)

(Benavides *et al*. 2007). This is its first report from the genus *Millettia* and a second report as a natural product.

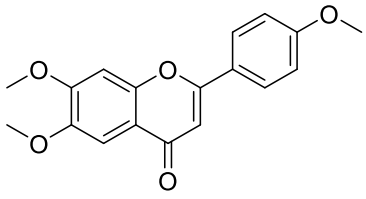

233

Table 4.24: NMR data of 6,7, 4′-trimethoxyflavone (233)

Position.	**δ_C**	**δ_H, *m*, (*J* Hz)**	**HMBC (H → C)**
2	160.2		
3	102.5	7.62, *s*	C-1′, C-4, C-10
4	174.9		
5	104.6	7.80, *s*	C-4, C-6, C-7, C-9, C-10
6	145.6		
7	152.1		
8	98.7	6.76, *s*	C-4, C-6, C-7, C-10
9	150.6		
10	113.7		
1′	124.4		
2′/6′	130.3	7.43, *d*, (8.7)	C-1′, C-2, C-2′/6′, C-4′
3′/5′	113.6	6.95, *d*, (8.7)	C-1′, C-3′/5′ C-4′
4′	159.5		
6-OCH_3	61.7	4.01, *s*	C-6
7-OCH_3	61.7	3.91, *s*	C-7
4′-OCH_3	55.3	3.83, *s*	C-4′

4.3.2.2 Taxasin (234)

Compound **234**, was gotten as a white solid. It was characterized to be an isoflavone Table 4.25 (Agrawal, 1989). The NMR spectrum showed peaks for a –OCH_3 ((δ_H 3.79 (*s*, 3H), δ_C 56.1) as the only substituent.

The AA′XX′ spin system in the ^{1}H NMR at δ_H 6.81 (H-3′/5′) and 7.34 (H-2′/6′), *d*, 2H, *J* = 8.6Hz,) suggested a *para* substitution in ring B. Further, the aromatic singlet protons at δ_H 7.84 and 6.73 were assignable to H-5 and H-8 respectively. The methoxy δ_H 3.79 correlated with δ_C 147.8 as H-8, allowing its placement to C-6. On this basis, C-7 and C-4′ were substituted with hydroxyl groups in accordance with the expected biogenetic oxygenation. The NMR data (Table 4.25) agreed with that in literature for 4′,7-dihydroxy-6-methoxyisoflavone, which was earlier reported as glycitein from soyabean seeds (Alnokari *et al*.,2016) and as taxasin (Agrawal, 1989).

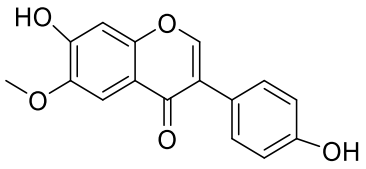

234

Table 4.25: NMR data of taxasin (234)

Position.	**δ_C**	**δ_H, *m*, (*J* in Hz)**	**HMBC (H → C)**
2	152.5	8.15,*s*	C-1′, C-4, C-9
3	128.5		
4	174.6		
5	127.2	7.84, *s*	C-4, C-7, C-9
6	147.8		
7	157.4		
8	102.3	6.69, *s*	C-6, C-7, C-9, C-10
9	166.5		
10	115.4		
1′	123.1		
2′/6′	130.4	7.34, *d*, (8.6)	C-1′, C-2′/6′, C-3, C-4′
3′/5′	115.5	6.81, *d*, (8.6)	C-1′, C-2′/6′, C-3′/5′, C-4′
4′	158.1		
6-OCH_3	55.7	3.78, *s*	C-6

4.3.2.3 6, 7, 4′-Trimethoxyisoflavone (235)

This compound had comparable spectral data to compound **234** Table 4.26 and it was therefore deduced to be an isoflavone. The ^{1}H spectra gave three substituent peaks δ_H 3.87, 3.95 and 4.06 (*s*, 3H) characteristic for methoxy groups. This compound had the same aromatic proton substitution pattern as compound **224**.

The more shielded methoxy group δ_H 3.87 correlated with δ_C 159.5 allowing its placement at C-4′. The methoxy group at δ_H 3.95 correlated with δ_C 151.4 while δ_H 4.06 correlated with δ_C 145.6 directing their placement at C-7 as well as C-6 respectively. The complete HMBC correlations Table (4.26) enabled characterization of this compound as 6, 7, 4′-trimethoxyisoflavone reported by (Agrawal, 1989). This again is the first report of this compound from this genus (Jha *et al*., 1980)

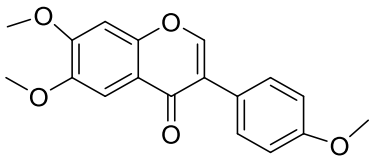

235

Table 4.26: NMR data of 6, 7, 4′-trimethoxyisoflavone (235)

Position.	δ_C	δ_H, *m*, (*J* in Hz)	HMBC (H → C)
2	152.1	7.97,*s*	C-1′, C-2, C-4, C-9
3	123.9		
4	175.3		
5	102.5	7.01, *s*	C-4, C-6, C-7, C-9, C-10
6	145.6		
7	151.4		
8	98.7	6.80, *s*	C-6, C-7, C-9, C-10
9	153.9		
10	117.8		
1′	124.5		
2′/6′	130.2	7.52, *d*, (7.8)	C-1′, C-2′/6′, C-3′/5′, C-3, C-4′
3′/5′	113.6	7.00, *d*, (7.8)	C-1′, C-3′/5′, C-4′
4′	159.5		
6-OCH_3	61.7	4.06, *s*	C-6
7-OCH_3	61.8	3.95, *s*	C-7
4′-OCH_3	55.3	3.87, *s*	C-4′

4.3.2.4 Paraben Acid (236)

The ^{13}C NMR of this compound had only 5-peaks (δ_C 168.7, 161.9, 131.6, 121.4 & 114.6). The ^{1}H NMR showed AA′XX′ spinning protons δ_H 6.85 and 7.92 (*d*, 2H, *J* = 8.8Hz). The proton at δ_H 7.98 (H-2/6) correlated with the carboxyl δ_C 168.7 and the quaternary at δ_C 161.9. This compound was identified as *p*-hydroxybenzoic acid previously reported as paraben acid (Harvey and Everett 2004; Soni *et al*., 2005; Kucekova *et al*., 2011).

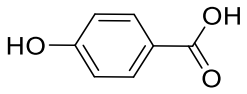

236

Table 4.27: NMR data of paraben acid (236)

Position.	δ_C	δ_H, *m*, (*J* in Hz)	HMBC (H → C)
1	121.4		
2/6	131.6	7.92, *d*, (8.8)	C-2/6, C-3/5, C-4, C=O
3/5	114.6	6.85, *d*, (8.8)	C-1, C-2/6, C-3/5, C-4, C=O
4	161.9		
C=O	168.7		

4.3.2.5 Maackiain (237)

This compound was obtained as a white solid. The ^{1}H NMR signals δ_H 3.58 (*d*, 1H *J* = 10.0Hz) and 4.23 (*dd*, 1H, *J* = 4.2, 10.0Hz) for the non-equivalent oxymethylene protons (H-2α/β), 3.69 (*m*) for the methine proton H-3 as well as 5.50 (*d*, 1H, *J* = 7.2Hz) for the oxymethine proton H-4 suggested **237** was a pterocarpan (Niu *et al*., 2013). The corresponding carborn peaks in the ^{13}C NMR at δ_C 66.3 (in the range 65.5-67.7) for the oxymethylene C-2, 39.7 (in the range 39.3-41.3) for the methine C-3 and 78.5 (in the range 77.4-79.1) for the oxymethine C-4, were typical of a C-2 unsubstituted pterocarpan (Agrawal, 1989). Additional quaternary signals δ_C 118.9 (in the range 117.3-119.4) for C-1′ and δ_C 154.2 (in the range 153.6-160.6) for C-6′ that make up the epoxide ring D of a pterocarpan (Agrawal, 1989) were evident in the ^{13}C NMR.

The NMR further showed signals δ_C 101.5, δ_H 5.93 (*s*, 2H) for a methylenedioxy and δ_H 9.64 (*s*, 1H) for a hydroxyl substituent. In addition, the ^{1}H NMR showed a pair of singlet δ_H 6.97 (*s*, 1H) and 6.52 (*s*, 1H), as well as an ABX spin system δ_H 7.23 (*d*, 1H, *J* = 8.6Hz), 6.47 (*dd*, 1H, *J* = 8.6, 2.5Hz) and 6.27 (*d*, 1H, *J* = 2.5Hz).

The hydroxyl δ_H 9.64 was fixed at C-7 on its correlation with the same carbons δ_C 109.3 (C-6), 158.7 (C-7) and 102.8 (C-8) as the ABX proton system. The δ_H 5.93 showing HMB cross peaks with δ_C 141.0 and 147.4, enabled the –OCH_2O- group to be placed between C-3′ and C-4′ allowing for the *para* singlet protons H-2′ and H-5′. Comparing data with literature and HMBC correlations (Table 4.28), Compound **237** was identified to be maackiain isolated from stem wood of *M. leucantha* (Chatsumpun *et al*., 2010), twigs of *M leptobotrya* Dunn (Zhi Na *et al*., 2013) and *M. dura* (RB) (Marco *et al*., 2017b).

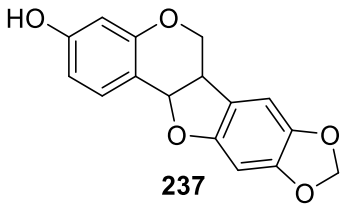

237

Table 4.28: NMR data of maackiain (237)

Position.	δ_C	δ_H, *m*, (*J* in Hz)	HMBC (H → C)
2	66.3	3.58, *d*, (10.0) 4.23, *dd*, (4.2, 10.0)	C-1′, C-4, C-9
3	39.7	3.69, *m*	C-2′, C-2, C-3, C-6′ C-10
4	78.5	5.50,*d*, (7.2)	C-2, C-5, C-9, C-10

Position.	δ_C	δ_H, *m*, (*J* in Hz)	HMBC (H → C)
5	132.5	7.23, *d*, (8.6)	C-4, C-7, C-9
6	110.1	6.47, *dd*, (2.5, 8.6)	C-7, C-8, C-10
7	159.2		
8	103.3	6.27, *d*, (2.5)	C-6, C-6′, C-9
9	156.8		
10	111.7		
1′	118.9		
2′	105.8	6.97,*s*	C-3′, C-4′, C-6′
3′	141.5		
4′	147.9		
5′	93.7	6.52,*s*	C-1′, C-3′, C-4′, C-6′
6′	154.2		
OCH_2O	101.5	5.50, *s*	C-3′, C-4′
7-OH		9.64, *s*	C-6, C-7, C-8

4.4 Compounds Isolated and Characterized from *Millettia lasiantha*

The study on the leaves, stems and roots of *M. lasiantha* yielded twelve metabolites. Their elucidation is described in the subsequent subsections.

4.4.1 Characterization of compounds from the leaves of *Millettia lasiantha*

From the leaves of *Millettia lasiantha*, four compounds were isolated. These compounds were chrysin (**229**), apigenin (**230**), chrysin-7-*O*-*β*-glucoside (**231**) and Luteolin (**238**). Only compound **238** is discussed, having discussed the other compounds in section 4.4.

4.4.1.1 Luteolin (238)

It was obtained as a yellowish solid. In the ^{13}C spectra, δ_C 165.1 (C-2), δ_C 104.2 (C-3) and 183.0 (C-4), together with the proton singlet δ_H 6.58 (s, 1H, H-3) suggested this compound was a flavone. In addition, the de-shielded singlet δ_H 13.02 (*s*, 1H) for the peri 5–OH in the ^1H NMR, confirmed a 5-hydroxy flavone. There was no substituent peak in the NMR spectra.

The *meta*-coupled protons δ_H 6.25 and 6.52 (*d*, 1H, *J* = 2.1Hz) in the ^1H NMR, were assigned respectively to H-6 and H-8, with C-7 being substituted with an -OH to fulfill the expected biogenetic oxygenation. The ABX spin system δ_H 7.00 (*d*, 1H, *J* = 8.3Hz), 7.47 (*dd*, 1H, *J* = 2.3, 8.3Hz) and 7.50 (*d*, 1H, *J* = 2.3Hz) represented a 3, 4-disubstitution in ring B.

The HMBC correlation (Table 4.29) affirmed the assignments and compound (**238**) was identified as 3′ ,4′, 5, 7-tetrahydroxyflavone which was reported as luteolin from the aerial parts of *lespedeza*

virgata (Yan *et al*., 2008) and also from *eclipta prostrata*.L (aerial parts) (Qi-Mei *et al*., 2012). This one is the first report of luteolin from the genus *Millettia*.

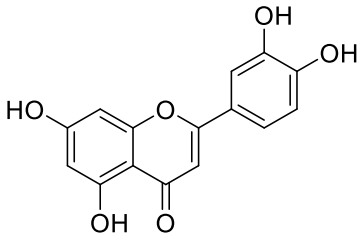

238

Table 4.29: NMR data of luteolin (238)

Position	δ_C	δ_H, *m*, (*J* in Hz)	HMBC (H → C)
2	165.1		
3	104.2	6.58, *s*	C-2, C-4, C-10, C-1′
4	183.0		
5	163.3		
6	99.7	6.25, *d*, (2.1)	C-5, C-7, C-8, C-10
7	164.9		
8	94.7	6.52, *d*, (2.1)	C-6, C-7, C-9, C-10
9	158.8		
10	105.3		
1′	123.7		
2′	114.1	7.50, *d*, (2.3)	C-2, C-3′, C-4′, C-6′
3′	146.5		
4′	150.1		
5′	116.6	7.00, *d*, (8.3)	C-1′, C-3′, C-4′
6′	120.1	7.47, *dd*, (8.3, 2.3)	C-2, C-2′, C-4′
5-OH		13.02, *s*	C-5, C-6, C-10

4.4.2 Characterization of compounds from the stem bark of *Millettia lasiantha*

Four compounds were identified from the stem bark comprising three known isoflavones formononetin (**91**), 6, 7, 4′-trimethoxyisoflavone (**235**), Geneistein (**239**) and a chalcone, isoliquiritigenin (**240**).

4.4.2.1 Genistein (239)

Genistein was obtained as white solid. The isoflavonoid skeltone was observed from δ_H 8.02 (*s*,1H), and δ_C 154.8 (C-2), 124.7 (C-3) and 182.2 (C-4). The ^{1}H NMR showed a deshielded singlet δ_H 12.81 (*s*, 1H) for 5-OH, indicating that compound **239** was a 5-hydroxyflavone (Table 4.30) (Agrawal, 1989).

The ^{1}H NMR revealed two AB spin protons δ_H 6.21 and 6.32 (*d*, *J* = 2.1Hz, 1H) attributed to ring A for the *meta* coupled protons H-6 and H-8. As well as an AA′XX′ spin system δ_H 6.85 and 7.92 (*d*, 2H, *J* = 8.8Hz) assignable to *ortho* coupled protons H-2′/6′ and H-3′/5′ respectively in ring B. C-7 and C-4′ had –OH substituents consistent with the expected biogenetic oxygenation.

The final structure was confirmed to be 4′, 5, 7-trihydroxyisoflavone from HMBC correlations Table 4.30. This compound was found to be genistein reported from *M. leptobotrya* Dunn. (twigs) (Zhi Na *et al*., 2013), also from the tuberous roots of *pueraria mirifica* (Chansakaow *et al*., 2000) as well as the heart wood of *Dalbergia boehmii* (Jean *et al*., 2017).

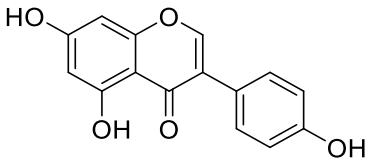

239

Table 4.30: NMR data of genistein (239)

Position	**δ_C**	**δ_H, *m*, (*J* in Hz)**	**HMBC (H→C)**
2	154.8	8.02, s	C-2,C-4,C-9, C-10, C-1′
3	124.7		
4	182.2		
5	163.8		
6	100.1	6.21, *d*, (2.1)	C-4, C-5, C-7, C-8, C-10
7	165.9		
8	94.8	6.32, *d*, (2.1)	C-4, C-6, C-7, C-9, C-10
9	159.5		
10	106.3		
1′	123.3		
2′/6′	131.4	7.36, *d*, (8.6)	C-2, C-2′/6′, C-4′
3′/5′	116.2	6.84, *d*, (8.6)	C-1′, C-2′/6′, C-3′/5′ C-4′
4′	158.8		
5-OH		12.81, *s*	

4.4.2.2 Isoliquiritigenin (240)

Compound (**240**) was obtained as a dirt brown gum. From the pair of trans-olefinic doublet protons (δ_H 7.59 (Hα) and 7.78 (Hβ), *d*, 1H, *J* = 15.4Hz,)) together with the corresponding δ_C 118.3 (C-α), 145.6 (C-β) and the conjugated carbonyl 193.5 in the NMR spectra, led to this compound being identified as a chalcone. The highly deshielded singlet δ_H 13.56, (*s*) for (2′-OH) in the ^{1}H NMR revealed it to be a 2′-hydroxychalcone (Agrawal, 1989).

The AA′BB′ system δ_H 7.60 (H-2/6) and 6.84 (H-3/5, *d*, 2H, *J* =8.6Hz,) in the ^{1}H NMR could only be assigned to ring B. The quaternary δ_C 158.2 (C-4) was oxygenated, a common pattern in ring B. Further, the ABX spin system at δ_H 6.28 (*d*, 1H, *J* = 2.4, H-3′), δ_H 6.41 (*dd*, 1H, *J* = 2.4, 8.8, H-5′) and δ_H 7.96 (*d*, 1H, *J* = 8.8, H-6′) were attributed to ring A with C-4′ being oxygenated, consistent with the expected biogenetic oxygenations.

Basing on the HMBC correlations (Table 4.31), compound **240** was characterized as 2′,4′,4-trihydroxychalcone earlier reported as isoliquiritigenin from the wood of *M. leucantha* (Rayanil *et al*., 2011), and also from the rhizomes and roots of *Glycyrrhiza uralensis*. Fisher (Tao *et al*., 2012; Bao *et al*., 2019) and *Sophora tonkinensis* (Yoo *et al*., 2014).

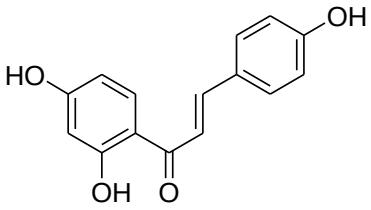

240

Table 4.31: NMR data of isoliquiritigenin (240)

Position	δ_C	δ_H, *m*, (*J* in Hz)	HMBC (H→C)
1	127.8		
2/6	131.8	7.60, *d*, (8.6)	C-1, C-2/6, C-3/5, C-4, C-β, C=O
3/5	116.9	6.84, *d*, (8.6)	C-1, C-2/6, C-3/5, C-4
4	161.5		
α	118.3	7.59, *d*, (15.4)	C-1, C-β, C=O
β	145.6	7.78, *d*, (15.4)	C-1, C-2/6, C-α, C=O
C=O	193.5		
1′	114.7		
2′	166.3		
3′	103.8	6.28, *d*, (2.4)	C-1′, C-2′, C-4′, C-5′
4′	167.5		
5′	109.1	6.41, *dd*, (8.8, 2.4)	C-1′, C-3′, C-4′
6′	133.4	7.96 ,*d*, (8.8)	C-1′, C-2′, C-3′, C-4′, C=O
2′-OH		13.56, *s*	

4.4.3 Characterization of compounds from the roots of *Millettia lasiantha*

Four compounds formononetin (**91**) and 7,3'-dihydroxy-2',4'-dimethoxycoumestan **(241)** trivial name lascoumestan, 7,5′-dihydroxy-6′,4′-dimethoxycoumaronochromone (**242**) trivial name lascoumaronochromone, and genistein-7-*O*-glucoside or genistin **(243)** where isolated from the roots, with **241** and **242** being novel.

4.4.3.1 3,8-dihydroxy-7,9-dimethoxycoumestan -trivial name lascoumestan (241)

Compound **241** was isolated as a white UV active solid. The HRESIMS gave $[M+H]^+$ at *m/z* = 329.0654 (calcd 329.0656) corresponding to $C_{17}H_{12}O_7$. The UV (λ_{max} at 254, 304 and 346nm) (Adityachaudhu and Gupta, 1973), the IR (3367 cm^{-1} for a free hydroxyl (Manki *et al*., 1981; Tao *et al*., 2012), 1716 cm^{-1} for δ-lactone carbonyl (Tamotsu and Shoji, 1969; Raju *et al*., 1981; Jacques *et al*., 2011), as well as 1625 and 1508 cm^{-1} for the two benzene rings (Pennaka *et al*. 2003) and the ^{13}C NMR (δ_C 160.6 (C-6), 103.4 (C-6a) and 157.2 (C-11a)) (Xianheng *et al*. 2019) suggested this compound was a coumestan derivative (Tamotsu and Shoji, 1969; Raju *et al*. 1981).

The NMR of this compound showed the presence of two methoxyl (δ_H 3.96 and 3.97 (3H, *s*); δ_C 57.0, 62.7) and two hydroxyls (δ_H 9.62 and 7.92 (1H, *s*)) substituents. The ^1H NMR further showed signals for three mutually coupled (δ_H 7.85 (1H, *d*, *J* = 8.6Hz), 6.98 (1H, *dd*, *J* = 8.6, 2.3Hz) and 6.91 (1H, *d*, *J* = 2.3Hz)) and a singlet (δ_H 7.22 (1H, *s*)) aromatic protons. HMBC correlations of the singlet aromatic proton (δ_H 7.22) with aromatic oxygenated carbons at δ_C 149.9, 149.6 and139.3 together with a quaternary non-oxygenated aromatic carbon at δ_C 111.5 allowed its placement at C-10 in ring D. The methoxy substituents at δ_H 3.96 (δ_C 62.7, HMQC) and 3.97 (δ_C 57, HMQC) were placed respectively, at C-7 (δ_C 141.4) and C-9 (δ_C 149.6) based on their corresponding HMBC correlations. The HMBC correlations of the hydroxyl at δ_H 7.69 with δ_C 149.6 (C-9), 141.4 (C-7) and 139.3 (C-8) permitted its placement at C-8 and thus the other hydroxyl at δ_H 9.62 at C-3. Hence, compound **241** was identified to be 3,8-dihydroxy-7,9-dimethoxycoumestan a new compound for which the trivial name lascoumestan is suggested. The structure was totally assigned based on COSY, HMQC and HMBC correlations, Table 4.32. This compound is novel, this being its first report.

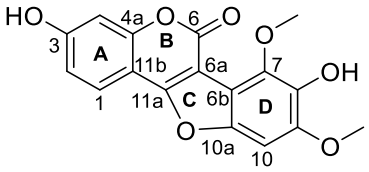

241

Table 4.32: NMR data for lascoumestan (241)

Position	δ_C	δ_H, *m*, (*J* in Hz)	HMBC (H→C)
1	123.6	7.85, *d*, (8.6)	C-3, C-4a
2	114.2	6.98, *dd*, (8.6, 2.3)	C-4, C-11b
3	161.9		
4	103.7	6.92, *d*, (2.3)	C-2, C-3,C-4a, C-11b
4a	156.1		
6	160.6		
6a	103.4		
6b	111.5		
7	141.4		
8	139.3		
9	149.6		
10	92.8	7.22, *s*	C-6b, C-8, C-9, C-10a
10a	149.9		
11a	157.2		
11b	105.8		
9-OCH_3	57.0	3.97, *s*	C-8
10-OCH_3	62.7	3.96, *s*	C-10
8-OH		7.69, *s*	C-7, C-8, C-9
3-OH		9.62, *s*	

4.4.3.2 7,5′-dihydroxy-4′,6′-dimethoxycoumaronochromone (lascoumaronochromone (242)

This compound was gotten as white non-crystalline solid. The HRESIMS molecular ion peak $[M+H]^+$ observed at *m/z* = 328.0587 (calcd 328.0583) corresponding to $C_{17}H_{12}O_7$. The ^{13}C-NMR gave signals at δc 161.9 (C-2), 114.7 (C-3), 173.1 (C-4), 111.5 (C-1′) and 150.0 (C-2′) that revealed presence of a coumaronochromone skeleton (Shou *et al*., 2009) characteristic for a 2,2'-epoxyisoflavone (Agrawal, 1989). The absence of a characteristic proton due to H-2 (usually appearing at δ ca 8) in the ^{1}H NMR spectrum confirmed a coumaronochromone skeleton (Shou *et al*., 2009).

The NMR of this compound showed two methoxyl substituents (δ_H 3.95 and 3.97 (3H, *s*); δ_C 57.0, 62.7). The ^{1}H NMR showed signals for three mutually coupled aromatic protons (δ_H 7.85 (1H, *d*, *J* = 8.4Hz), 6.98 (1H, *dd*, *J* = 8.4, 2.4Hz) and 6.91 (1H, *d*, *J* = 2.4Hz)) and a singlet (δ_H 7.20 (1H, *s*)). HMBC correlations of the aromatic singlet proton (δ_H 7.20) with aromatic oxygenated carbons at δ_C 150, 149.7 and 139.3 together with a quaternary non-oxygenated aromatic carbon at δ_C 111.5 allowed its placement at C-3′ in ring D. The methoxy substituents at δ_H 3.96 and 3.97 were placed respectively, at C-6′ (δ_C 141.5) and C-4′ (δ_C 149.7) based on their corresponding HMBC

correlations Table 4.33. This implied the three mutually coupled protons were assignable to a tri-substituted (Fang *et al*., 2019) phenyl ring A.

The complete NMR data shown in Table 4.33, led to identification of compound **242** as 7,5′-dihydroxy-6′,4′-dimethoxycoumaronochromone for which a trivial name lascoumaronochromone has been suggested. This compound is novel as well, as this is its first report.

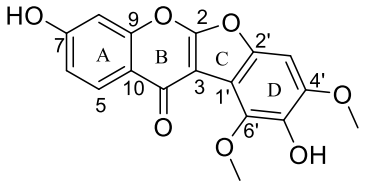

242

Table 4.33: NMR data of lascoumaronochromone (242)

Position	**δ_C**	**δ_H *m*, (*J* in Hz)**	**HMBC (H→C)**
2	161.9		
3	114.7		
4	173.1		
5	123.6	7.85, *d*, (8.4)	C-7, C-9
6	114.2	6.98, *dd*, (8.4, 2.4)	C-7, C-8, C-10
7	156.1		
8	103.7	6.91, *d*, (2.4)	C-6, C-7, , C-9, C-10
9	157.2		
10	105.8		
1′	111.5		
2′	150.0		
3′	92.9	7.20, *s*	C-1′, C-2′, C-4′, C-5′
4′	149.7		
5′	139.3		
6′	141.5		
6′-OCH_3	62.7	3.95, *s*	C-6′
4′-OCH_3	57.0	3.97, *s*	C-4′

4.4.3.3 Genistin (233)

Compound **233** was isolated as white solid. The ESIRMS gave $[M+H]^+$ m/z 433.1125 for $C_{21}H_{20}O_{10}$. The NMR showed signals δ_H 12.82, 8.15/ δ_C 155.3, 123.1 and 182.5 for a 5-hydroxyisoflavone (Agrawal, 1989). UV λmax 242, 264, 326nm was consistent with an isoflavone skeleton (Bandyukova and Kazakov, 1979; Li *et al*., 2011).

The ^{13}C NMR peaks at δ_C 62.4, 71.9, 74.7, 77.8, 78.4 and 101.6, together with δ_H 5.05 (*d*), 3.92 ,3.71 (*dd*), 3.53 (*dd*), 3.51 (*d*), 3.49 (*d*) and 3.42 (*d*) signals in the ^1H NMR revealed a glucose

moiety (P.K Agrawal 1989).The ^{1}H NMR signal δ_H 5.05 (*d*, *J* = 7.2Hz, 2H) is typical of an anomeric proton of a *β-D*-glucose moiety (Agrawal, 1989; Andersen and Markham, 2006).

The ^{1}H NMR showed a pair of *meta* coupled protons δ_H 6.52 and 6.71 (*d*, *J* = 2.3Hz, 1H) attributed to ring A as well as *ortho* coupled protons 6.85 and 7.31 (*d*, *J* = 8.6Hz, 1H) typical of a *para* substituted ring B. Correlation of the anomeric proton δ_H 5.05 with the oxygenated quaternary carbon δ_C 164.8 enabled the placement of the glucose moiety at C-7. Complete assignment was based on HMB correlations, Table 4.34 and compound 243 was found to be genistein-7-*O*-*β*-*D* -glucoside. It is a known isoflavone reported from roots of *Flemingia philippinensis* (Li *et al*., 2011), from *genista* (Bandyukova and Kazakov, 1979).

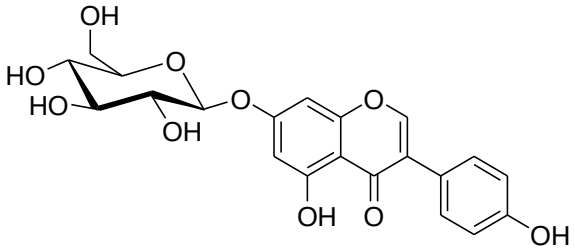

243

Table 4.34: NMR data of genistin (243)

Position	δ_C	δ_H, *m*, (*J* in Hz)	HMBC (C→H)
2	155.3	8.15, *s*	C-1', C-2, C-4, C-9
3	123.1		
4	182.5		
5	163.6		
6	101.1	6.52, *d*, (2.3)	C-5, C-7, C-8, C-10
7	164.8		
8	95.9	6.71, *d*, (2.3)	C-6, C-7, C-9, C-10
9	159.3		
10	108.0		
1'	125.1		
2'/6'	116.3	6.85, *d*, (8.6)	C-3, C-2'/6', C-4'
3'/5'	131.4	7.31, *d*, (8.6)	C-1, C-3'/5', C-4'
4'	159.0		
1"	101.6	5.05, *d*, (7.2)	C-7
2"	78.4	3.53, *dd*, (5.8)	C-4"
3"	74.7	3.49, *d*,	C-1", C-2", C-4", C-5"
4"	71.2	3.42, *d*, (9.4)	C-6", C-2"
5"	77.8	3.51, *d*, (1.8)	C-1", C-3"
6"	62.4	3.92, *dd*, (12.2, 2.1)	C-2", C-4"
		3.71, *dd*, (12.2, 2.1)	

4.5 Biological activities

Antiplasmodial and cytotoxicity studies were done on the extracts of *M. dura* and some of the pure compounds isolated. The subsections 4.7.1 and 4.7.2 give details of the results obtained.

4.5.1 Antiplasmodial results

The crude extracts (CH_2Cl_2/MeOH (1:1v/v)) of *Millettia dura* (Flowers, stem bark and seedpods) as well as ten compounds were tested for anti-*plasmodial* activity towards both chloroquine sensitive (D6) as well as chloroquine resistant (W2) *Plasmodium falciparum* strains. The common anti-malarial drug chloroquine was used as positive control.

The stem bark crude extract had the highest respective activities of 31.9±8.6 and 23.1±4.5µg/ml against W2 and D6. The Seeds extract had the least activities of 68.5±9.3 towards W2 and 79.1±9.8µg/ml against D6. Durmillone (**99**), Isoerythrine-A-4′-(3-methylbutyl-2-ethyl)ether (**102**), milletone (**172**) and milletosin (**173**) were the most active compounds against both strains, Table 4.35. The only flavone tested, kaempferol (**227**) had no activity towards either strain. In general, isoflavones have a better activity against W2 and D6 than flavones. Important still, the activity of the pure compounds isolated from the seed crude extract was far better than that of the crude itself, an effect attributable to antagonism of the compounds in the crude extract.

Table 4.35: Antiplasmodial results

	IC_{50} in (µM±SD)	
Sample tested	**W2**	**D6**
Calopogoniumisoflavone-A (**97**)	69.6±7.5	47.7±6.9
Jamaicin (**98**)	50.2±2.9	56.4±2.1
Durmillone (**99**)	36.7±2.9	39.3±7.8
Durallone (**100**)	53.6±2.3	42.8±2.3
Isoerythrine-A-4′-(3-methylbutyl-2-ethyl)ether(**102**)	37.2±8.1	41.3±9.4
Barbigerone (**114**)	39.5±8.5	53.2±9.1
Ichthynone (**123**)	>100	62.1±8.2
Millettone (**172**)	33.1±3.7	27.4±3.1
Millettosin (**173**)	44.0±4.5	33.3±12.1
Kaempferol (**227**)	>100	>100
Flower extract	56.6±4.1	56.8±13.1
Stem bark extract	31.9±4.3	23.1±4.5
Seeds extract	68.5±9.3	79.1±9.8
Chloroquine (standard)	0.082±0.011	0.008±0.046

4.5.2 Cytotoxicity isoflavones from *Millettia dura*

Twelve flavonoids isolated from *M. dura* were assessed for cytotoxicity (Table 4.36) towards five cell-lines; A549, Hep-G2, BEAS-2B, LO2 and CCD 19Lu, the latter three are non-cancerous controls.

Table 4.36: Cytotoxicity of isoflavones from *Millettia dura*

Key: (N)-Normal cell-line, (C)-Cancer cell-line, NT- Not Tested;

	Normal Cell-line			Cancer Cell-line	
Compound	**BEAS-2B(N)**	**LO2 (N)**	**CCD19Lu (N)**	**A549 (C)**	**HepG2 (C)**
Calopogonium isoflavone A (**97**)	>100	6.3±0.8	>100	>100	24.2±2.9
Jamaicin (**98**)	>100	68.7±10.6	>100	11.4±5.0	44.3±3.1
Durmillone (**99**)	58.4±2.8	78.4±2.8	>100	6.6±1.2	>100
Durallone (**100**)	>100	>100	>100	>100	>100
Ichthynone (**123**)	>100	>100	NT	> 100	>100
Kaempferol (**227**)	57.1±6.4	>100	NT	>100	>100
Isoerythrin-A-4′-(3-methylbut-2-enyl)ether (**102**)	21.2 ± 3.8	55.8±3.1	NT	14.3±1.2	37.7±3.8
Maximaisoflavone-B (**94**)	55.8±7.9	38.6±2.2	NT	48.5±9.0	>100
Maximaisoflavone-G (**115**)	100	67.5±1.5	NT	84.5±17.3	>100
7,2′-Dimethoxy-4′, 5′-methylenedioxyisoflavone (**93**)	>100	>100	>100	>100	88.4±4.1
Maximaisoflavone D (**92**)	47.9±3.8	29.5±3.2	49.6	>100	10.4±1.1
Isojamaicin (**105**)	>100	75.5±2.8	>100	>100	34.5±3.9
Tephrosin (**171**)	NT	NT	NT	3.14	NT
Milletone (**172**)	NT	NT	NT	29.3	NT
Milletosin (**173**)	NT	NT	NT	48.6	NT
Paclitaxel (standard)	<0.1	<0.1	<0.1	0.0033	0.19

Key: (N)-Normal cell-line, (C)-Cancer cell-line, NT- Not Tested;

Tephrosin (**171**) and durmillone (**99**) were the most active compound showing selective cytotoxicity against A549 adenocarcinomic human alveolar basal epithelial cancer cell line, with respective IC_{50} values of 3.1±1.2 and 6.6±1.2µM. Jamaicin (**98**) showed toxicity to the cancer cell lines A549 (IC_{50} 11.4±5.0µM) and HePG2 (44.3±3.2µM) without significant toxicity against the normal cells BEAS-2B and CCD19Lu (IC_{50} >100µM) but it is cytotoxic to LO2 (IC_{50} 68.7±10.6µM). Apart from maximaisoflavone D (**92**), the other active metabolites have a 2,2-dimethylchromene to ring A between C-7 and C-8. The additional C_5 unit made from cyclization of isoprenoid moiety at C-8 rises lipophilicity alongside membrane penetrability, explaining the observed activities as observed (Sasaki *et al*., 2011). Jamaicin (**98**) and isojamaicin (**105**) were also screened towards DLD-1WT (cancerous cells) and DLD-1 DKO (normal cells), and jamaicin (**98**) showing modest activity for the cancerous cells DLD-1WT (IC_{50} = 20.9±0.9µM) with no toxicity towards the normal cells DLD-1 DKO, while the isomeric isoflavone isojamacin (**105**)

was toxic against both cell lines (IC_{50} =14.5±3.4 9μM against DLD-1WT) and (IC_{50} =13.5±0.6μM) against DLD. The only tested flavonol, kaempferol (**227**), was cytotoxic to the normal cell line BEAS-2B having an IC_{50} value of 57.1±6.4μM and was not active to the other cell lines (IC_{50} > 100μM).

4.6 Chemotaxonomic significance of the flavonoids of *M. dura* and *M. ferruginea*

Millettia ferruginea (Hochst.) Baker which is endemic to Ethiopia (Gillet *et al*., 1971) has an infraspecific taxon, *M. ferruginea* ssp. *darassana* (The Plant List, 2013). It is morphologically related to *M. dura*. The only difference between the two species is that, *M. dura* has narrower pods, longer and more spreading indumentum of its calyx and pedicel, in addition to having no cylindrical disc observed in *M. ferruginea* (Gillet *et al*., 1971). Phytochemically, chalcones, a flavanone and flavononol, isoflavones, rotenoids and pterocarpanoids have been reported (Table 4.37) from these taxa (Buyinza *et al*., 2020).

4.6.1. Chemotaxonomic significance of chalcones, flavonones and flavanol

From *M. dura* and *M. ferruginea*, a total of five chalcones (**26**, **28**, **43**, **228** and **244**) have been reported (Table 4.37). Whereas compounds **28** and **288** isolated from *M. dura* are simple chalcones which appear to be precursors to several flavonoids of these taxa, compounds **43** and **244** are C-prenylated. Compound **26** is gerenylated and has only been reported from *M. ferruginea* ssp. *darasana* (Dagne, *et al*., 1989) but its occurrence has also been reported in *M. usaramensis* (Yenesew *et al*., 1998; Deyou *et al*., 2015). Approximately 80% of the chalcones have been reported from *dura* and are concentrated in the roots and stem bark (Buyinza *et al*., 2020).

A flavonol (**227**) isolated from the flowers of *M. dura* (Buyinza *et al*., 2019) and a flavonone (**49**) from stem bark of *M. ferruginea* (Dagne *et al*., 1989) represent simple flavonoids which occur widely in different genera of the family Fabaceae and are of little chemotaxonomic value.

4.6.2 Chemotaxonomic significance of isoflavones

A total of 33 isoflavones have so far been reported from *M. dura* and *M. ferruginea*; among these 23 contain a prenyl group at C-8 or its modification into a 2,2-dimthylchromene ring involving the hydroxy group at C-7 (Buyinza *et al*., 2020). Such compounds occur in all the three taxa (Table 4.37). *C*-Prenylation has only been observed at C-8, while there are 5 examples of *O*-prenylated

isoflavones (**94**, **102**, **109**, **112** and **245**) at either C-7 or C-4′, occurring in *M. dura*, with **109** also reported from *M. ferruginea* ssp. *darassana*. There is only one example of *O*-geranylated isoflavone (compound **246**) reported from *M. ferruginea* ssp. *darassana* (Table 4.37). The rest of the 14 isoflavones are simpler isoflavones substituted with methoxy and/or methylenedioxy groups. There are 9 isoflavones (Table 4.37) with free hydroxy groups, and except for 6-demethyldurallone (**103**), the free hydroxy group in the isoflavones of these taxa is always at C-7. These isoflavones, upon methylation or cyclization involving the adjacent prenyl group, produce the corresponding alkylated isoflavones which co-occur in these plants.

Except for three isoflavones (**247**, **248** and **249**) which only occur in *M. ferruginea* ssp. *darasana*, all the isoflavones reported from these taxa are 5-deoxy derivatives, indicating that they are derived from trihydroxychalcone (isoliquiritigenin) through the flavanone liquiritigenin mediated by the enzyme CHI (Andrej *et al*., 2004). In ring A, in addition to the biogenetically expected oxygenation at C-7, oxygenation has been observed at C-6 in 12 of these isoflavones (Table 4.37, **103**, **100**, **99**, **154**, **247**, **123**, **248,101,116**, **249**, **107** and **251**). Of which, six (**100**, **99**, **123**, **101**, **116** and **107**) were reported from *M. dura*, six (**99**, **247**, **123**, **248**, **249** and **251**) from *M. ferruginea* ssp. *darasana* and three (**103, 99** and **248**) from *M. ferruginea.* Among the C-6 oxygenated isoflavones, only compound **99** is shared among these three taxa. On the other hand, oxygenation at C-8 is rare and is observed only in three isoflavones (**108**, **92** and **106**), all of which isolated from *M. dura*.

A methylenedioxy group in ring A has been reported for compounds **92** and **106**, both of which isolated from *M. dura.* However, this is a more common feature in ring B as found in 17 isoflavones (Table 4.37; **104**, **93**, **95**, **99, 154, 118**, **247**, **123**, **105, 98, 94**, **115**, **106**, **248**, **249**, **251** and **252**). In ring B, in addition to the biogenetic expected oxygenation at C-4′, oxygenation has also been observed at C-2′ or C-6′ in 7 isoflavones (**144**, **95**, **118**, **123**, **98**, **250**, and **252**). The more preferred additional oxygenation in this ring is at C-3′ or C-5′, with 24 isoflavones (Table 4.37) oxygenated at one of these two positions. Among these, 6 compounds (**93**, **105**, **115**, **116**, **118** and **252**) are oxygenated at both C-3′ and C-5′, a feature more common in *M. dura*, having 5 compounds (**93**, **105**, **115**, **116** and **118**) than in *M. ferruginea* ssp. *darasana* (one isoflavone, **118**) and *M. ferruginea*, (two isoflavones, **105** and **118**).

4.6.3 Chemotaxonomic significance of rotenoids

A total of seven rotenoids have been reported from both *M. dura* and the two taxon of *M. ferruginea,* all of which having a pyran (**170**, **183**, **172**, **173** and **171**) or furan (**202** and **174)** group attached to ring D, at C-8/C-9. Two of these (**172**, and **173**) have a methylenedioxy group between C-2 and C-3 in ring A, while the rest have methoxy groups at these positions. All the reported rotenoids are C-11 deoxygenated and only **183** is a 6a,12a-dehydrorotenoid. It is only tephrosin (**171**) which has been reported across the three taxa, while **170** and **174** are shared between *M. dura* and *M. ferruginea*, while compound **202** is shared between *M. dura* and *M. ferruginea* ssp *darasana*. Compounds **183**, **172** and **173** reported only from *M. dura*, can distinguish this taxon from *M. ferruginea* (Buyinza *et al*., 2020). The B/C ring junction in these rotenoids and 12a-hydroxyrotenoids is *cis*-oriented, and have the same absolute configuration with 6a*S*,12a*S* designation for the rotenoids (**170**, **172**, and **174**), and 6a*R*,12a*R* designation for the 12a-hydroxyrotenoids (**202**, **173** and **171**) as determined by ORD (Ollis *et al*., 1967). Of the two pterocarpans reported, flemichapparin B (**153**) is shared between *M. dura* and *M. ferruginea* ssp *darasana,* while 3-*O*-prenylmaackianin (**166**) has only been reported from *M. dura*.

4.6.4 Chemotaxonomic significance of flavonoids and isoflavanoids

Whereas C-6 oxygenated isoflavones are common in all the three taxa, at C-8 (**108**, **92** and **106**), oxygenation has only been observed in *M. dura* but not in the two taxon of *M. ferruginea* and *M. ferruginea* ssp *darasana.* The *O*-prenylated isoflavoneisoerythrine A 4′-(3-methylbut-2-enyl)ether (**102**), the isoflavones 6-demethyldurallone (**103**), durallone (**100**), durlettone (**245**) have only been reported from *M. dura*. The rotenoids millettone (**173**) and Millettosine (**171**) with methylenedioxy group at C-2/C-3 appears to delineate *M. dura* from the two taxon of *M. ferruginea.* The C-5 oxygenated isoflavones 7-hydroxy-5,6-dimethoxy-3′,4′-methylenedioxyisoflavone (**247**), 5-methoxydurmillone (**248**) and pre-5-methoxydurmillone (**249**) from the two taxon of *M. ferruginea,* have not been reported in *M. dura*. The two taxon of *M. ferruginea* can be distinguished by the presence of the geranylated chalcone 4′-*O*-geranylisoliquiritigenin (**26**) and the isoflavones, 7-*O*-geranylformononetin (**246**) in *M. ferruginea* ssp *darasana* which have not yet been found in *M. ferruginea.*

Table 4.37: Distribution of flavonoids in different parts of *M. dura* and *M. ferruginea*

COMPOUND	Occurrence			
	Millettia dura	***M. ferruginea* ssp. *darassana***	***M. ferruginea***	**Other *Millettia* Sources**
Chalcones				
4′-*O*-Geranylisoliquiritigenin (**26**)		RB (Dagne *et al*., 1990b)		*M. usaramensis* ssp *usaramensis* (RB, SB) Deyou *et al*., 2015; (Yenesew *et al*., 2003b, 1998)
Butein (**28**)	RB (Marco *et al*., 2017)			
4-Hydroxyderricin (**43**)	SB, RB (Dagne *et al*., 1991)			
4,2′-Dihydroxy-4′-methoxychalcone (**228**)	FL (Buyinza *et al*., 2019)			
4-Hydroxylonchocarpin (**244**)	SB (Dagne *et al*., 1991)		SB (Dagne *et al*., 1989)	
Flavones				
Kampferol (**227**)	FL (Buyinza *et al*., 2019)			
Flavanone				
4′-Hydroxyisolonchocarpin (**49**)			SB (Dagne *et al*., 1989)	*M. pachycarpa* (SD) (Yanbe et al. 2019)
Isoflavones				
Barbigerone (**114**)	SB (Buyinza *et al*., 2019)	SD (Dagne and Bekele 1990a)	SD (Dagne and Bekele 1990a)	*M. usaramensis* (SB) (Yenesew, *et al.*, 1998), *M. dielsiana* Harms (ST) (Ye et al. 2014), *M. pachycarpa* (SD) (Tu et al. 2019)
Calopogoniumisoflavone A (**97**)	FL (Buyinza *et al*., 2019), SD, SB (Yenesew *et al.*, 1996)	SD (Dagne and Bekele 1990a)	SD (Dagne and Bekele 1990a)	*M. oblate* (SB) (Derese et al. 2014d), *M. dielsiana* (SB) (Ye *et al*., 2014)
Calopogoniumisoflavone B (**104**)	RB (Dagne *et al*., 1991; Marco *et al*., 2017)		SB (Dagne *et al*., 1989)	*M. griffoniana* (Yankep *et al*., 1997)
6-Demethyldurallone (**103**)	SB (Yenesew *et al*., 1996)			
7,2′-Dimethoxy-4′, 5′-methylenedioxyisoflavone (**93**)	RB (Dagne *et al*., 1991; Marco *et al*., 2017)			

COMPOUND	Occurrence			
	Millettia dura	***M. ferruginea* ssp. *darassana***	***M. ferruginea***	**Other *Millettia* Sources**
7,3′-Dimethoxy-4′,5′-methylenedioxyisoflavone (**95**)	SB (Derese *et al*., 2003)			
7-Hydroxy-8,3′,4′-trimethoxylisoflavor (**108**)	RB (Marco *et al*., 2017)			*M. usaramensis* (RB) (Deyo *et al*., 2015)
Durallone (**100**)	FL (Buyinza *et al*., 2019); SD, SB (Yenesew *et al*., 1996)			*M. oblata* (ST) (Derese *et al*., 2014) and *M. dielsiana* (ST) (Ye *et al*., 2014).
Durlettone (**245**)	SD (Ollis *et al*., 1967; Dagne *et al*., 1991)			
Durmillone (**99**)	FL (Buyinza *et al*., 2019); SB (Yenesew *et al*., 1996); RB (Marco *et al*., 2017); SD (Ollis *et al*., 1967)	SP (Dagne *et al*., 1989); SD (Dagne and Bekele 1990a)	SD (Dagne and Bekele 1990a)	*M. grifoniana* (RB) (Yankep *et al*., 1997),
6,7-Dimethoxy-3′,4′-methylenedioxy-8-(3,3-dimethylallyl)isoflavone (**154**)			SD (Deyou and Jang 2018)	
Ferrugone (**118**)	SB (Buyinza *et al*., 2019); SD (Ollis *et al*., 1967); SP (Yenesew *et al*., 1997)	SB (Dagne *et al*., 1989); SD (Dagne and Bekele 1990a)	SB (Dagne *et al*., 1989); SD (Dagne and Bekele 1990a)	
Formononetin (**91**)	FL (Buyinza *et al*., 2019); SP (Yenesew *et al*., 1997)			
7-*O*-Geranylformononetin (**246**)		RB (Dagne et al. 1990b)		
7-Hydroxy-5,6-dimethoxy-3′,4′-methylenedioxisoflavone (**247**)		SB (Dagne *et al*., 1989)		
Ichthynone (1**23**)	FL (Buyinza *et al*., 2019); SB (Ollis *et al*., 1967)	SB (Dagne *et al*., 1989)		*M. caerulea* (FT) (Ren *et al*., 2016), *M. pachyloba* (GR) (Mai et al. 2010), *M. dielsiana* (ST) (Ye *et al*., 2014)
Isoerythrin A, 4′-(3-methylbut-2-enyl) ether (**102**)	SB (Yenesew *et al*., 1996); RB (Derese *et al*., 2003; Marco *et al*., 2017)			
Isojamaicin (**105**)	SB (Derese *et al*., 2003)		SB (Dagne *et al*., 1989)	*M. usaramensis* ssp *usaramensis* (SB) (Derese

COMPOUND	Occurrence			
	Millettia dura	***M. ferruginea* ssp. *darassana***	***M. ferruginea***	**Other *Millettia* Sources**
				et al., 2003; Yenesew *et al*., 1998)
Jamaicin (**98**)	FL, SB (Buyinza *et al*., 2019); SP (Yenesew *et al.*, 1997)	SB (Dagne *et al*., 1989); RB (Dagne and Bekele 1990a)	SB (Dagne *et al*., 1989)	*M. usaramensis* ssp. *usaramensis* (SB) (Yenesew *et al*., 1998), *M. grifoniana* (RB), *M. pachyloba* (GR) (Mai *et al*., 2010).
Maximaisoflavone B (**94**)	SB (Dagne *et al*., 1991); RB (Marco *et al*., 2017)			*M. oblata* (LV) (Deyou *et al*., 2017)
Maximaisoflavone D (**92**)	SB (Yenesew *et al*., 1996)			
Maximaisoflavone G (**115**)	SB (Buyinza *et al*., 2019)			*M. oblata* (LV) (Deyou *et al*., 2017)
Maximaisoflavone H (**106**)	SB & RB (Dagne *et al*., 1991; Yenesew *et al.*, 1996)			*M. oblata* (RB) (Deyou *et al*., 2015)
Maximaisoflavone J (**112**)	FL,SB (Buyinza *et al*., 2019)			*M. oblate ssp* (ST, LV) (Deyou *et al*., 2017)
5-Methoxydurmillone (**248**)		SB (Dagne *et al*., 1989) , RB (Dagne and Bekele 1990a)	SB (Dagne *et al*., 1989)	
6-Methoxylcalopogoniumisoflavone A (**101**)	FL (Buyinza *et al*., 2019); SD (Yenesew, *et al.*, 1997)			*M. dielsiana* (ST) (Ye *et al*., 2014), *M. oblata* (ST) (Derese *et al*., 2014)
Mildurone (**116**)	SD (Ollis *et al*., 1967)			*M. oblata* (LV) (Deyou *et al*., 2017)
Nordurlettone (**109**)	RB (Derese *et al*., 2003)	(RB) (Dagne *et al*., 1990b)		
Pre-5-methoxydurmillone (**249**)		RB (Dagne and Bekele 1990a)		
Prebarbigerone (**250**)			SD (Dagne and Bekele 1990a)	
Predurallone (**107**)	SP (Yenesew *et al.*, 1996)			

COMPOUND	Occurrence			
	Millettia dura	***M. ferruginea* ssp. *darassana***	***M. ferruginea***	**Other *Millettia* Sources**
Predurmillone (**251**)		SD (Dagne and Bekele 1990a)		
Preferrugone (**252**)		SD (Dagne and Bekele 1990a)		
Rotenoids				
Deguelin (**170**)	SD (Ollis *et al*, 1967); SP (Buyinza *et al*., 2019)		SD (Dagne *et al*., 1991)	*M. pachycarpa* (SD) (Tu *et al*., 2019)
6a,12a-Dehydrodeguelin (**183**)	SD (Ollis *et al*., 1967)			*M. oblata* (LV) (Deyou *et al*., 2017)
12a-Hydroxyrotenone (**202**)	(Dagne *et al*., 1991)	SD (Dagne and Bekele 1990a)		*M. pachycarpa* (SD) (Tu *et al*., 2019)
Millettone (**172**)	SD (Ollis *et al*, 1967); SP (Yenesew *et al*., 1997)			
Millettosin (**173**)	SD (Ollis *et al*, 1967)			*M. usaramensis* (RB, SB) (Deyou *et al*., 2015, Yenesew *et al*., 1998)
Rotenone (**174**)	SD (Ollis *et al*., 1967)		SD (Dagne and Bekele 1990a)	*M. pachycarpa* (SD), (Ashok *et al*., 1982)
Tephrosin (**171**)	SD (Ollis *et al*, 1967); SP (Yenesew *et al*., 1997; Buyinza *et al*., 2019)	SD (Dagne and Bekele 1990a)		*M. oblata* (RB, LV) (Deyou *et al*., 2015; 2017), *M. usaramensis* (SD) (Yenesew *et al*., 1998), *M. usaramensi* (RB) (Deyou *et al*., 2015), *M. pachycarpa* (SD) (Tu *et al*., 2019)
Pterocarpene				
Flemichapparin B (**253**)	SB (Dagne *et al*., 1989)	SB (Dagne *et al*., 1989)		
3-*O*-Prenylmaackiain (**166**)	RB (Marco *et al*., 2017			

Key: LV Leaves, FL Flowers, SP Seed pods, SD seeds, FT Fruits, GR Grains, SB Stem bark, ST Stems, RB Root bark

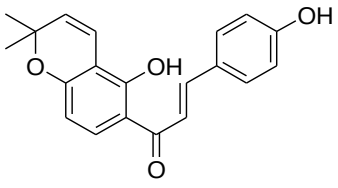

244

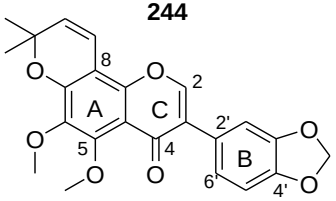

248

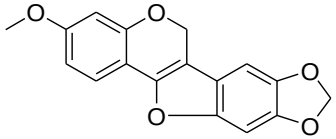

253

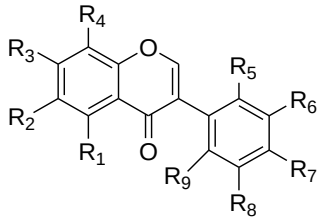

	R_1	R_2	R_3	R_4	R_5	R_6	R_7	R_8	R_9
245	H	H	OMe	H	H	H	O-Prenyl	H	H
246	H	H	O-Geranyl	H	H	H	OMe	H	H
247	OMe	OMe	OH	H	H	OCH_2O		H	H
249	OMe	OMe	OH	Prenyl	H	OCH_2O		H	H
250	H	H	OMe	Prenyl	OMe	H	OMe	OMe	H
251	H	OMe	OH	Prenyl	H	OCH_2O		H	H
252	H	H	OH	Prenyl	OMe	OCH_2O		OMe	H

Figure 4.1: Additional compounds from M. dura and M. ferruginea from Table 4.37

CHAPTER FIVE
CONCLUSIONS AND RECOMMENDATIONS

5.1 Conclusions

Three species of the genus *Millettia*; *M. dura*, *M. leucantha* and *M. lasiantha* were studied and the following conclusions are drawn;

i. In total, fiftyone compounds were isolated and characterized including thirtytwo isoflavones, nine flavanones, four rotenoids, two chalcones, two pterocarpanoids, a flavonol and a benzoic acid. This serves to be the first report of Kaempferol (**227**), 4,2′-dihydroxy-4′-methoxychalcone (**228**), 6,7,4'-timethoxyflavone (**233**), taxasin (**234**), 6,7,4'-timethoxyisoflavone (**235**) and paraben acid (**236**) from the genus. From the roots of *M. lasiantha* the new flavonids 3,8-dihydroxy-7,9-dimethoxycoumestan (**241**) and 7,5′-dihydroxy-6′,4′-dimethoxycoumaronochromone (**242**) were obtained.

ii. Out of the crude extracts tested for antiplasmodial activity, the stem bark extract from *M. dura*, showed the highest activities of 31.9±8.6 and 23.1±4.5 μg/ml for W2 and D6 strains of *P. falciparum*, repectively. Among the compounds tested, durmillone (**99**), isoerythrine-A-4′-(3-methylbutyl-2-ethyl)ether (**102**), milletone (**172**) and milletosin (**173**) were the most active compounds against both strains.

iii. Out of the twelve flavonoids evaluated for cytotoxicity, tephrosin (**171**) and durmillone (**99**) were the most active. They showed selective cytotoxicity against A549 adenocarcinomic human alveolar basal epithelial cancer cell line, with respective strong IC_{50} values of 3.1±1.2 and 6.6±1.2 μM.

iv. This study has provided a more enriched chemotaxonomic relationship between *M. dura*, *M. ferruginea* and *M. ferruginea* ssp *darrasana*. Oxygenation at C-8 and a methylenedioxy in ring A have only been observed in isoflavones from *M. dura*. Millettone (**172**) and millettosine (**173**) only observed in the seeds/pods of *M. dura* delineates it from the two taxa of *M. ferruginea*, in support of the morphological difference only observed in their seed pods. The two taxa of *M. ferruginea* could well be distinguished by the presence of the geranylated chalcone, 4′-*O*-geranylisoliquiritigenin (**26**) and isoflavones 7-*O*-geranylformononetin (**246**) so far reported only from *M. ferruginea* ssp *darasana* (RB). The presence of isoflavones as the major metabolites in the three taxa reviewed is a strong marker for the genus *Millettia*.

5.2 Recommendations

Basing on the observations from this study, the following recommendations are noted:

i. Tephrosin (IC_{50} 3.14µM) and durmillone (IC_{50} 6.6µM) having shown such strong cytotoxicites (Kuete and Effert, 2015) against A549 cancer cell line, can be followed up for anticancer product developement.

ii. Seed pods of *M. dura* having the following rotenoids, tephrosin (IC_{50} 3.14µM), milletone (IC_{50} 29.3µM) and milletosine (IC_{50} 48.6µM) with good to moderate toxicities, can be developed into insecticide and or larvaecides for malaria vector control.

iii. For conclusive delineation of *M. dura* from *M. ferruginea*, an HPLC profiling and DNA sequencing is needed (chemophenetic studies). Also, the roots of *M. ferruginea* should be investigated for presence/absence of geranylated chalcones so far observed only in *M. ferruginea* ssp. *darassana*.

iv. Considering the new flavonoids from the roots of *M. lasiantha* having interesting scaffolds of a coumestan and coumaronochromone, the roots of this plant be exhaustively examined for such metabolites.

REFERENCES

Adesanwo J. K.1, Shode F. O, Aiyelaagbe O, Oyede R. T and Baijnath H (**2009**). Isolation and characterization of a new chalcone from the leaves of *Heteropyxis natalensis*. *Internationational Journal of Medicine* and *Medical Sciences*, **1**, 028–032.

Adityachaudhu N and Gupta P. K (**1973**). A new Pterocarpan and Coumestan in the Roots of *Fflemingia Chappar*. *Phytochemistry*, **12**, 425–428.

Aftab T, Naeem M, Masroor M and Khan A (**2017**). *Artemisia annua:* Prospects, Applications and Therapeutic Uses (1st ed.). *CRC Press*.

Agrawal P. K (**1989**). *Carbon-13 NMR of Flavonoids* Vol. **39**. *Elsevier science publishers* b.v. Amsterdam, The Netherlands

Ajaegbu E. E, Eboka C. J, Okoye F. B. C and Proksch P (**2018**). New pterocarpan and derrisisoflavones from the root of *Millettia aboensis*. *ResearchGate*, 1–2.

Alnokari S, Antoun A and Ahmad S. A (**2016**). Extraction and Determination of Isoflavones in Soybean Seeds. *Int. J. Pharm*. Sci, **41**, 1–3.

Amaral G. R, Sara A. S, Luciana N. A, Patrícia S and Adriana A. C (**2019**). Natural Products as Treatment against Cancer: A Historical and Current Vision. *Clinics in Oncology*, **4**, 1–5.

American Cancer Society (**2018**). Global Cancer Facts and Figures 4th Edition. Atlanta. *American Cancer Society*, 1–76.

American Cancer Society (**2019**). Cancer Facts and Figures 2019. *American Cancer Society*.

Amirah A, Fei W. C, Jeremy R. S, Jonathan W. K. L and Yee L. L (**2018**). *Plasmodium knowlesi malaria: Current research perspectives*. **11**, 1145–1155.

Andersen Ø. M and Markham K. R (Eds.) (**2006**). Flavonoids*:* Chemistry, biochemistry and applications. *CRC Taylor and Francis*. 925-928.

Andrej J, Juraj F, Ivana P and Tibor M (**2004**). Approaches to flavonoid production in plant tissue Cultures-Review. *Biologia, Bratislava*, **59**, 697–710.

Ashok K. S, Itankar P. S, Jogendra N. B, Serengolam V. G and Werner H (**1982**). Rotenoids from Roots of *Millettia pachycarpa*. *Phytochemistry*, **21**, 949–951.

Ashoka H, Prashanth H, Manasa K. H, Chandraprasad M, Pradeep S and Ashok K. S (**2017**). Isolation and Detection of Vinca Alkaloids from Endophytes Isolated from *Canthranthus roseus*. *European Journal* of *Biomedical* and *Pharmaceutical Sciences*, **4**, 675–683.

Atilaw Y, Duffy S, Heydenreich M, Muiva-Mutisya L, Avery V, Erdélyi M and Yenesew A (**2017**). Three Chalconoids and a Pterocarpene from the Roots of *Tephrosia aequilata*. *Molecules*, **22**, 318.

Aung T. N, Qu Z, Kortschak R. D and Adelson D. L (**2017**). Understanding the Effectiveness of Natural Compound Mixtures in Cancer through their Molecular Mode of Action. *International Journal of Molecular Sciences*, **18**, 656.

Aye M, Aung H, Sein M and Armijos C (**2019**). A Review on the Phytochemistry, Medicinal Properties and Pharmacological Activities of 15 Selected Myanmar Medicinal Plants. *Molecules*, **24**, 293.

Ayine-Tora D, Kingsford-Adaboh R, Asomaning W, Harrison J, Mills-Robertson F, Bukari Y, Sakyi P, Kaminta S and Reynisson J (**2016**). Coumarin Antifungal Lead Compounds from *Millettia thonningii* and their Predicted Mechanism of Action. *Molecules*, **21**, 1369.

Ayuko T. A, Njau R. N, Wanjala C, Nyangasi L and Ndiege I. O (**2009**). "In Vitro Antiplasmodial Activity and Toxicity Assessment of Plant Extracts Used in Traditional Malaria Therapy in the Lake Victoria Region." *Memórias Do Instituto Oswaldo Cruz* **104**,689–94.

Baird J. K (**2005**). Effectiveness of antimalarial drugs. *New England Journal of Medicine*, **352**, 1565–1577.

Bandyukova V. A and Kazakov A. L (**1979**). Advances in the Chemistry of Natural Isoflavonoids. *UDC*, **547**, 569–586.

Banzouzi J. T, Prost A, Rajemiarimiraho M and Congo P (**2008**). Traditional Uses of the African *Millettia* species (Fabacea). *International Journal of Botany*, **4**, 406–420.

Bao F, Bai H.-Y, Wu Z. R and Yang Z. G (**2019**). Phenolic compounds from cultivated *Glycyrrhiza uralensis* and their PD-1/PD-L1 inhibitory activities. *Natural Product Research*, 1–8.

Barasa L. (**2011**). Phytochemical Investigation of the Stem Bark of *Millettia oblata* ssp. *teiensis* for Antiplasmodial and Larvicidal Principles [Thesis]. University of Nairobi.

Basco L. K, Mitaku S, Skaltsounis A. L, Ravelomanantsoa N, Tillequin F, Koch M and Le Bras J (**1994**). In vitro activities of furoquinoline and acridone alkaloids against Plasmodium falciparum. *Antimicrobial Agents* and *Chemotherapy*, **38**, 1169–1171.

Batista R, De Jesus S. J. A and De Oliveira A. B (**2009**). Plant-derived antimalarial agents: New leads and efficient phytomedicines. Part II. Non-alkaloidal natural products. *Molecules*, **14**, 3037–3072.

Belofsky G, Aronica M, Foss E, Diamond J, Santana F, Darley J, Dowd P. F, Coleman C. M and Ferreira D (**2014**). Antimicrobial and antiinsectan phenolic metabolites of dalea searlsiae. *Journal of Natural Products*, **77**, 1140–1149.

Benavides A, Bassarello C, Montoro P, Vilegas W, Piacente S and Pizza C (**2007**). Flavonoids and isoflavonoids from Gynerium sagittatum. *Phytochemistry*, **68**, 1277–1284.

Biagini G, Oneill P, Bray P and Ward S (**2005**). Current drug development portfolio for antimalarial therapies. *Current Opinion in Pharmacology*, **5**, 473–478.

Blazquez A. G, Fernandez-Dolon M, Sanchez-Vicente L, Maestre A. D, Gomez-San Miguel A. B, Alvarez M, Serrano M. A, Jansen H, Efferth T, Marin J. J. G and Romero M. R (**2013**). Novel artemisinin derivatives with potential usefulness against liver/colon cancer and viral hepatitis. *Bioorganic and Medicinal Chemistry*, **21**, 4432–4441.

Bloom D. E, Cafiero E. T, Jané-Llopis E, Abrahams-Gessel S, Bloom L. R, Fathima S, Feigl A. B, Gaziano T, Mowafi M, Pandya A, Prettner K, Rosenberg L, Seligman B, Stein A. Z and Weinstein C (**2011**). The Global Economic Burden of Noncommunicable Diseases. Geneva*: World Economic Forum*.

Boik John (**2001**). Natural Compounds in Cancer Therapy (1st ed.). *Oregon Medical Press*, LLC, 521

Bosire C. M, Deyou T, Kabaru J. M, Kimata D. M and Yenesew A (**2014**). Larvicidal activities of the stem bark extract and rotenoids of *Millettia* usaramensis subspecies usaramensis on Aedes aegypti L. (Diptera: Culicidae). *Journal of Asia-Pacific Entomology*, **17**, 531–535.

Bray F, Ferlay J, Soerjomataram I, Siegel R. L, Torre L. A and Jemal A (**2018**). Global cancer statistics 2018: Globocan estimates of incidence and mortality worldwide for 36 cancers in 185 countries. *CA: A Cancer Journal for Clinicians*, **68**, 394–424.

Bruce-Chwatt L. J, and Bruce-Chwatt J. M (**1950**). Antimalarial Drugs in West Africa, with Particular Reference to Proguanil: Results of a Survey in Nigeria. *The British Medical Journal*, **2**, 7–14.

Bueno P. L, Pan L, Muñoz A. U, Li J, Chai H. B, Gallucci J. C, Ninh T. N, Carcache De Blanco E. J, Soejarto D. D and Kinghorn A. D (**2014**). Caeruleanone A, a rotenoid with a new

arrangement of the D-ring from the fruits of *Millettia caerulea*. *Organic Letters*, **16**, 1462–1465.

Buyinza D, Chalo D. M, Derese S, Ndakala A, Yenesew A (**2020**). Flavonoids and Isoflavonoids of *Millettia dura* and *Millettia ferruginea*: Phytochemical Review and Chemotaxonomic Values. *Biochemical Systematics* and *Ecology* **91**,1-6

Buyinza D, Yang L. J, Derese S, Ndakala A, Coghi P, Heydenreich M, Wong V. K. W, M€oller H. M and Yenesew A (**2019**). Cytotoxicity of isoflavones from *Millettia dura*. *Natural Product Research*, **XX**, 1–5.

Chansakaow S, Tsutomu I, Keiko S, Mineaki O, Yoshihiro H, Momoe K and Chaiyo C (**2000**). Isoflavonoids from *Pueraria mirifica* and their Estrogenic Activity. *Planta Medica*, **66**, 572–575.

Chatsumpun M, Sritularak B and Likhitwitayawuid K (**2010**). Phenolic Compounds from Stem Wood of *Millettia leucantha*. *Chemistry of Natural Compounds*, **46**, 634–635.

Chen M, Wang X, Zha D, Fangfang C, Wenjing Z, Yan H, Qilai H, Hongqin Z, and Zi-Chun H (**2016**). "Apigenin Potentiates TRAIL Therapy of Non-Small Cell Lung Cancer via Upregulating DR4/DR5 Expression in a P53-Dependent Manner." *Scientific Reports* **6**, 35468.

Commonwealth. (**2019**). CommonWealth Malaria Report. *CommonWealth Malaria Commitment*.

Dagne E and Bekele A. (**1990a**). C-prenylated isoflavones from *Millettia ferruginea*. *Phytochemistry*, **29**, 2679–2682.

Dagne E, Bekele A, Noguchi H, Shibuya M and Sankawa U (**1990b**). O-Geranylated and O-prenylated flavonoids from *Millettia ferruginea*. *Phytochemistry*, **29**, 2671–2673.

Dagne E, Bekele A and Waterman P. G (**1989**). The Flvonoids of *Millettia ferruginea* ssp. *ferruginea* and *ssp. darassana* in Ethiopia. *Phytochemistry*, **28**, 1897–1900.

Dagne E, Wendimagegn M and Bekele A (**1991**). Flavanoids of *Millettia dura*. *Phytochemistry*, **5**, 81–86.

Dat L. D, Tu N. T. M, Duc N. V, Luyen B. T. T, Huyen C. T. T, Jang H. J, Thu D. T, Huong T. T, Tram L. H, Thong N. V, Hung N. D, Kim Y. H and Thao N. P (**2019**). Anti-inflammatory secondary metabolites from the stems of *Millettia dielsiana* Harms ex Diels. *Carbohydrate Research*, **484**, 1-19.

Deardorff K, Ray W, Winterstein E, Brown M, McCornack J, Cardenas-Garcia B, Jones K, McNutt S, Fulkerson S, Ferreira D, Gény C, Chen X, Belofsky G and Dondji B (**2016**).

Phenolic Metabolites of Dalea ornata Affect Both Survival and Motility of the Human Pathogenic Hookworm Ancylostoma ceylanicum. *Journal of Natural Products*, **79**, 2296–2303.

Deoraj C. M, Iqbal P, Volmink J, Estambale B, Salim S. A. K, Ralph M and Robin F (**2015**). Changing Disease Pattern in Africa. *Network of African Science Academies (NASAC)*, 1–36.

Derese S (**2004**). Antiplasmodial Flavonoids from Some Kenyan *Papilinoideae* Species [Thesis]. University of Nairobi.

Derese S, Barasa L, Akala H. M, Yusuf A. O, Kamau E, Heydenreich M and Yenesew A (**2014a**). 4′-Prenyloxyderrone from the stem bark of *Millettia oblata* ssp. teitensis and the antiplasmodial activities of isoflavones from some *Millettia* species. *Phytochemistry Letters*, **8**, 69–72.

Derese S, Yenesew A, Midiwo J. O, Heydenreich M and Peter M. G (**2003**). A new isoflavone from stem bark of *Millettia dura*. *Bulletin of the Chemical Society of Ethiopia*, **17**, 113–115.

Desjardins R. E, Craig J. C. J, David H and Jeffrey D. C (**1979**). Quantitative Assessment of Antimalarial Activity In Vitro by a Semiautomated Microdilution Technique. *Antimicrobial Agents and Chemotherapy*, 710–718.

Deyou T and Jang Y. P (**2018**). A new prenylated isoflavone from seeds of *Millettia ferruginea* ssp. *ferruginea*. *South African Journal of Botany*, **117**, 155–157.

Deyou T, Marco M, Heydenreich M, Pan F, Gruhonjic A, Fitzpatrick P. A, Koch A, Derese S, Pelletier J, Rissanen K, Yenesew A and Erdélyi M (**2017a**). Isoflavones and Rotenoids from the Leaves of *Millettia oblata* ssp. *teitensis*. *Journal of Natural Products*, **80**, 2060–2066.

Deyou T, Gumula I, Pang F, Gruhonjic A, Mumo M, Holleran J, Duffy S, Fitzpatrick P. A, Heydenreich M, Landberg G, Derese S, Avery V, Rissanen K, Erdélyi M and Yenesew A (**2015a**). Rotenoids, Flavonoids, and Chalcones from the Root Bark of *Millettia usaramensis*. *Journal of Natural Products*, **78**, 2932–2939.

Deyou T. W (**2015**). Phytochemical nvestigation of Selected *Millettia* (Leguminosae) and *Ochina* (Ochnaceae) Species for Anticancer Activities [Thesis] University of Nairobi.

Dominguez X. A, Sergio S. G, Williams H. J, Ortiz C, Scott A. I and Reibenspies I. J. H. (**1989**). Kukulkanins a and b, new chalcones from *Mimosa tenuefolia*. *Journal of Natural Products*, **52**, 864–867.

Foley M and Tilley L (**1998**). Quinoline antimalarials: Mechanisms of action and resistance and prospects for new agents. *Pharmacology and Therapeutics*, **79**, 55–87.

Frimpong-Boateng K (**2010**). Infectious Disease and Cancer in Africa—A medical and Demographical Reality. *Global Health and Molecular Medicine. Hannover*, 1–12.

Giovanna P, Philippe R, Elena F, Marcello N and Corrado G (**2003**). Prenylated isoflavonoids from *Millettia pervilleana*. *Elsevier*, **63**, 471–474.

Globocan (**2018**). *910- East -African-Fact-Sheets*. 1–2.

González-Vallinas M, González-Castejón M, Rodríguez-Casado A, and Ramírez A. M (**2013**). "Dietary Phytochemicals in Cancer Prevention and Therapy: A Complementary Approach with Promising Perspectives." *Nutrition Reviews* **71**:585–99.

Gumula I (**2014**). Phytochemical Investigation of Three Leguminosae Plants for Cancer Chemopreventive Agents [Thesis] University of Nairobi

Gumula I, Heydenreich M, Derese S, Ndiege I. O and Yenesew A (**2012**). Four isoflavanones from the stem bark of *Platycelphium voënse*. *Phytochemistry Letters*, **5**, 150–154.

Gunjan A, Andaleeb S and Vipin C. K (**2017**). Drug Resistance in Bacteria, Fungi, Malaria, and Cancer (Vol. 3). *Springer*.

Haque Md, Uzzal N. F and Sadiur R. S (**2016**). Anti-Cancer Agents Derived from Plants and Dietary ources*:* A REVIEW, 55–66.

Harvey P. W and Everett D. J (**2004**). Significance of the Detection of Esters of *p*-Hydroxybenzoic Acid(Parabens) in Human Breast Tumours. *Journal of Applied Toxicology* **24**, 1–4.

Harrison J. J. E. K, Ayine-Tora M. D, Appiagyei B, Mills-Robertson F. C, Asomaning W. A, Achel D. G, Ishida H and Kingsford, R (**2019**). Crystal structure and in vitro antimicrobial activity studies of Robustic acid and other Alpinumisoflavones isolated from *Millettia thoningii*. *Zeitschrift Für Kristallographie - Crystalline Materials*, **234**, 229–235.

Havyarimana L, Ndendoung S. T, de Dieu T. J, de Théodore A. A and Tanyi J. M (**2012**). Chemical constituents of *Millettia barteri* and their antimicrobial and antioxidant activities. *Pharmaceutical Biology*, ***50***, 141–146.

Highet R. J and Highet P. F (**1967**). Structure of two isoflavones from the Abyssinian Berebera tree. *The Journal of Organic Chemistry*, **32**, 1055–1058.

International Agency for Research on Cancer. (**2018**). Latest global cancer data. *World Health Organization*, 1–3.

Iqbal J, Abbasi B. A, Mahmood T, Kanwal S, Ali B, Shah S. A and Khalil A. T (**2017**). Plant-derived anticancer agents: A green anticancer approach. *Asian Pacific Journal of Tropical Biomedicine*, **7**, 1129–1150.

Jacques K, Laure B, Mabeku K, Jules R, Kuiate A. T, Tiabou and Zacharias T. F (**2011**). Antimicrobial Glycosides and Derivatives from Roots of *Picralima nitida*. *International Journal of Chemistry*, **3**, 23–31.

Jean P. A, Jean M, Achyut A, Nole T, Alembert T. T, Muhammad I. C and Augustin E. N (**2017**). New coumestan and oumaronochromone derivatives from *Dalbergia boehmii* Taub. (Fabaceae). *Phytochemistry Letters*, **21**, 109–113.

Jha H. C, Zilliken F and Breitmaier E (**1980**). Carbon-13 Chemical Shift Assignments of Chromones and Isoflavones. *Canadian Journal of Chemistry* **58**, 1211–19.

Karimov A. M, Slobodyanyuk T. N and Botirov E. K (**2017**). Flavonoids from the Aerial Part of Scutellaria intermedia. *Chemistry of Natural Compounds*, **53**, 745–746.

Kim A, Choi J, Htwe K. M, Chin Y.-W, Kim J and Yoon K. D (**2015**). Flavonoid glycosides from the aerial parts of *Acacia pennata* in Myanmar. *Phytochemistry*, **118**, 17–22.

Kuete V and Efferth T (**2015**). African Flora Has the Potential to Fight Multidrug Resistance of Cancer. *BioMed Research International* **2015**, 1–24.

Kucekova Z, Jiri M, Petr H, Otakar R, Pavel V and Petr S (**2011**). Phenolic Compounds from Allium Schoenoprasum, Tragopogon Pratensis and Rumex Acetosa and Their Antiproliferative Effects. *Molecules* **16**, 9207–17.

Kumar A, Paliwal D, Saini D, Thakur A, Aggarwal S and Kaushik D (**2014**). A comprehensive review on synthetic approach for antimalarial agents. *European Journal of Medicinal Chemistry*, **85**, 147–178.

Kumar A, Patil D, Rajamohanan P. R and Ahmad A (**2013**). Isolation, Purification and Characterization of Vinblastine and Vincristine from Endophytic Fungus Fusarium oxysporum Isolated from *Catharanthus roseus*. *PLoS ONE*, **8**, 1–10.

Larit F, Benyahia S, Benayache S, Léon F, Brouard I and Bermijo J (**2012**). Flavonoïds from *Calycotome spinosa* (L.). Lamk. *Internationational Journal of Medicinal Aromatic Plants*, **2**, 34–37.

Lee S, An H, Chang D.-J, Jang J, Kim K, Sim J, Lee J and Suh Y.-G (**2015**). Total synthesis of (-)-deguelin via an iterative pyran-ring formation strategy. *Chemical Communications (Cambridge, England)*, **51**, 9026–9029.

Li L, Xueyang D, Lixia Z, Pan S and Minjian Q (**2011**). A new coumestan with immunosuppressive activities from *Flemingia philippinensis*. *Fitoterapia*, **82**, 615–619.

Lynette B. P, Pan L, Muñoz U, Li J, Chai H.-B, Gallucci J. C, Ninh T. N, Carcache de Blanco E. J, Soejarto D. D and Kinghorn A. D (**2014**). Caeruleanone A, a Rotenoid with a New Arrangement of the D-Ring from the Fruits of *Millettia caerulea*. *Organic Letters*, **16**, 1462–1465.

Madhushree (**2016**). *Cancer Therapy with Vinca Aakaloids*. *International Journal of Experimental Research and Review***, 7**, 38–43.

Mai H. D. T, Nguyen T. T. O, Cuong V, Pham M. L, Guéritte F and Tran D. T (**2010**). Cytotoxic Prenylated Isoflavone and Bipterocarpan from *Millettia*. *Planta Medica*, **76**, 1739–1742.

Marco M, Deyou T, Gruhonjic A, Holleran J, Duffy S, Heydenreich M, Firtzpatrick P. A, Landberg G, Koch A, Derese S, Pelletier J, Avery V. M, Erdélyi M and Yenesew A (**2017a**). Pterocarpans and isoflavones from the root bark of *Millettia micans* and of *Millettia dura*. *Phytochemistry Letters*, **21**, 216–220.

Marco M (**2015**). *Phytochemical Investigation of Three Leguminosae Plants for Larvicidal Activity Against Aedes Aegypti* [Thesis]. University of Nairobi.

Maundu P and Tengnäs B (**2005**). Useful trees and shrubs for Kenya. *World Agroforestry Centre.* http://agris.fao.org/agris-search/search.do?recordID=SO2007100022.

Maurie M. M. D (**1991**). Taxol: An Important New Drug in the Management of Epithelial Ovarian Cancer. *The yale journal of biology and medicine,* **64**, 583-590.

Maxine C, Walker M and Shaw M (**2018a**). Global Malarial Report, and Advice on Malarial Prophylaxis for General Practitioners. *RNZCGP, Auckland and Northland Divisions, 1-22*

Mushtaque Md. S (**2015**). Reemergence of chloroquine (CQ) analogs as multi-targeting antimalarial agents: A review. *European Journal of Medicinal Chemistry*, **90**, 280–295.

Meng C. Y, Han Y, Duan Y. X, Chen J. X, Hu Q. F and Gao X. M (**2013**). Isolation of chalcones from the root of codonopsis cordifolioidea and their antitobacco mosaic virus activities. *Asian Journal of Chemistry*, **25**, 9517–9519.

Willcox M, Bodeker G and Rasoanaivo P (**2004**). Traditional Medicinal Plants and Malaria. *CRC Press*. (Vol. 4).

Michael M. M (**2008**). Phytochemical Investigation of the Roots of Millettia Usaramensis Subspecies Usaramensis for Antiplasmodial Principles[Thesis]. University of Nairobi.

Na Z, Song Q.-S and Hu H.-B (**2014**). Flavonoids from Twigs of *Millettia pubinervis*. *Natural Product Communications*, **9**, 1934578X1400901214.

Namukobe J, Kiremire B. T, Byamukama R, Kasenene J. M, Akala H. M, Kamau E, and Dumontet V (**2015**). Antiplasmodial compounds from the stem bark of *Neoboutonia macrocalyx* pax. *Journal of Ethnopharmacology*, **162**, 317–322.

Nayak M and Kim I (**2015**). Alkyne Carbonyl Metathesis As a Means to Make 4-Acyl Chromenes: Syntheses of (±)-Deguelin and (±)-Munduserone. *Journal of Organic Chemistry*, **80**, 11460–11467.

Ndjateu F. S. T, Tsafack R. B. N, Nganou B. K, Awouafack M. D, Wabo H. K, Tene M, Tane P and Eloff J. N (**2014**). Antimicrobial and antioxidant activities of extracts and ten compounds from three Cameroonian medicinal plants: Dissotis perkinsiae (Melastomaceae), Adenocarpus mannii (Fabaceae) and Barteria fistulosa (Passifloraceae). *South African Journal of Botany*, **91**, 37–42.

Niu D. Y, Li Y. K, Wu X. X, Shi Y. D, Hu Q. F and Gao X. M (**2013**). Pterocarpan derivatives from *clinopodium urticifolium* and their cytotoxicity. *Asian Journal of Chemistry*, **25**, 9672–9674.

Noble R. L (**1990**). The discovery of the vinca alkaloids—Chemotherapeutic agents against cancer. *Biochemistry and Cell Biology*, **68**, 1344–1351.

Nogueira C. R and Lopes L. M (**2011**). Antiplasmodial natural products. *Molecules*, **16**, 2146–2190.

Ojima I, Lichtenthal B, Lee S, Wang C and Wang X (**2016**). Taxane anticancer agents: A patent perspective. *Expert Opinion on Therapeutic Patents*, **26**, 1–20.

Ollis W. D, Rhodes C. A and Sutherland I. O (**1967**). The extractives of *Millettia dura* (Dunn): The constitutions of durlettone, durmillone, milldurone, millettone and millettosin. *Tetrahedron*, **23**, 4741–4760.

O'Neill M. J, Bray D. H, Boardman P, Phillipson J. D and Warhurst D. C (**1985**). Plants as sources of antimalarial drugs. Part 1. In vitro test method for the evaluation of crude extracts from plants. *Planta Medica*, **5**, 394–398.

PAHOWHO (**2018**). Epidemiological Update Increase of malaria in the Americas. *Pan American Health Organization and World Health Organization*, 1–6.

Pailee P, Mahidol C, Ruchirawat S and Prachyawarakorn V (**2019**). Diverse flavonoids from the roots of *Millettia brandisiana*. *Phytochemistry*, **162**, 157–164.

Pelter B. A, Ward R. S, Gray T. I, Park S, Sa S, I-ettevs T, Ternai B, Markham K. K, Nathan P. J, Mares J, Hernandez M. C and Perkin J. C. S. I (**1976**). The Carbon-I 3 Nuclear Magnetic Resonance Spectra of Flavonoids and Related Compounds. *Journal of the Chemical Society Perkin Transactions 1*, **2002**, 2475–2483.

Pennaka H. K, Mopuru V. B. R, Duvvuru G, Madugula M. M, Cristelle C and Bernard B (**2003**). A New Coumestan from *Tephrosia calophylla*. *Chem. Pharm. Bull*, **51**, 194–196.

Perumalsamy H, Jang M. J, Kim J.-R, Kadarkarai M and Ahn Y.-J (**2015**). Larvicidal activity and possible mode of action of four flavonoids and two fatty acids identified in *Millettia* pinnata seed toward three mosquito species. *Parasites and Vectors*, **8**, 237.

Phrutivorapongkul A, Lipipun V, Ruangrungsi N, Kirtikara K, Nishikawa K, Maruyama S, Watanabe T and Ishikawa T (**2003**). Studies on the chemical constituents of stem bark of *Millettia* leucantha: Isolation of new chalcones with cytotoxic, anti-herpes simplex virus and anti-inflammatory activities. *Chemical and Pharmaceutical Bulletin*, **51**, 187–190.

Qiao-li Z, Zeng-bao W. U, Zhi-hui Z, Xin-hua L. U, Hong L and Wei C (**2011**). 显脉羊蹄甲中酚酸类成分研究. **46**, 946–950.

Qi-Mei L, Zhao H.-Y, Zhong X.-K and Jiang J.-G (**2012**). Eclipta prostrata L. phytochemicals: Isolation, structure elucidation, and their antitumor activity. *Food and Chemical Texicology*, **50**, 4016–4022.

Raju K. V. S, Srimannarayana G, Ternai B, Stanley R and Markham K. R (**1981**). ^{13}C NMR studies of some complex natural oxygen heterocyclics. *Tetrahedron*, **37**, 957–962.

Raksat A, Maneerat W, Rujanapun N, Andersen R. J, Pyne S. G and Laphookhieo S (**2019**). Antibacterial and Inhibitory Activities against Nitric Oxide Production of Coumaronochromones and Prenylated Isoflavones from *Millettia extensa*. *Journal of Natural Products*, **82**, 2343–2348.

Rastrelli L, Berger I, Kubelka W, Caceres A, De Tommasi N and De Simone F (**1999**). New 12a-hydroxyrotenoids from *Gliricidia sepium* bark. *Journal of Natural Products*, **62**, 188–190.

Rayanil B. P and Tuntiwachwuttikul P (**2011**). A new phenolic compound with anticancer activity from the wood of *Millettia leucantha*. *Archives of Pharmacal Research*, **34**, 881–886.

Ren Y, Benatrehina P. A, Muñoz Acuña U, Yuan C, Chai H. B, Ninh T. N, Carcache De Blanco E. J, Soejarto D. D and Kinghorn A. D (**2016**). Isolation of Bioactive Rotenoids and Isoflavonoids from the Fruits of *Millettia caerulea*. *Planta Medica*, **82**, 1096–1104.

Sen P, Kumar P. S, Ranjita H, Kamlesh K. S, Pushpa P and Amit R (**2016**). Apigenin Naturally Occurring Flavonoids: Occurrence and Bioactivity. *UK Journal of Pharmaceutical and Biosciences*, **4**, 56–68.

Senait K, Sambe D, Allarangar Y and Wondimagegnehu A (**2010**). Trends of Major Disease Outbreaks in the African Region. *East African Journal of Public Health*, **7**, 20–29.

Shan S, Shi J, Yang P, Jia B, Wu H, Zhang X and Li Z (**2017**). Apigenin Restrains Colon Cancer Cell Proliferation via Targeted Blocking of Pyruvate Kinase M2-Dependent Glycolysis. *Journal of Agricultural and Food Chemistry*, **65**, 8136–8144.

Shou Q. Y, Qing T and Zheng W. S (**2009**). Hirtellanines A and B, a pair of isomeric isoflavonoid derivatives from *Campylotropis hirtella* and their immunosuppressive activities. *Bioorganic and Medicinal Chemistry*, **19**, 3389–3391.

Siegel R. L, Miller K. D and Jemal A (**2019**). Cancer statistics, 2019. CA: *A Cancer Journal for Clinicians.*

Soni M. G, Carabin I. G and Burdock G. A (**2005**). Safety Assessment of Esters of P-Hydroxybenzoic Acid (Parabens). *Food and Chemical Toxicology* **43**, 985–1015.

Stierle A, Strobel G and Stierle D (**1993**). Taxol and taxane production by *Taxomyces andreanae*, an endophytic fungus of Pacific yew. *Science*, **260**, 214–216.

Taj U. R, Khanzadi F. K, Wajiha L, Khair Z, Khair Z and Syed G. M (**2015**). Characterization of one Novel Flavone and four New Source Compounds from the Bark of *Millettia ovalifolia* and In-Vitro Inhibition of Carbonic Anhydrase-II by the Novel Flavonoid. *Rec. Nat. Prod.* **9**, 553–560.

Tamotsu S and Shoji S (**1969**). Chemical Studies on the Oriental Plant Drugs. Some New Constituents of *Licorice* Root. Glycyrol, 5-O-Methylglycyrol and Isoglycyrol. *Chem. Pharm. Bull*, **17**, 729–734.

Tao W.-W, Duan J.-A, Yang N.-Y, Tang Y.-P, Liu M.-Z and Qian Y.-F (**2012**). Antithrombotic phenolic compounds from *Glycyrrhiza uralensis*. *Fitoterapia*, **83**, 422–425.

The Plant List (**2013**). A Working List of all Plant Species; www.worldfloraonline.org.(accessed 09th April, 2020).

Trager W and Jensen J. B (**1976**). Human malaria parasites in Continuous culture. *Science*, **193**, 673–675.

Tu Y, Xiao T, Gong G, Bian Y and Li Y (**2019**). A new isoflavone with anti-inflammatory effect from the seeds of *Millettia pachycarpa*. *Natural Product Research*, 1–7.

Upadhyay K. S, Ramesh C. R, Rekha G, Ashutosh P, Poonam G and Penny J (**2017**). Drug Resistance in Cancer. In *Drug Resistance in Bacteria, Fungi, Malaria and Cancer*. *Springer International Publishing*, 449–473.

Uraiwan S, Chavi Y, Siriporn T, Jongjai S and Auemporn J (**2018**). Flavonoids from *Milletia leucantha* and Their Cytotoxicity. *Natural Product Communications*, **13**, 961–962.

Vandekerckhove S and D'hooghe M (**2015**). Quinoline-based antimalarial hybrid compounds. *Bioorganic and Medicinal Chemistry*, **23**, 5098–5119.

Wani M. C H, Taylor L, Monroe E, Wall P, Coggon and A. T. McPhail (**1971**). The Isolation and Structure of Taxol, a Novel Antileukemic and Antitumor Agent from *Taxus brevifolia*. *Journal of the American Chemical Society*, **93**, 2323–2325.

Weaver B. A (**2014**). How Taxol/paclitaxel kills cancer cells. *Molecular Biology of the Cell*, **25**, 2677–2681.

Wei Z, Yang Y, Xie C, Li C, Wang G, Ma L, Xiang M, Sun J, Wei Y and Chen L (**2014**). Synthesis and biological evaluation of pyranoisoflavone derivatives as anti-inflammatory agents. *Fitoterapia*, **97**, 172–183.

White N J, Pukrittayakamee S, Tinh H. T, Faiz M. A, Mokuolu O. A and Dondorp A. M. (**2014**). *Malaria Online*, **383**, 723–735.

WHO (**2018c**). Pricing of cancer medicines and its impacts (Technical CC BY-NC-SA 3.0 IGO; pp. 1–171).

WHO (**2018b**). Pricing of cancer medicines and its impacts. Geneva. 1–171.

WHO (**2018a**). World malaria report 2018, Geneva.

Woodrow C. J (**2005**). Artemisinins. *Postgraduate Medical Journal*, **81**, 71–78.

Woon-Chien T, Ho Han K, Rossarin S and Hwee-Ling K (**2016**). Medicinal Plants and Malaria Applications, Trends, and Prospects. *Traditional Herbal Medicines for Modern Times Book 16 1st edn CRC Taylor & Francis*. pp472.

Wright C. W (**2005**). Traditional antimalarials and the development of novel antimalarial drugs. *Journal of Ethnopharmacology*, **100**, 67–71.

Xianheng S, Xiang L, Jianfei S, Jianheng L, Zefeng Z, Zhibo D, Hui M, Meng Y, Mingkang L and Yong Z (**2019**). Copper-catalyzed intramolecular cross dehydrogenative coupling approach to coumestans from 20-hydroxyl-3-arylcoumarins. *RSC Advances*, **9**, 17391–17398.

Xiaowei H, Leilei Z, Li G, Yan G, Lijing Z, Liyong L, Jianyong S and Li C (**2015**). Antiinflammatory and Analgesic Activities of Ethanol Extract and Isolated Compounds from *Millettia pulchra*. *Biol. Pharm. Bull*, **38**, 1328–1336.

Yan C, Xiaoyi W, Haihui X and Hongzhu D (**2008**). Antioxidant 2-Phenylbenzofurans and a Coumestan from Lespedeza Wirgata. *Journal of Natural Products*, **71**, 929–932.

Yanbei T, Wu C, Kang Y, Li Q, Zhu C and Li Y (**2019**). Bioactivity-guided identification of flavonoids with cholinesterase and β-amyloid peptide aggregation inhibitory effects from the seeds of *Millettia pachycarpa*. *Bioorganic and Medicinal Chemistry Letters*, **29**, 1194–1198.

Yankep E, Fomum Z. T and Dagne E (**1997**). An O-geranylated isoflavone from *Millettia griffoniana*. *Phytochemistry*, **46**, 591–593.

Ye H, Wu W, Liu Z, Xie C, Tang M, Li S, Yang J, Tang H, Chen K, Long C, Peng A, Wei Y and Chen L (**2014**). Bioactivity-guided isolation of anti-inflammation flavonoids from the stems of *Millettia dielsiana* Harms. *Fitoterapia*, **95**, 154–159.

Yenesew A, Midiwo J. O and Waterman P. G (**1996**). Four Isoflavones from Seed Pods of *Millettia dura*. *Phytochemistry*, **41**, 951–955.

Yenesew A, Midiwo J. O and Waterman P. G. (**1996a**). Four isoflavones from seed pods of *Millettia dura*. *Phytochemistry*, **41**, 951–955.

Yenesew A, Midiwo J. O and Waterman P. G (**1997**). 6-methoxycalpogonium isoflavone a: A new isoflavone from the seed pods of *Millettia dura*. *Journal of Natural Products*, **60**, 806–807.

Yenesew A, Midiwo J. O and Waterman P. G (**1997a**). 6-Methoxycalpogonium Isoflavone A: A New Isoflavone from the Seed Pods of *Millettia dura*. *Journal of Natural Products*, **60**, 806–807.

Yenesew A, Midiwo J. O and Waterman P. G (**1998b**). Rotenoids, isoflavones and chalcones from the stem bark of *Millettia* usaramensis subspecies usaramensis. *Phytochemistry*, **47**, 295–300.

Yenesew A, Derese S, Midiwo J. O, Heydenreich M and Peter M. G (**2003a**). Effect of rotenoids from the seeds of *Millettia dura* on larvae of Aedes aegypti. *Pest Management Science*, **59**, 1159–1161.

Yenesew A, Derese S, Midiwo J. O, Oketch-Rabah H. A, Lisgarten J, Palmer R, Heydenreich M, Peter M. G, Akala H, Wangui J, Liyala P and Waters N. C (**2003b**). Anti-plasmodial

activities and X-ray crystal structures of rotenoids from *Millettia usaramensis* subspecies *usaramensis*. *Phytochemistry*, **64**, 773–779.

Yoo H, Chae H. S, Kim Y. M, Kang M, Ryu K. H, Ahn H. C, Yoon K. D, Chin Y. W and Kim J (**2014a**). Flavonoids and arylbenzofurans from the rhizomes and roots of *Sophora tonkinensis* with IL-6 production inhibitory activity. *Bioorganic and Medicinal Chemistry Letters*, **24**, 5644–5647.

Yunyao K, Yanbei T, Xuefei M, Qin L, Chao Z and Yanfang L (**2017**). A New Flavonol Glycoside from *Millettia pachycarpa*. *Natural Product Communications*, **12**, 1447–1449.

Zhao Z, Liu P, Wang S and Ma S (**2017**). Optimization of ultrasound, microwave and Soxhlet extraction of flavonoids from *Millettia speciosa* Champ and evaluation of antioxidant activities in vitro. *Journal of Food Measurement and Characterization*, **11**, 1947–1958.

Zhenyu Z, Pinghuai L, Shasha M, Shenglin W, Ang L, Jiguang L and Meng W (**2017**). Botanical Characteristics, Chemical and Nutritional Composition and Pharmacological and Toxicological Effects of Medicinal and Edible Plant *Millettia speciosa Champ. Food Science*, **38**, 1-14.

Zhi-Na, Fan Q.-F, Song Q.-S and Hu H.-B (**2017**). Three new flavonoids from *Millettia pachyloba*. *Phytochemistry Letters*, **19**, 215–219.

Zhi-Na, Qishi S and Huabin H (**2013**). *Flavonoids from Twigs of Millettia leptobotrya Dunn*. *Rec. Nat. Prod*, **7**, 307–312.

Zingue S, Ntsa D. M, Magne N. C. B, Michel T, Ndinteh D. T, Clyne C and Njamen D (**2019**). Lupeol, the major compound of the dichloromethane extract of *Millettia macrophylia* Benth (Fabaceae), displays estrogenic effects in ovariectomized rats. *Phytotherapy Research*, **33**, 949–957.

APPENDICES

Appendix 1: NMR Spectra for Formononetin (91)

Appendix 1a: ^{1}H NMR for Compound 91

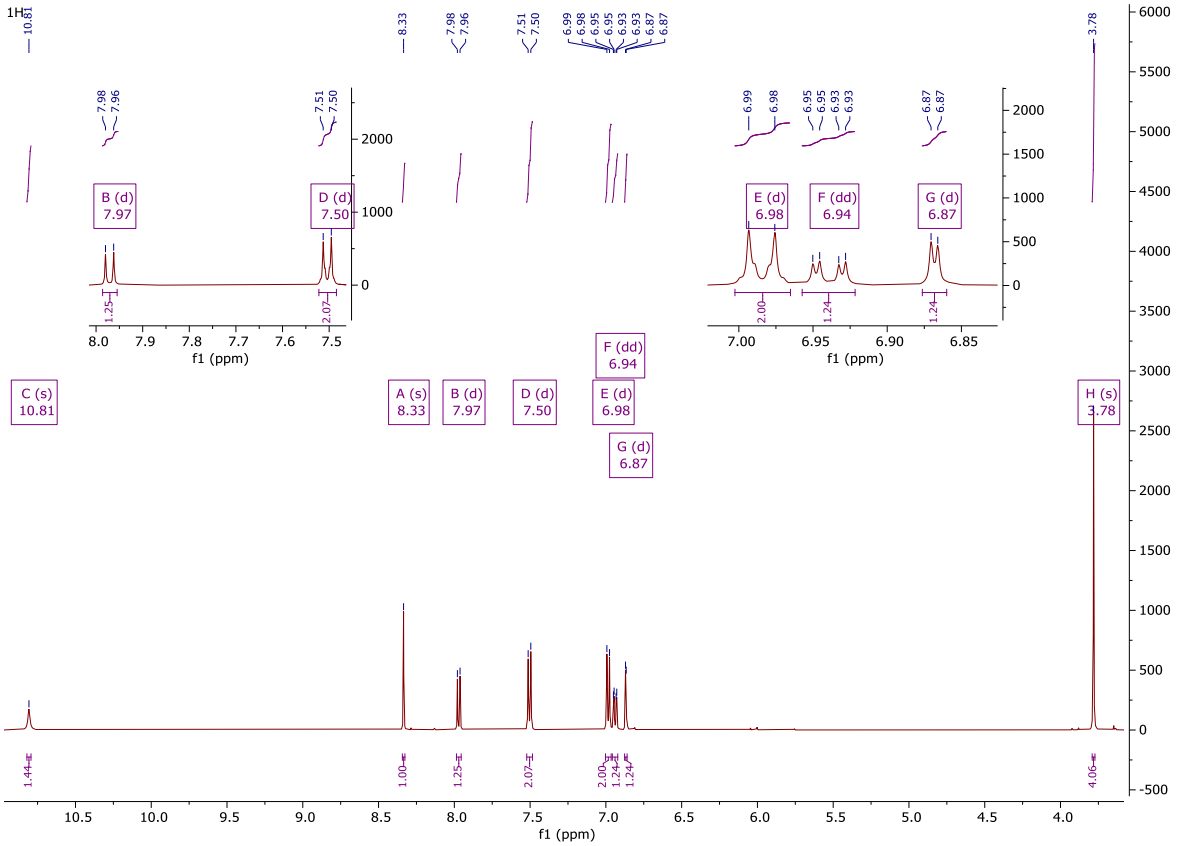

Appendix 1b: ^{13}C NMR for Compound 91

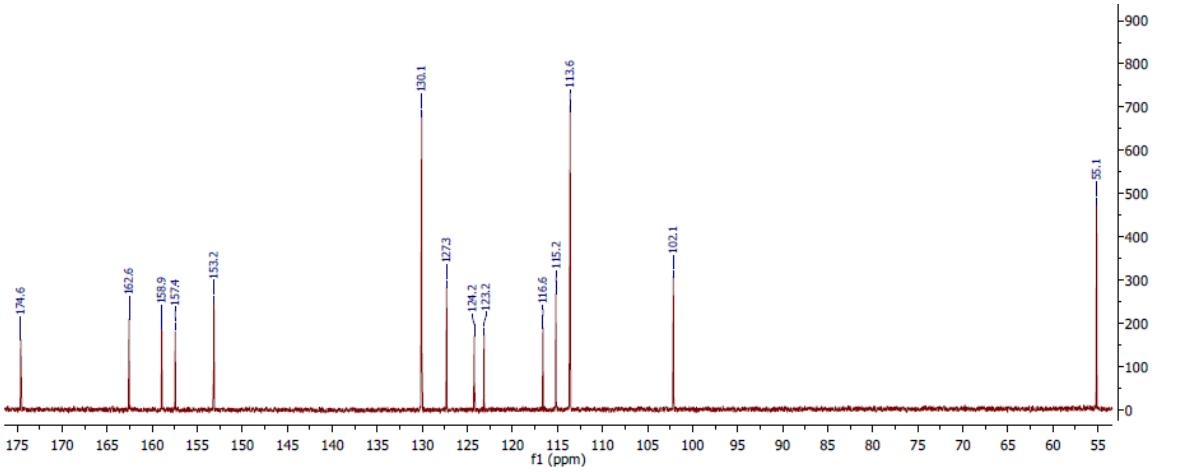

Appendix 1c: H H-Cosy for Compound 91

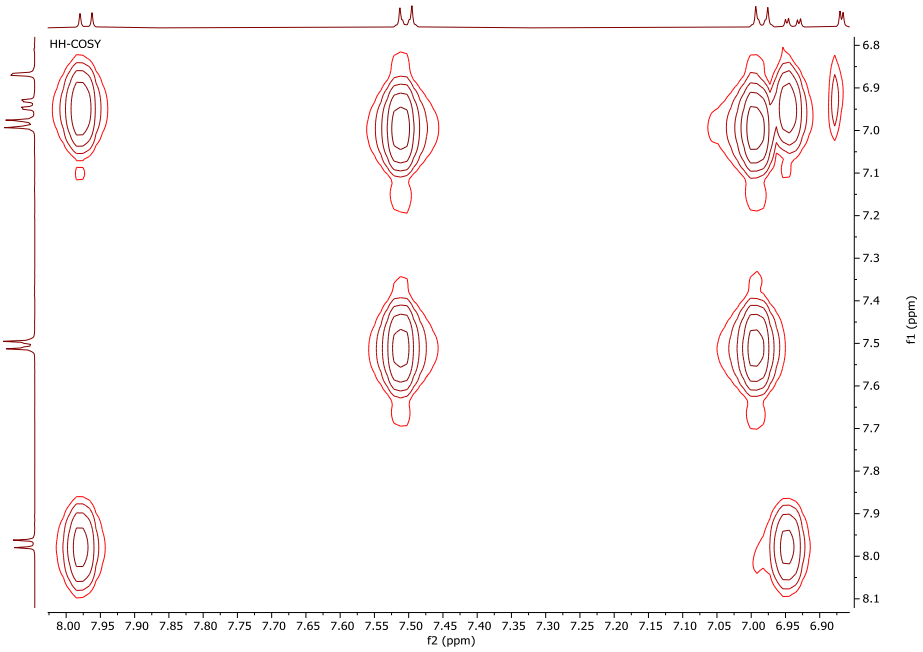

Appendix 1d: HSQC for Compound 91

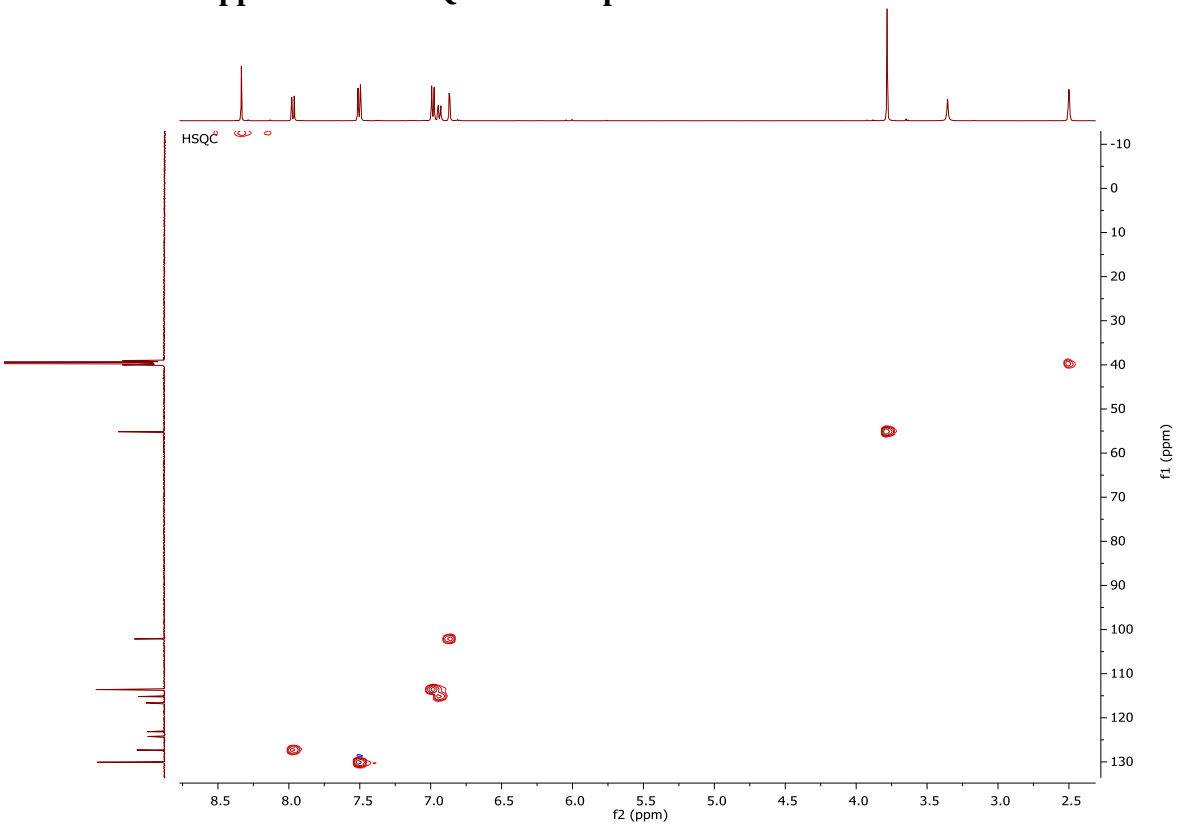

Appendix 1e: HMBC for Compound 91

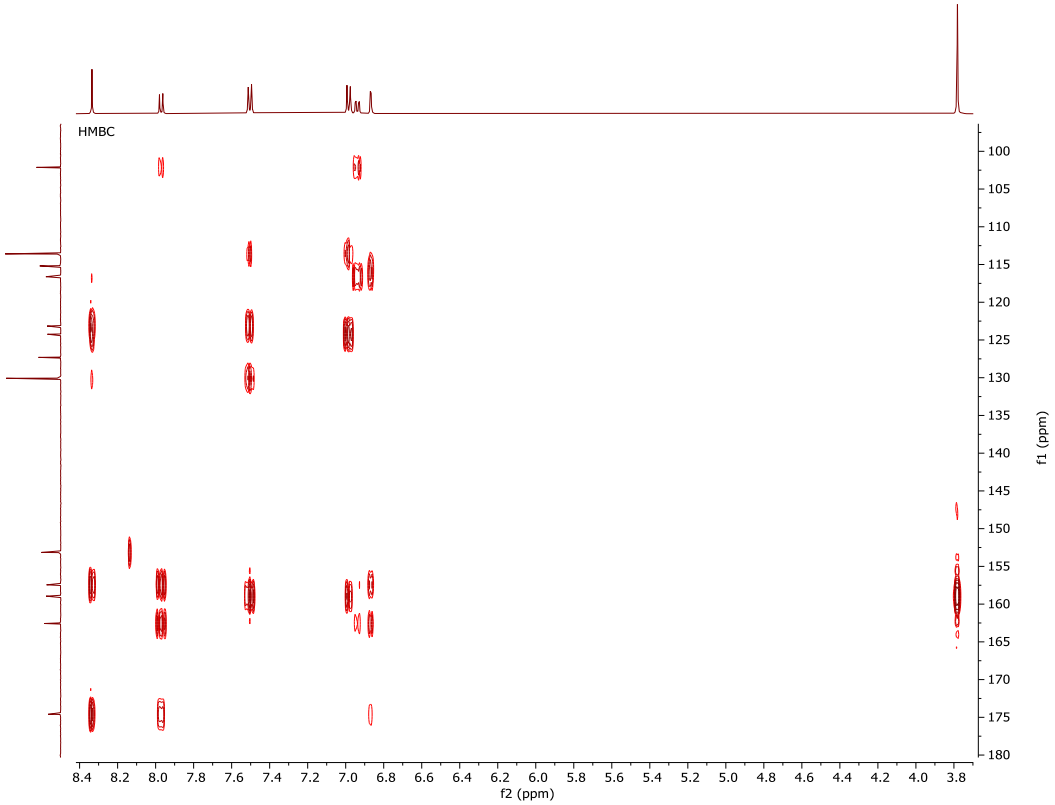

Appendix 2: NMR Spectra for Maximaisoflavone D (92)

Appendix 2a: ^{1}H NMR for Compound 92

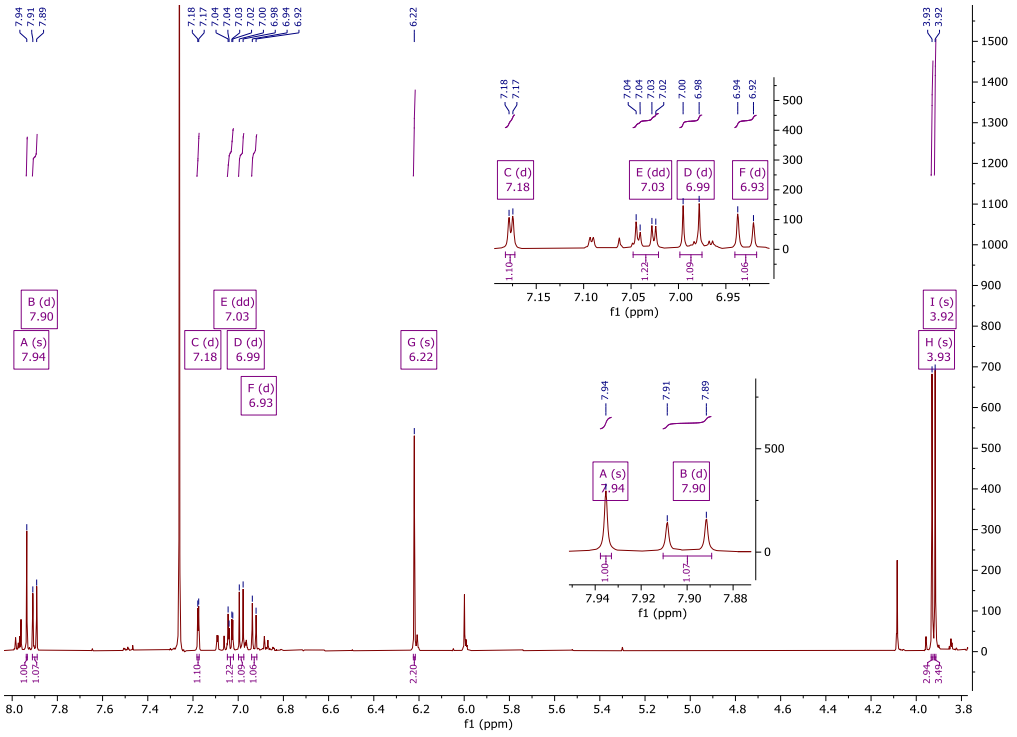

Appendix 2b: ^{13}C NMR for Compound 91

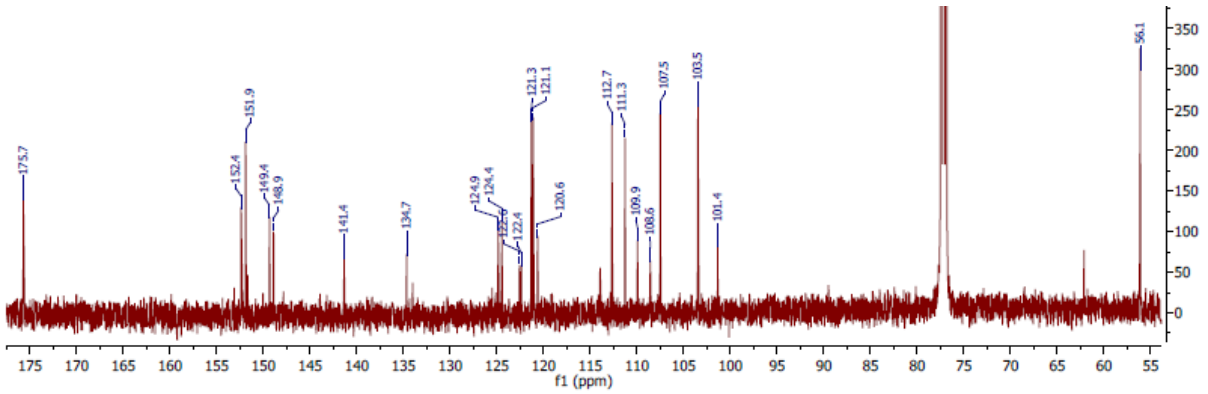

Appendix 2c: H H-Cosy for Compound 92

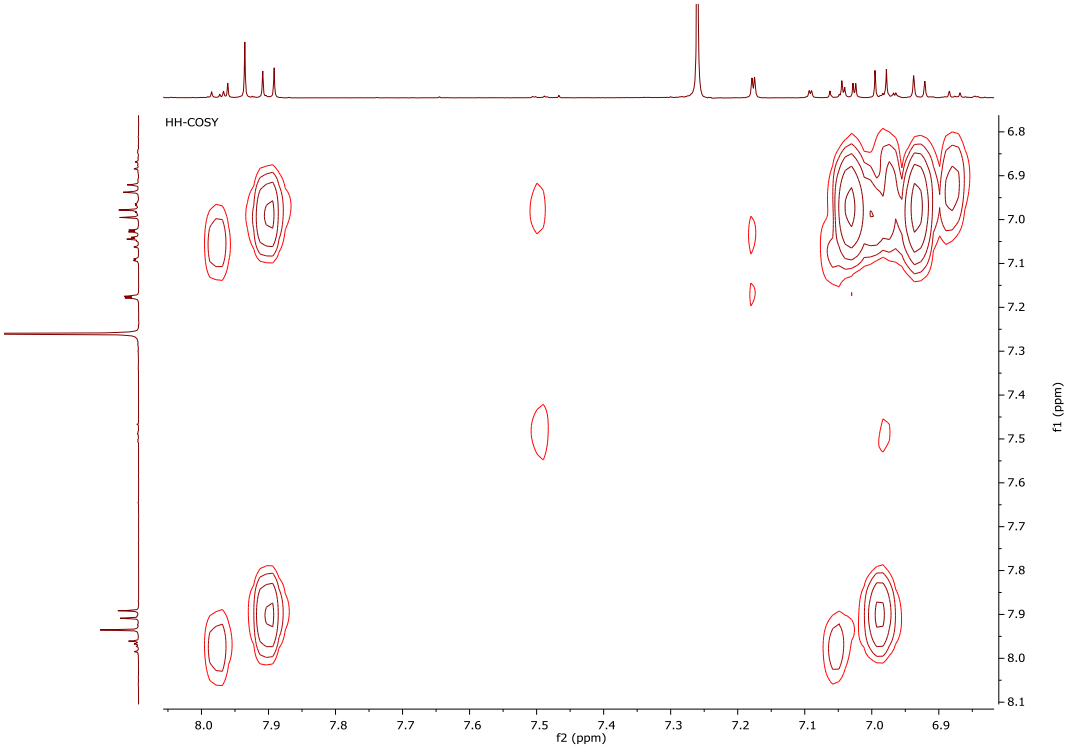

Appendix 2d: HSQC for Compound 92

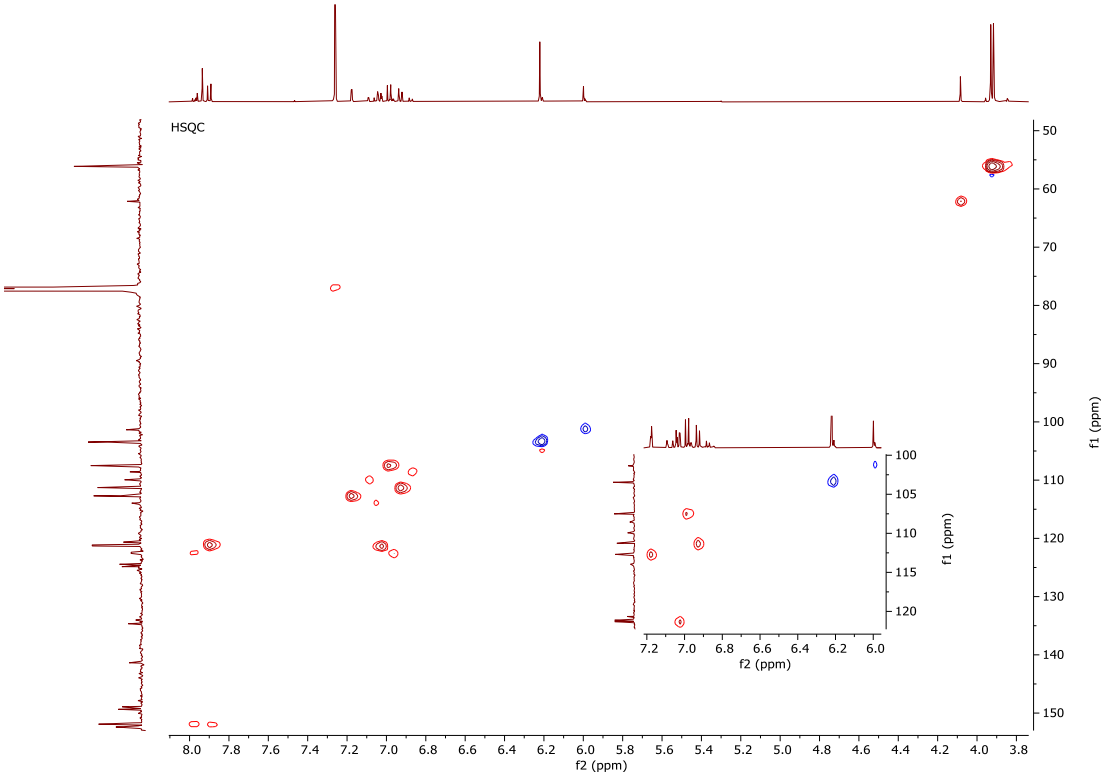

Appendix 2e: HMBC for Compound 92

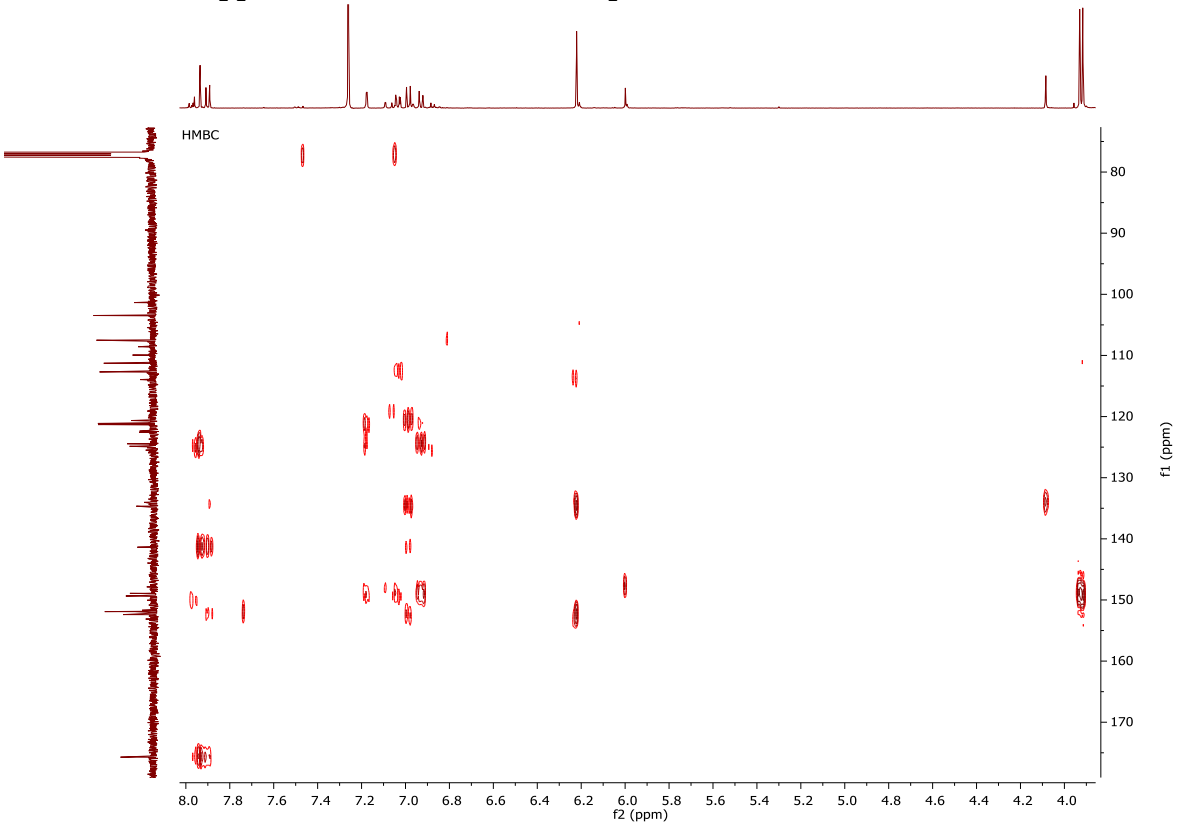

Appendix 3: NMR Data for Maximaisoflavone B (94)

Appendix 3a: ^{1}H NMR for Compound 94

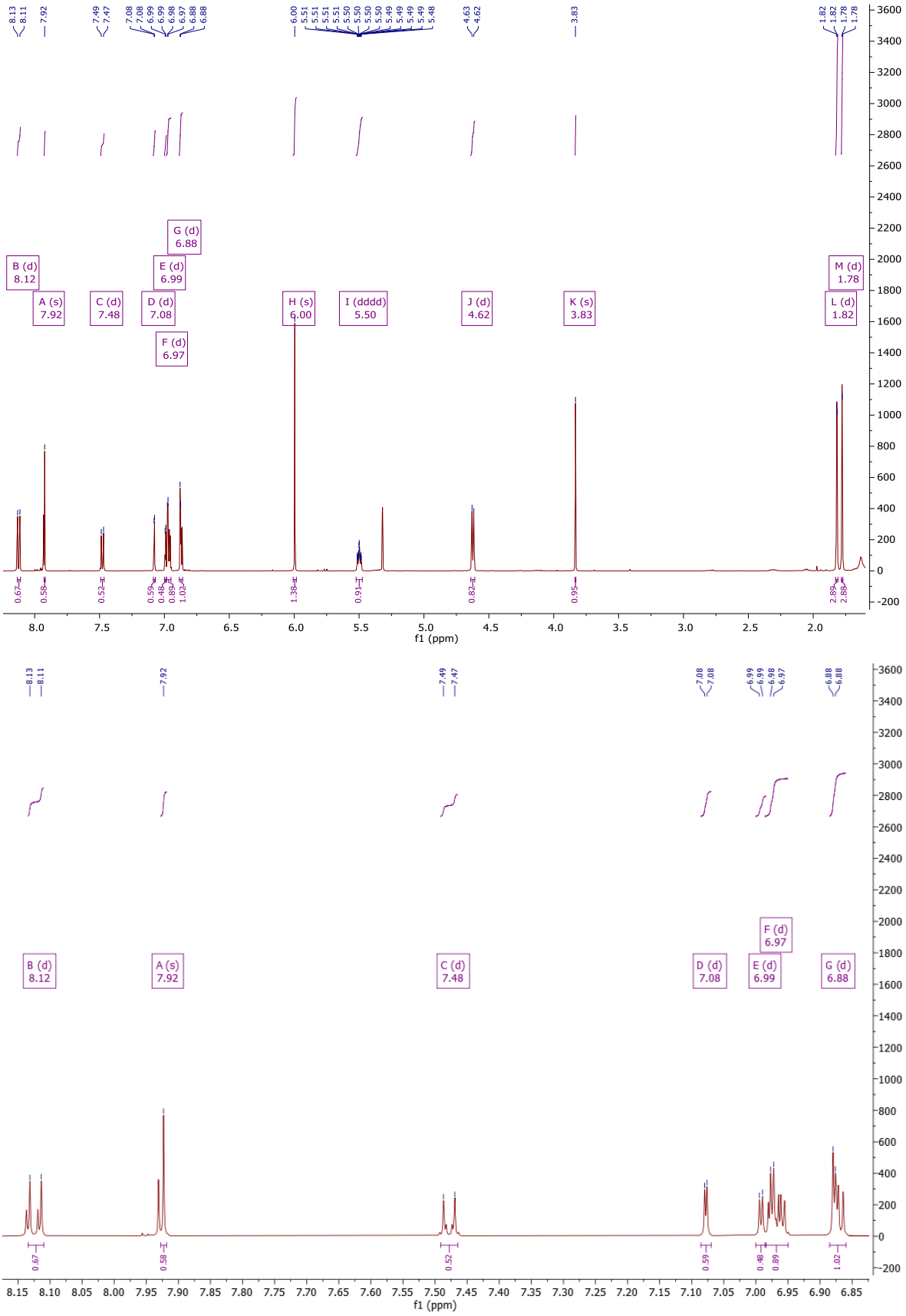

Appendix 3b: ^{13}C NMR for Compound 94

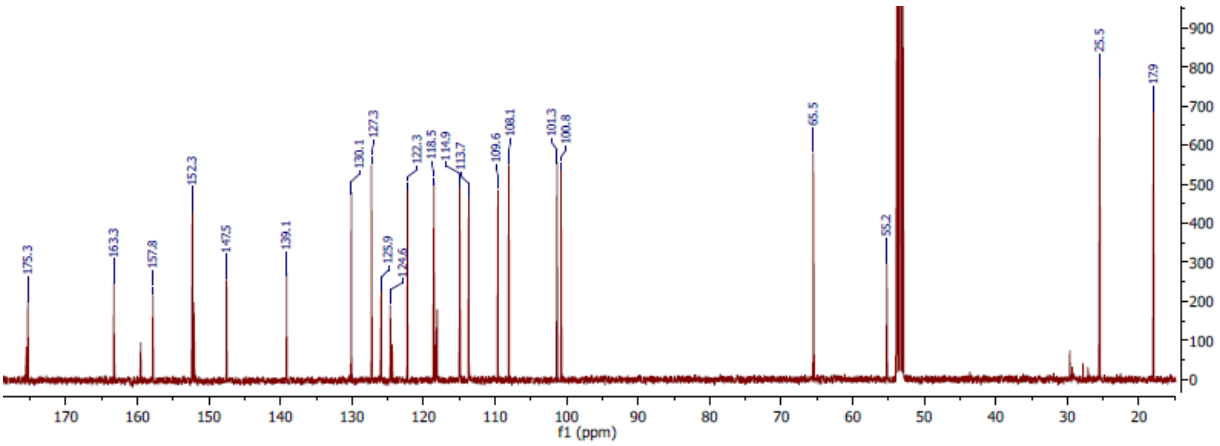

Appendix 3c H H-Cosy: NMR for Compound 94

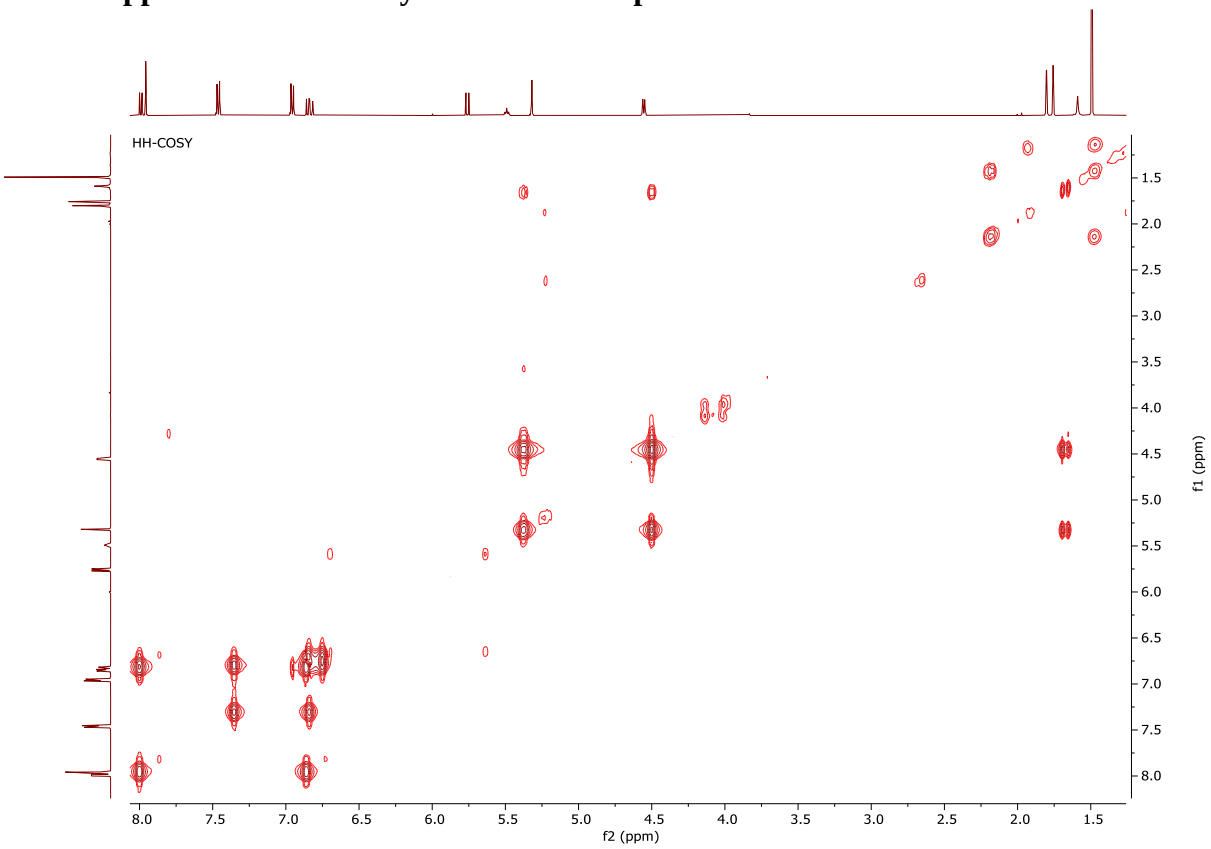

Appendix 3d HSQC for Compound 94

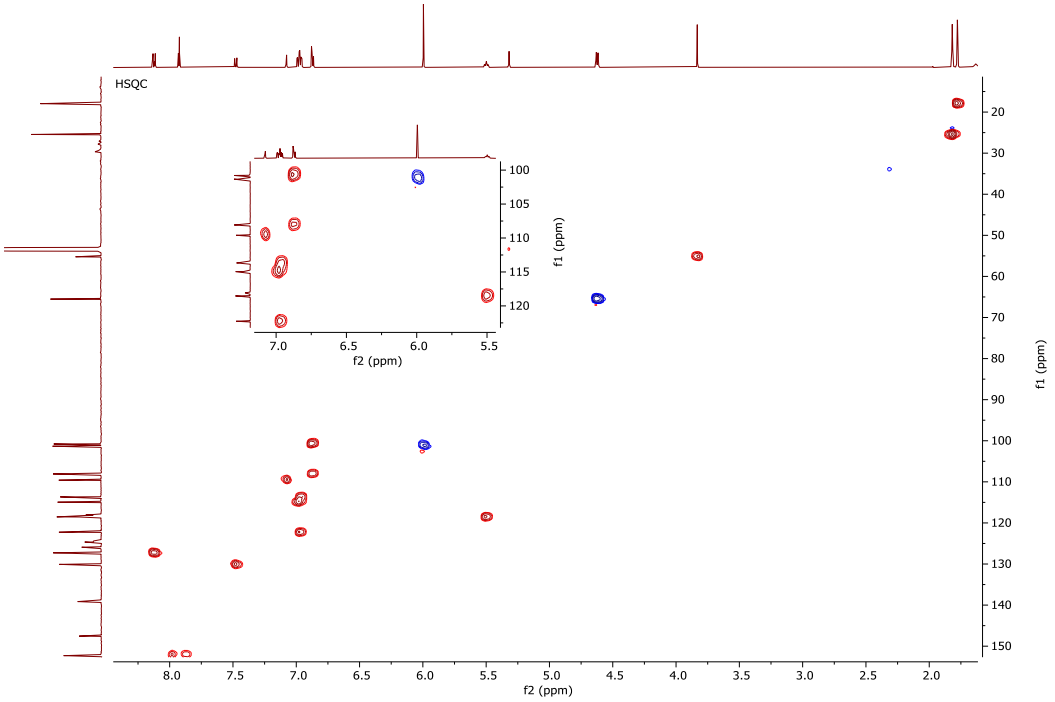

Appendix 3e: HMBC for Compound 94

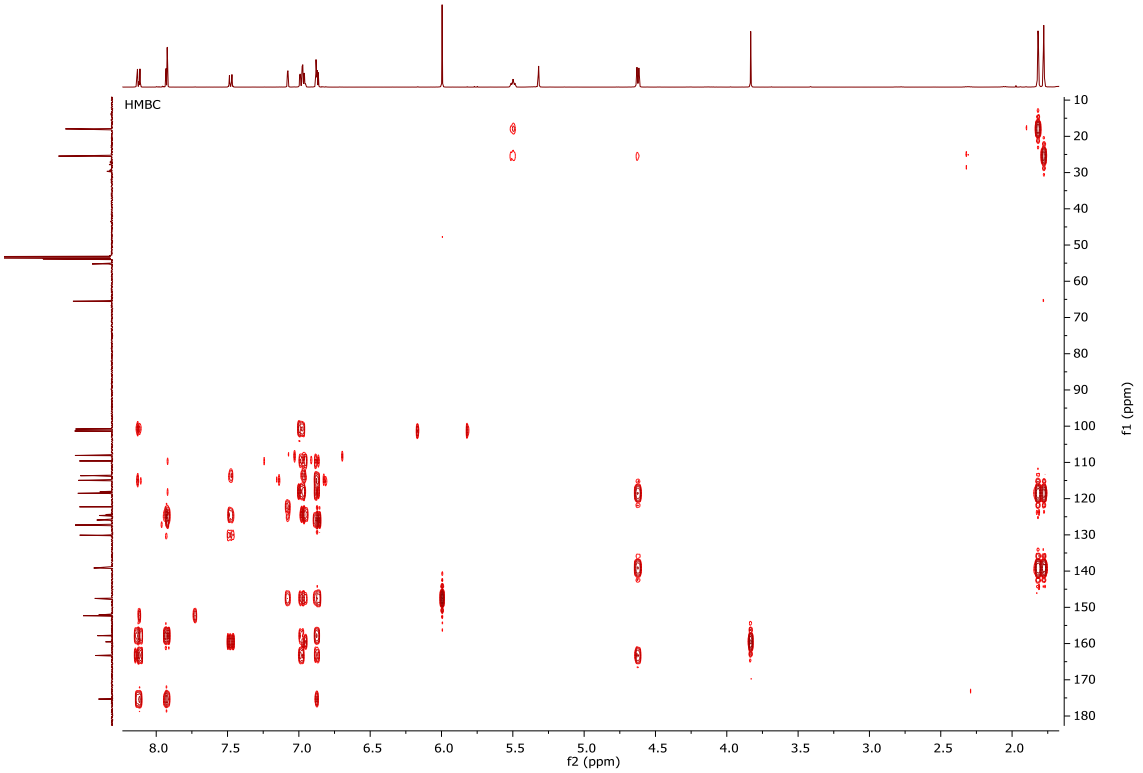

Appendix 3e: HMBC for Compound 94

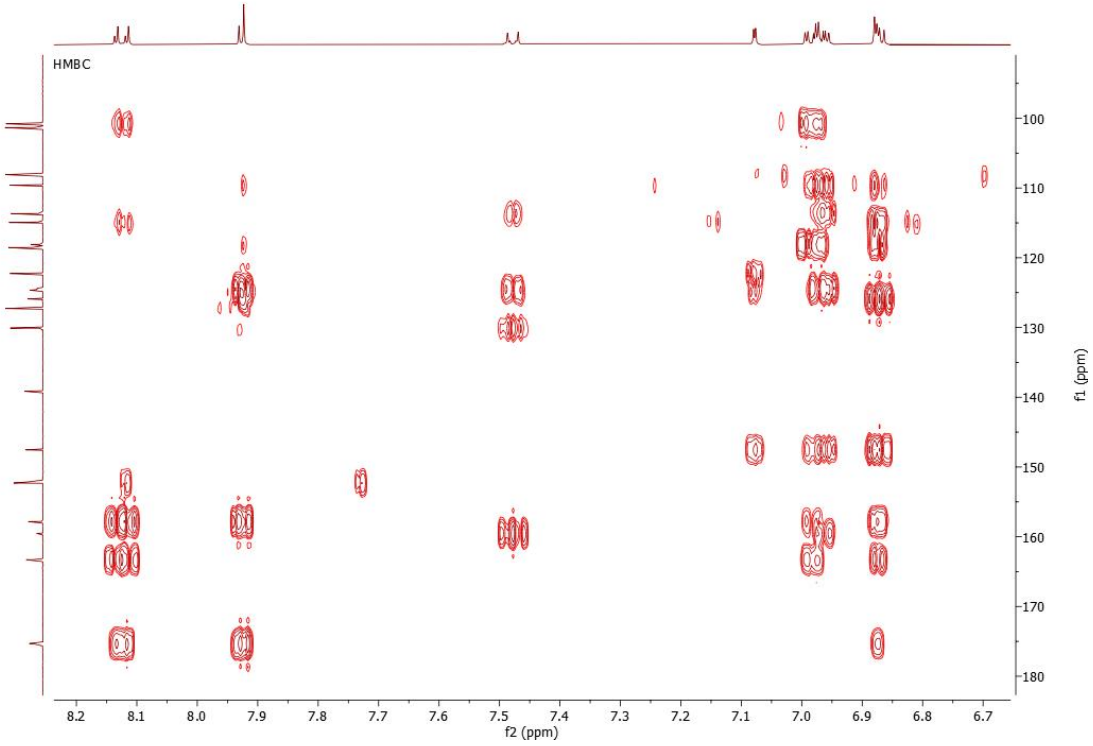

Appendix 4: NMR Spectra for Calopogogiumisoflavone A (97)

Appendix 4a: ^{1}H NMR for Compound 97

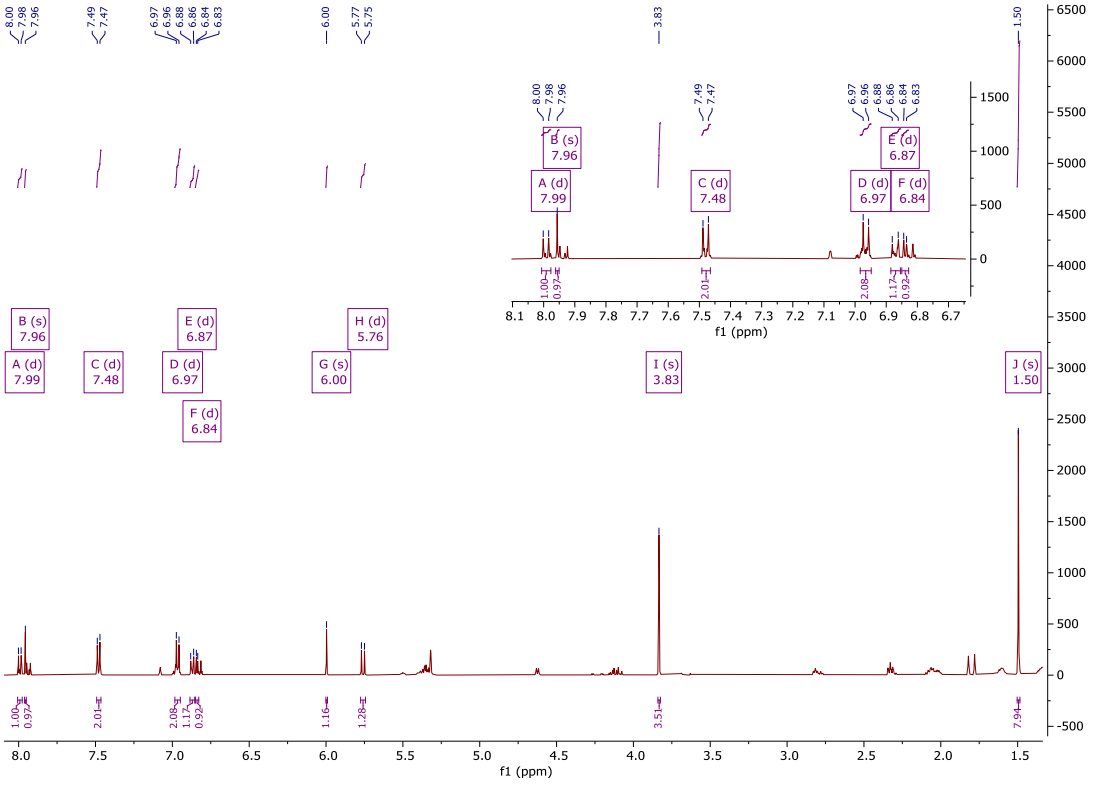

Appendix 4b: ^{13}C NMR for Compound 94

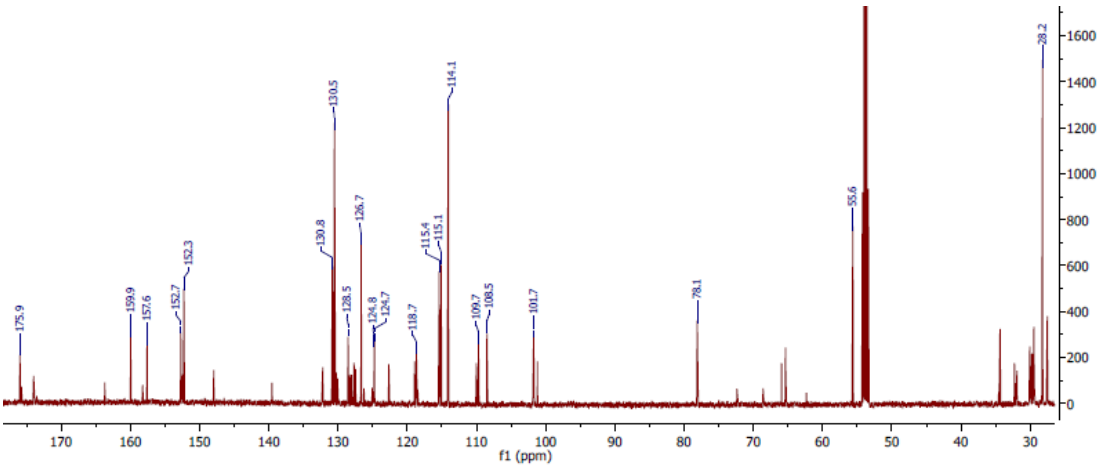

Appendix 4c: HSQC for Compound 97

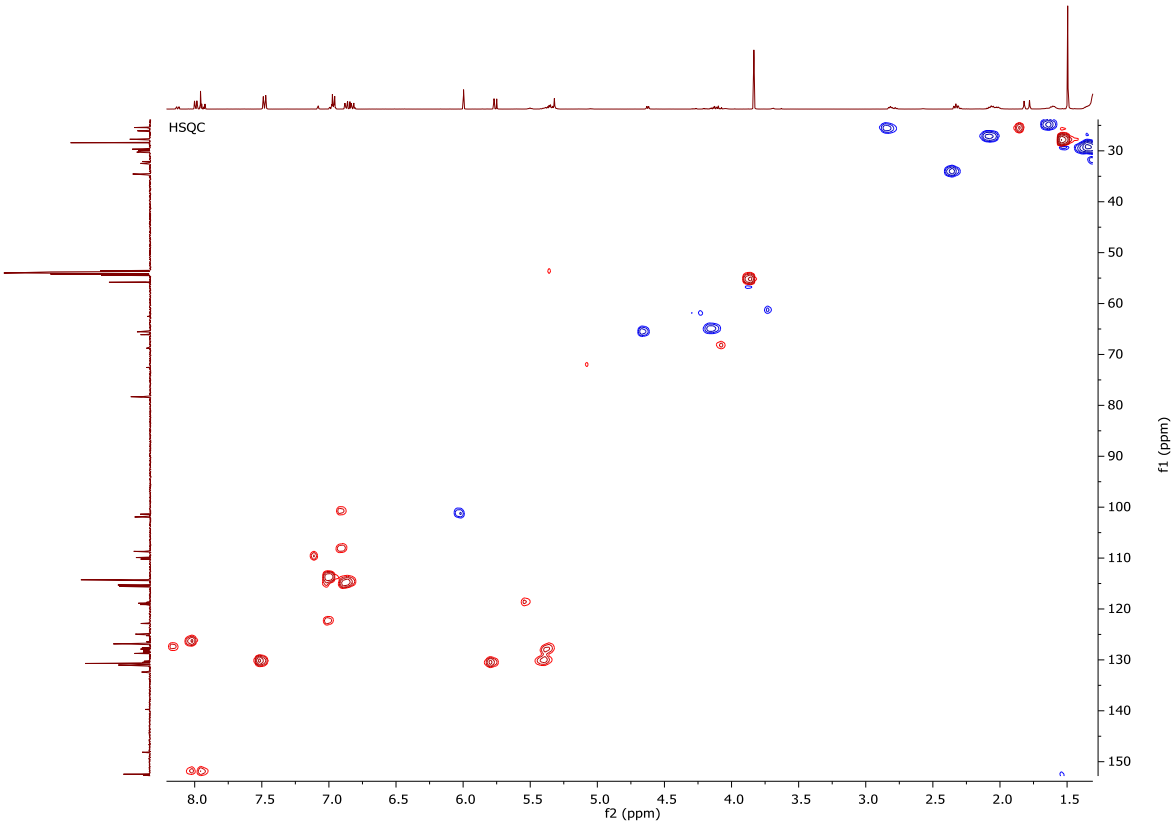

Appendix 4e: HMBC for Compound 97

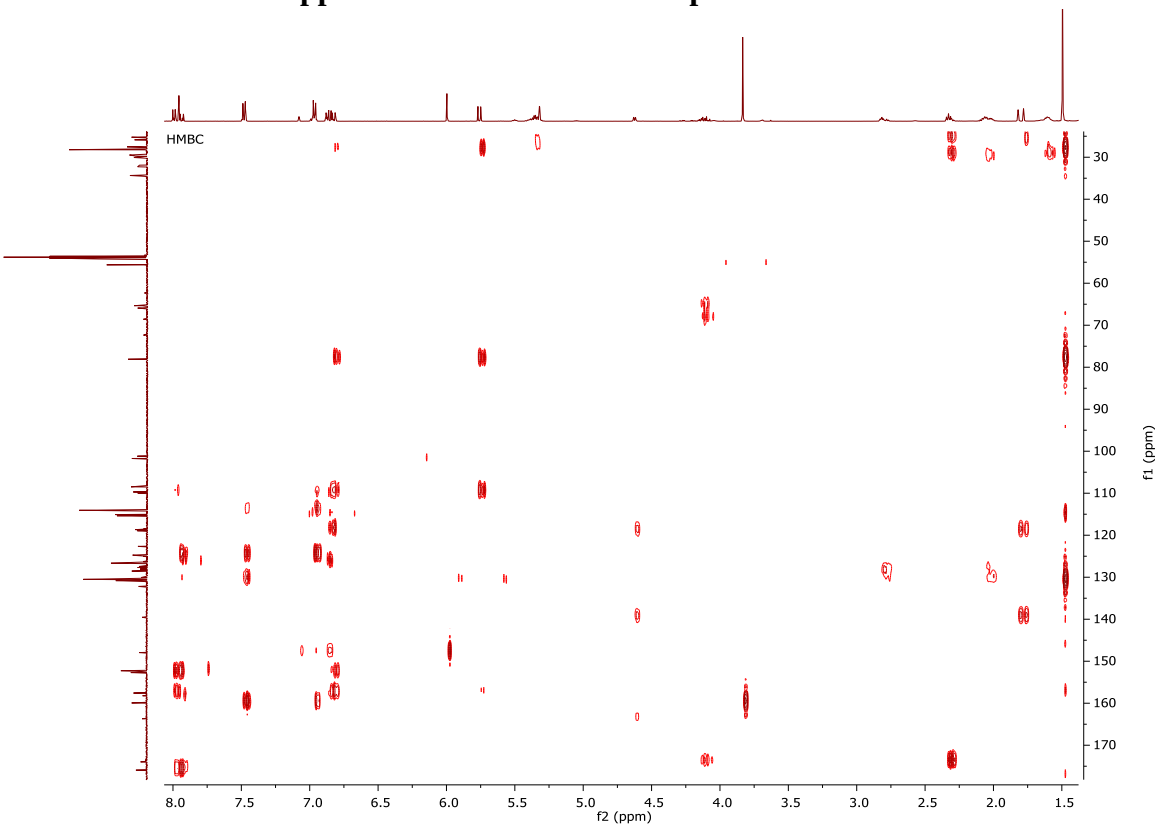

Appendix 5: NMR Spectra for Jamaicin (98)

Appendix 5a: ^{1}H NMR for Compound 98

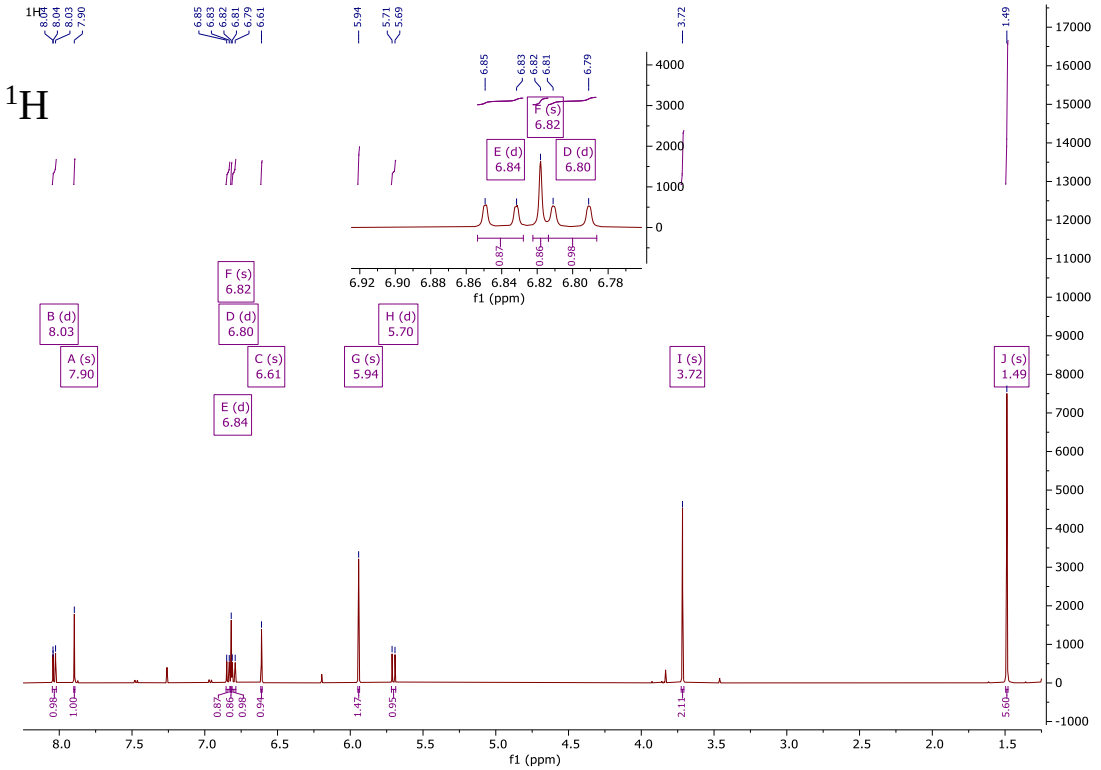

Appendix 5b: ^{13}C NMR for Compound 98

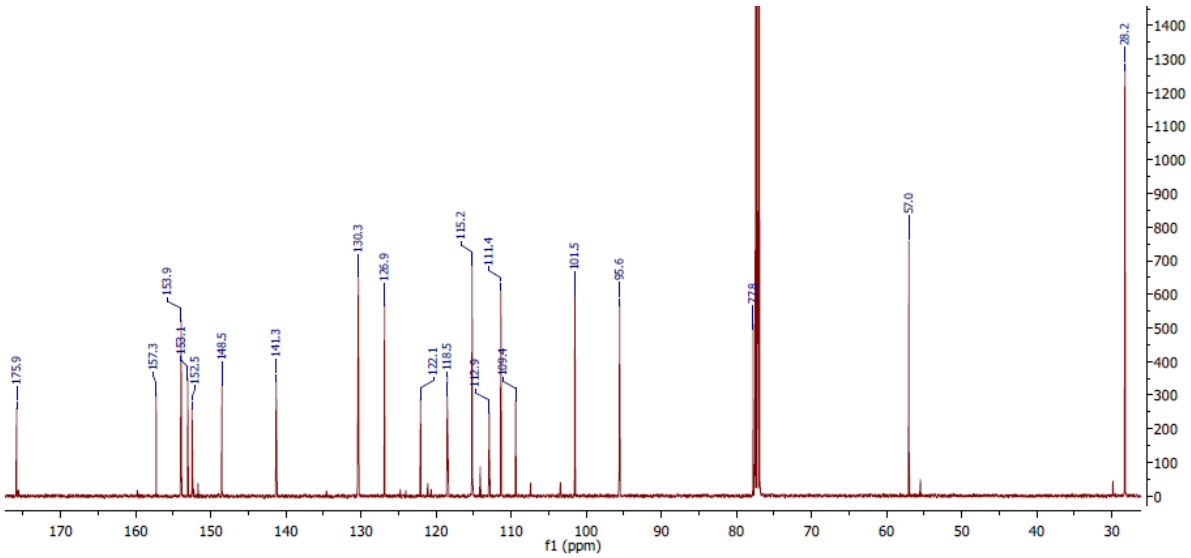

Appendix 5c: H H-Cosy for Compound 98

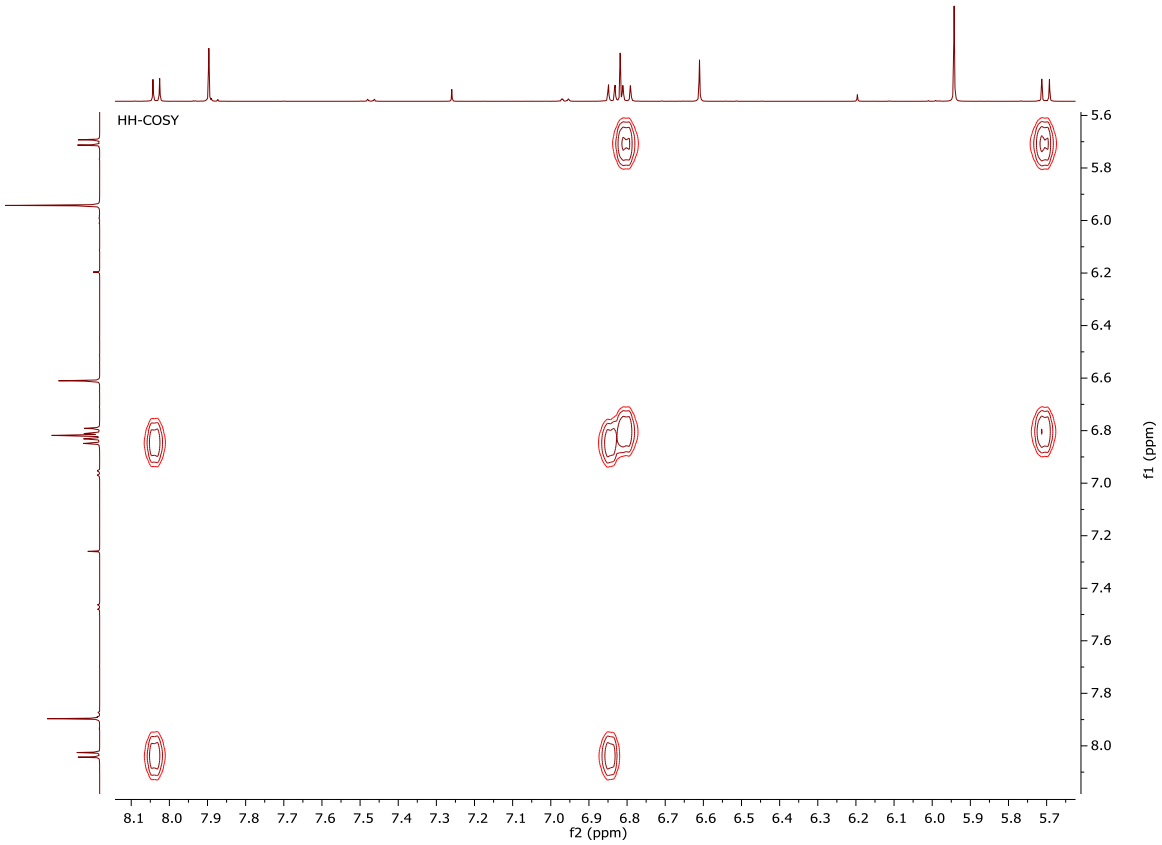

Appendix 5d: HSQC for Compound 97

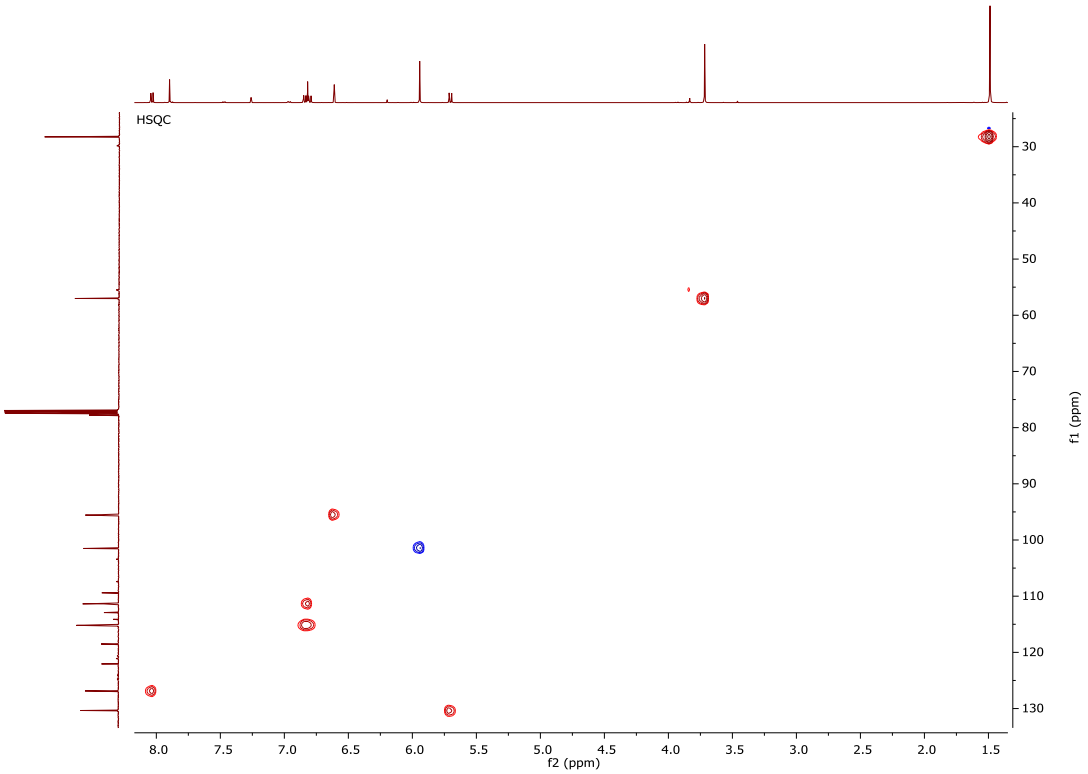

Appendix 5e: HMBC for Compound 98

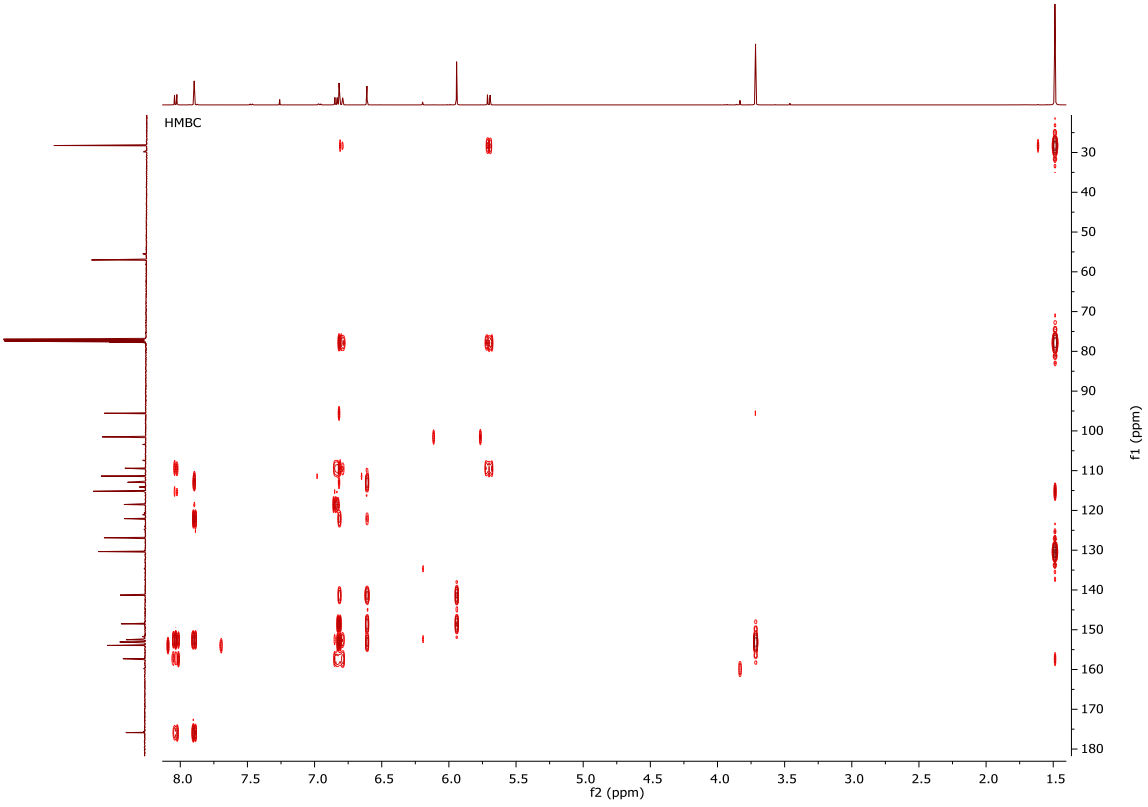

Appendix 6: NMR Spectra for Durmillone (99)

Appendix 6a: ^{1}H NMR for Compound 99

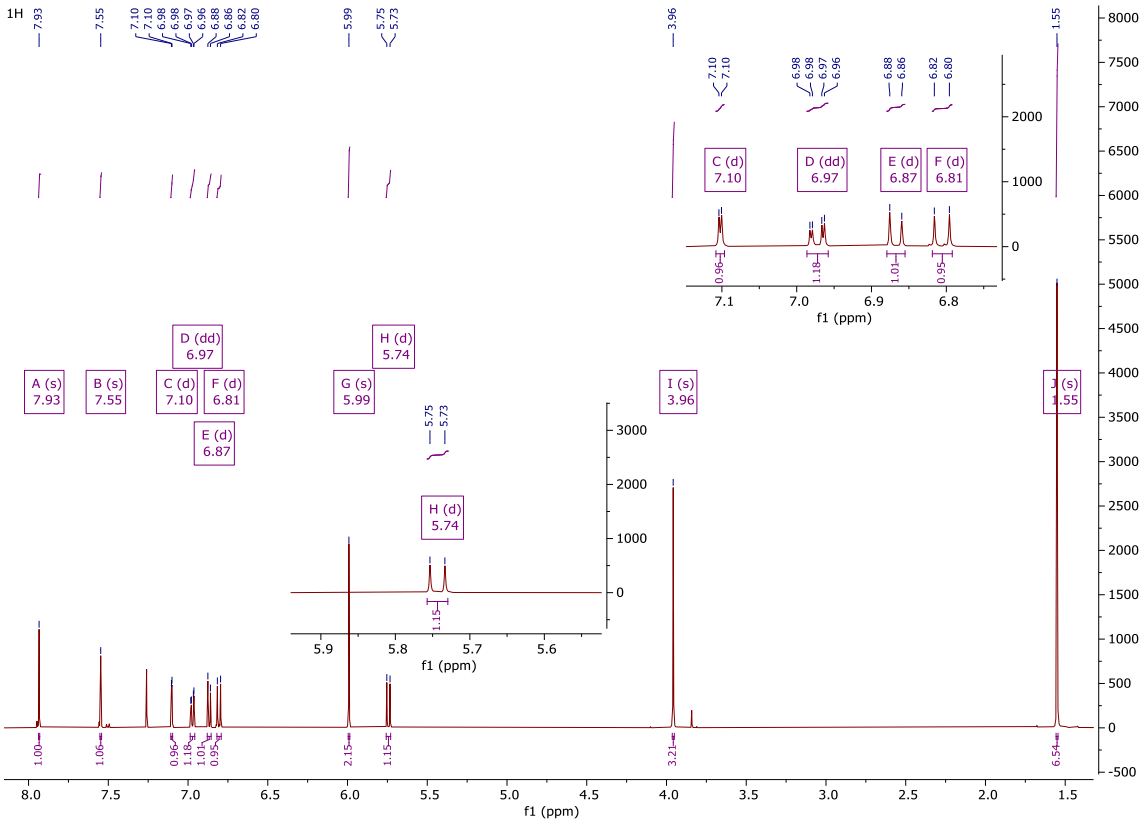

Appendix 6b: ^{13}C NMR for Compound 99

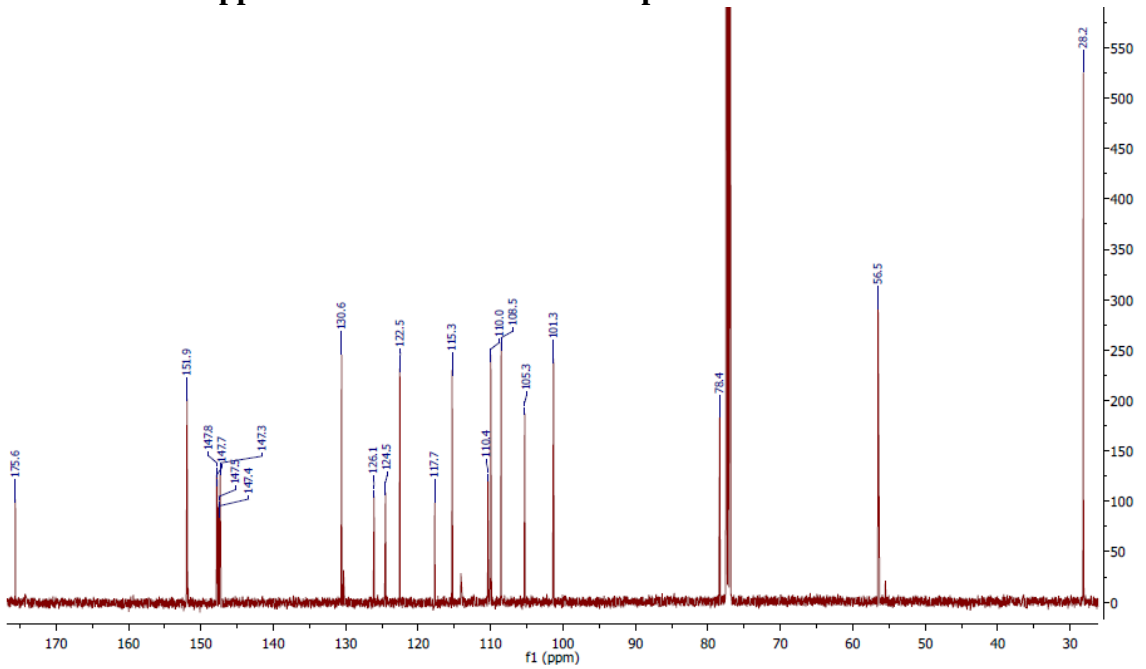

Appendix 6c: H H-Cosy for Compound 99

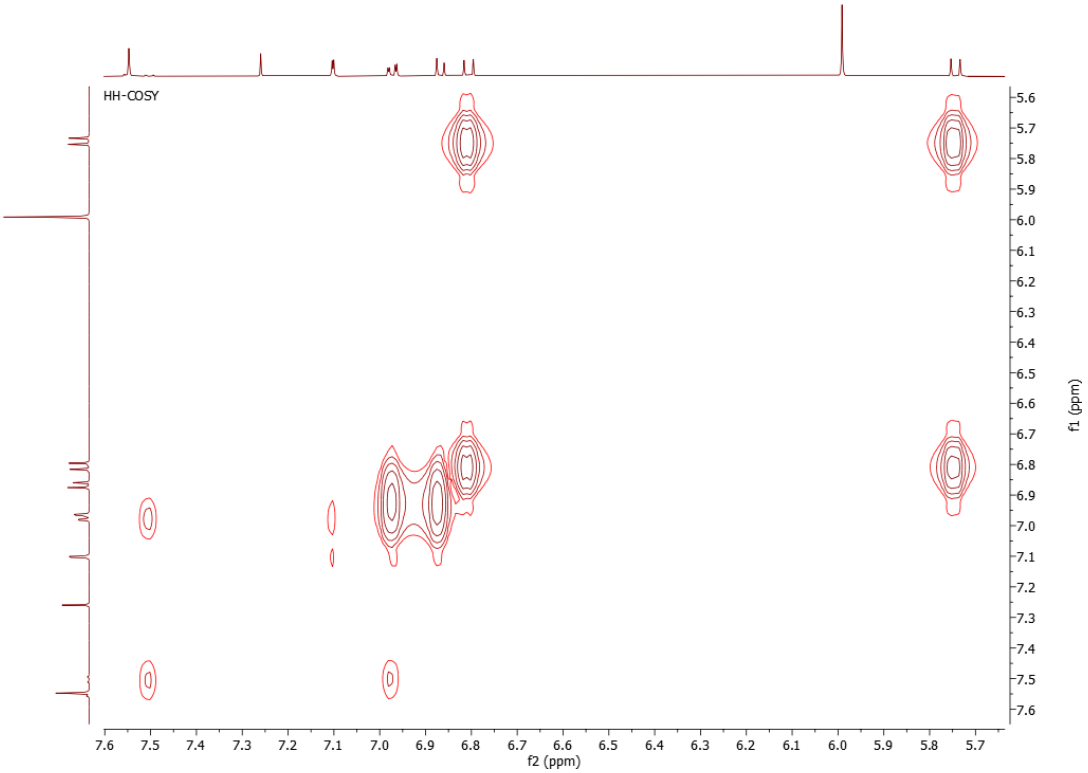

Appendix 6d: HSQC for Compound 99

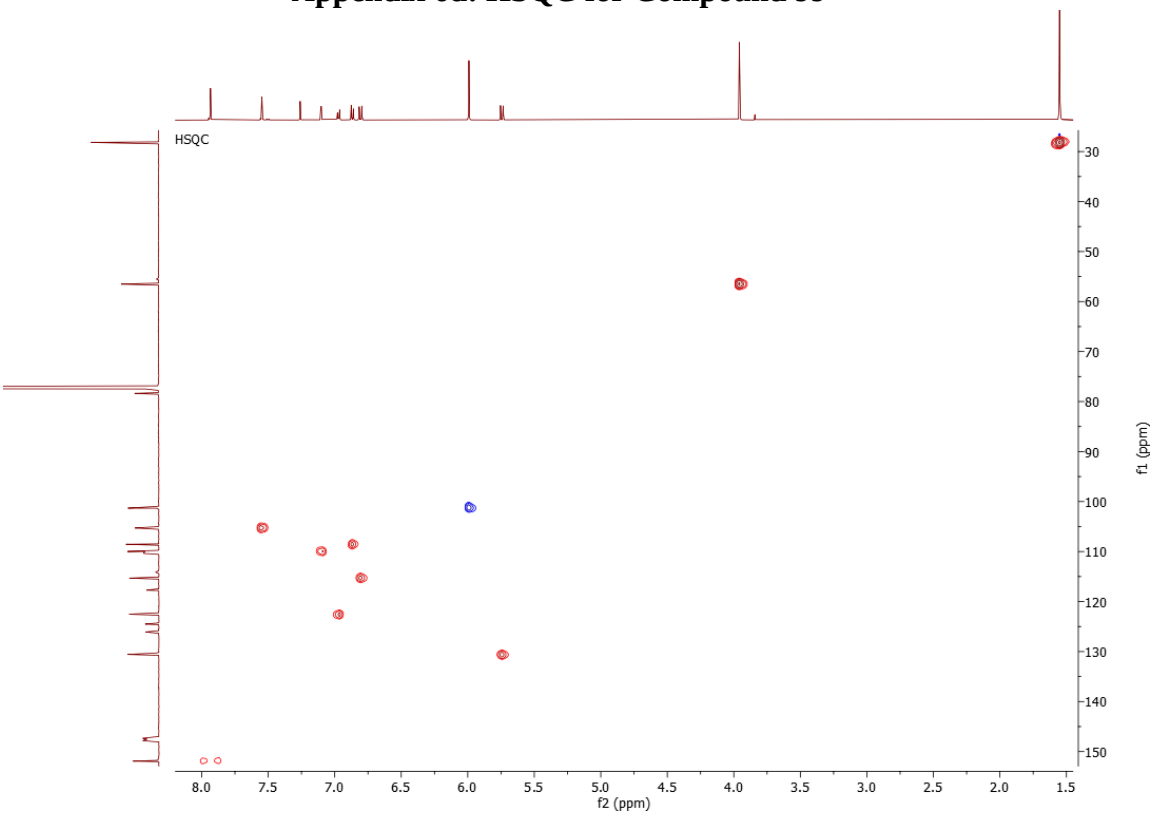

Appendix 6e: HMBC for Compound 99

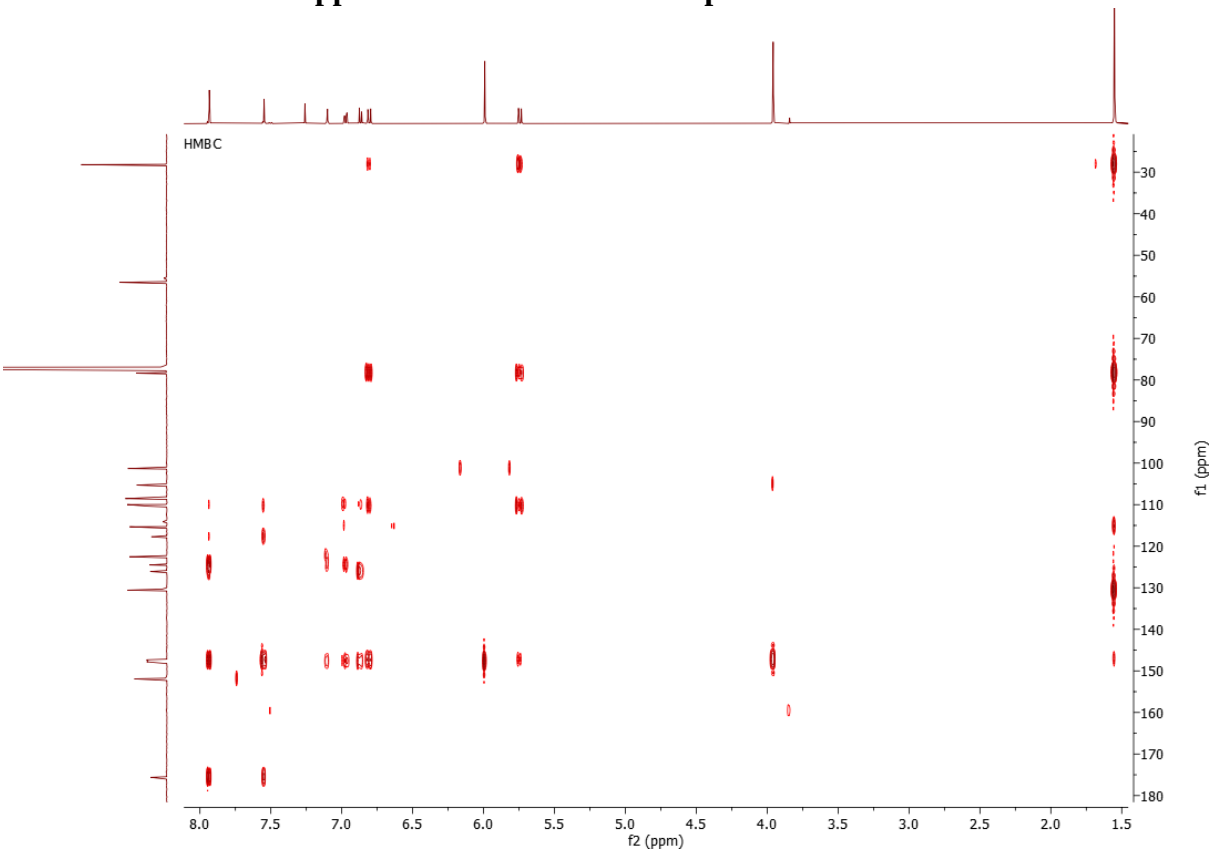

Appendix 7: NMR Spectra for Durallone (100)

Appendix 7a: ^{1}H NMR for Compound 100

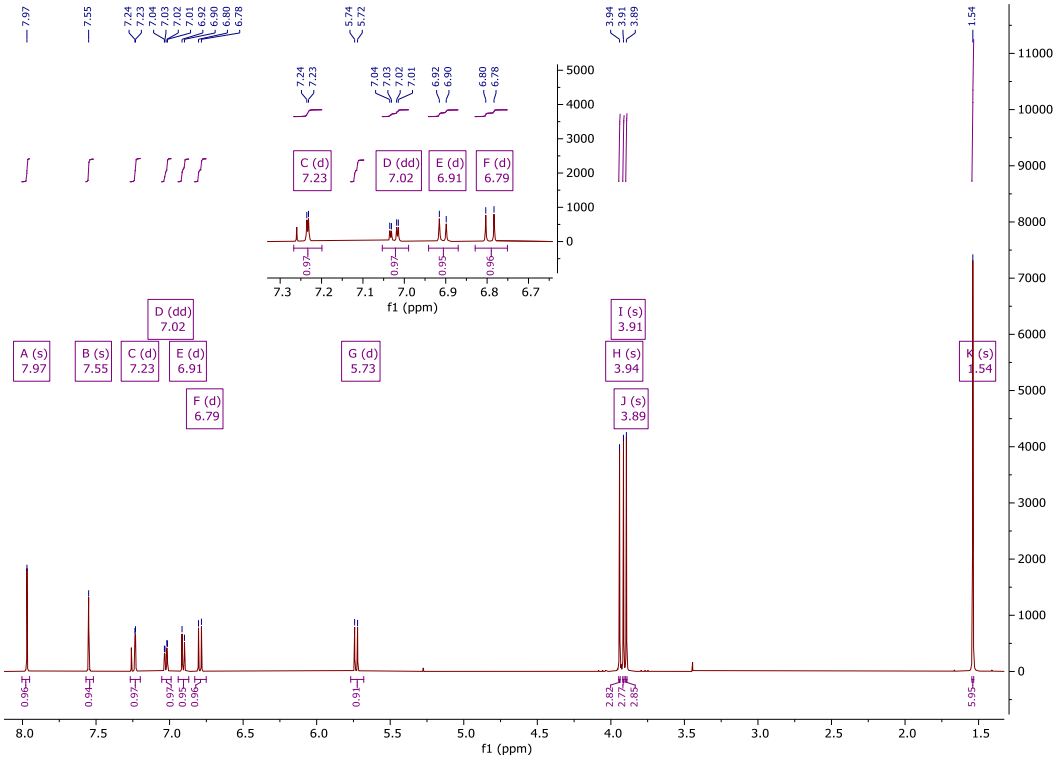

Appendix 7b: ^{13}C NMR for Compound 100

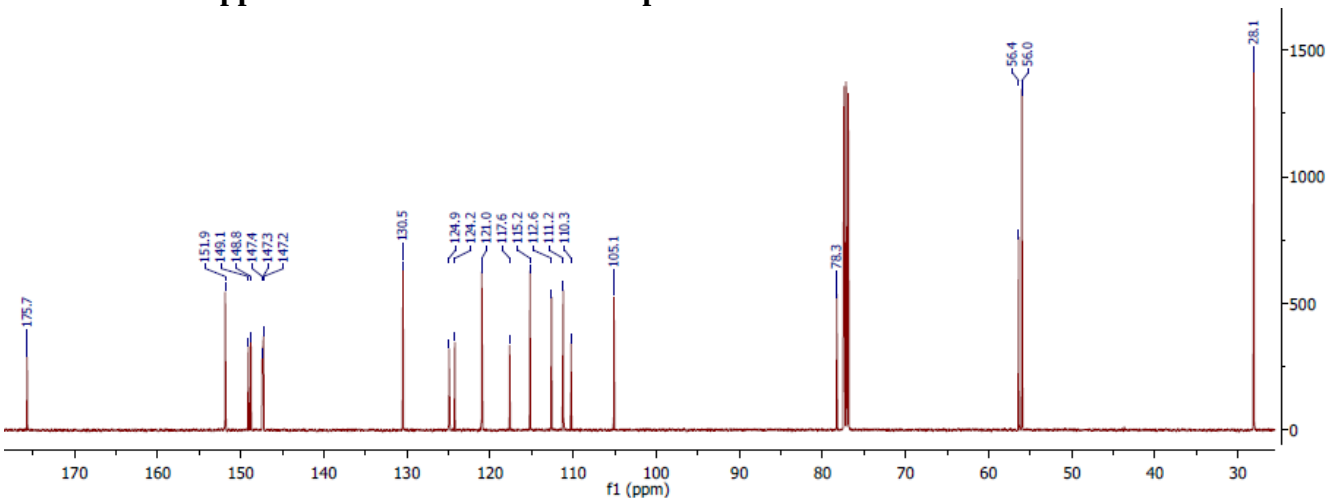

Appendix 7c: H H-Cosy for Compound 100

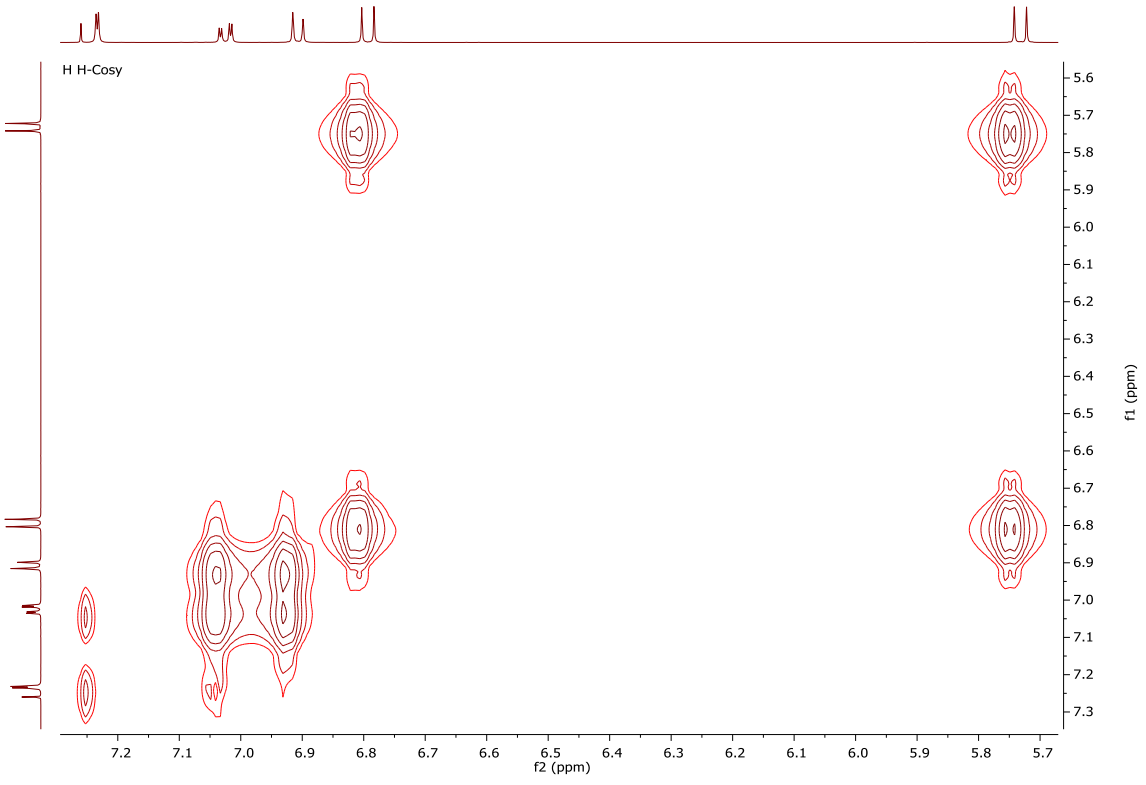

Appendix 7c: HSQC for Compound 100

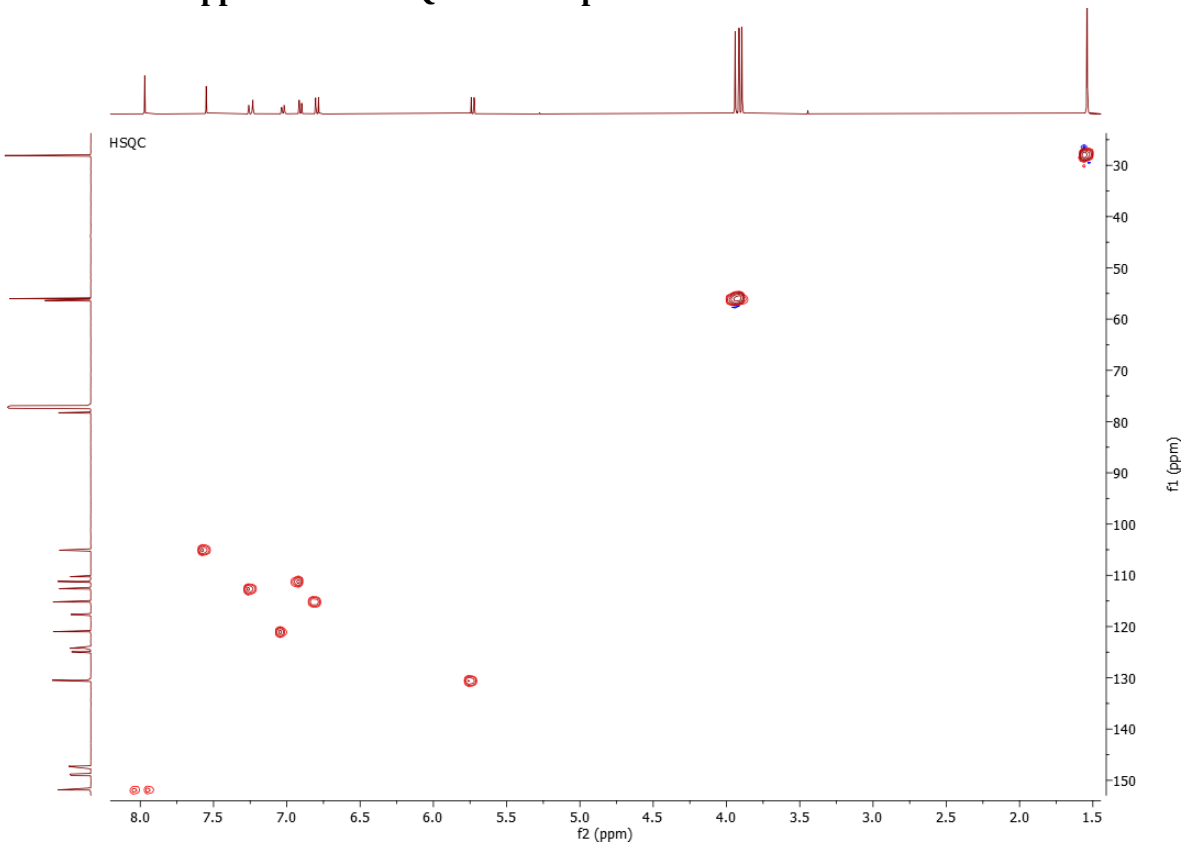

Appendix 7c: HSQC for Compound 100

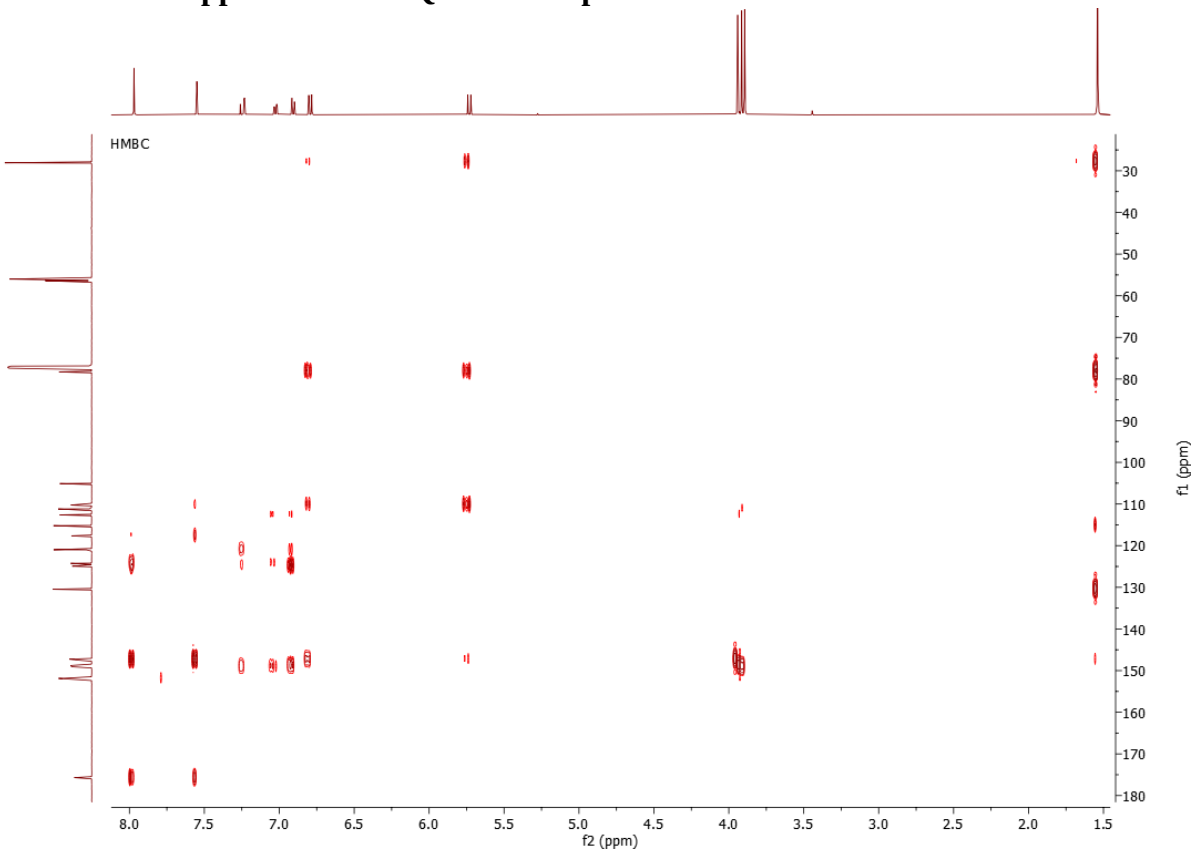

Appendix 8: NMR Spectra for 6-Methoxycalopogogiumisoflavone A (101)

Appendix 8a: ^{1}H NMR for Compound 101

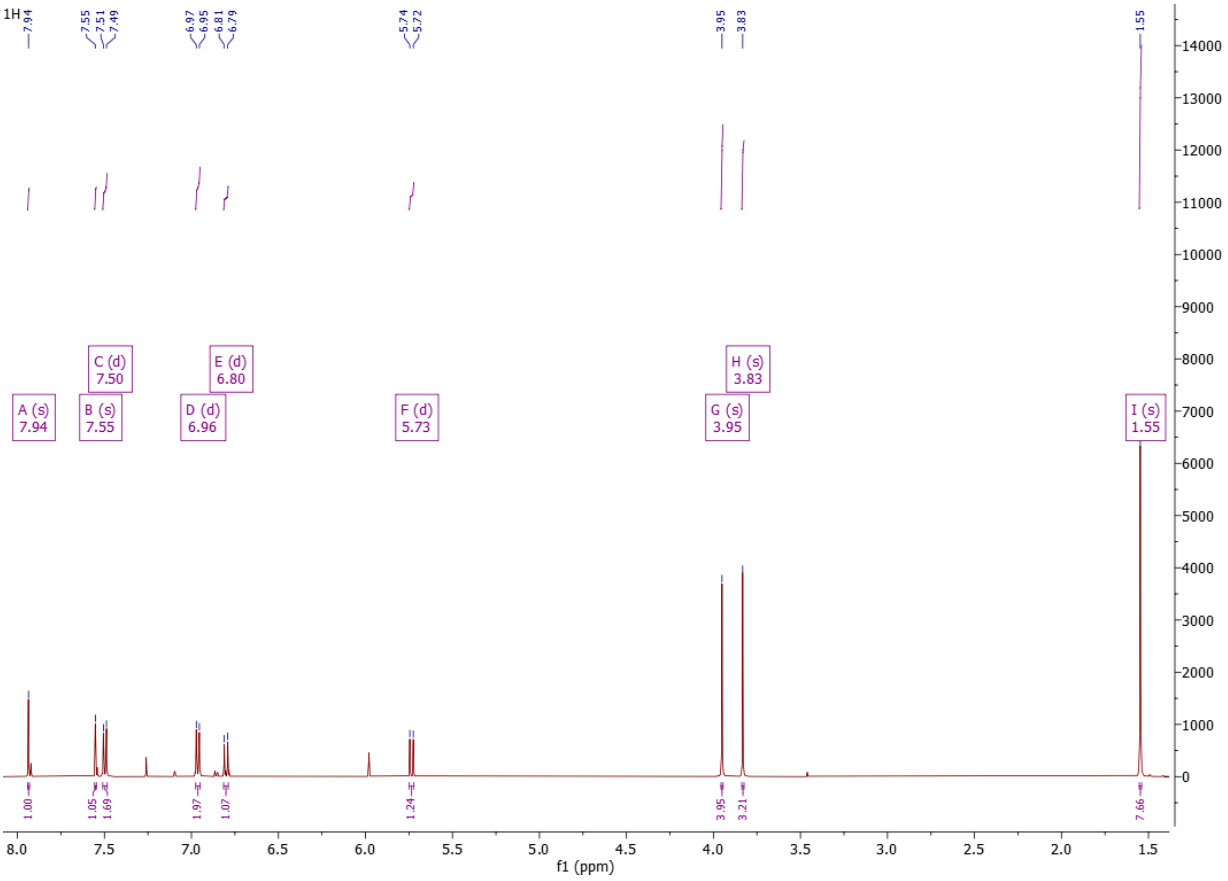

Appendix 8b: ^{13}C NMR for Compound 101

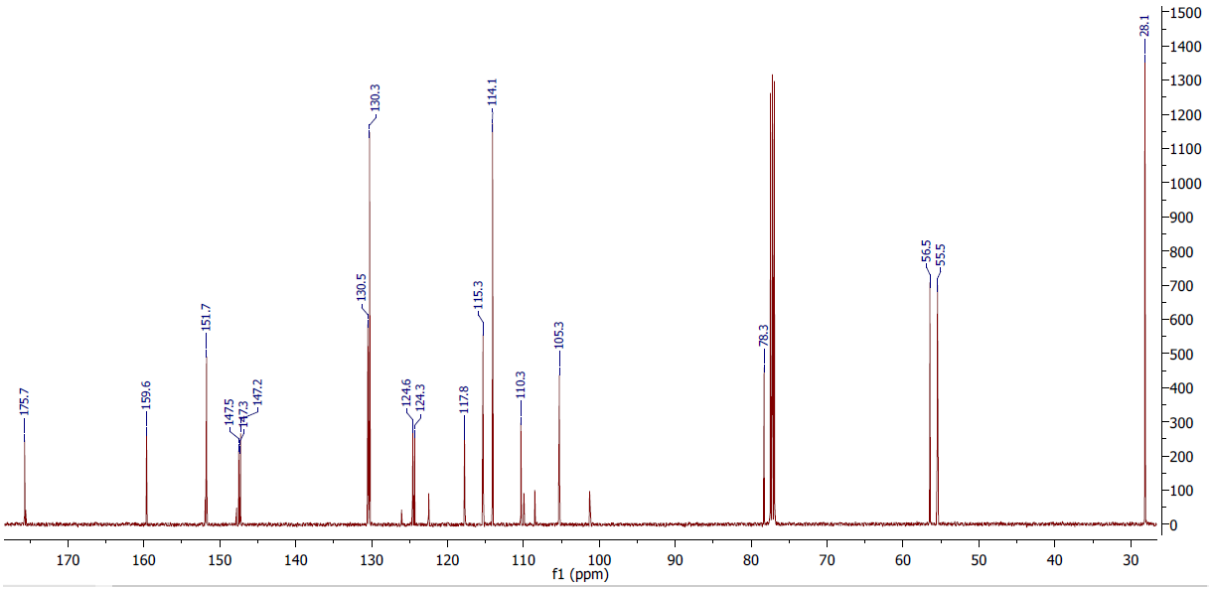

Appendix 8c: H H-Cosy for Compound 101

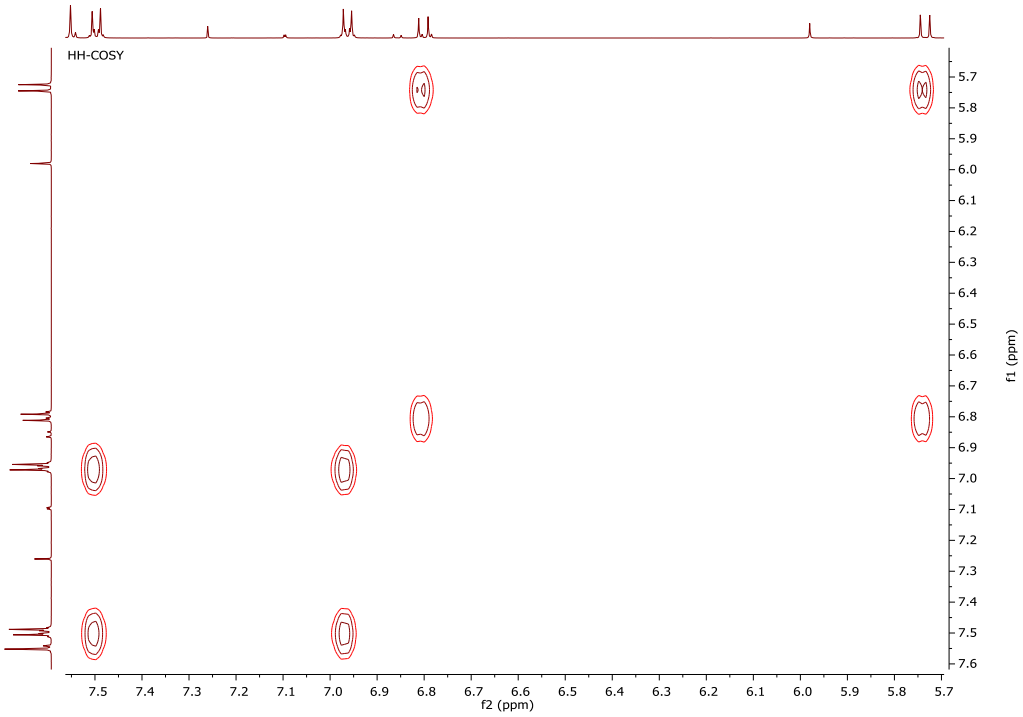

Appendix 8d: H SQC for Compound 101

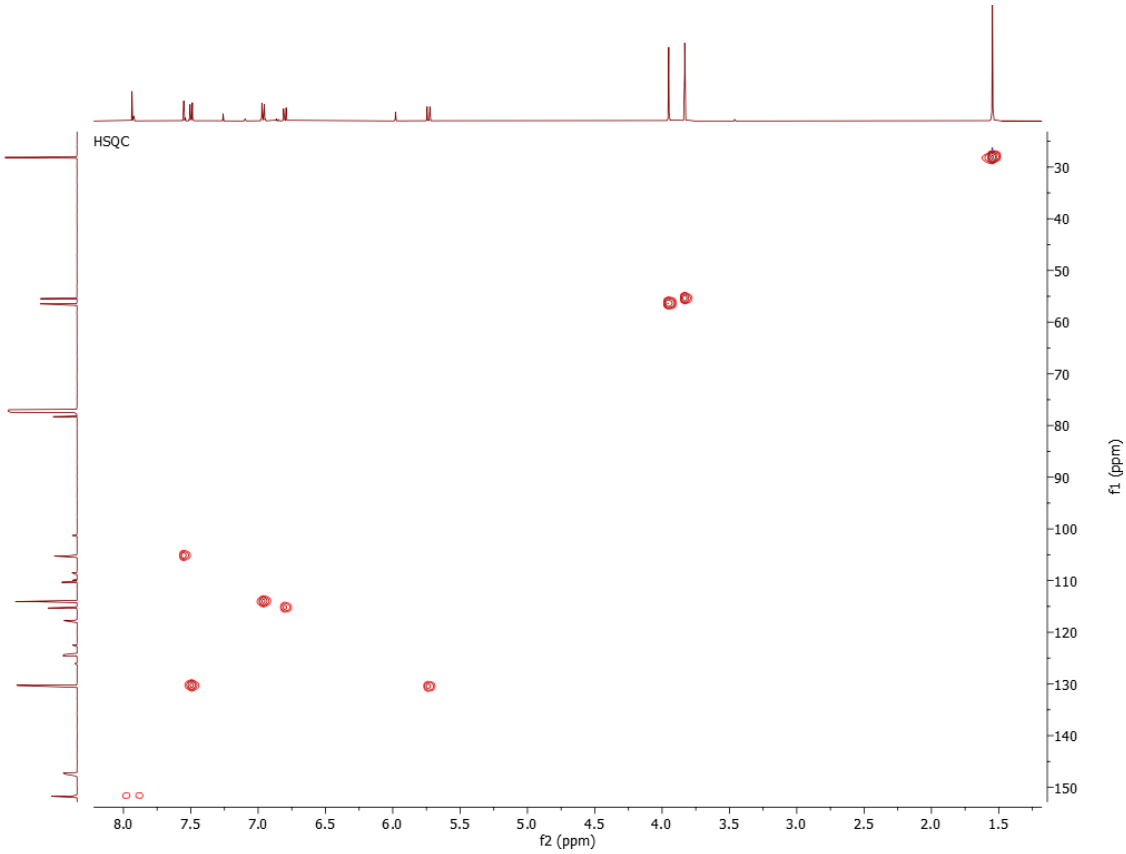

Appendix 8e: HMBC for Compound 101

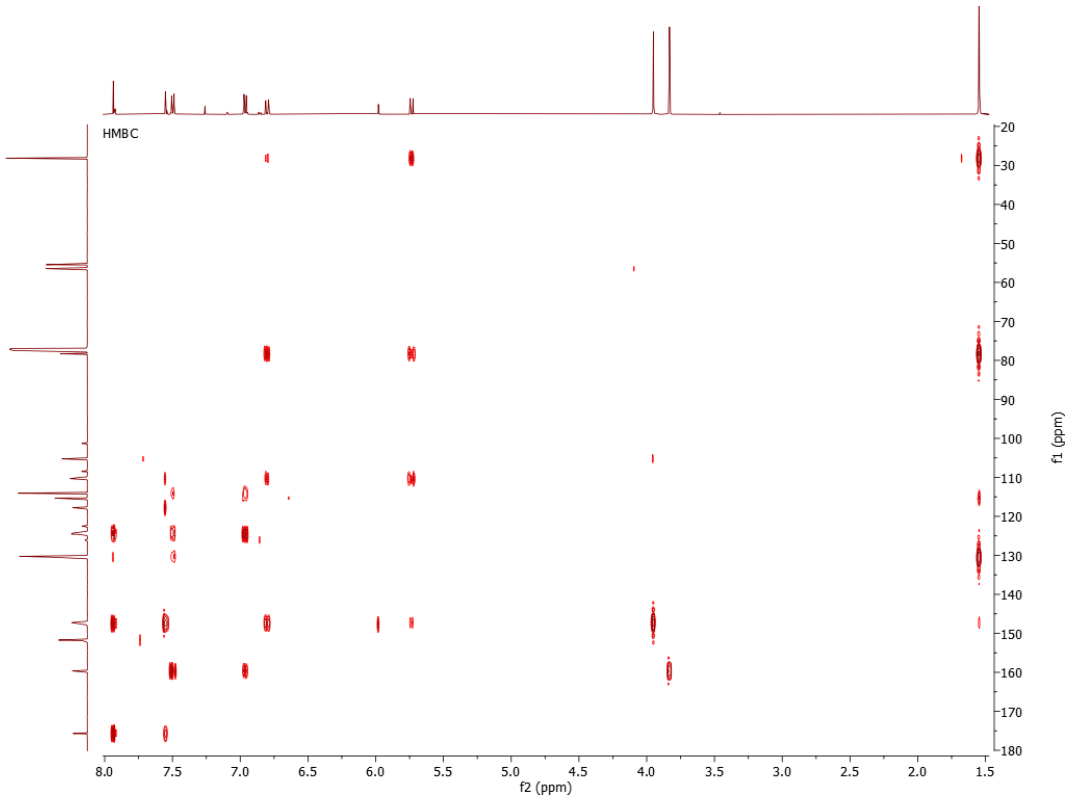

Appendix 9: NMR Spectra for Isoerythrin-A-4′-(3-methylbut-2-enyl)ether (102)

Appendix 9a: ^{1}H NMR for Compound 102

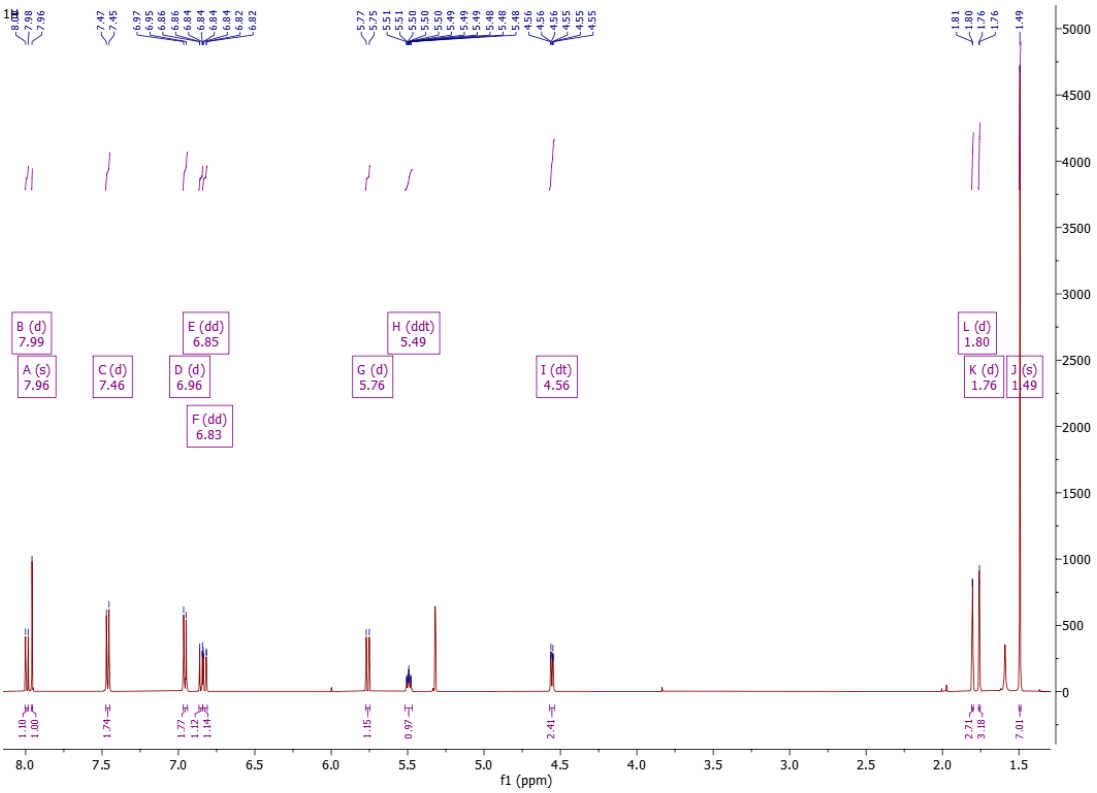

Appendix 9b: ^{13}C NMR for Compound 102

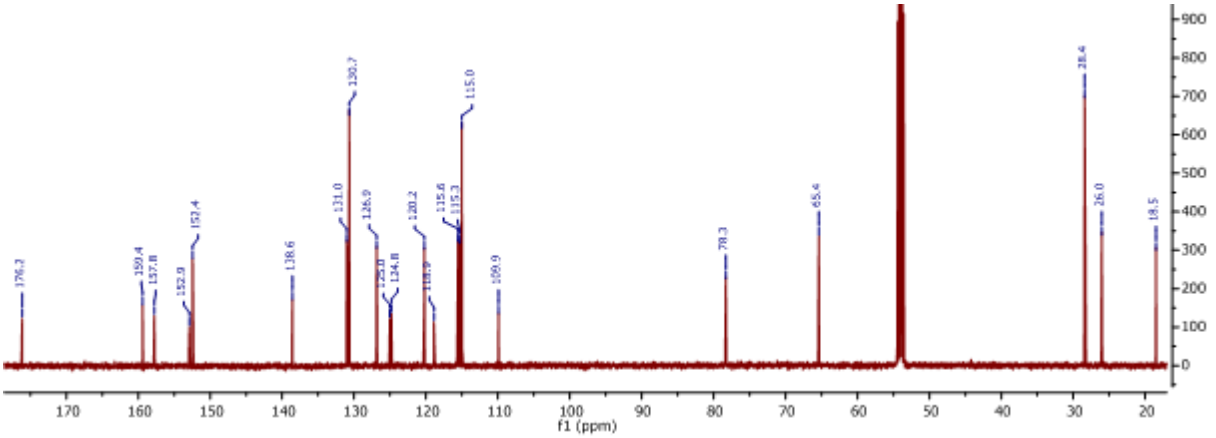

Appendix 9c: H H-Cosy for Compound 102

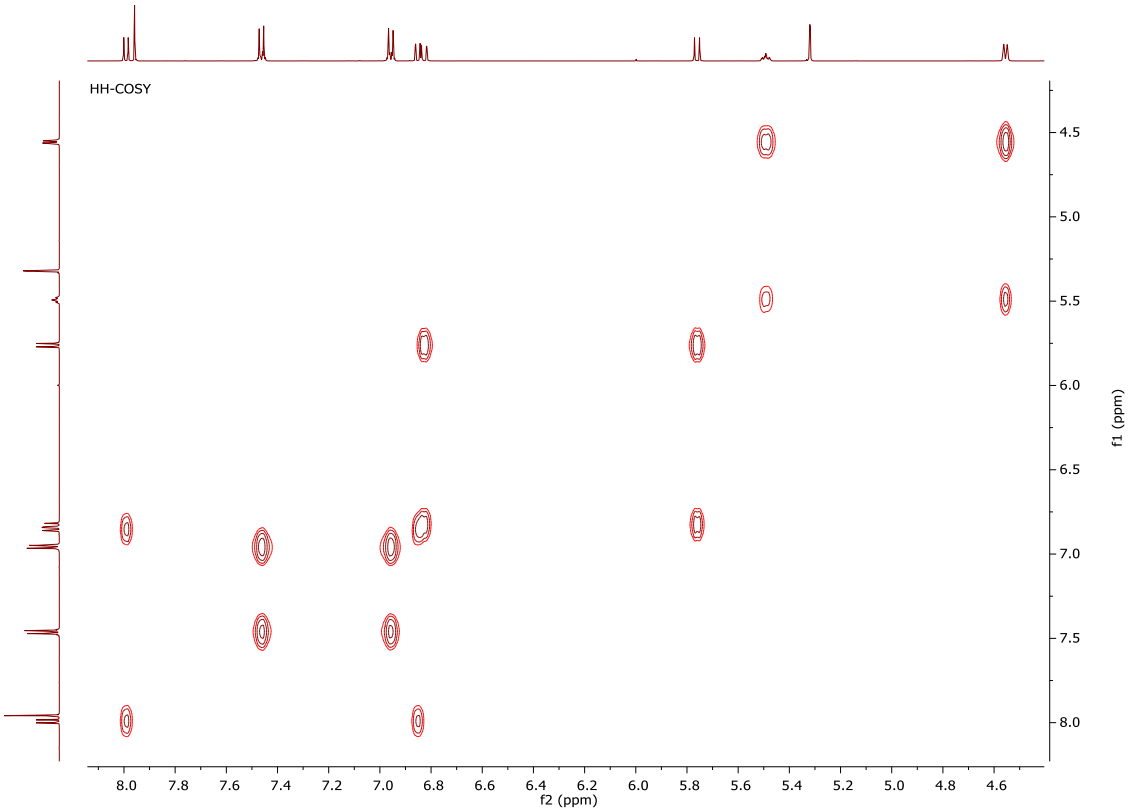

Appendix 9d: HSQC for Compound 102

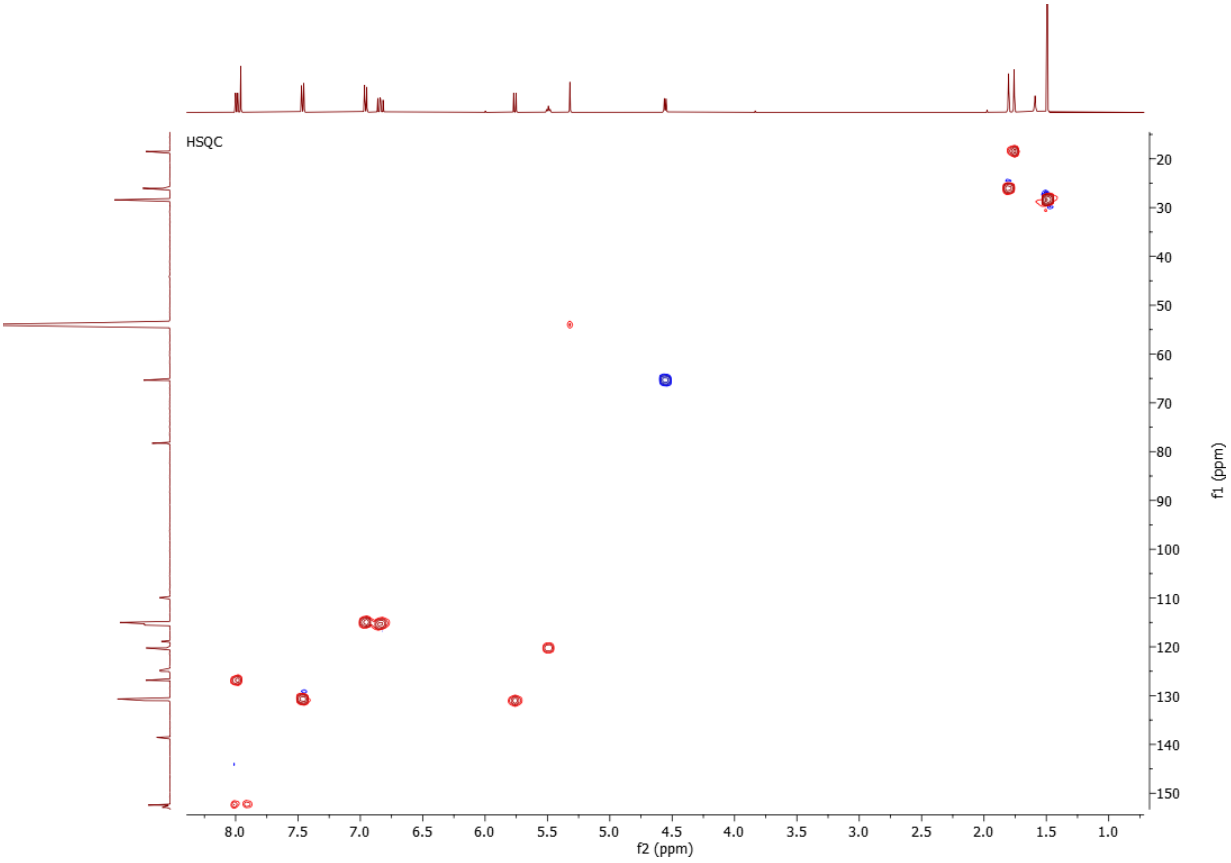

Appendix 9e: HMBC for Compound 102

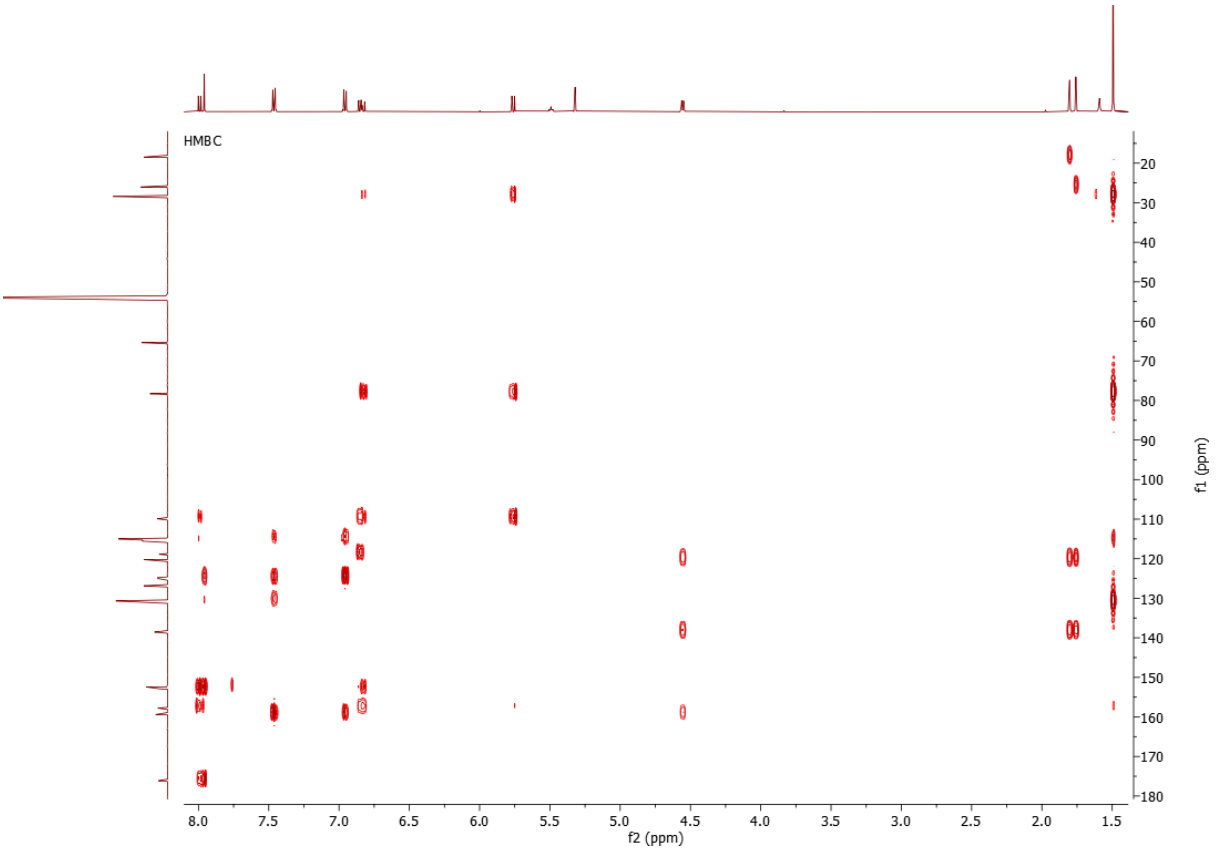

Appendix 10: NMR Spectra for Barbigerone (114)

Appendix 10a: ^{1}H NMR for Compound 114

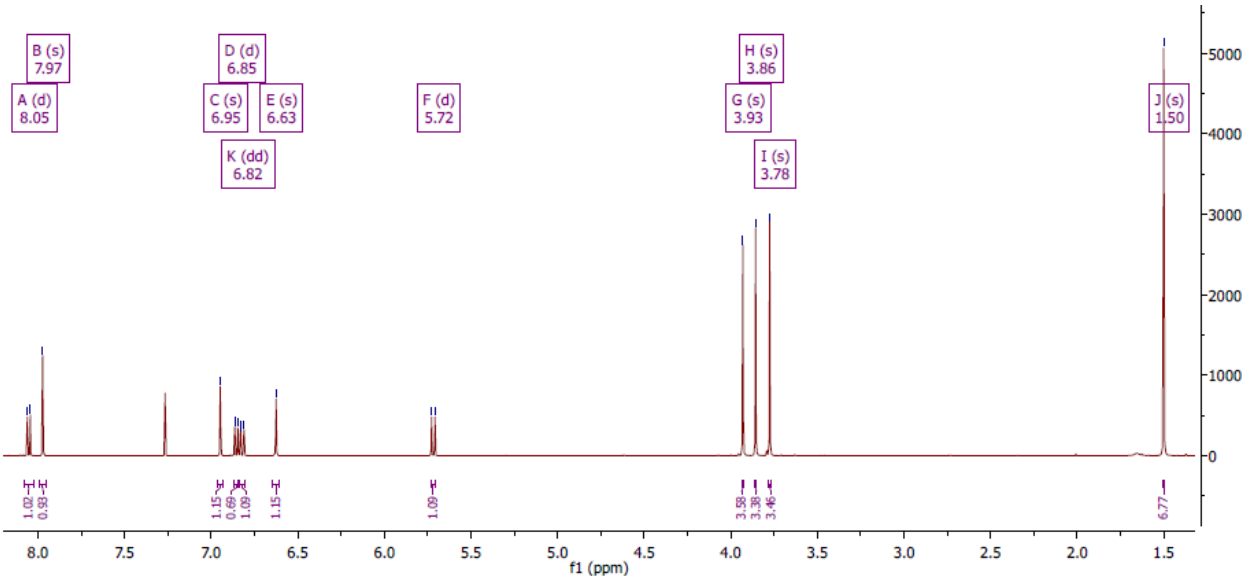

Appendix 10b: ^{13}C NMR for Compound 114

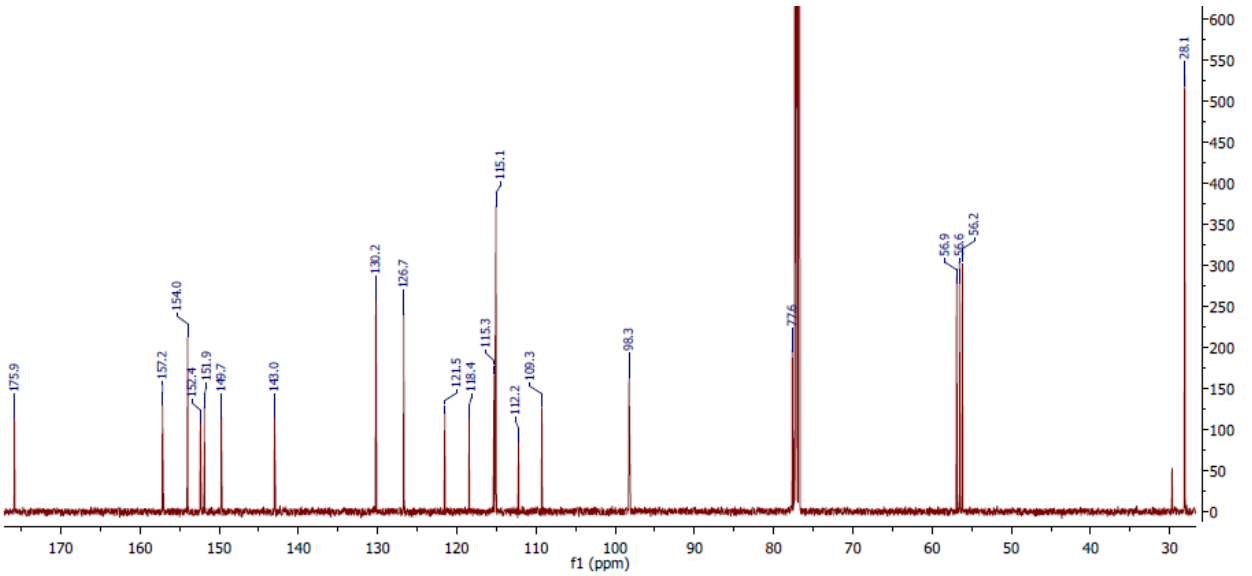

Appendix 10c: H H-Cosy for Compound 114

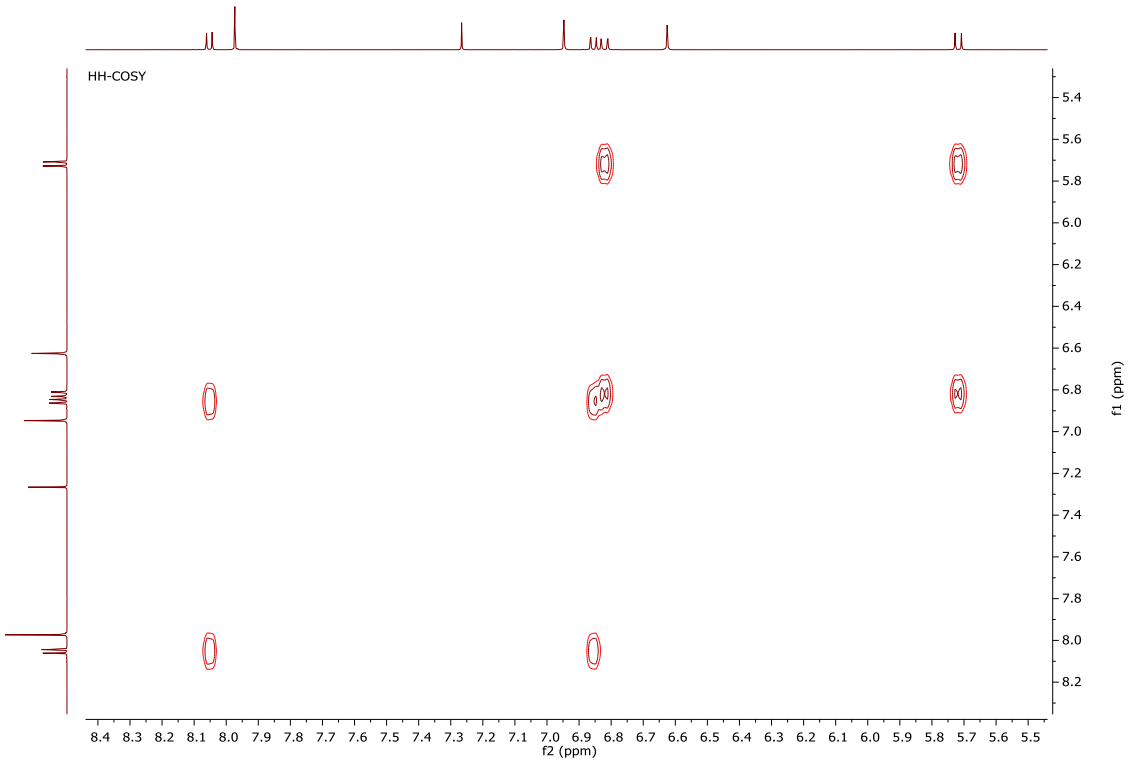

Appendix 10d: HSQC for Compound 114

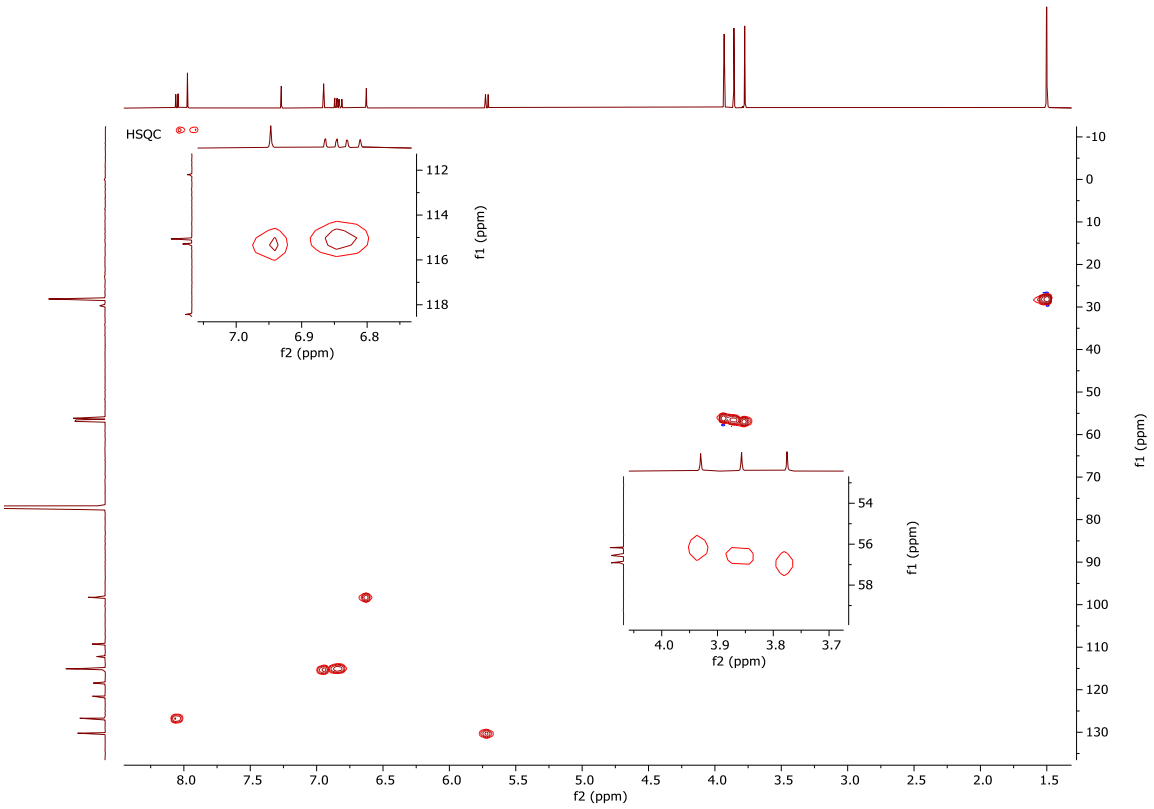

Appendix 10e: HMBC for Compound 114

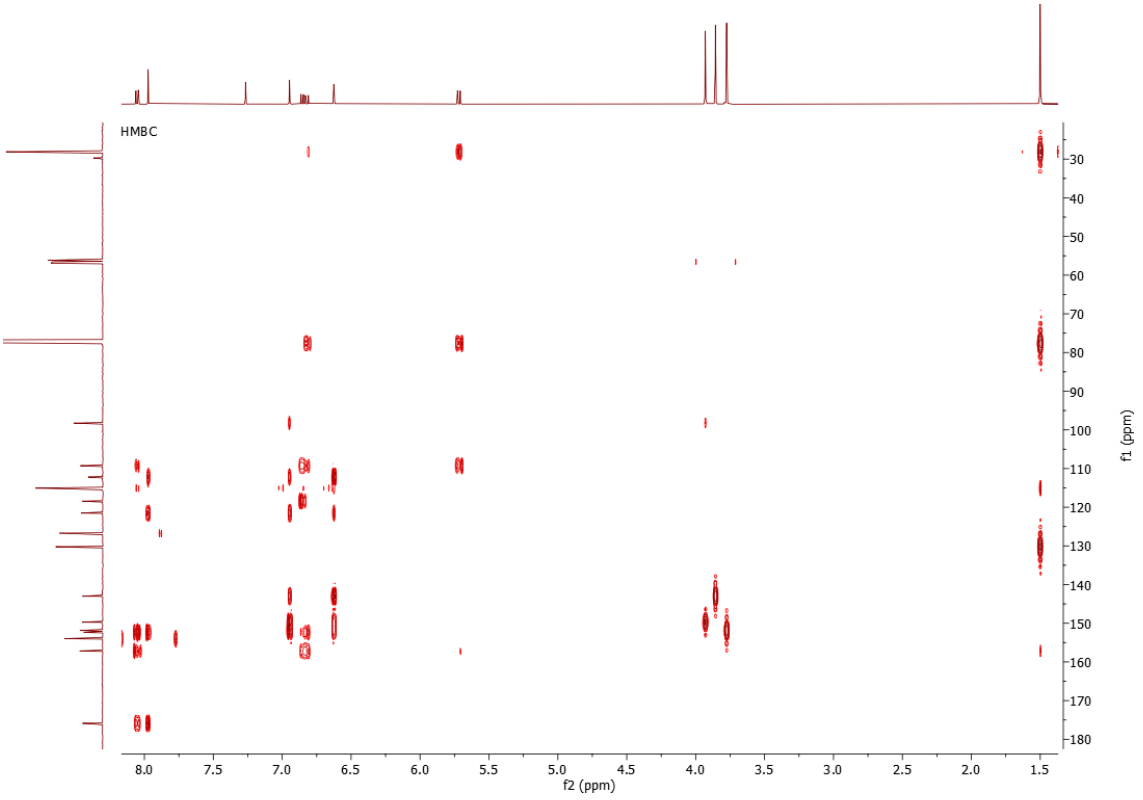

Appendix 11: NMR Data for Maximaisoflavone G (115)

Appendix 11a: ^{1}H NMR for Compound 115

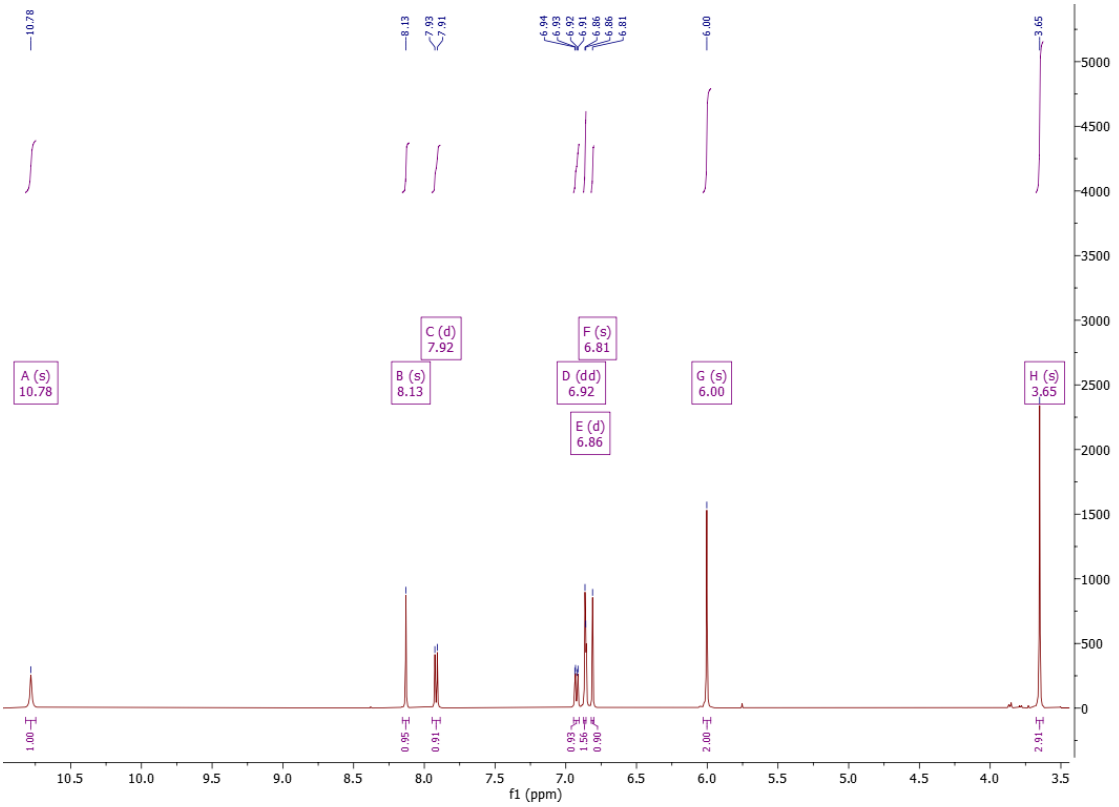

Appendix 11b: ^{13}C NMR for Compound 115

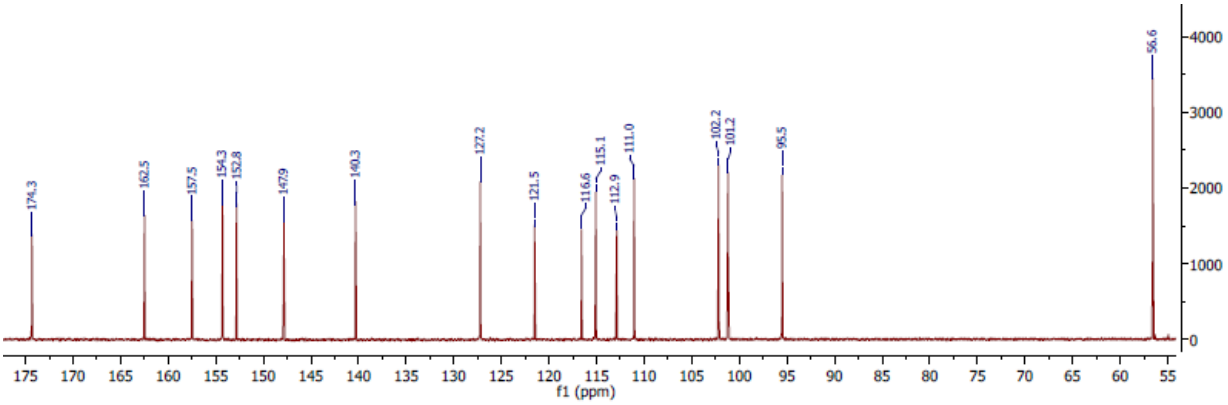

Appendix 11c: H H-Cosy for Compound 115

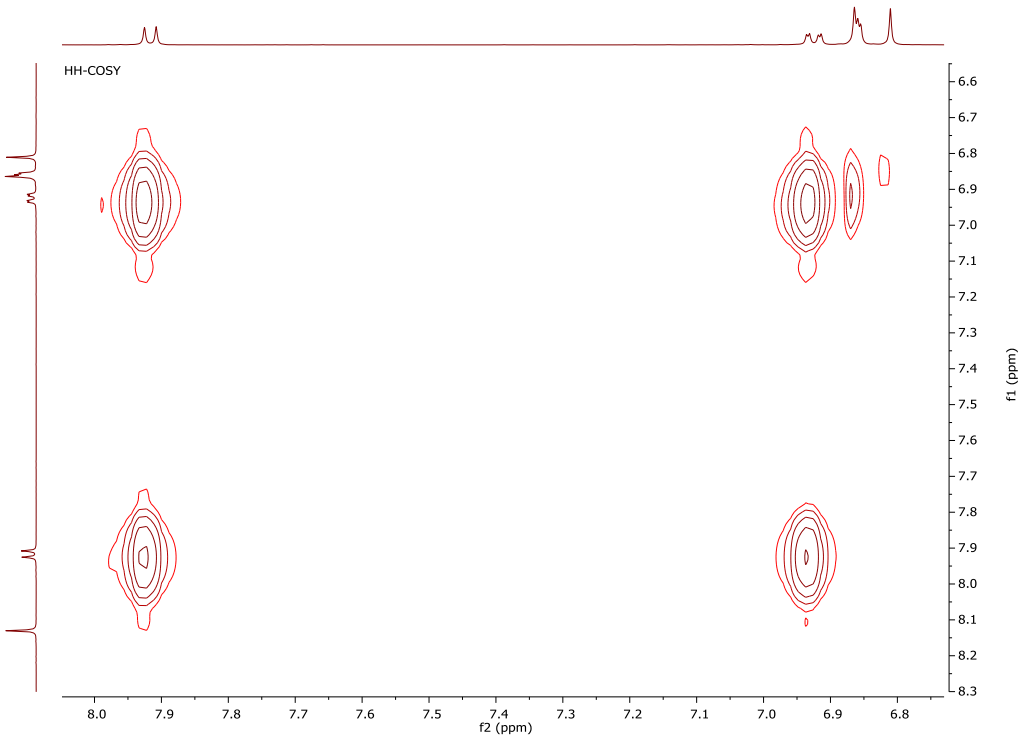

Appendix 11d: HSQC NMR for Compound 115

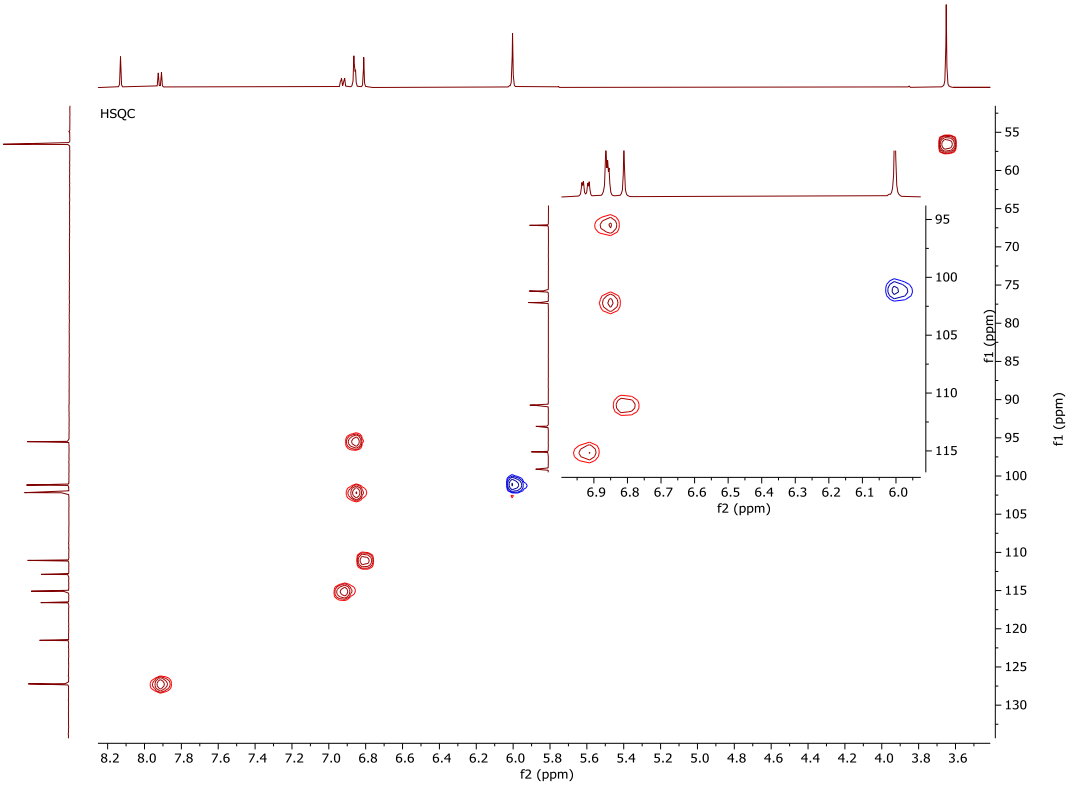

Appendix 11e: HMBC for Compound 115

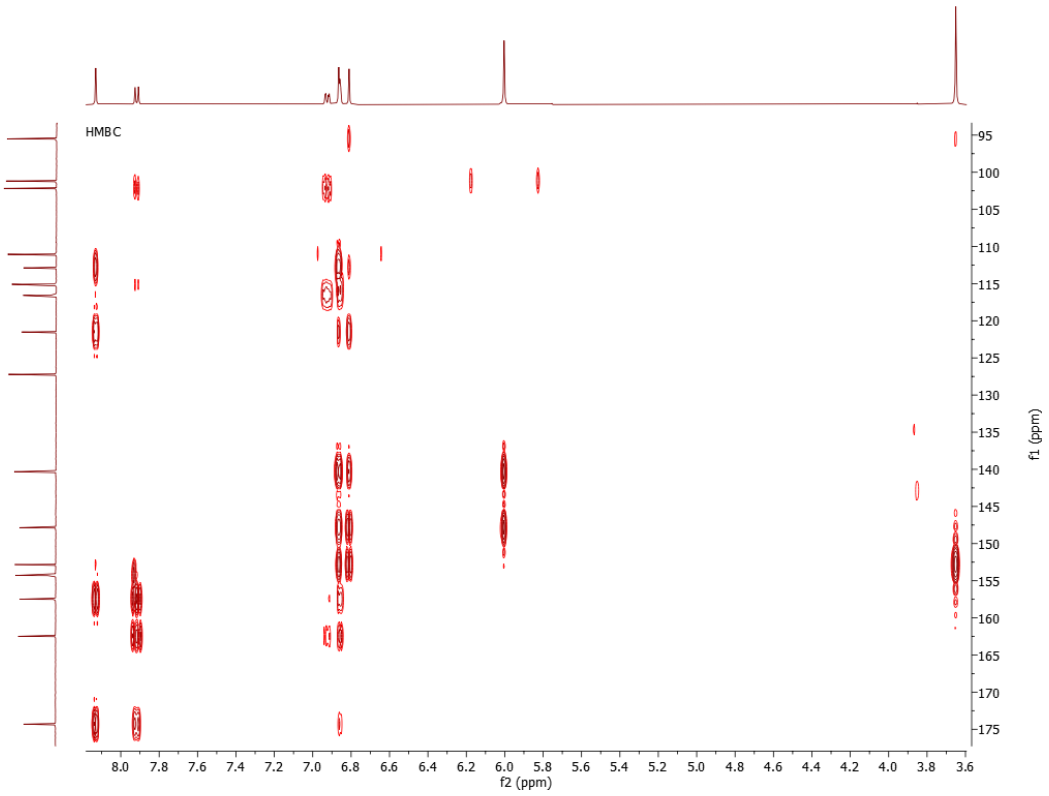

Appendix 12: NMR Spectra for Ferrugone (118)

Appendix 12a: ^{1}H NMR for Compound 118

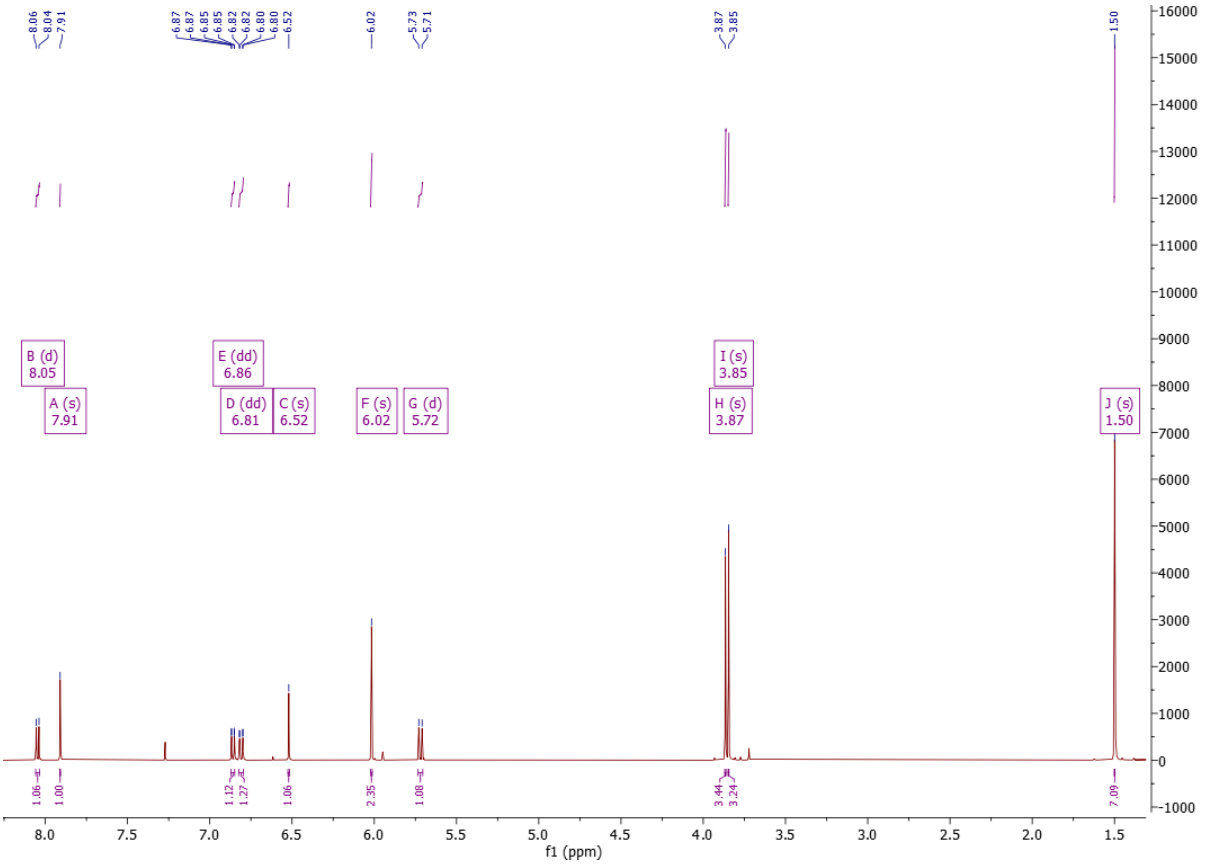

Appendix 12b: ^{13}C NMR for Compound 118

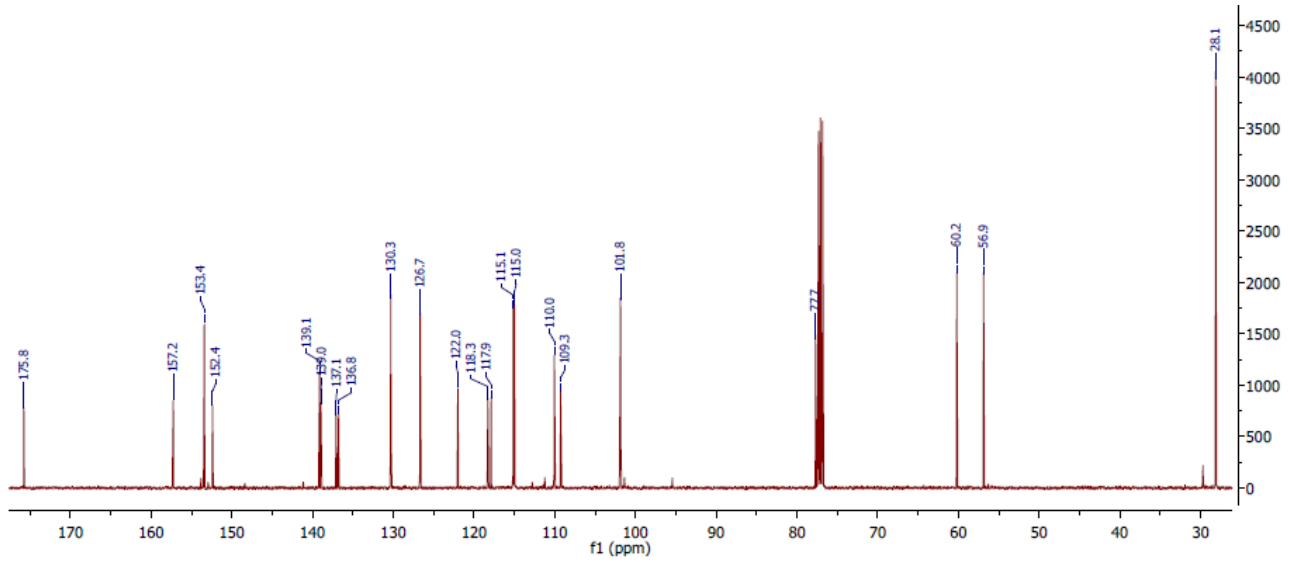

Appendix 12c: H H-Cosy for Compound 118

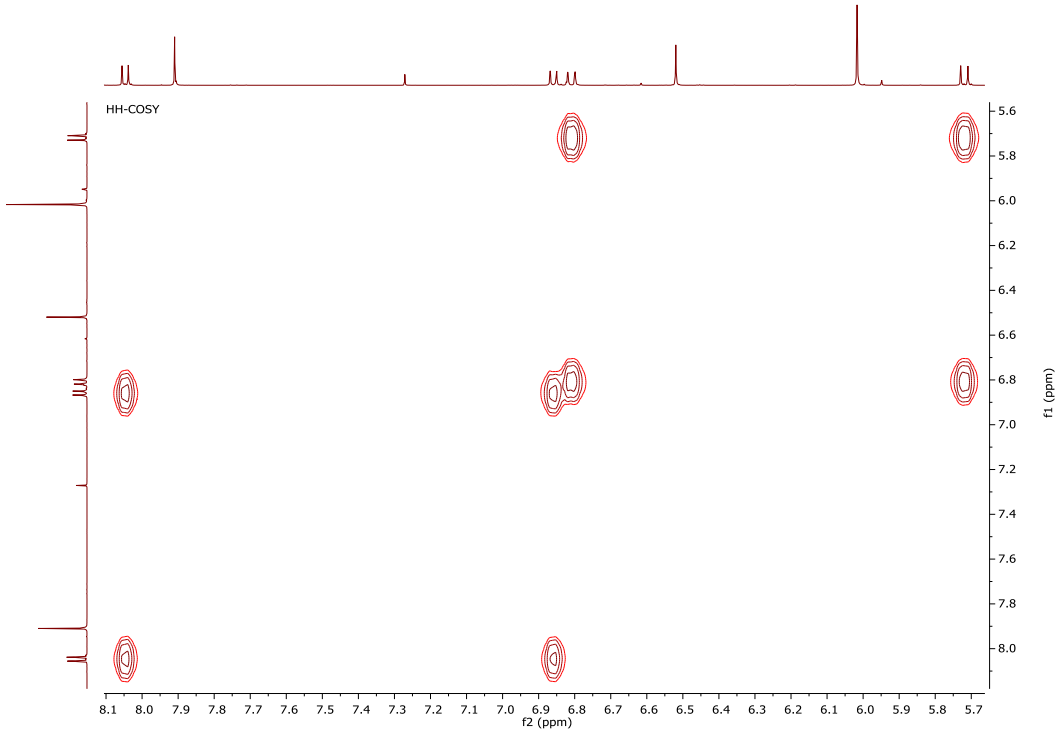

Appendix 12d: HSQC for Compound 118

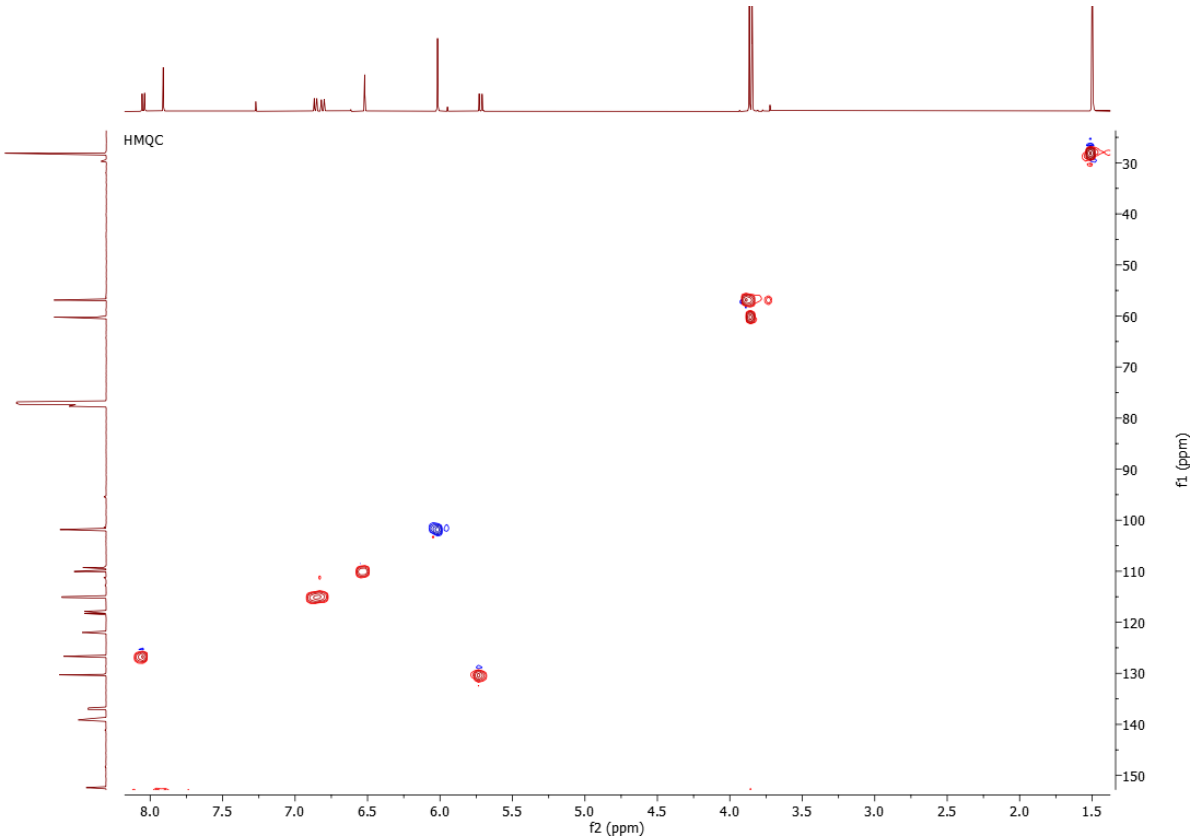

Appendix 12e: HMBC for Compound 118

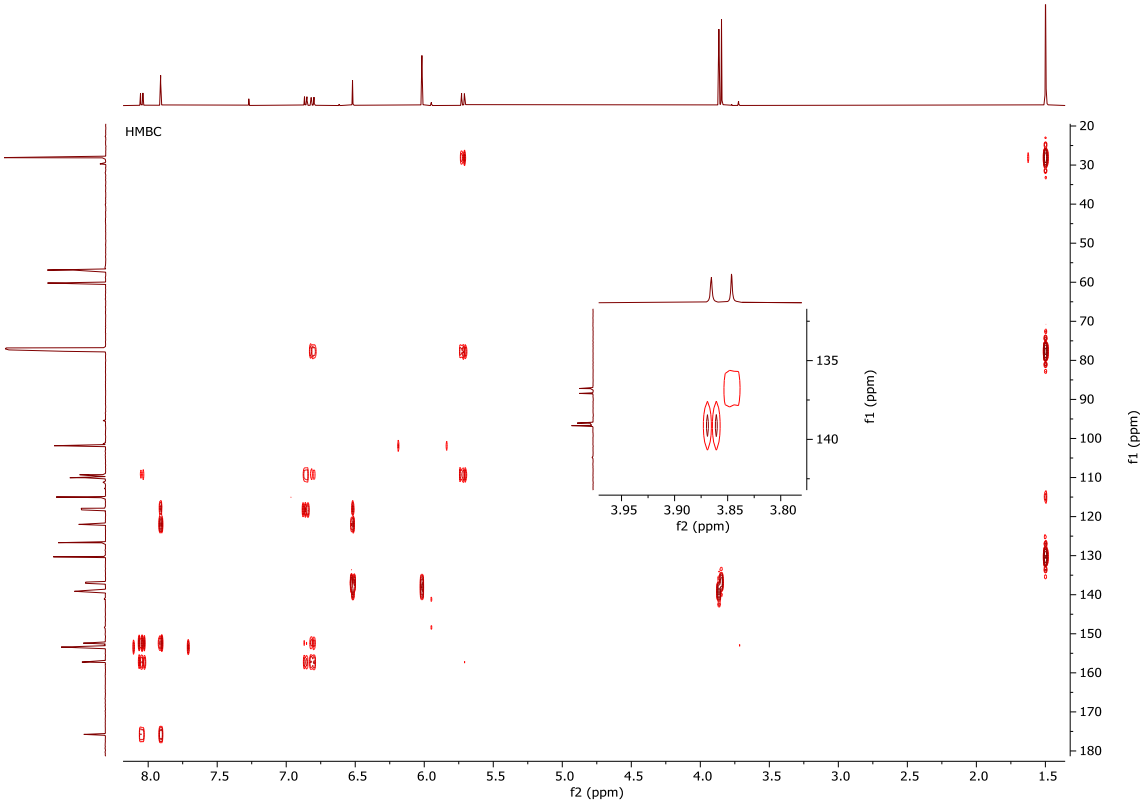

Appendix 13: NMR Spectra for Ichthynone (123)

Appendix 13a: ^{1}H NMR for Compound 123

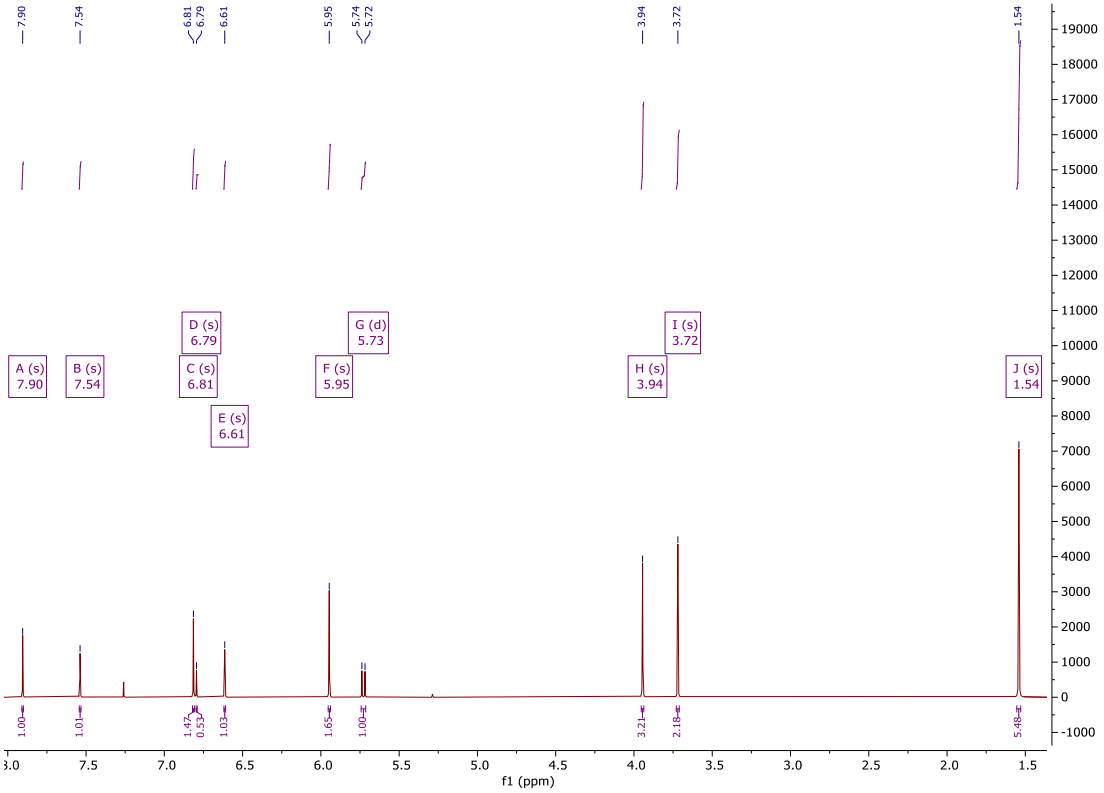

Appendix 13b: ^{13}C NMR for Compound 123

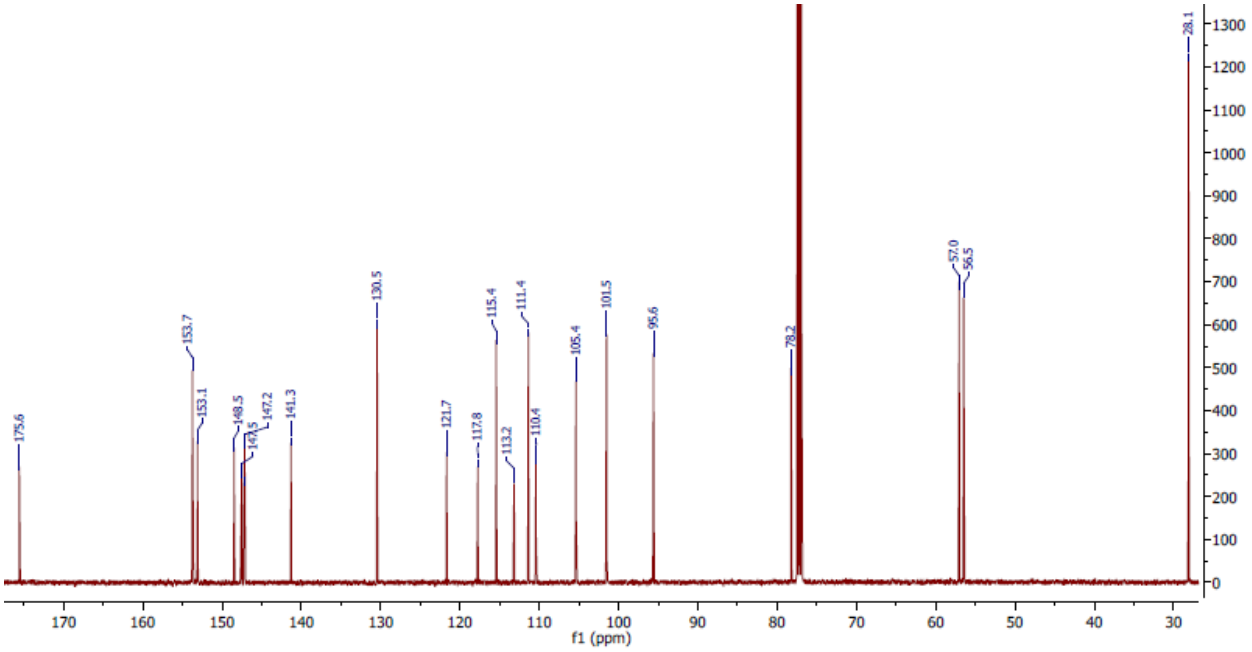

Appendix: H H-Cosy for Compound 123

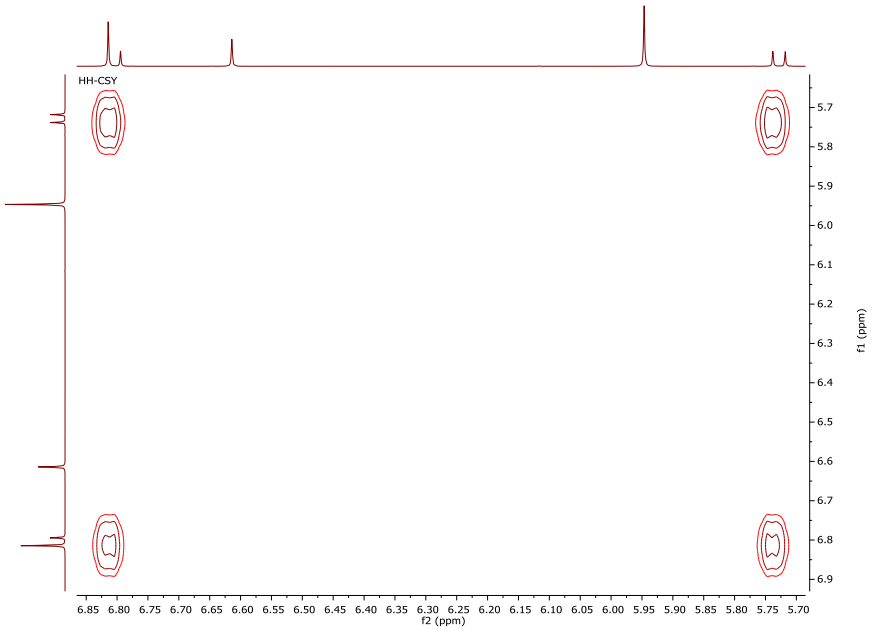

Appendix 13d: HSQC for Compound 123

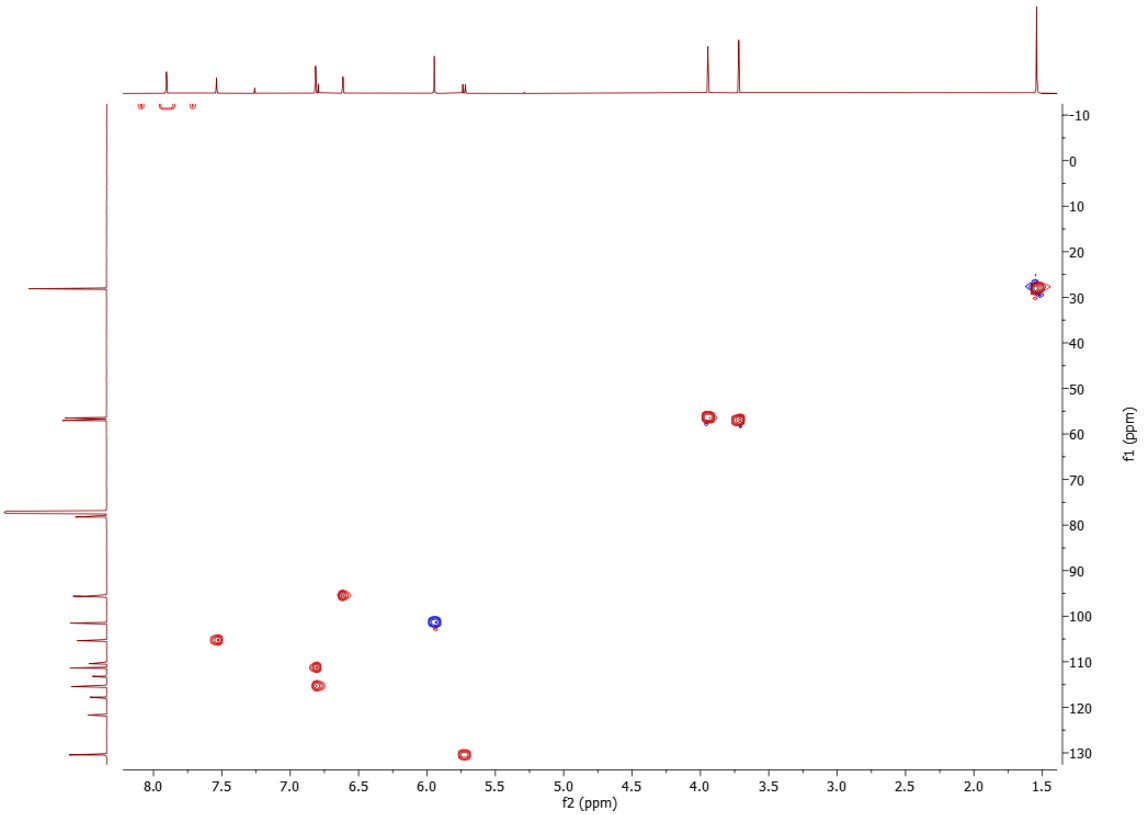

Appendix 13e: HMBC for Compound 123

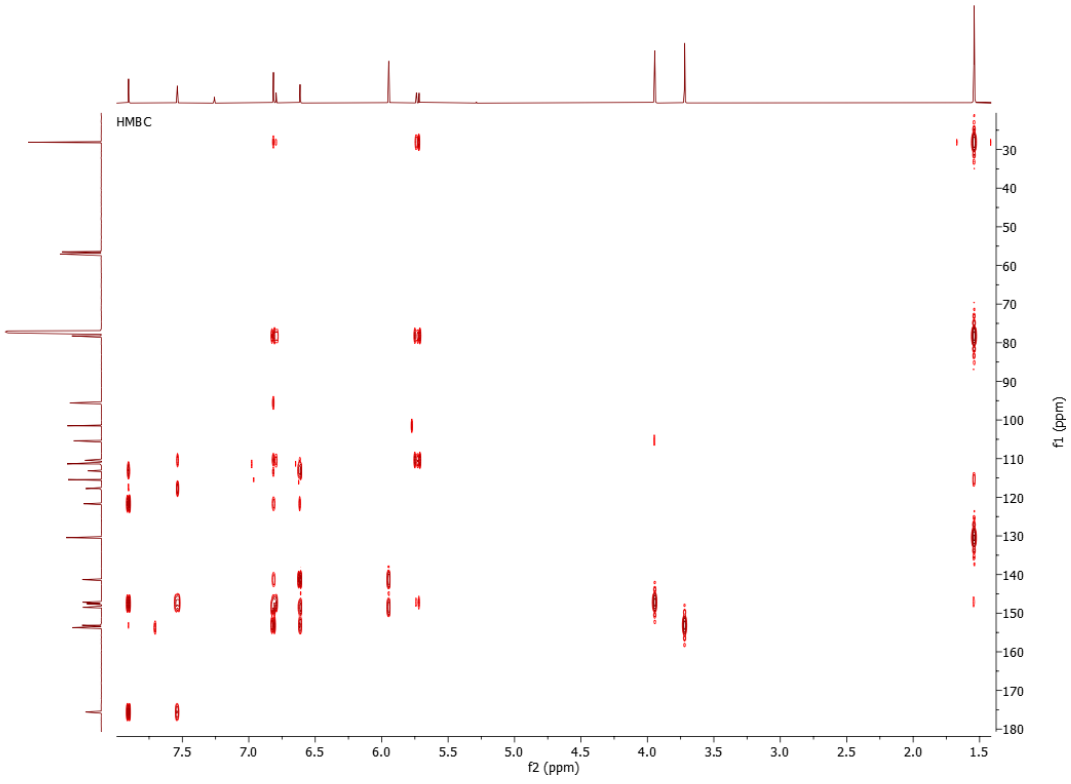

Appendix 14: NMR Data for Deguelin (170)

Appendix 14a: ^{1}H NMR for Compound 170

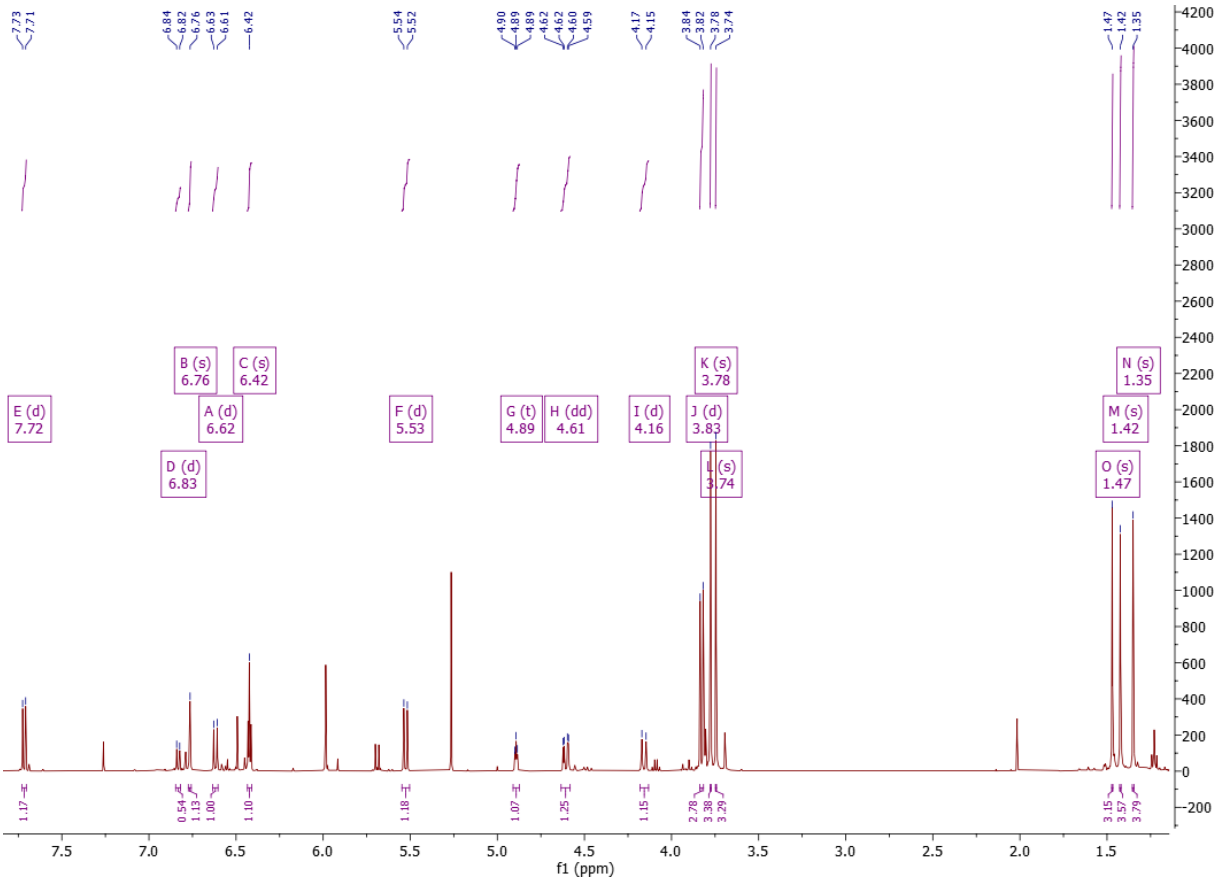

Appendix 14b: ^{13}C NMR for Compound 170

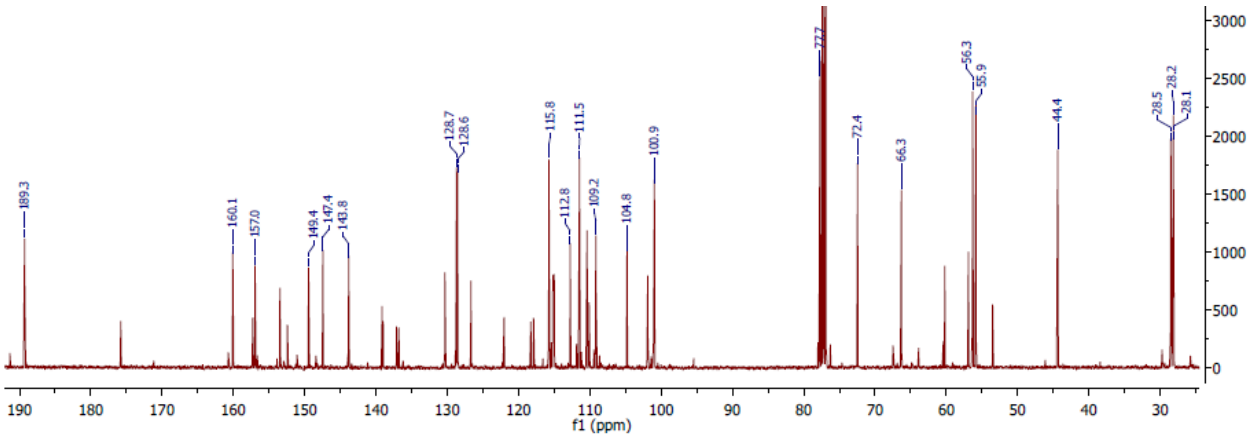

Appendix 14c: H H-Cosy for Compound 170

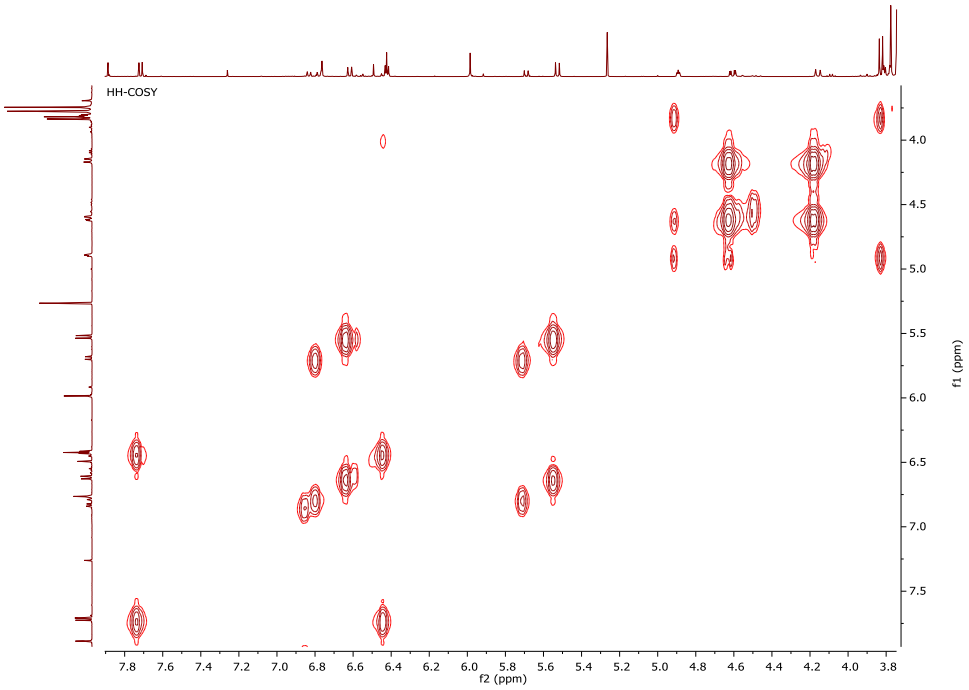

Appendix 14d: HSQC for Compound 170

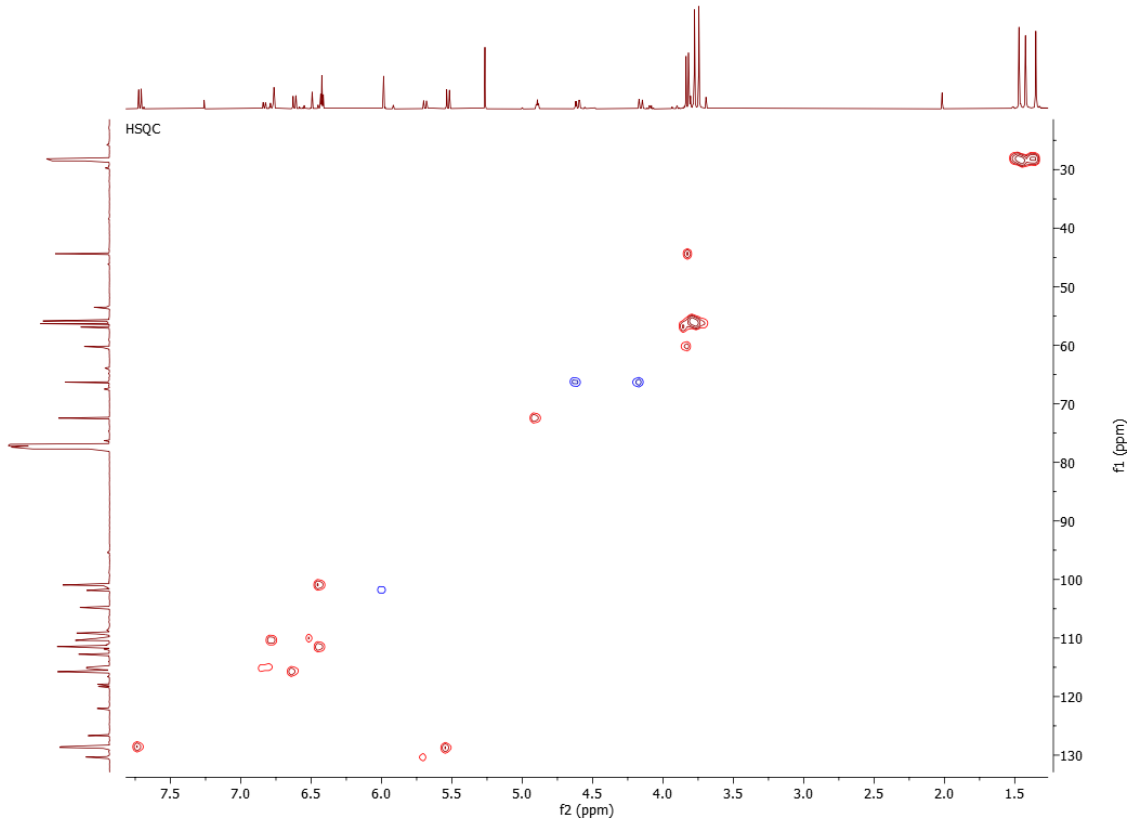

Appendix 14e: HMBC for Compound 170

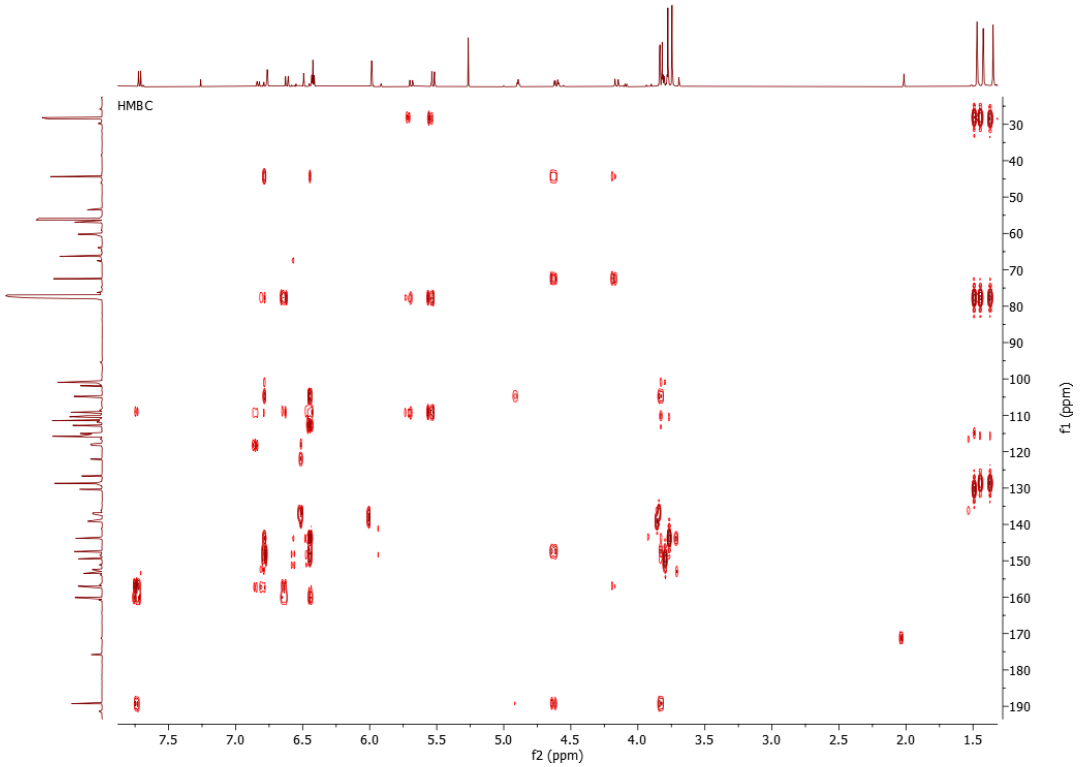

Appendix 15: NMR Data for Tephrosin (171)

Appendix 15a: ^{1}H NMR for Compound 171

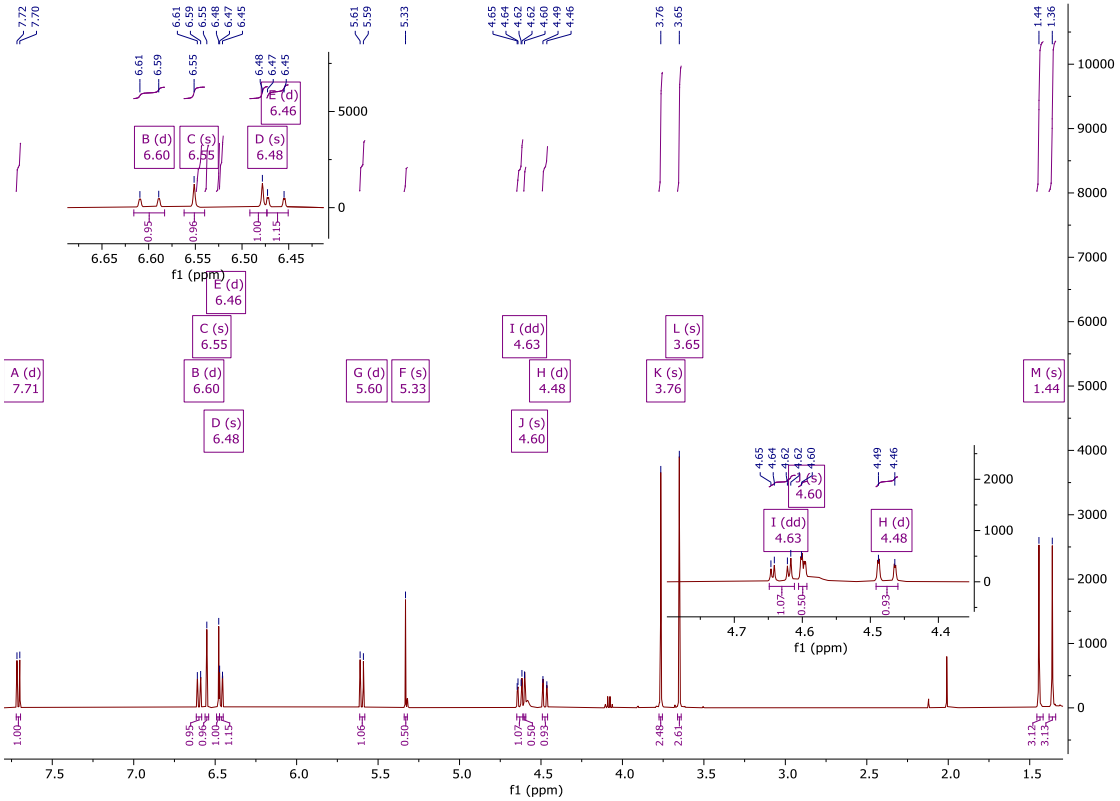

Appendix 15b: ^{13}C NMR for Compound 171

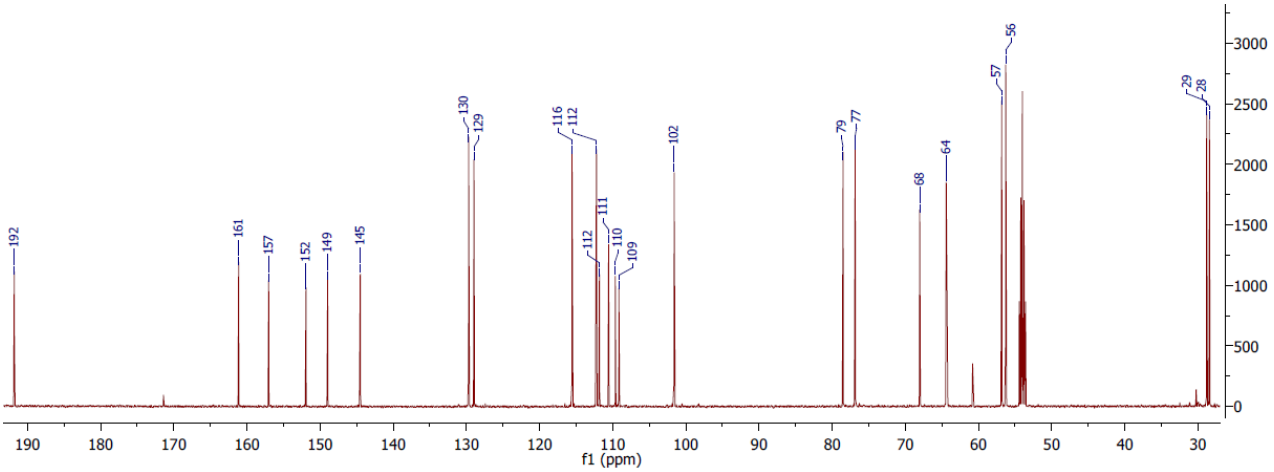

Appendix 15c: H H-Cocsy for Compound 171

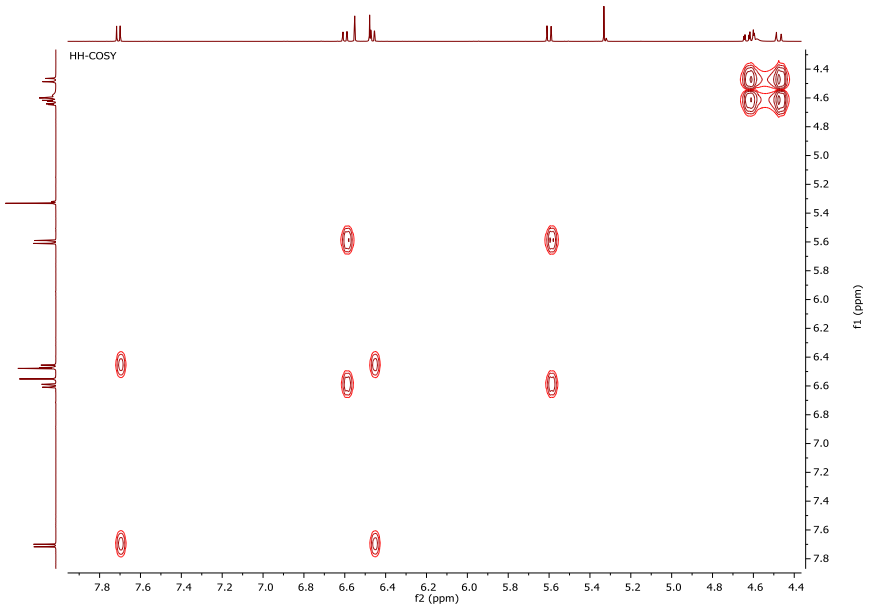

Appendix 15d: HSQC for Compound 171

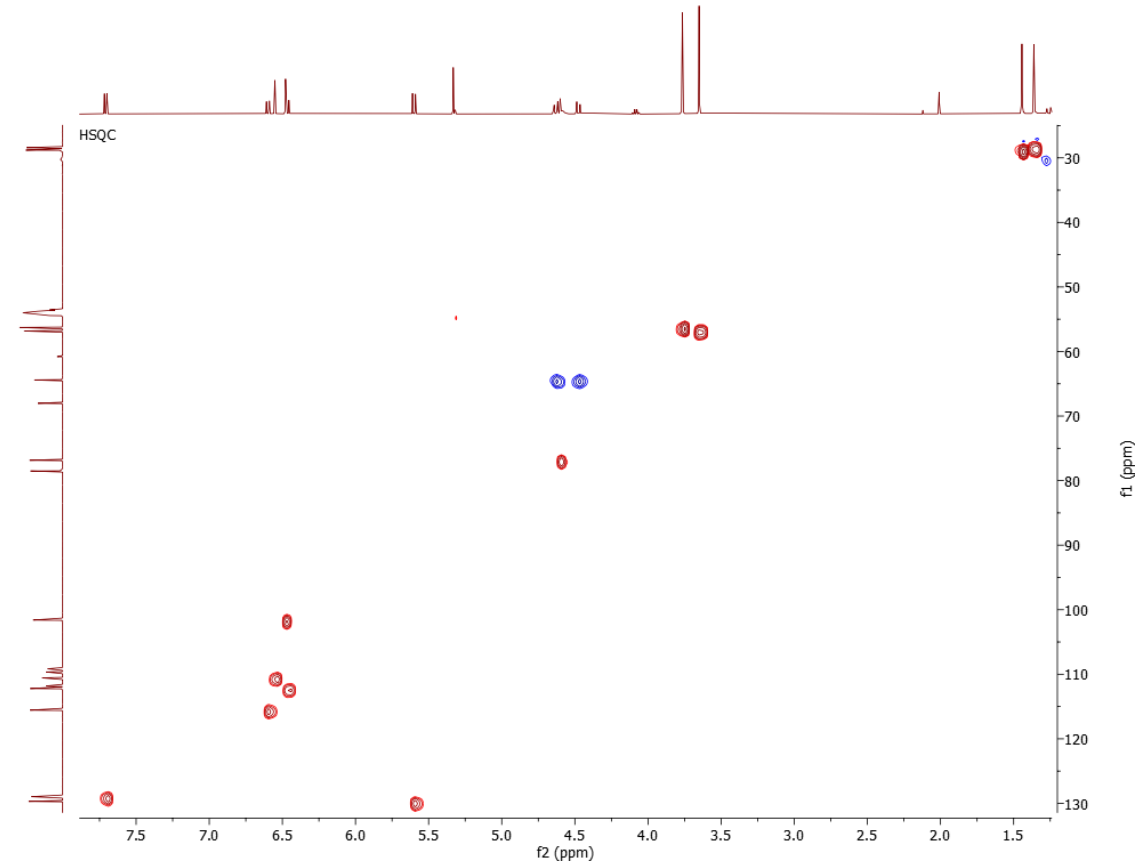

Appendix 15e: HMBC for Compound 171

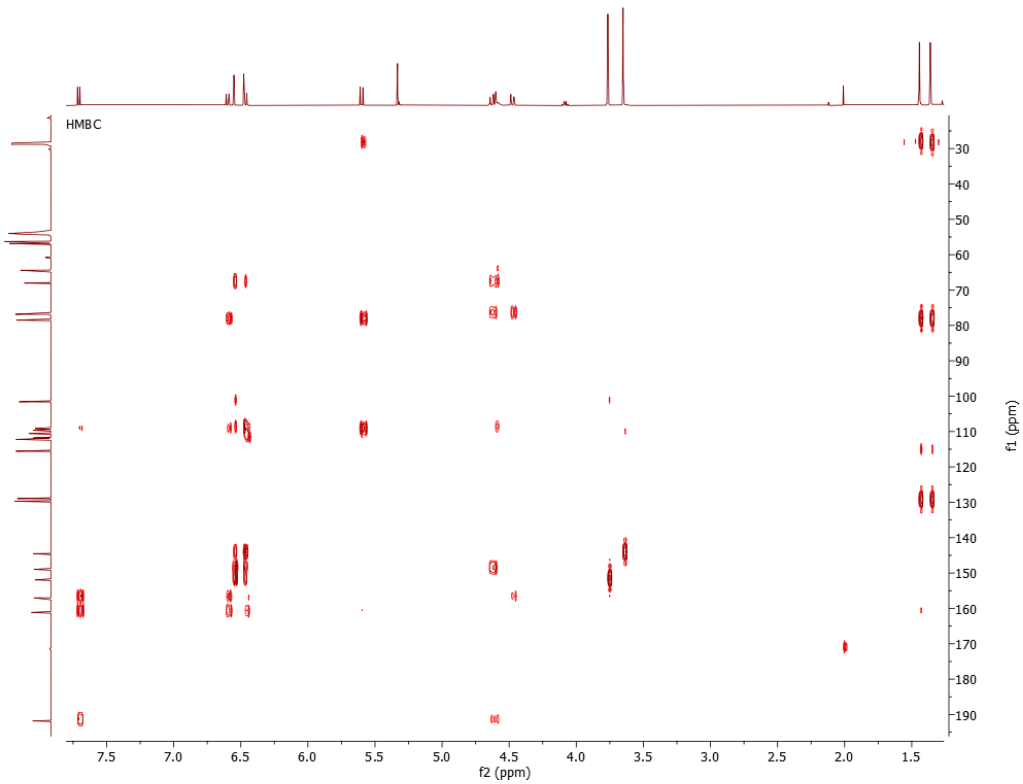

Appendix 16: NMR Data for Milletone (172)

Appendix 16a: ^{1}H NMR for Compound (172)

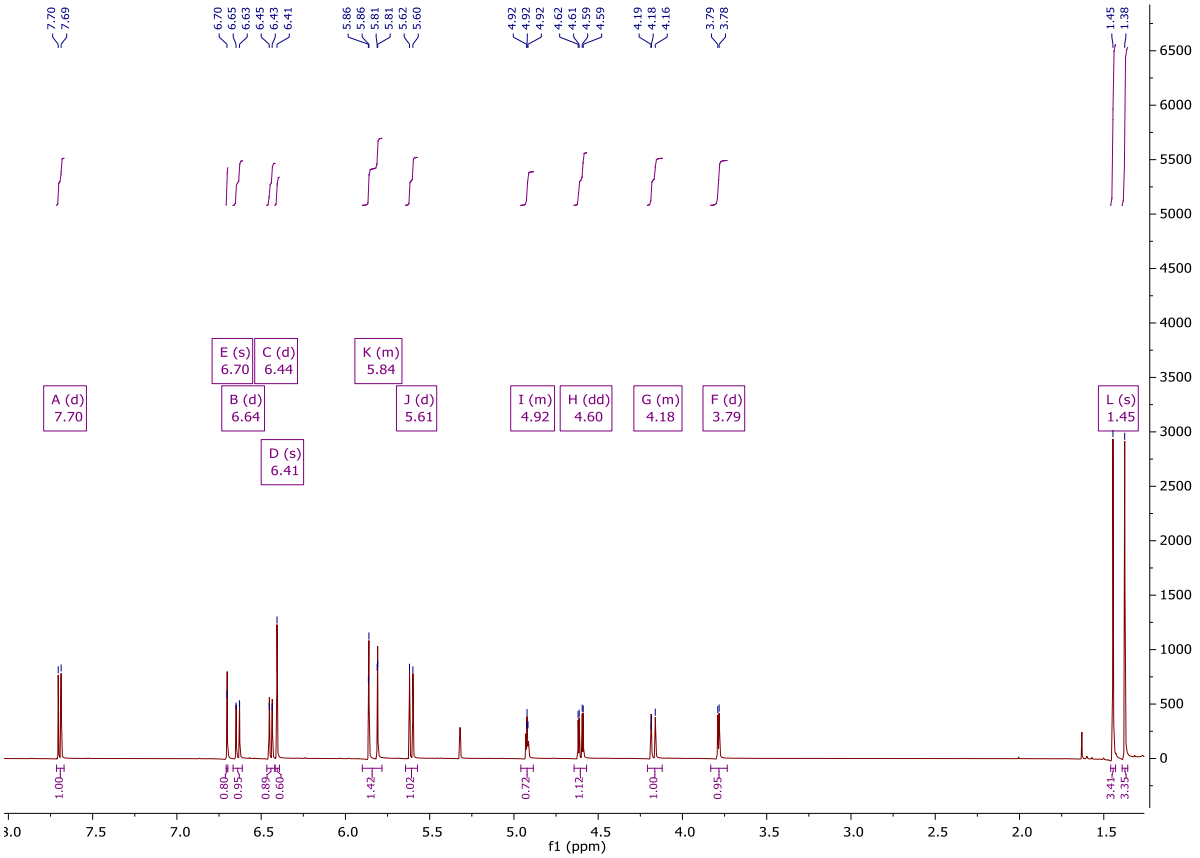

Appendix 16b: ^{13}C NMR for Compound 172

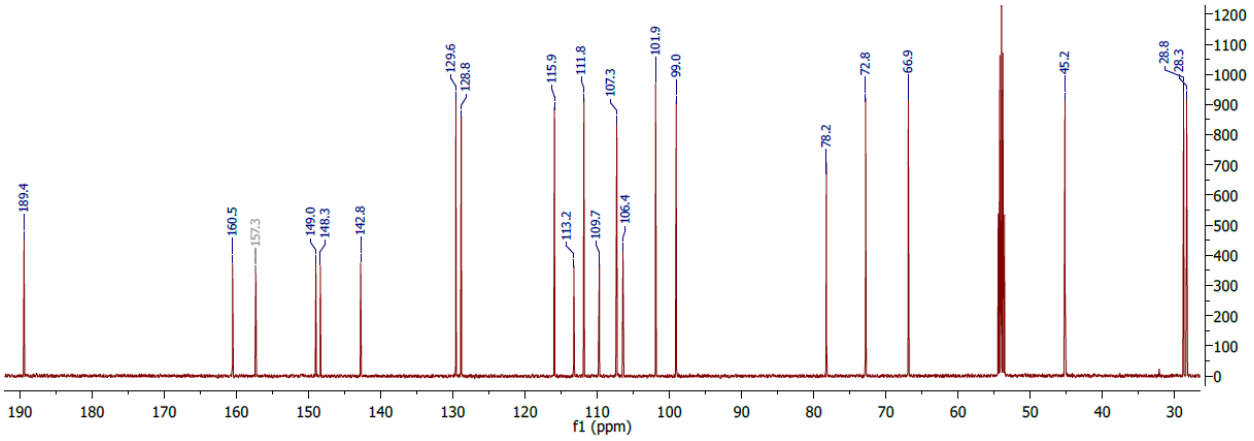

Appendix 16c: H H-Cosy for Compound 172

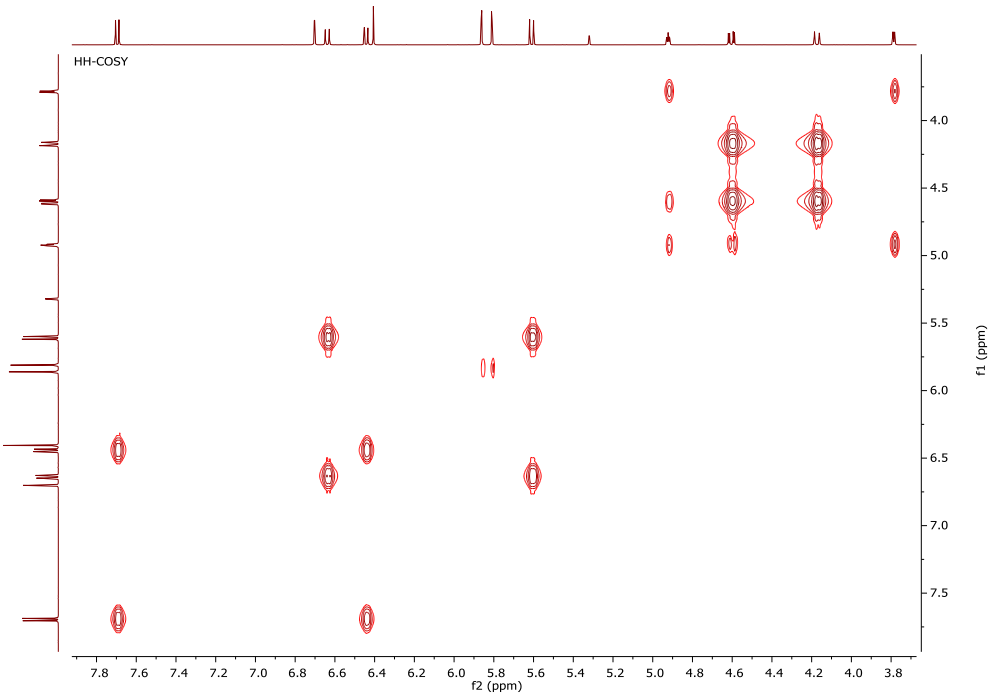

Appendix 16d: HSQC for Compound 172

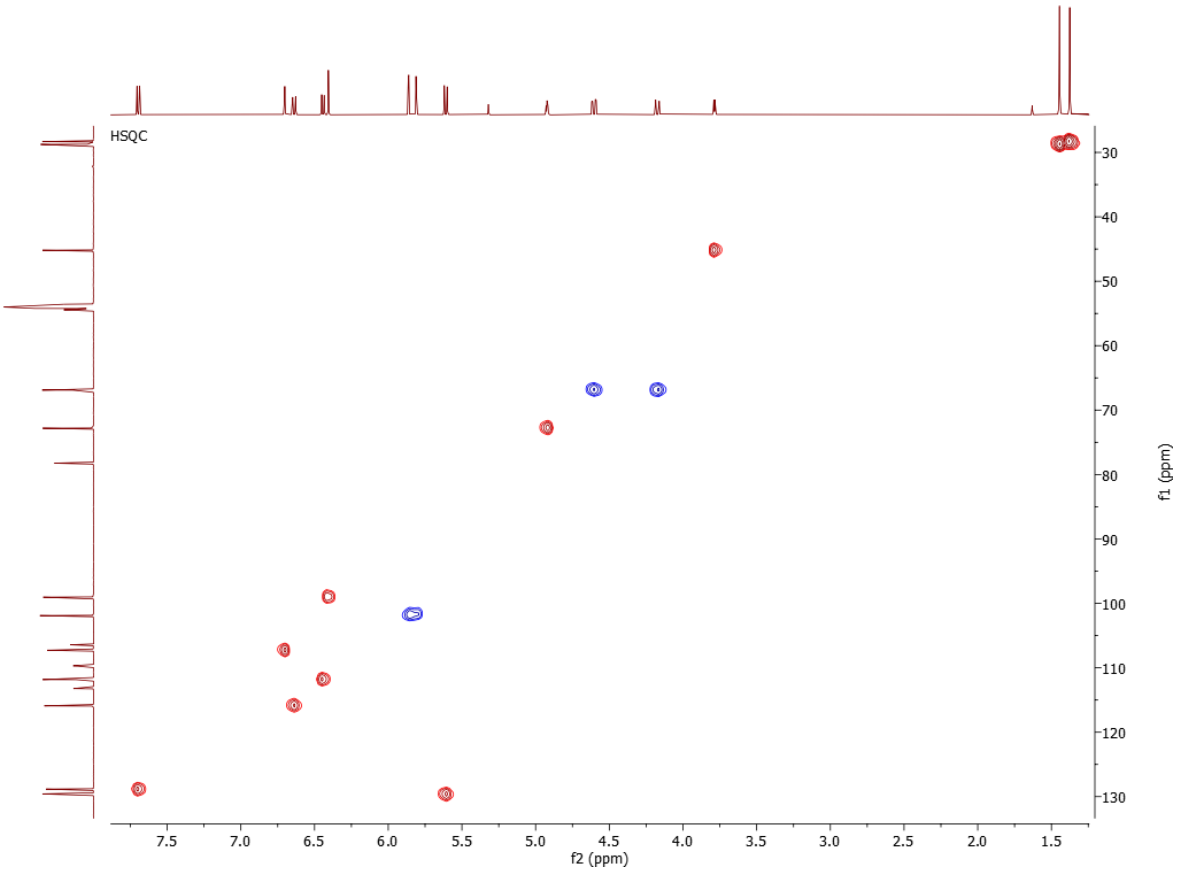

Appendix 16e: HMBC for Compound 172

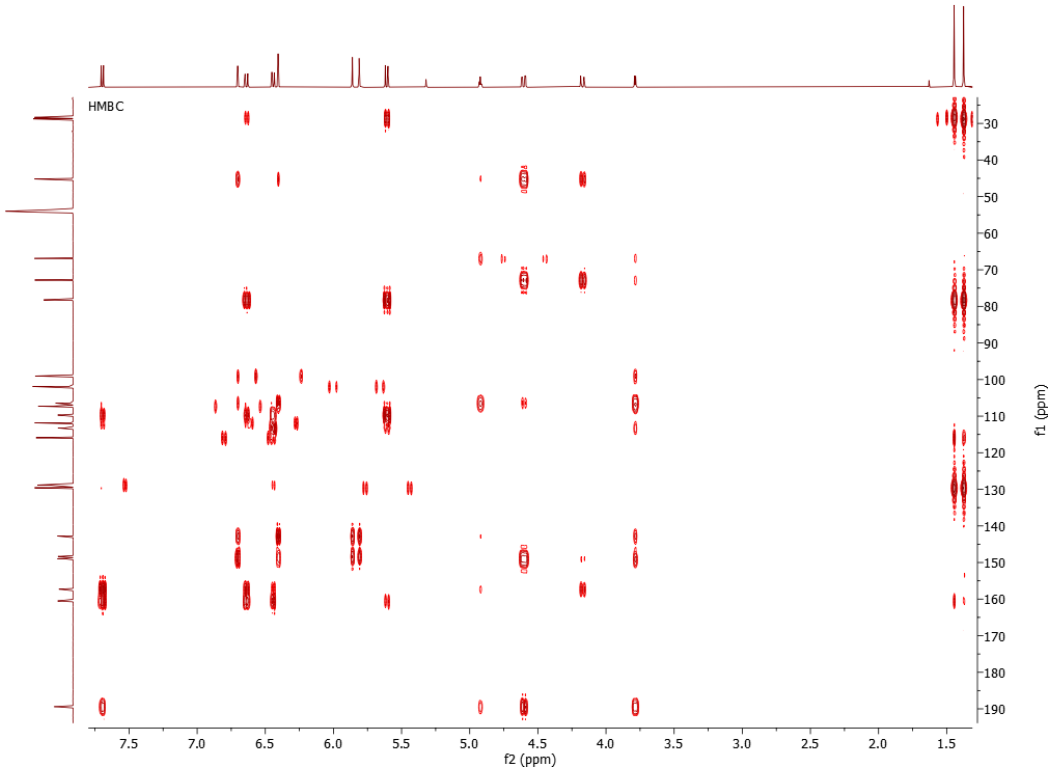

Appendix 17: NMR Data for Milletosin (173)

Appendix 17a: ^{1}H NMR for Compound 173

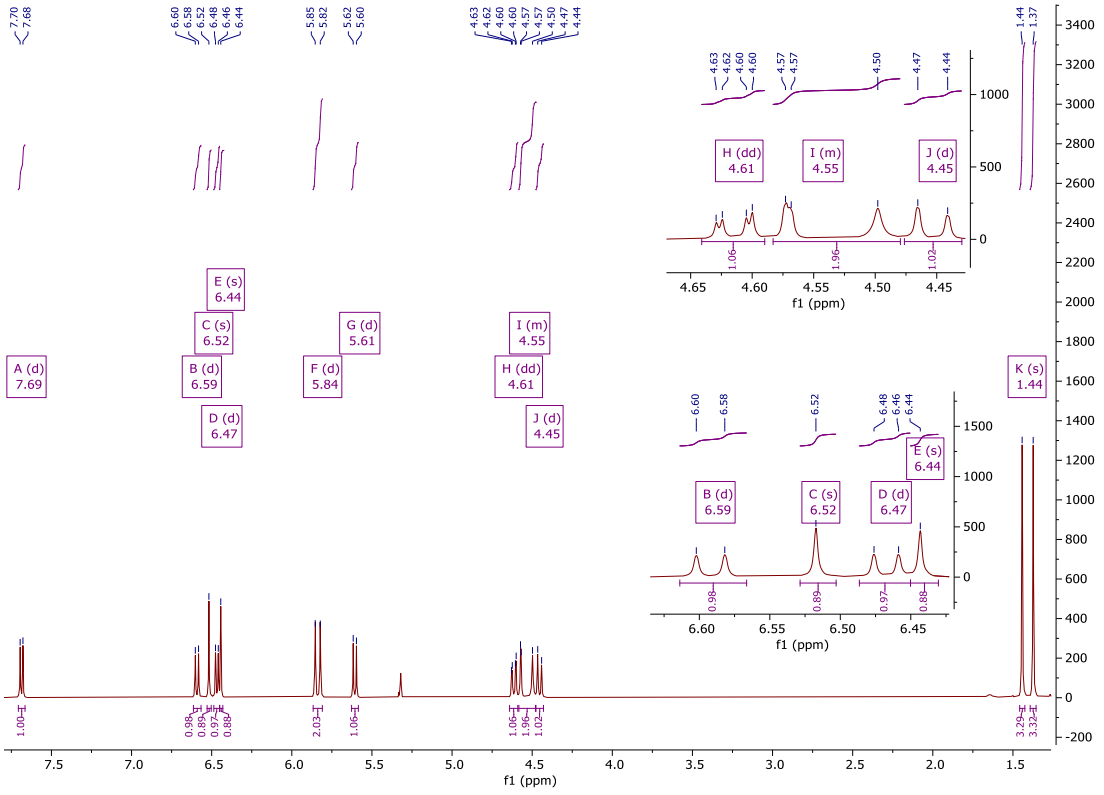

Appendix 17b: ^{13}C NMR for Compound 173

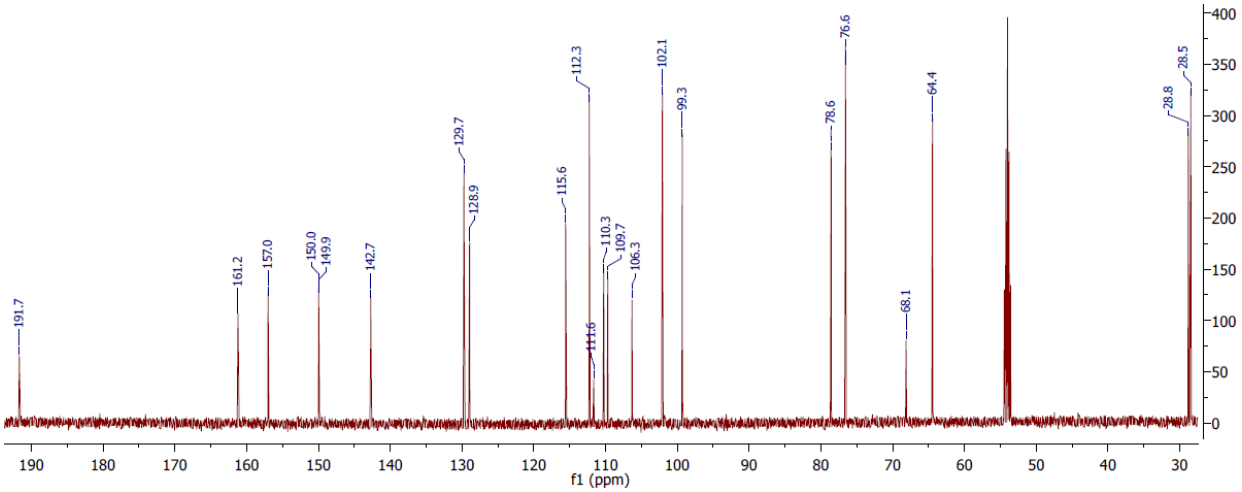

Appendix 17c: H H-Cosy for Compound 173

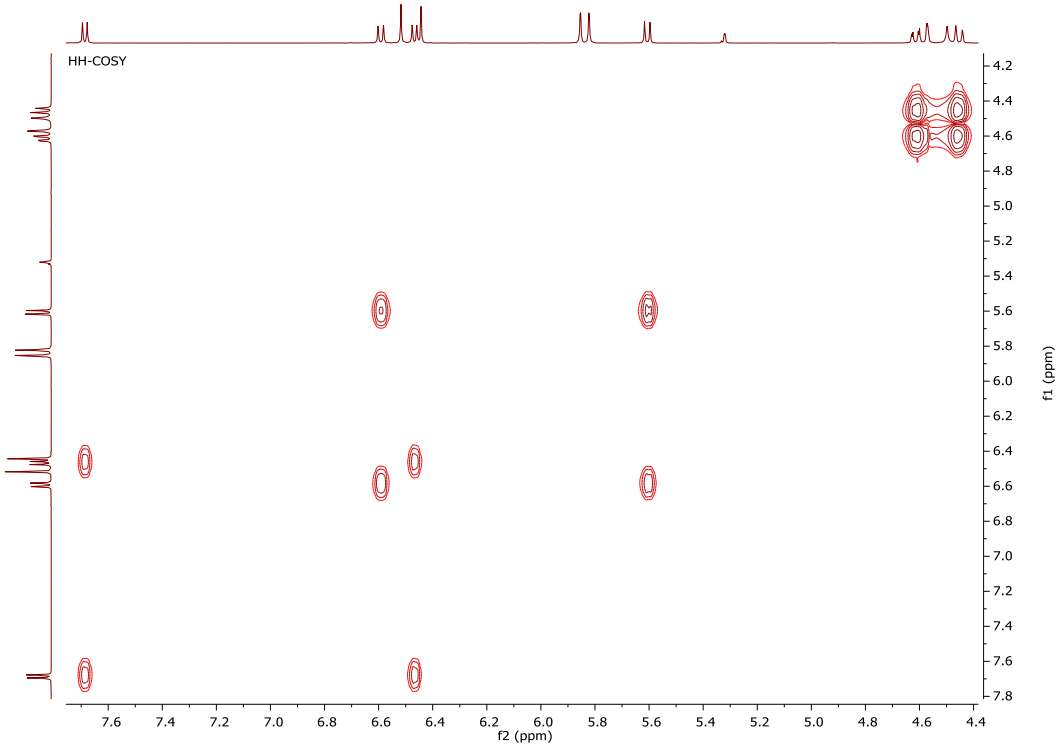

Appendix 17c: HSQC for Compound 173

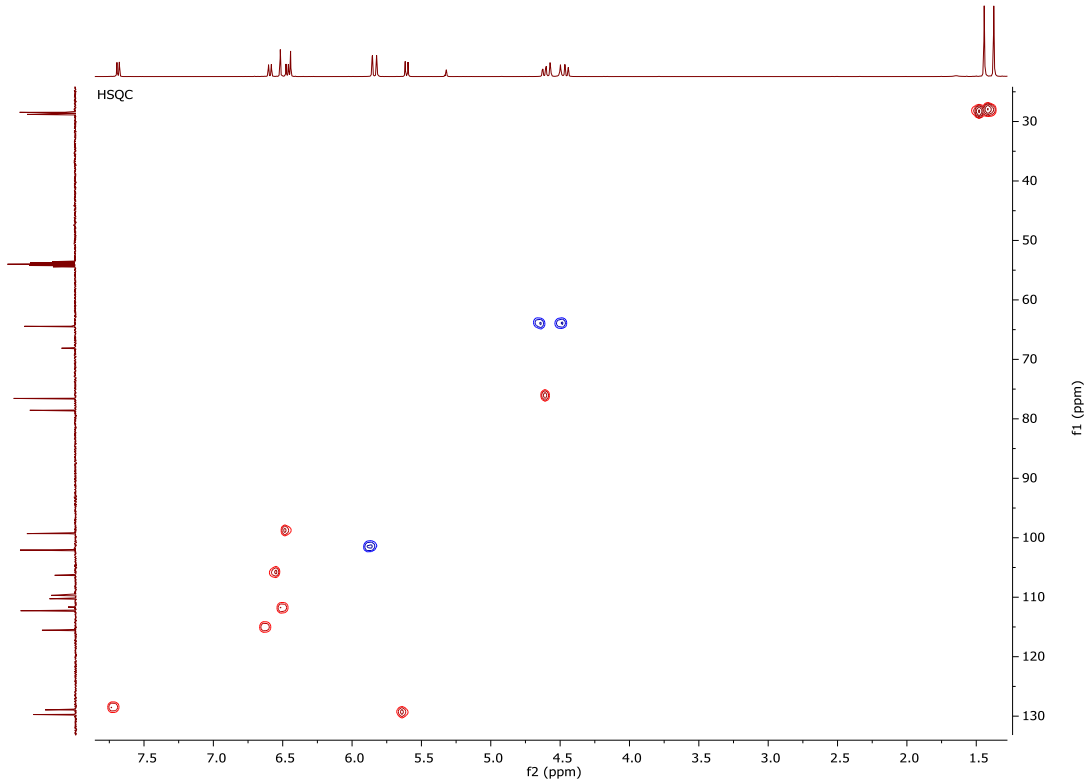

Appendix 17c: HMBC for Compound 173

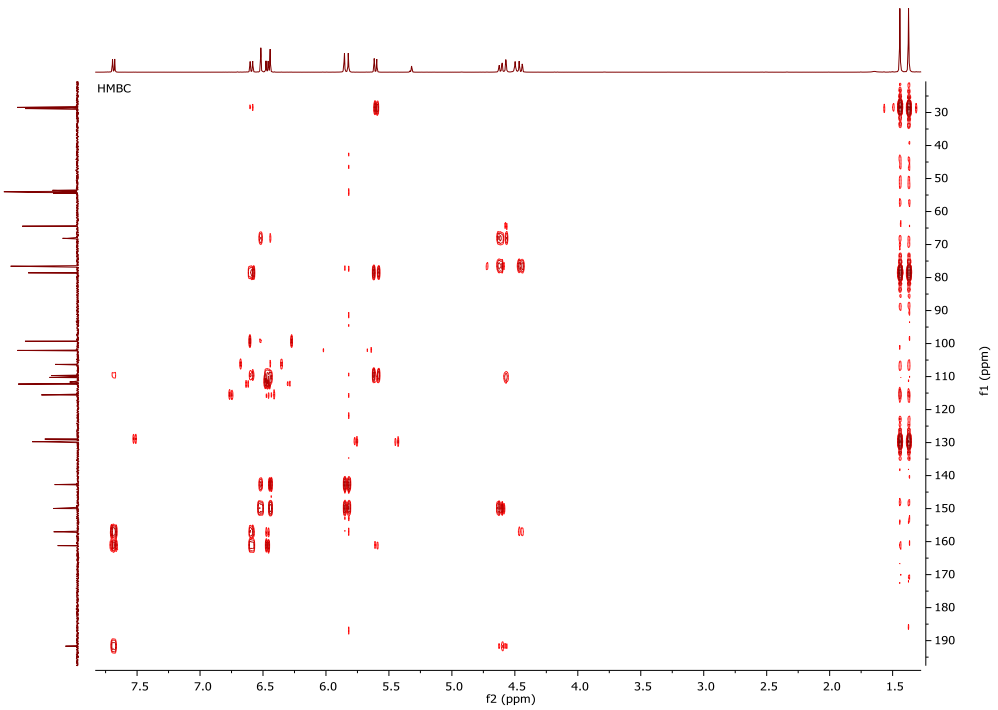

Appendix 18: NMR Spectra for Kaempferol (227)

Appendix 18a: ^{1}H NMR for Compound 227

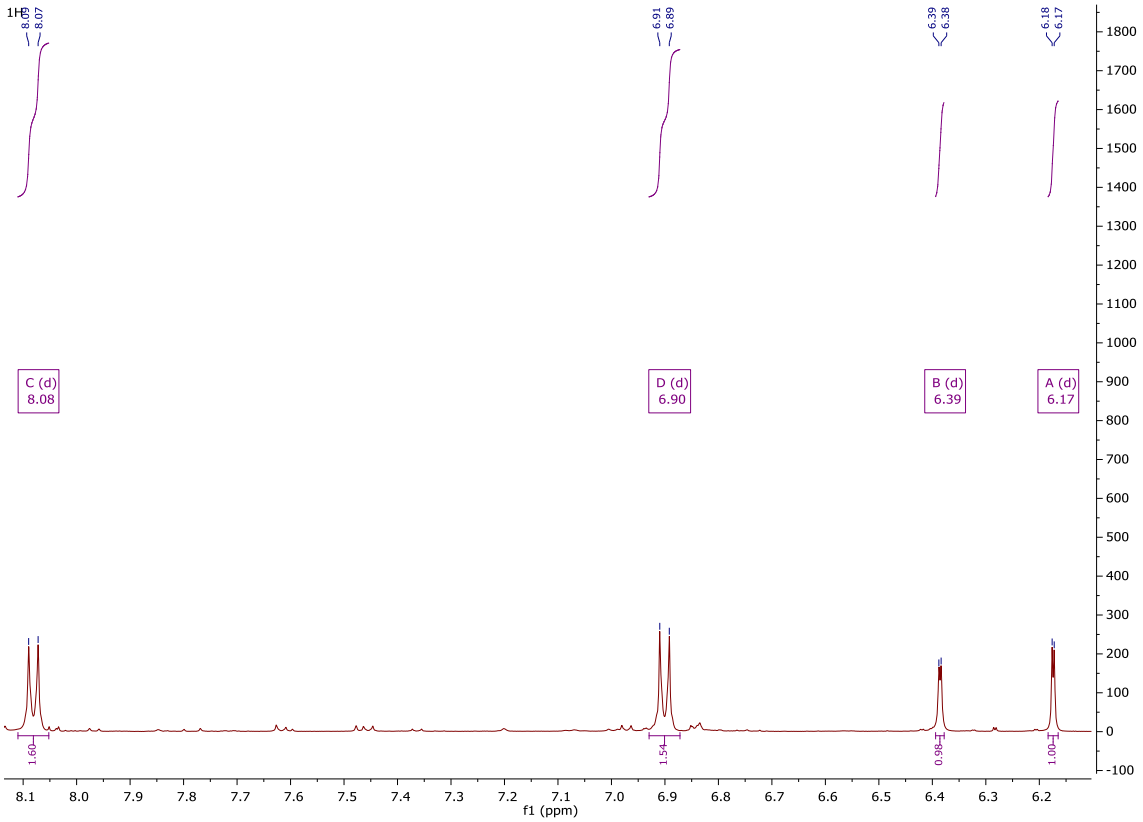

Appendix 18b: ^{13}C NMR for Compound 227

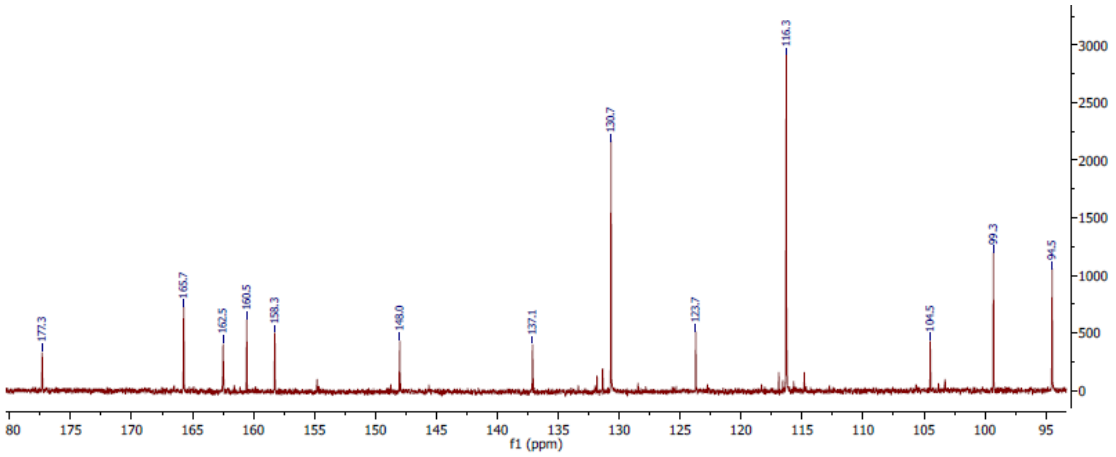

Appendix 18c: H H-Cosy for Compound 227

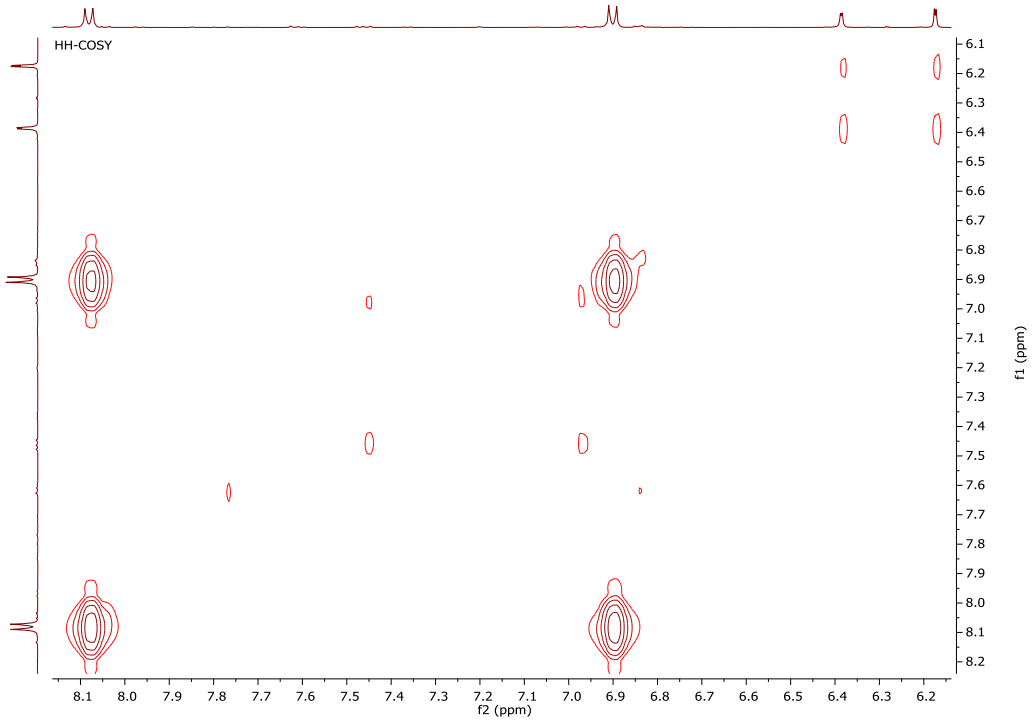

Appendix 18d: HSQC for Compound 227

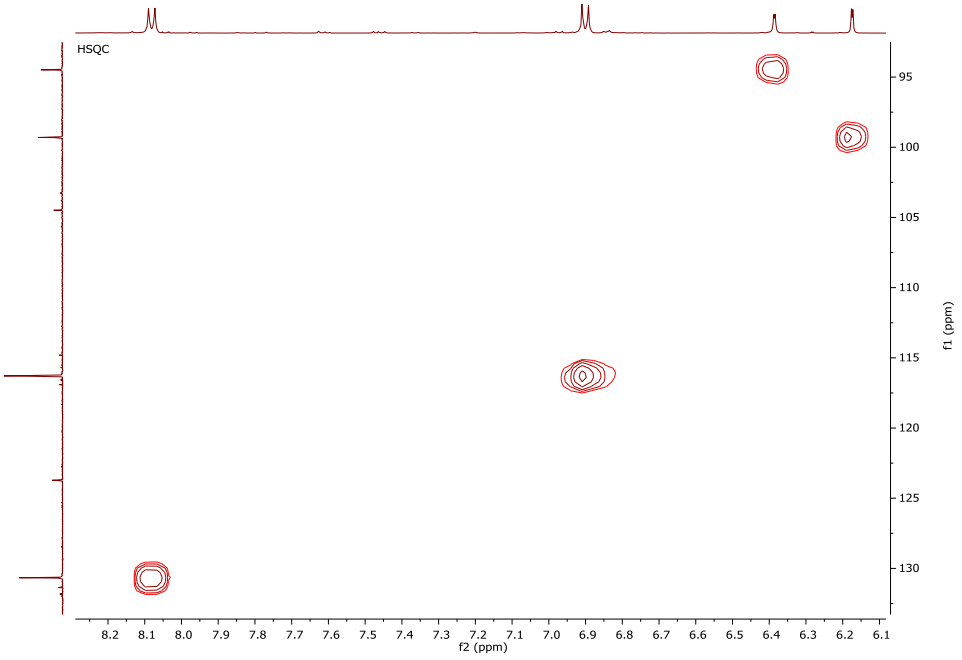

Appendix 18e: HMBC for Compound 227

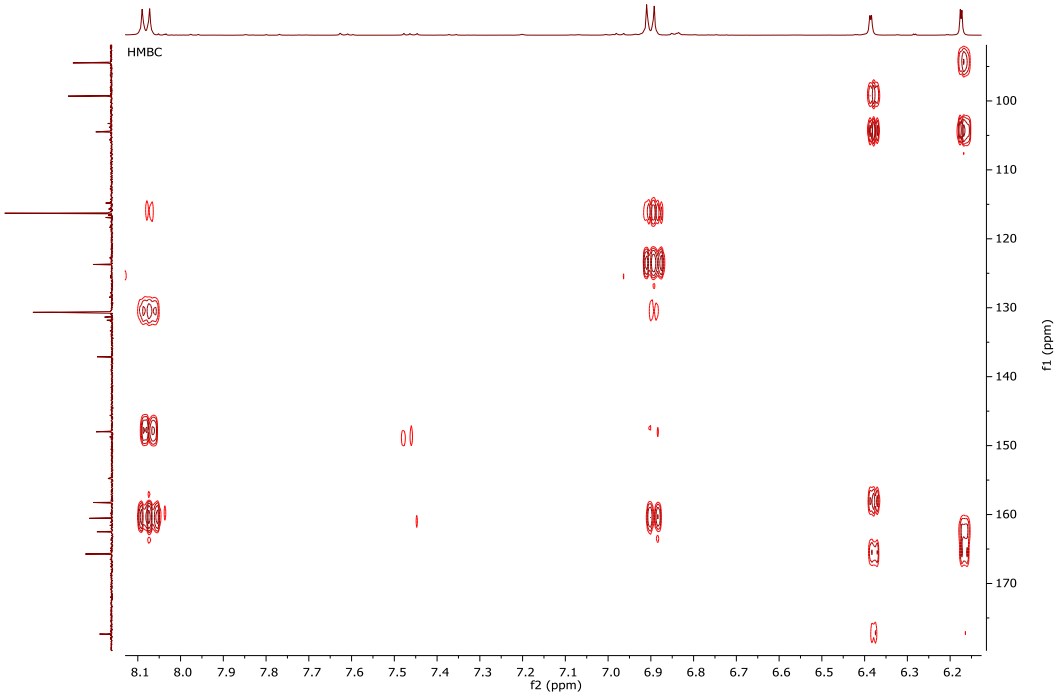

Appendix 19: NMR Spectra for 4,2-Dihydroxy-4-methoxy chalcone (228)

Appendix 19a: ^{1}H NMR for Compound 228

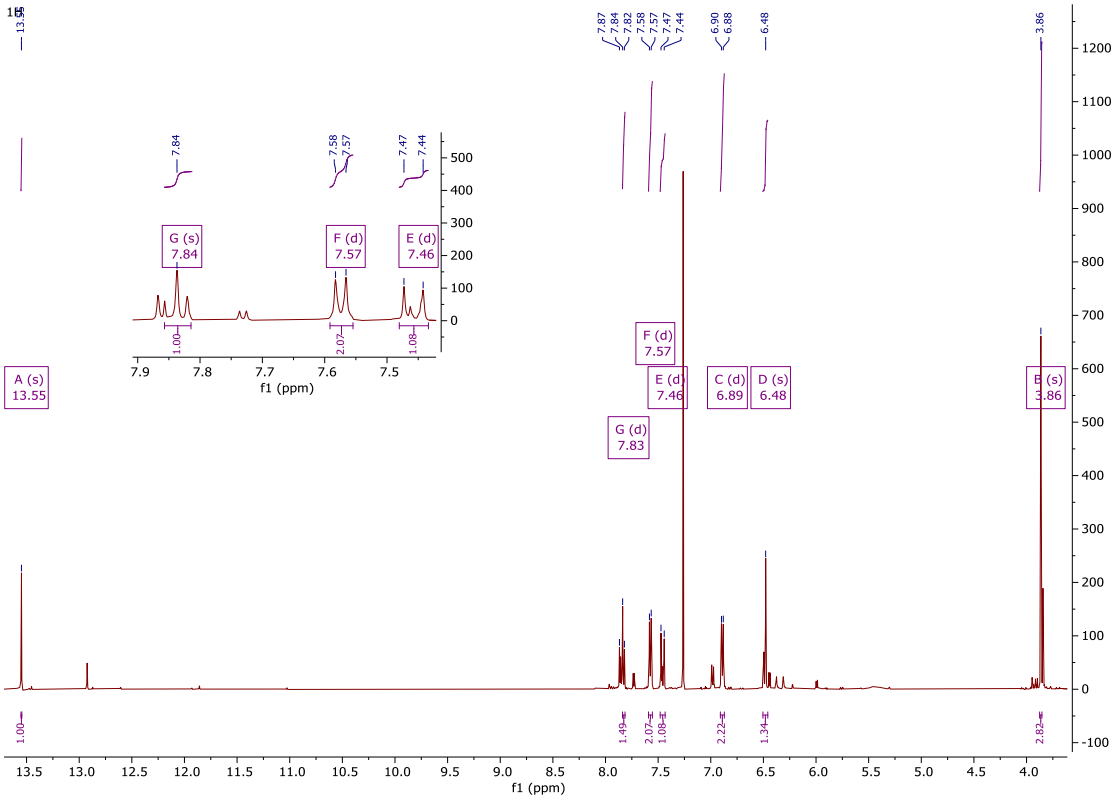

Appendix 19b: ^{13}C NMR for Compound 228

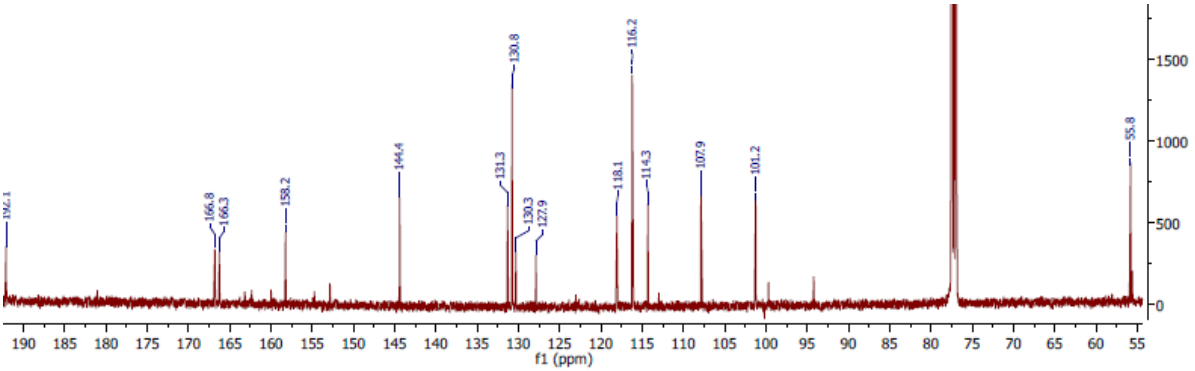

Appendix 19c: H H-Cosy for Compound 228

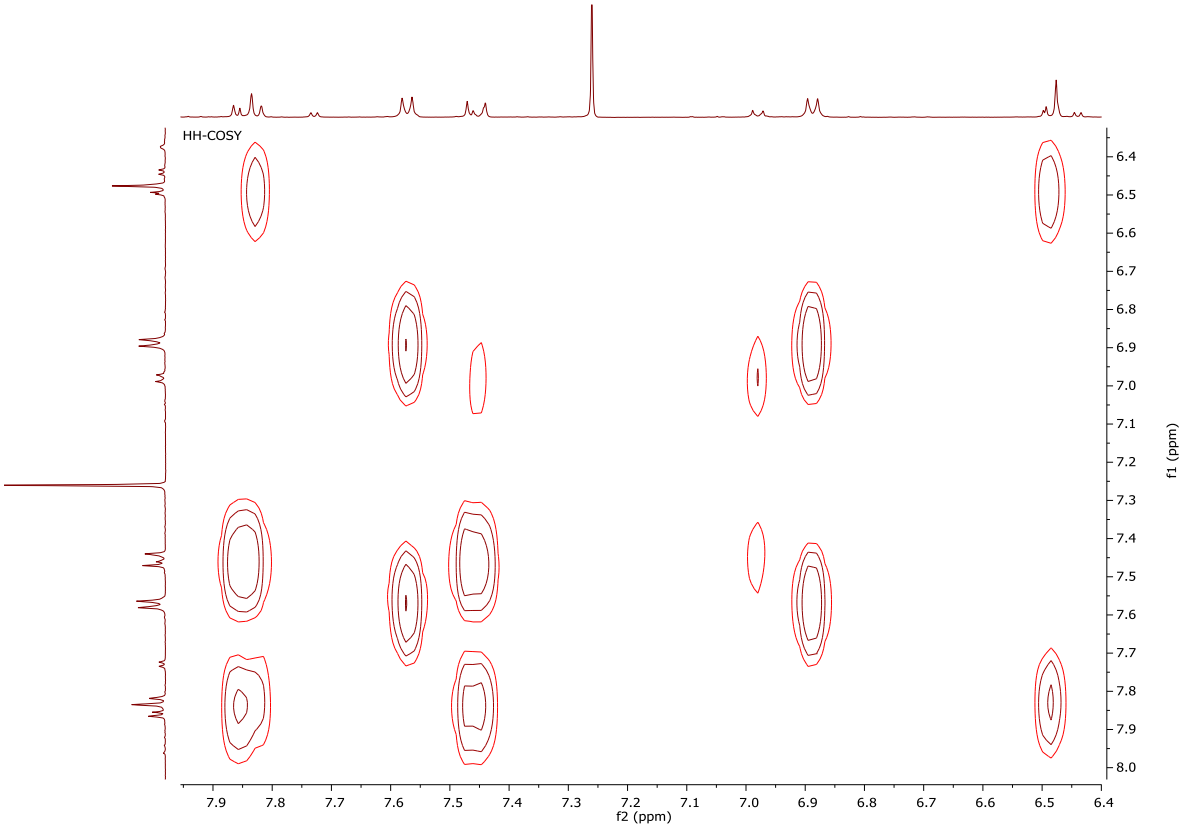

Appendix 19d: HSQC for Compound 228

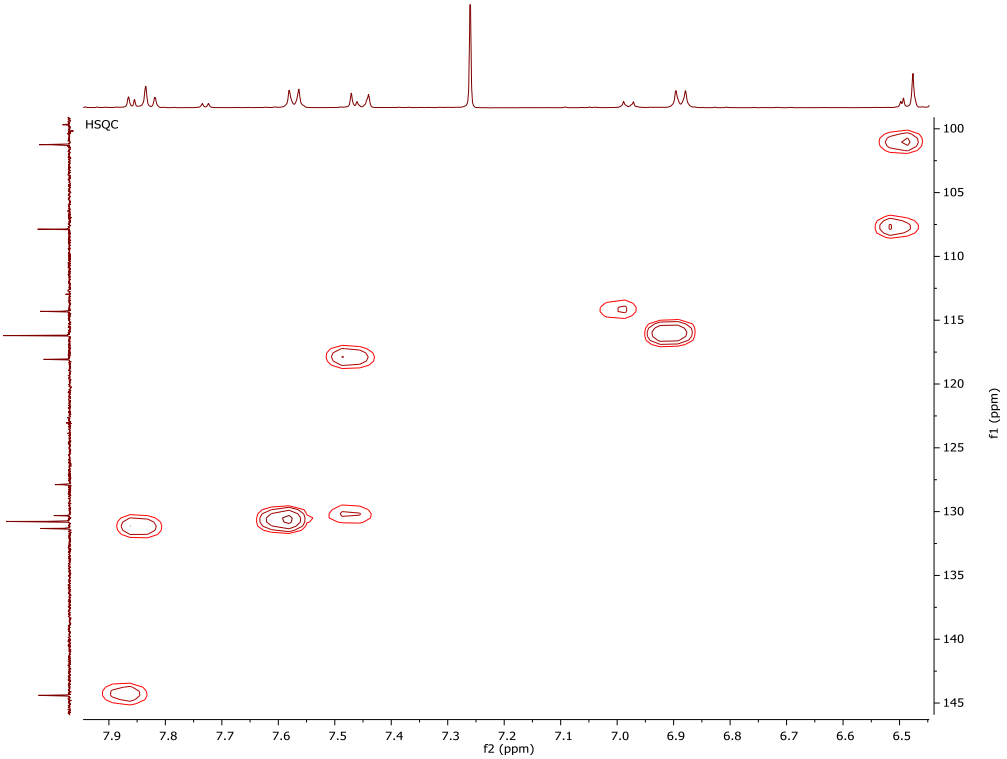

Appendix 19e: HMBC for Compound 228

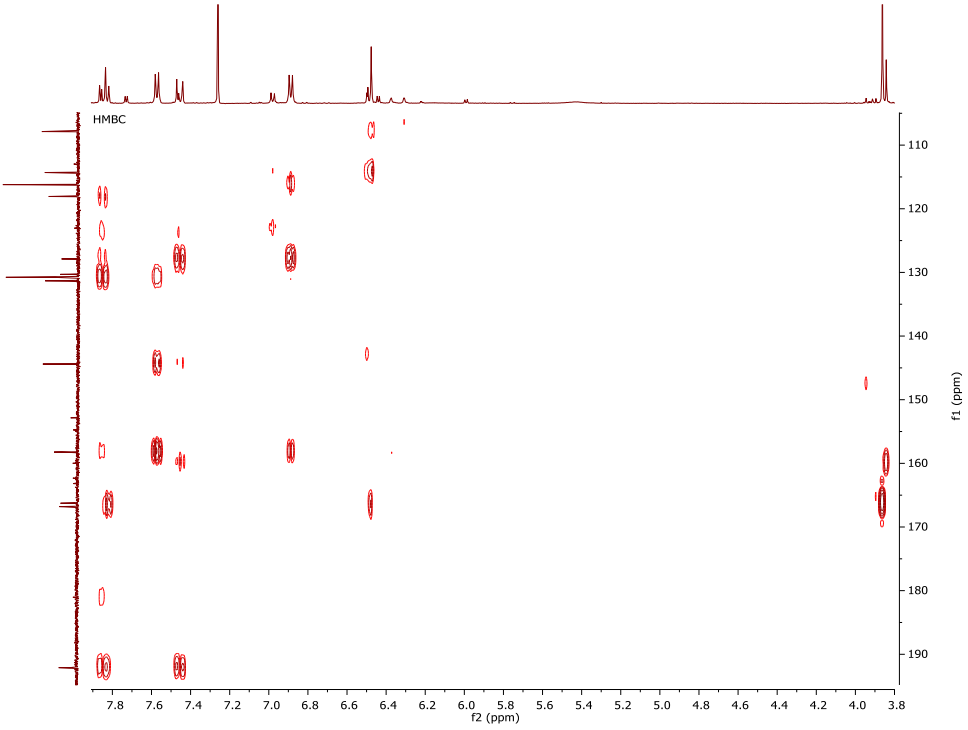

Appendix 20: NMR Spectra for Chrysin (229)

Appendix 20a: ^{1}H NMR for Compound 229

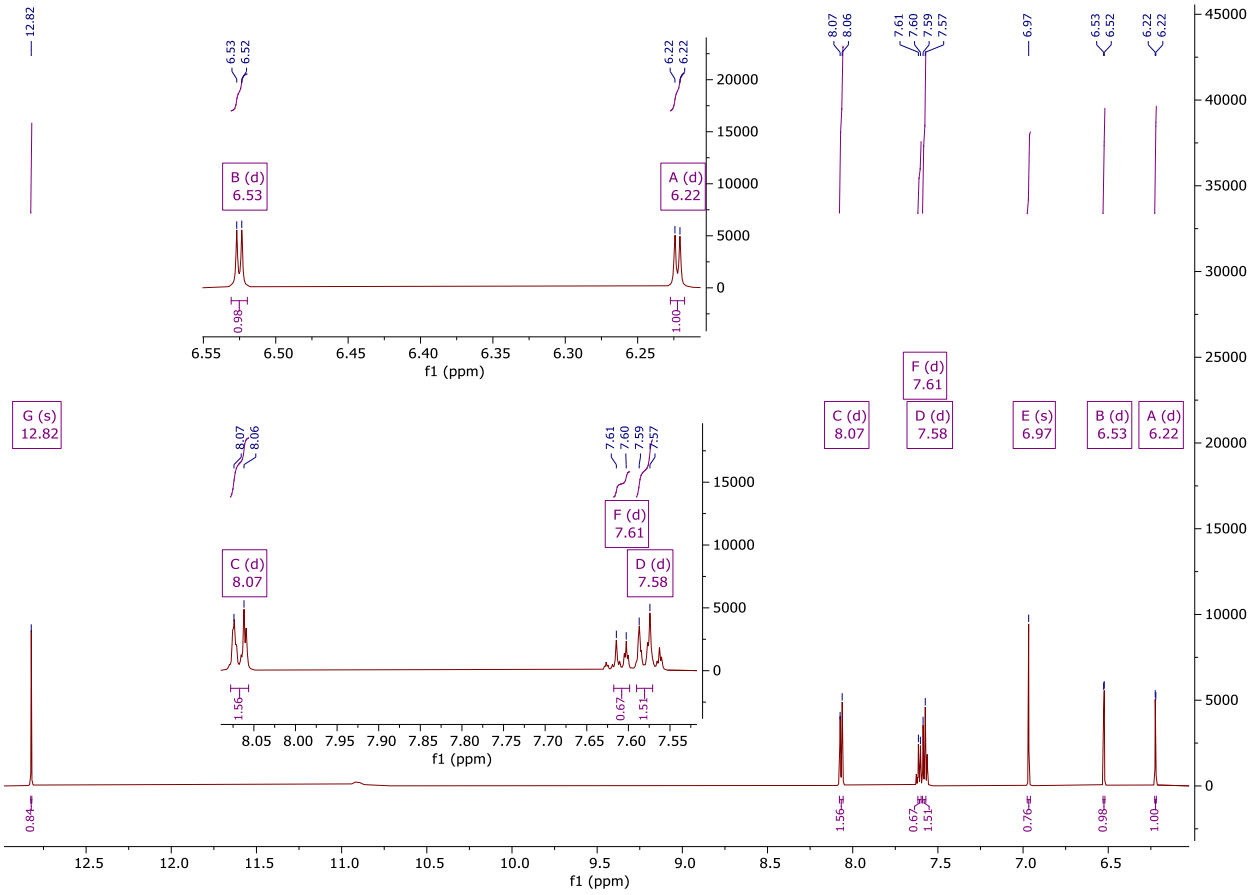

Appendix 20b: ^{13}C NMR for Compound 229

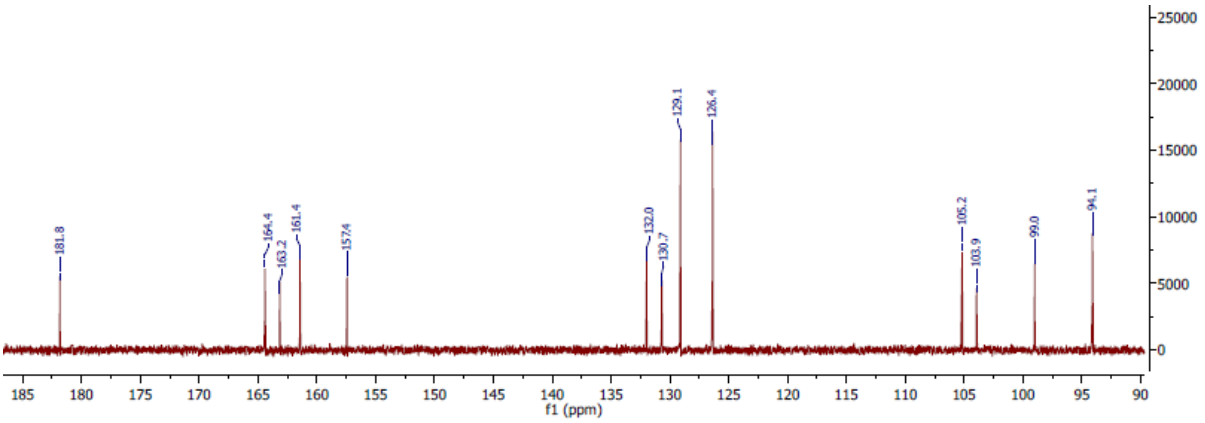

Appendix 20a: H H-Cosy NMR for Compound 229

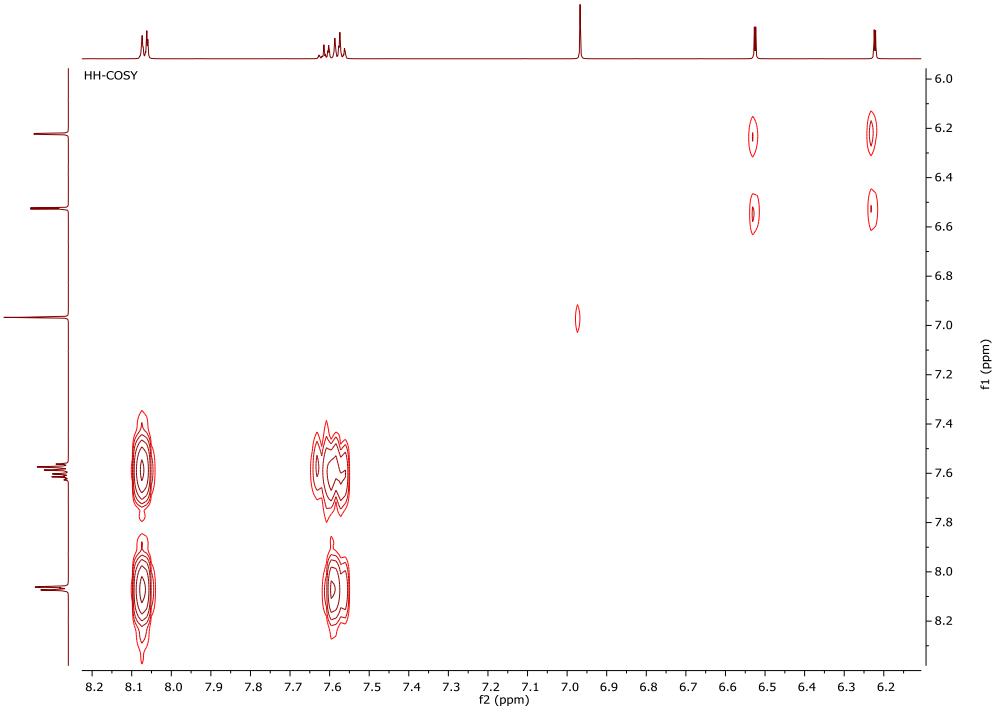

Appendix 20c: HSQC NMR for Compound 229

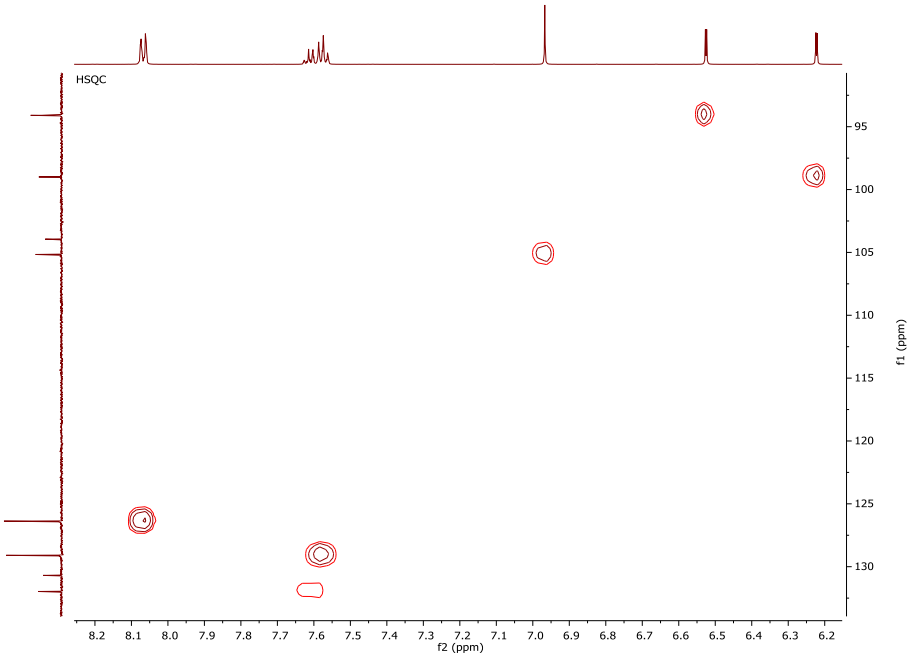

Appendix 20a: ^{1}H NMR for Compound 229

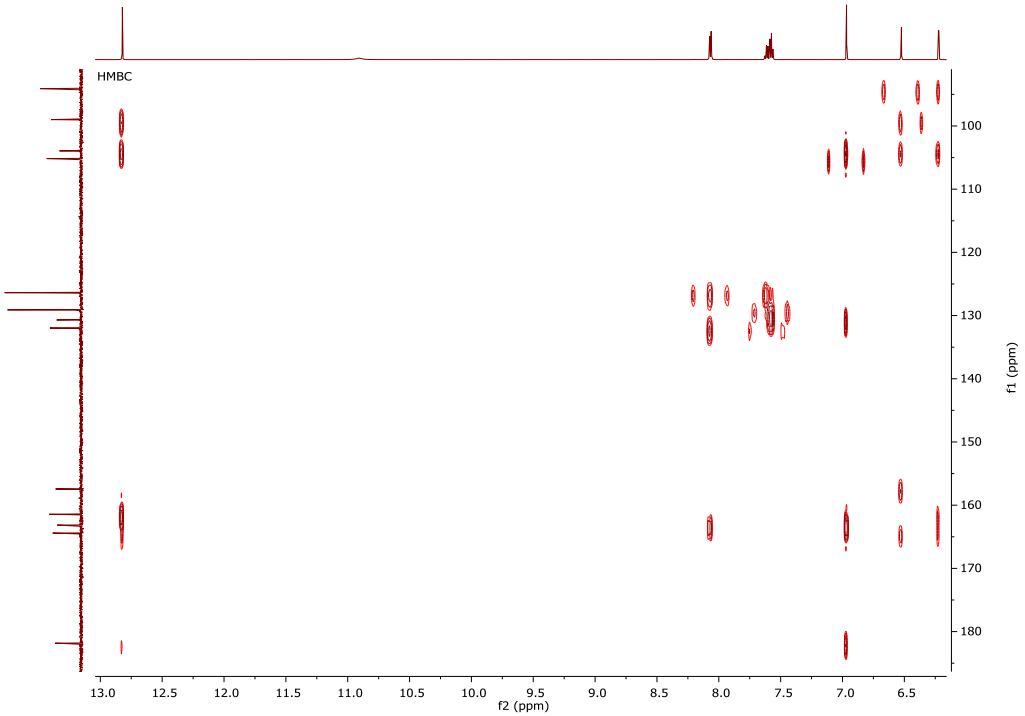

Appendix 21: NMR Data for Apigenin (230)

Appendix 21a: ^{1}H NMR for Compound 230

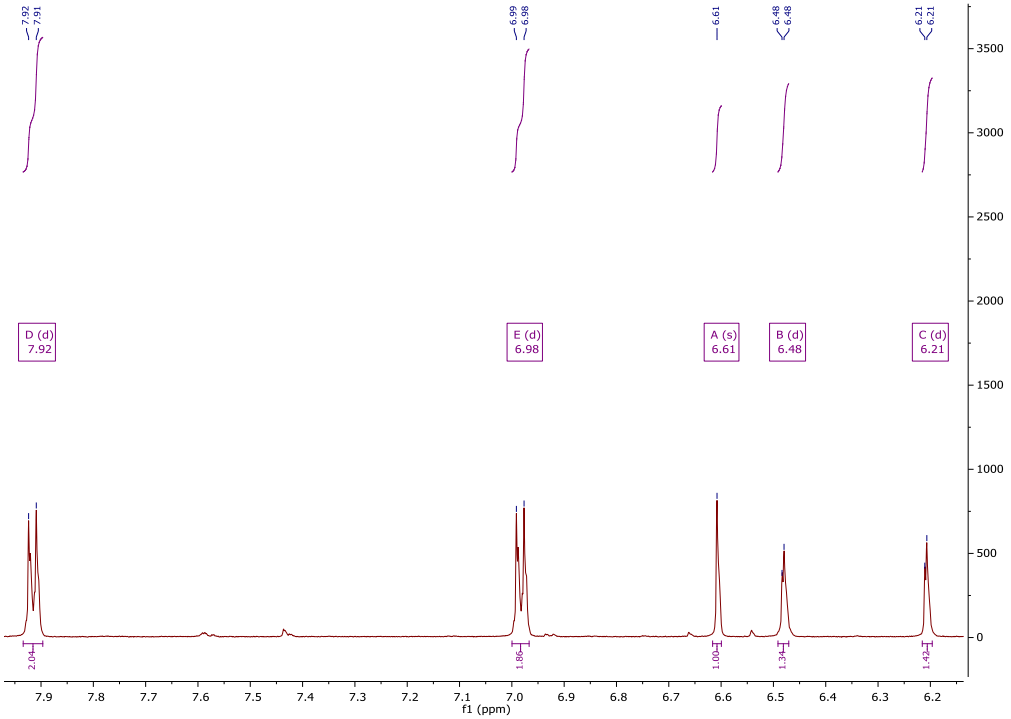

Appendix 21b: ^{13}C NMR for Compound 230

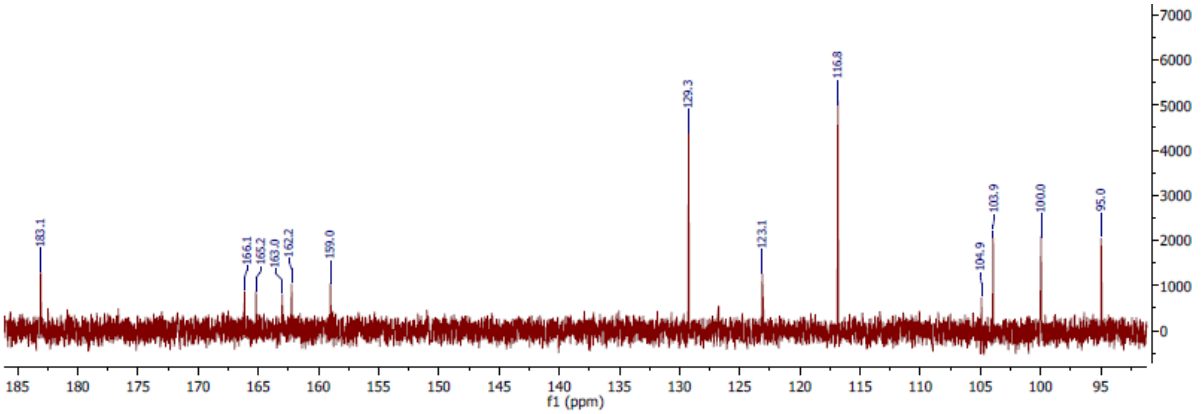

Appendix 21c: H H-Cosy for Compound 230

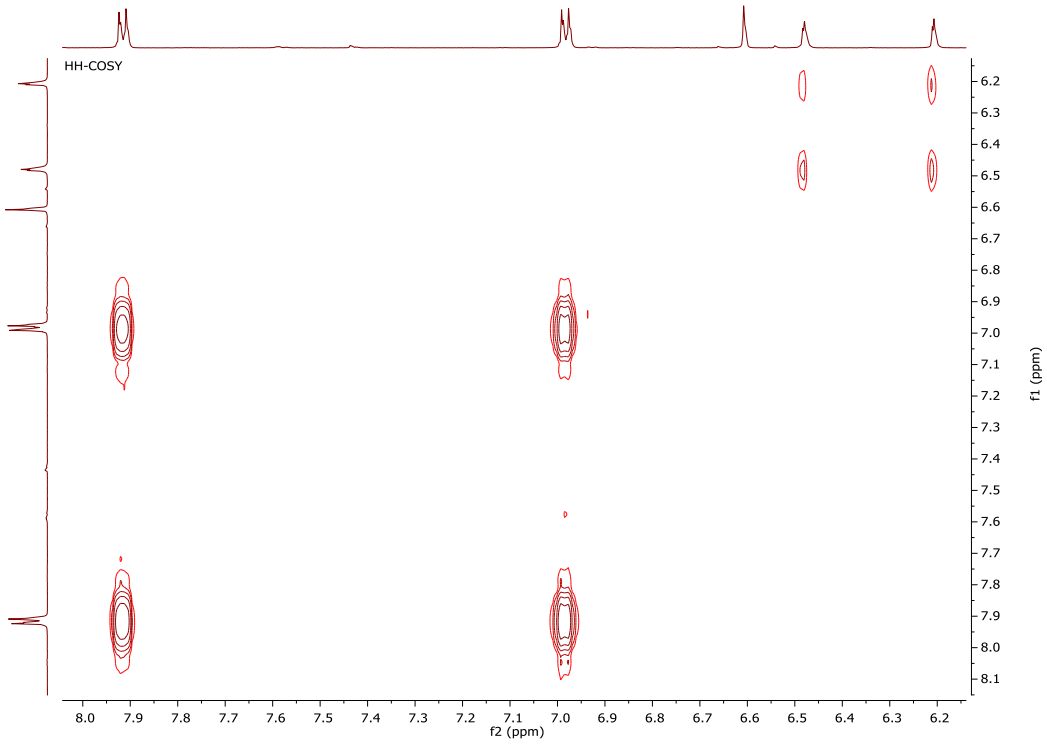

Appendix 21d: HSQC for Compound 230

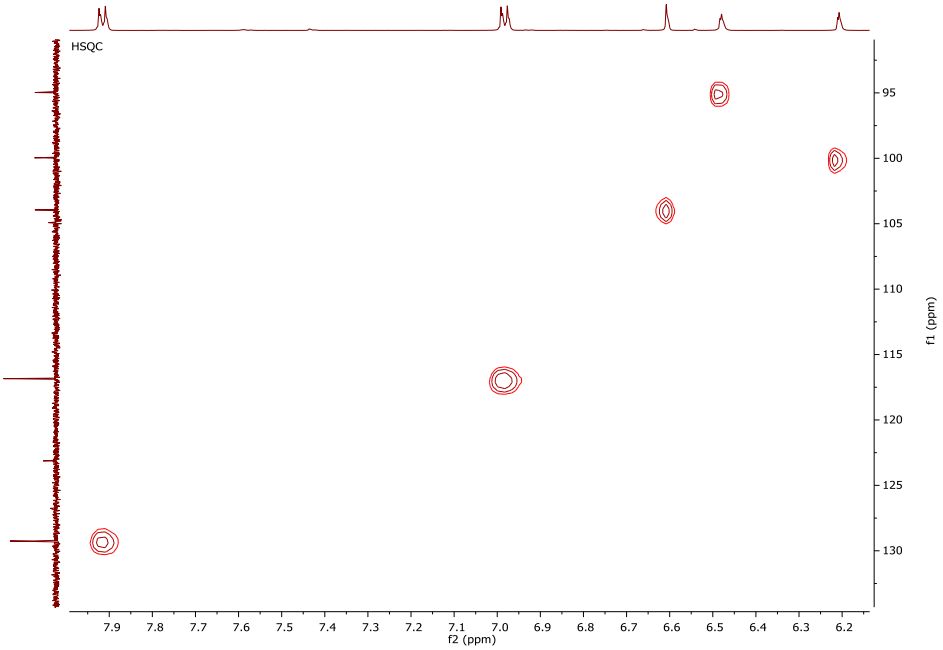

Appendix 21e: HMBC for Compound 230

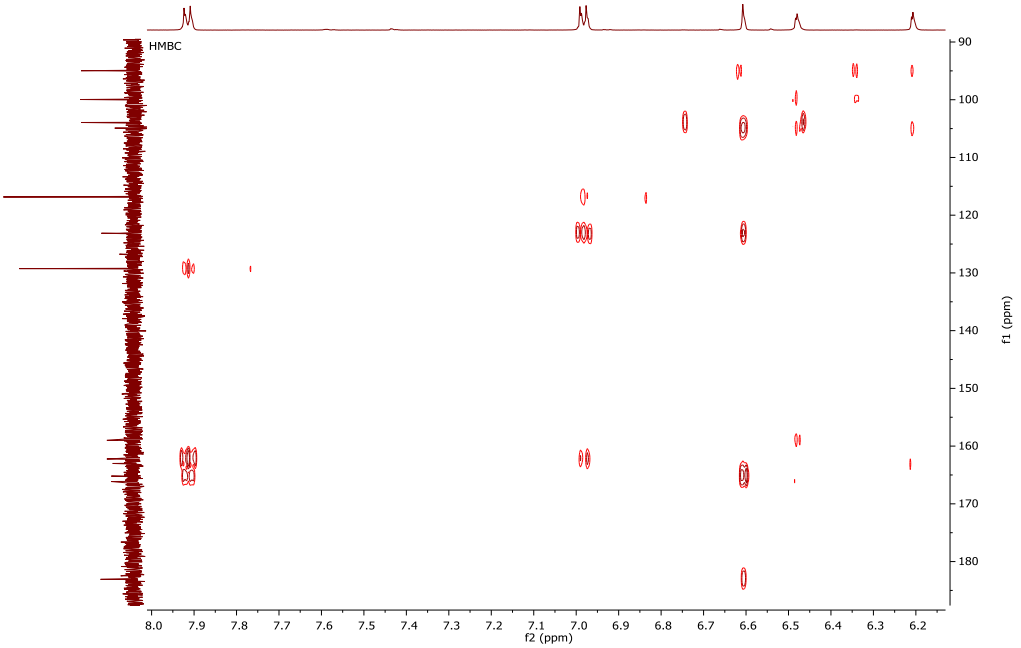

Appendix 22: NMR Data for Chrysin-7-*O*-*β*-D-glucoside (231)

Appendix 22a: ^{1}H NMR for Compound 231

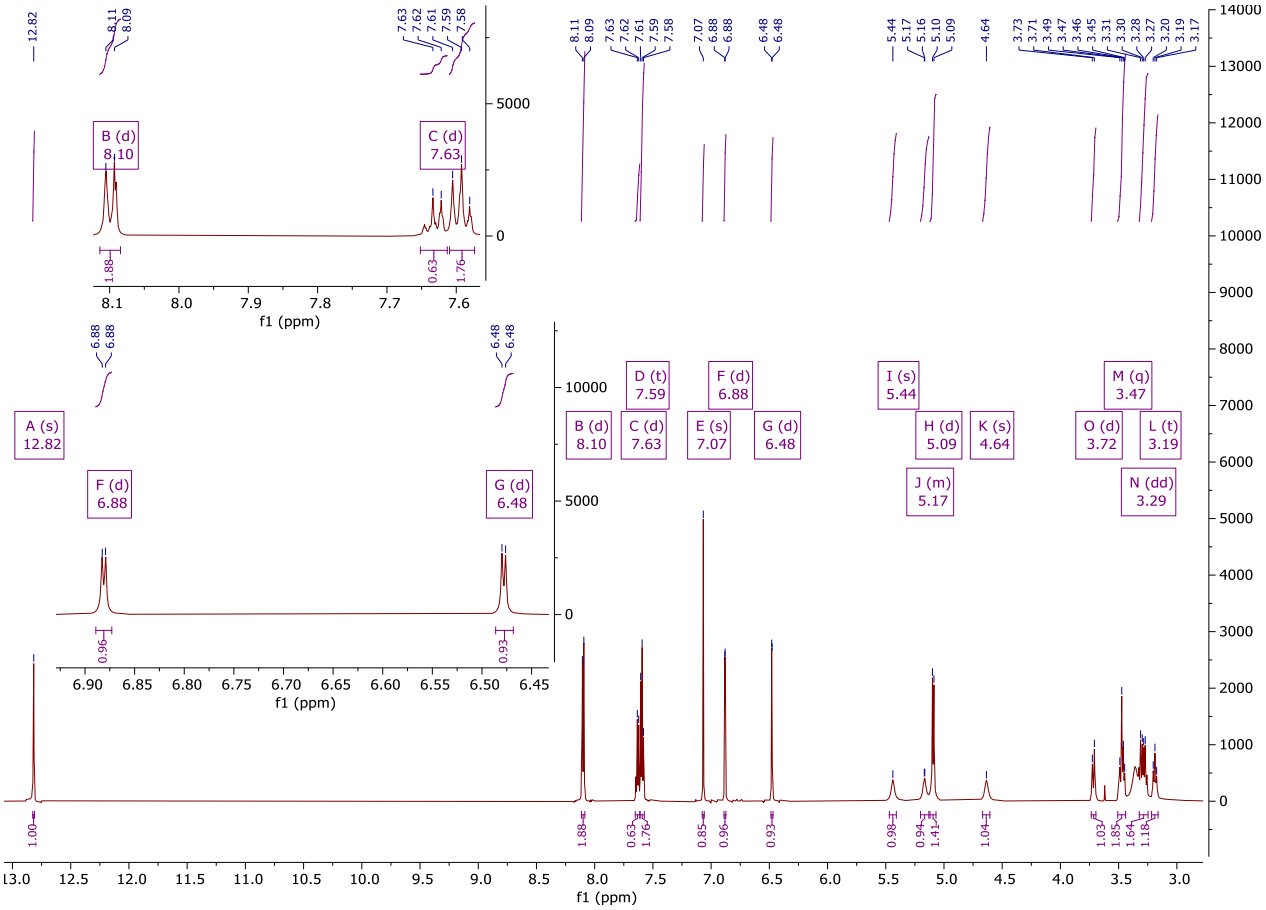

Appendix 22b: ^{13}C NMR for Compound 231

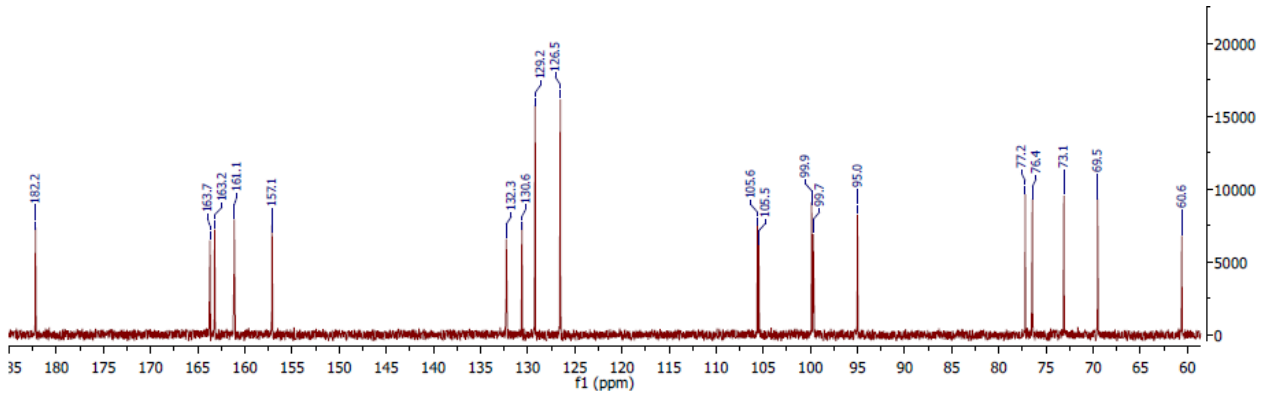

Appendix 22b: H H-Cosy for Compound 231

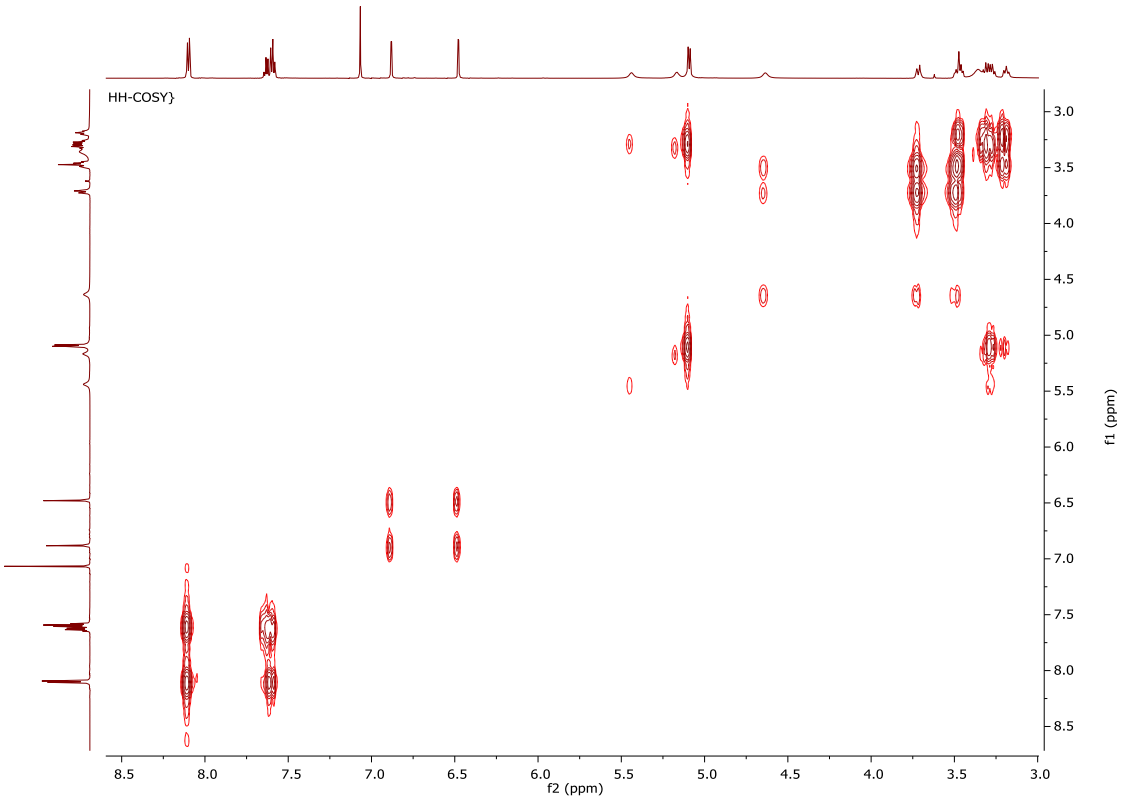

Appendix 22c: HSQC for Compound 231

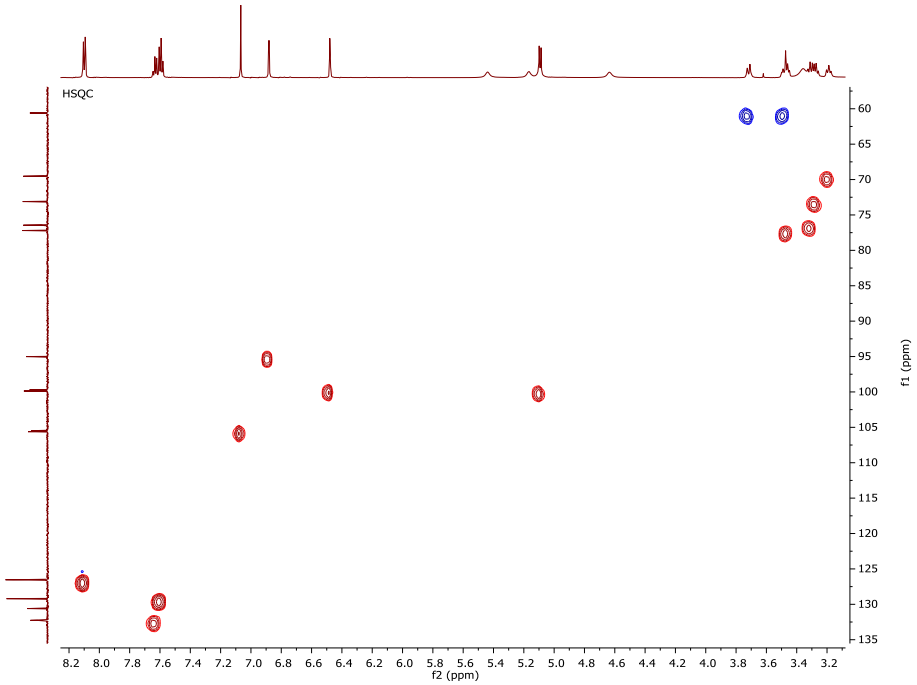

Appendix 22e: HMBC for Compound 231

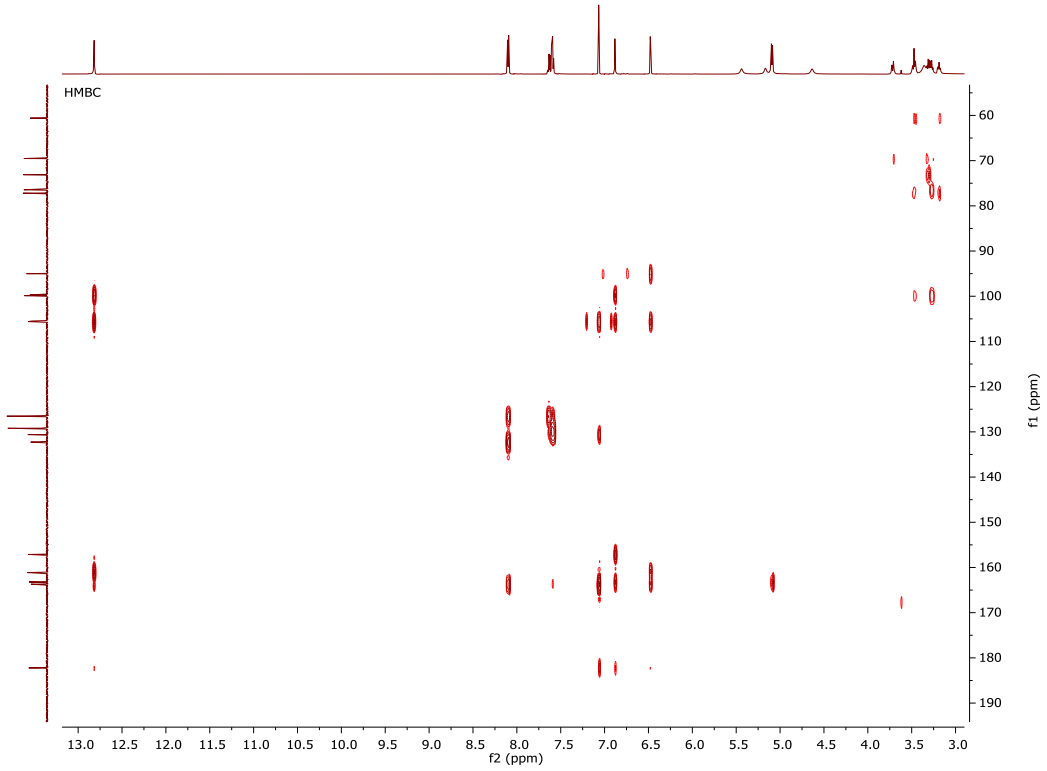

Appendix 23: NMR Data for Genkwanin (232)

Appendix 23a: ^{1}H NMR for Compound 232

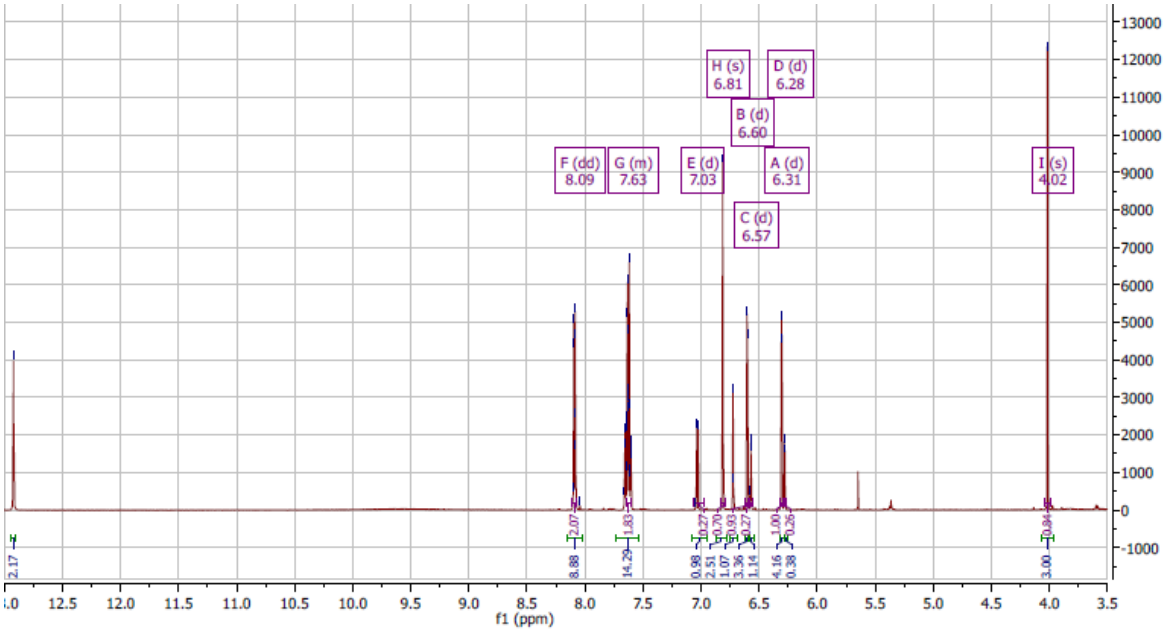

Appendix 23a: ^{1}H NMR for Compound 232

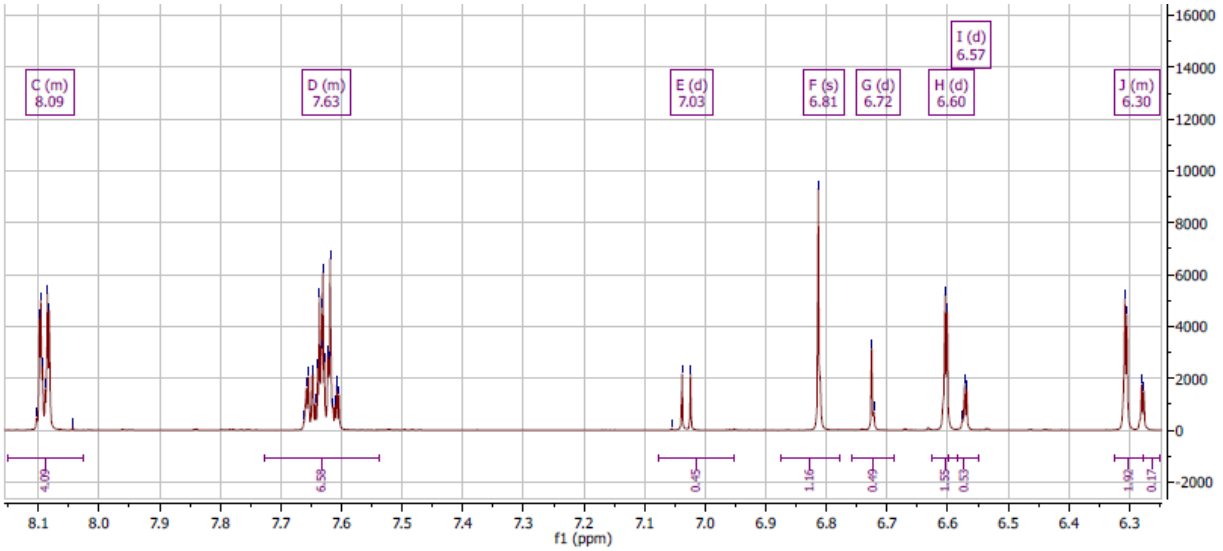

Appendix 23b: ^{13}C NMR for Compound 232

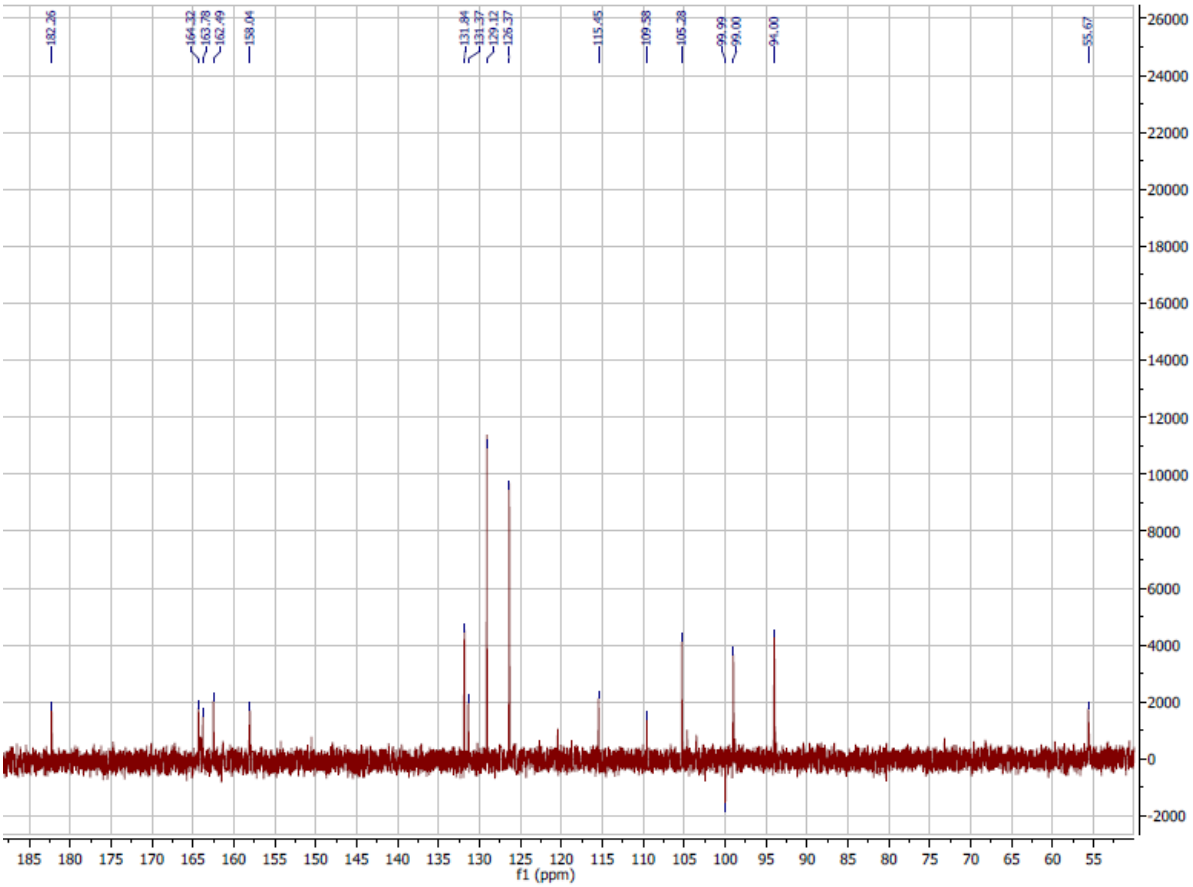

Appendix 23c: H H-Cosy for Compound 232

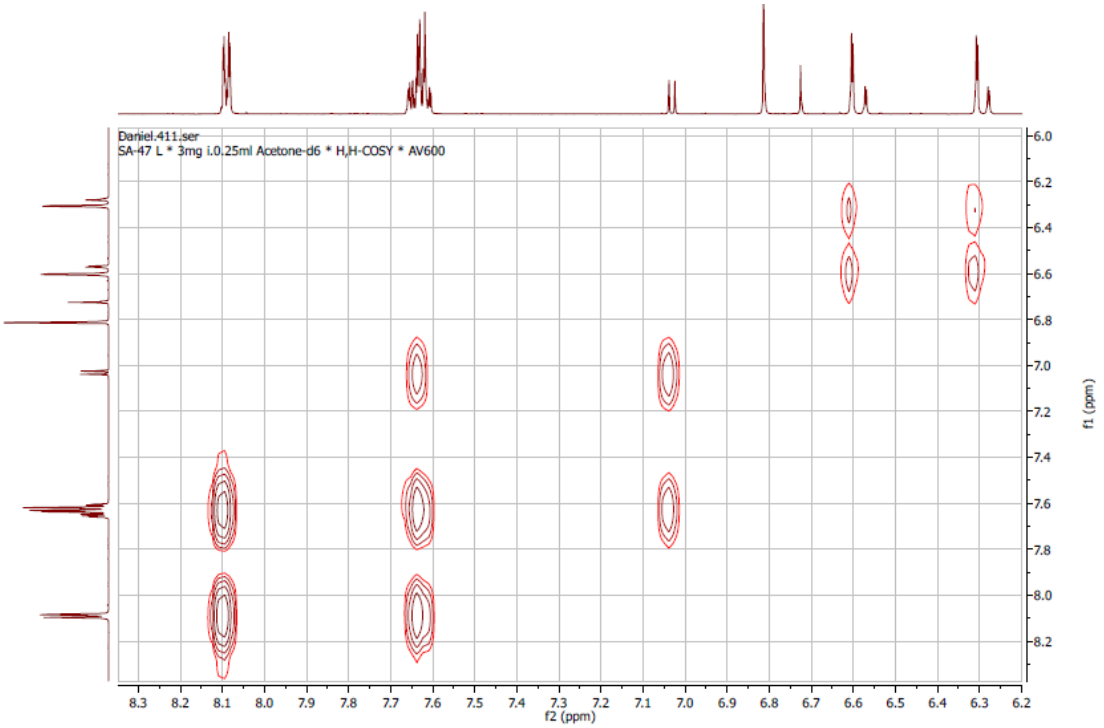

Appendix 23d: HSQC for Compound 232

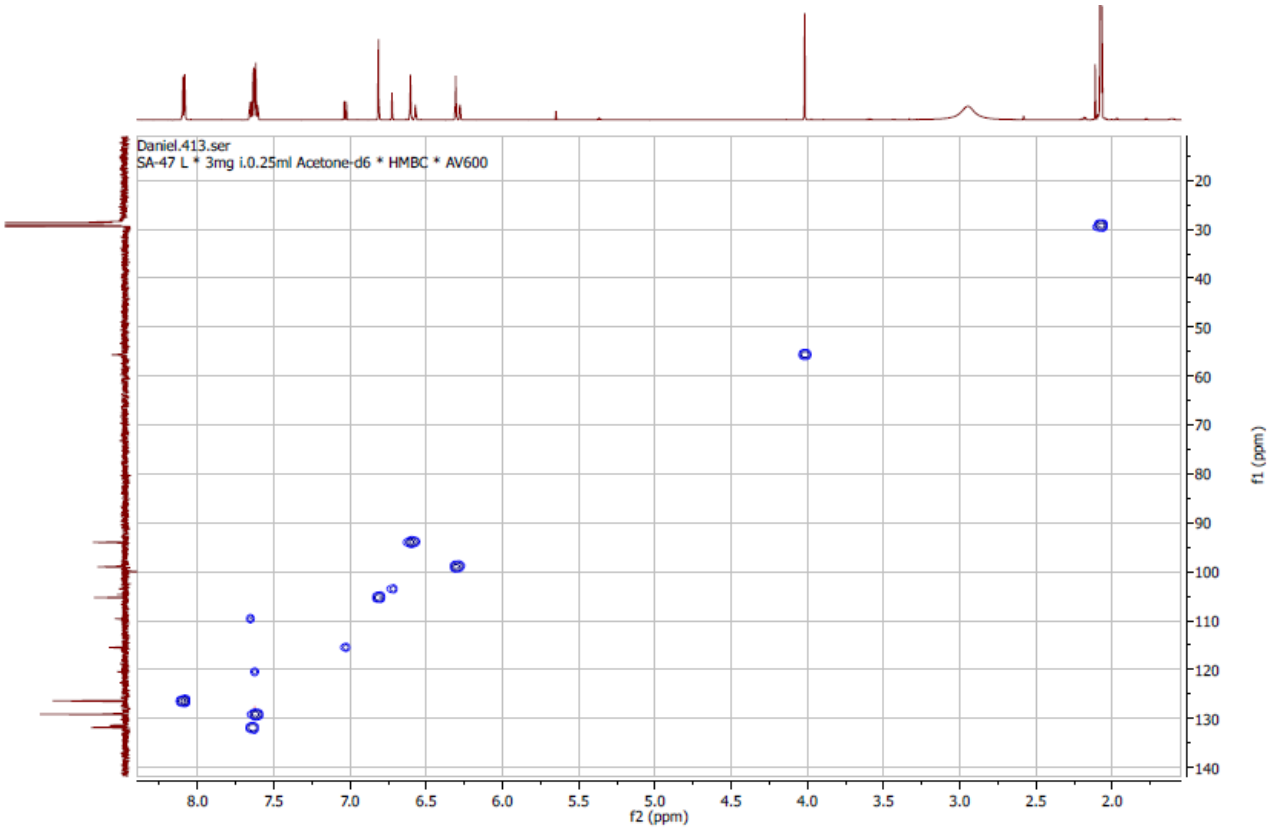

Appendix 23e: ^{1}H NMR for Compound 232

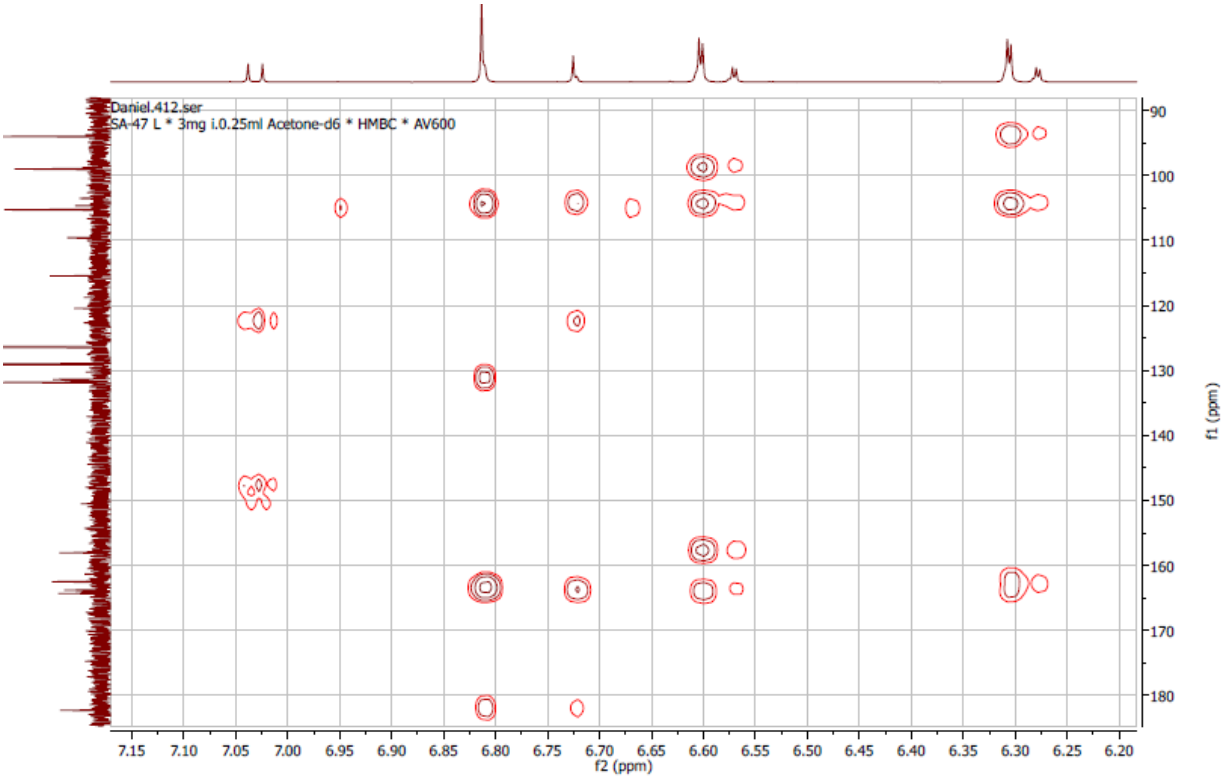

Appendix 24: NMR Data for 6,7,4′-Trimethoxyflavone (233)

Appendix 24a: ^{1}H NMR for Compound 233

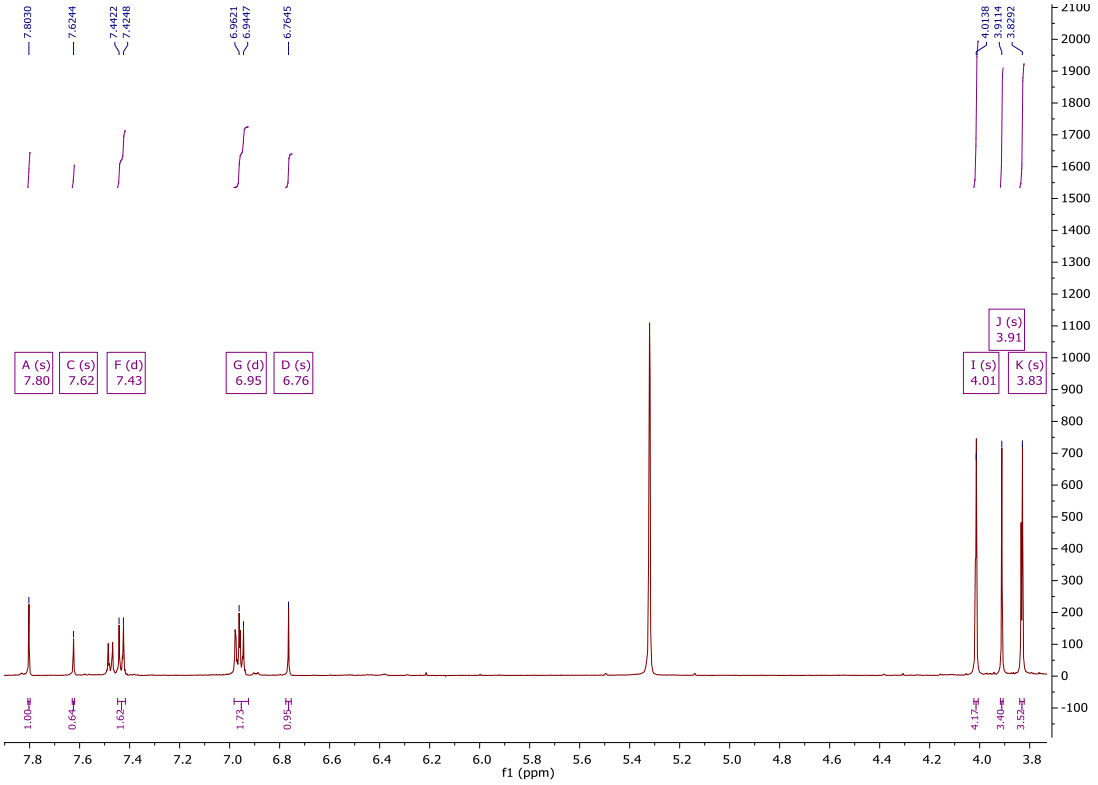

Appendix 24b: H H-Cosy NMR for Compound 233

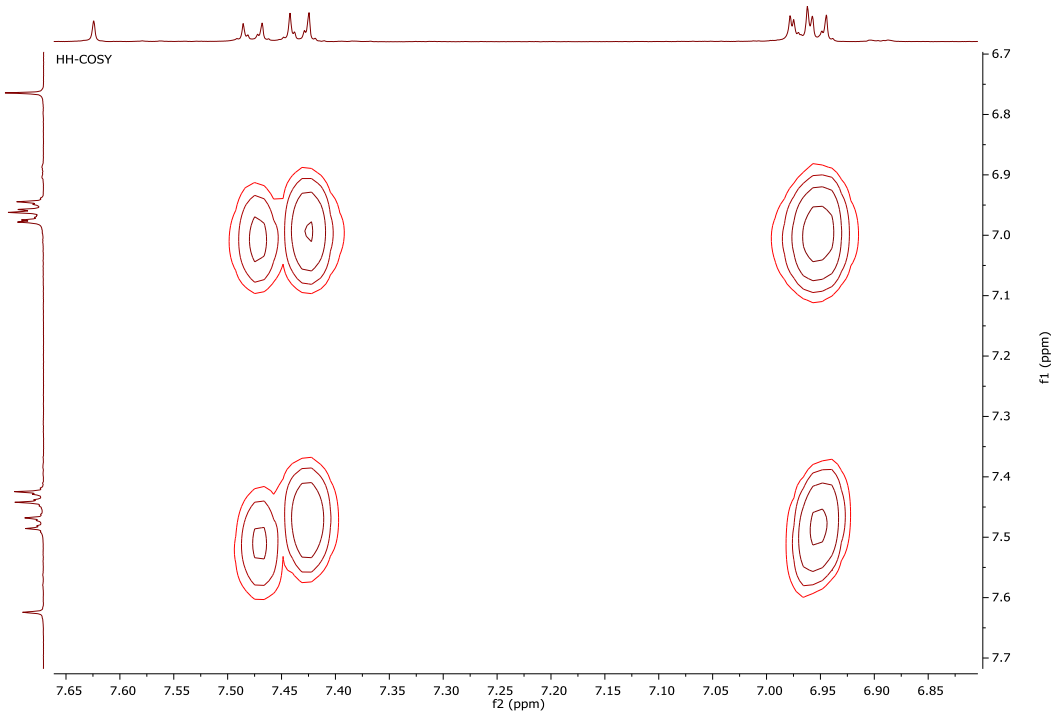

Appendix 24c: HSQC for Compound 233

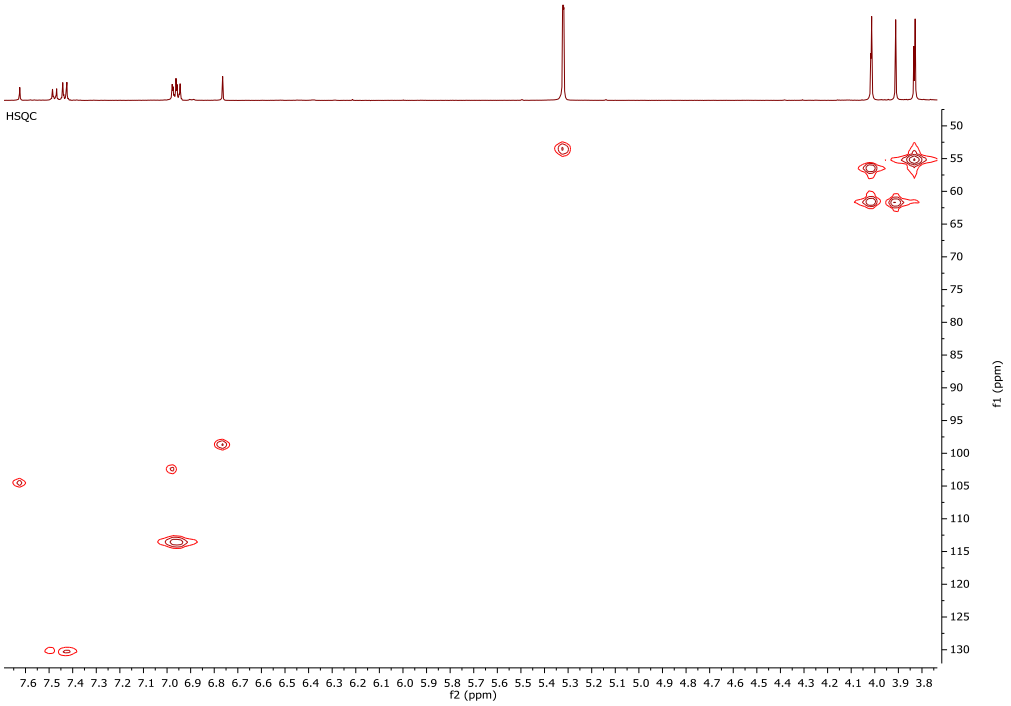

Appendix 24e: ^{1}H NMR for Compound 233

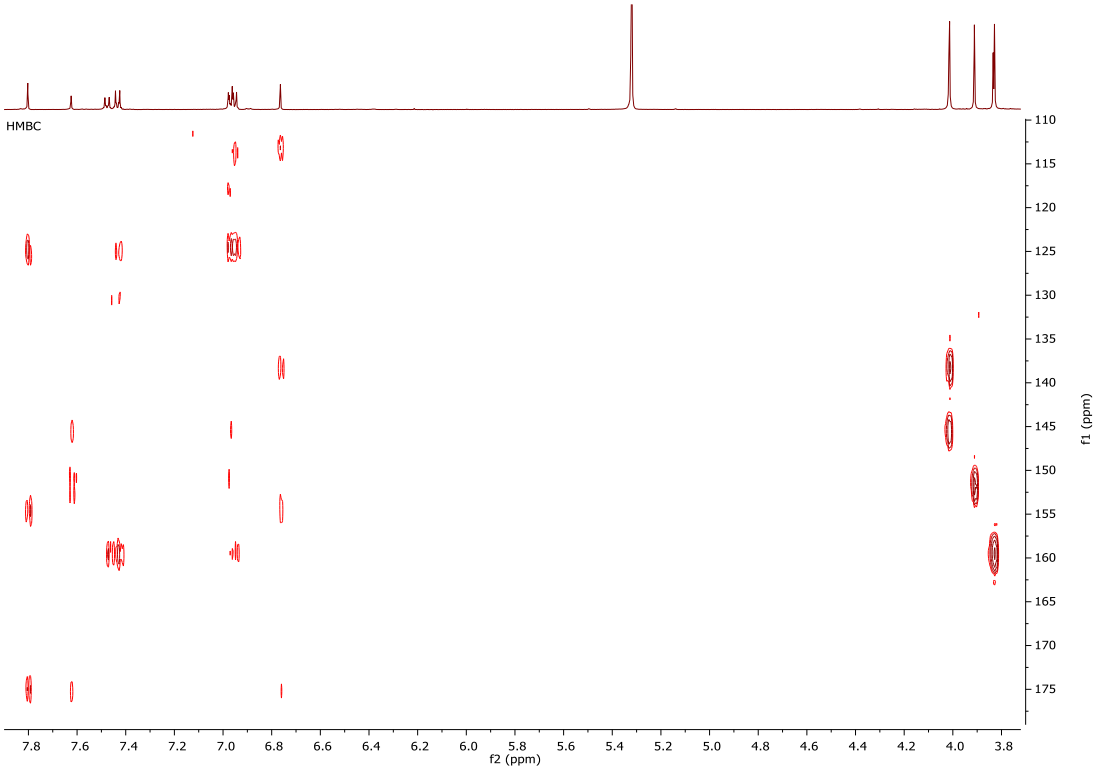

Appendix 25: NMR Spectra for Taxasin (234)

Appendix 25a: ^{1}H NMR for Compound 234

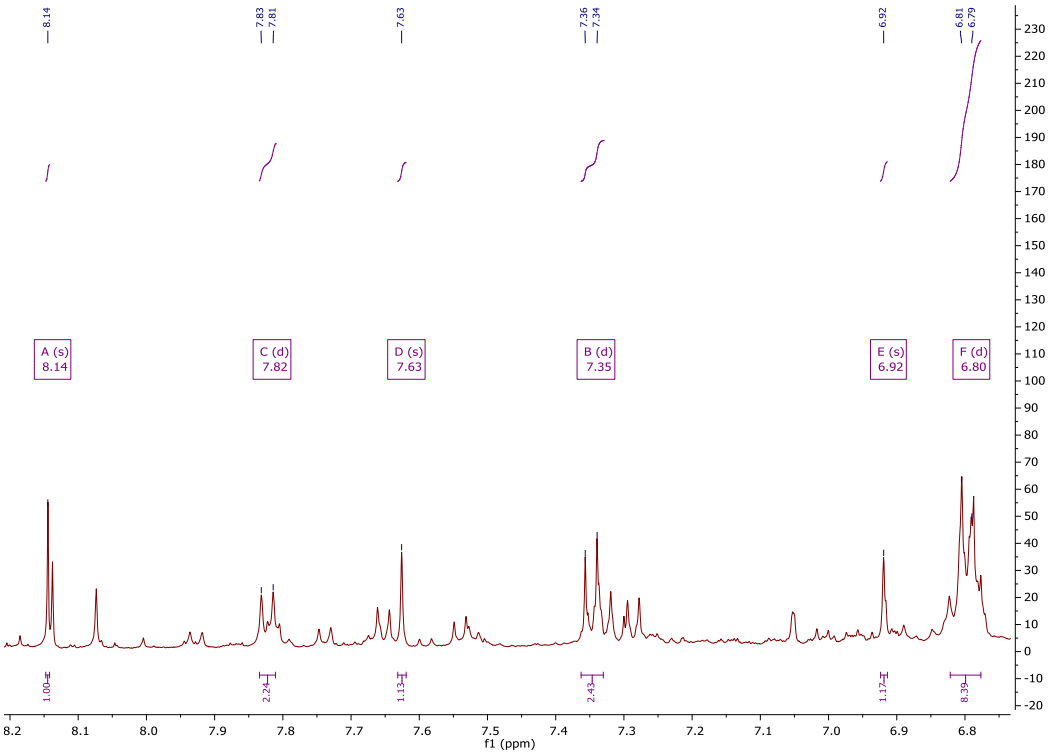

Appendix 25b: ^{13}C NMR for Compound 234

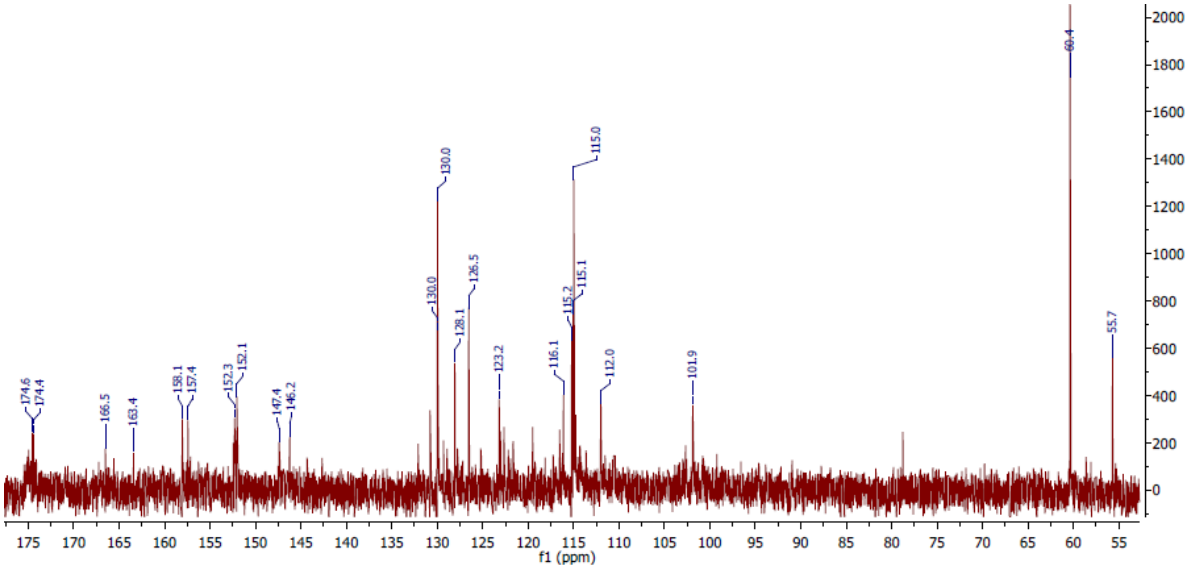

Appendix 25c: H H-Cosy for Compound 234

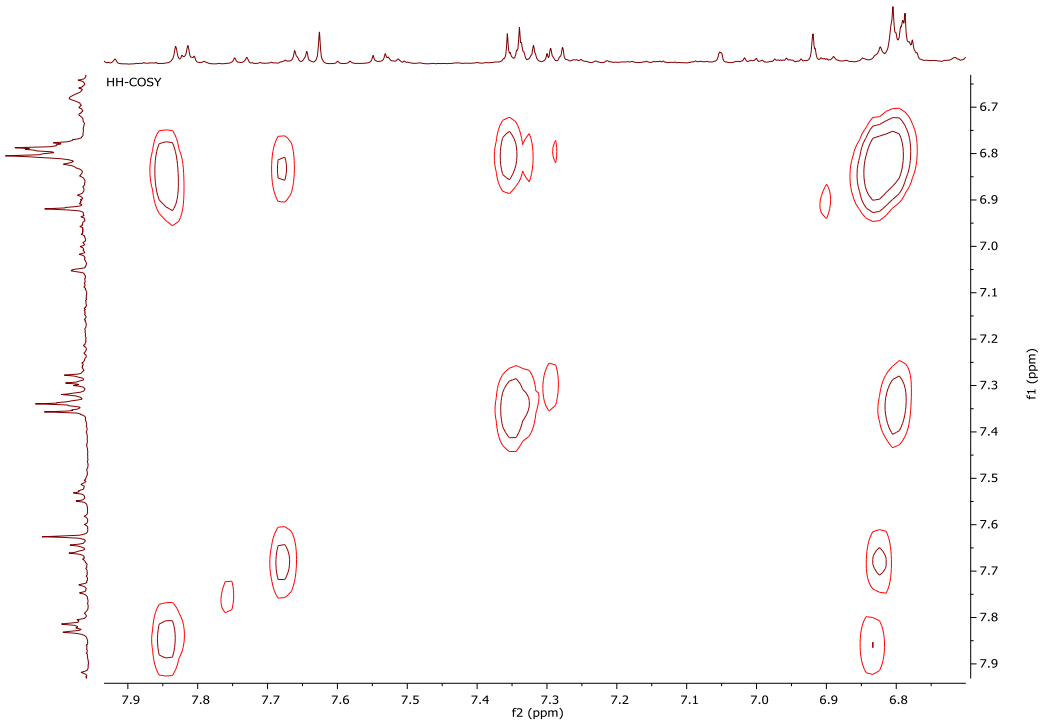

Appendix 25c: H H-Cosy for Compound 234

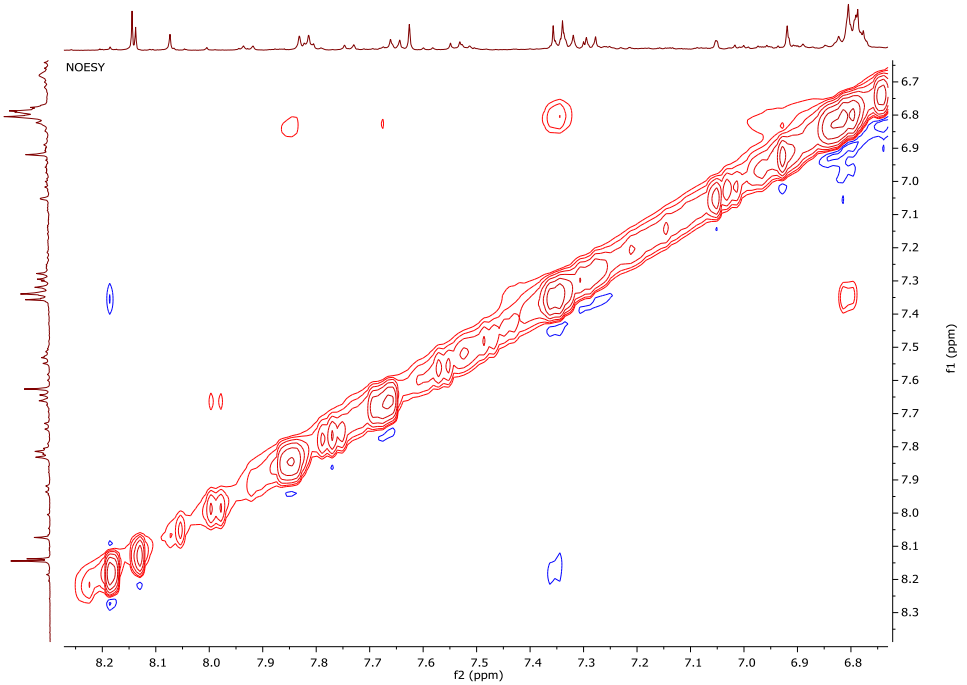

Appendix 25d: HSQC for Compound 234

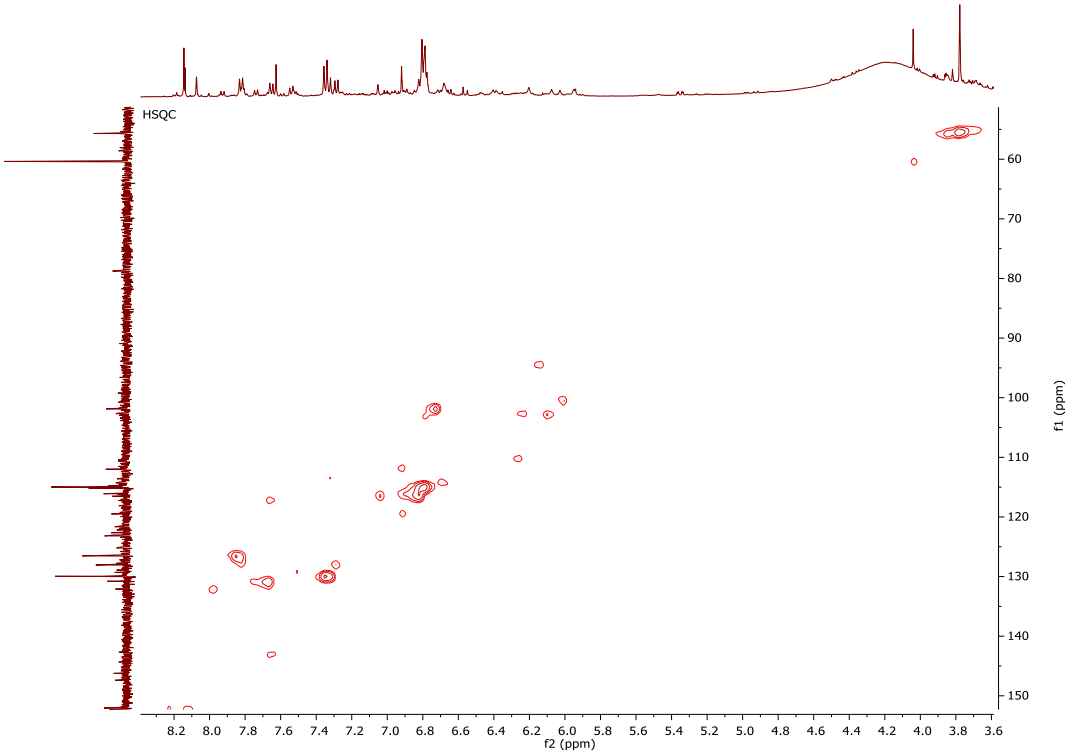

Appendix 25e: HMBC for Compound 234

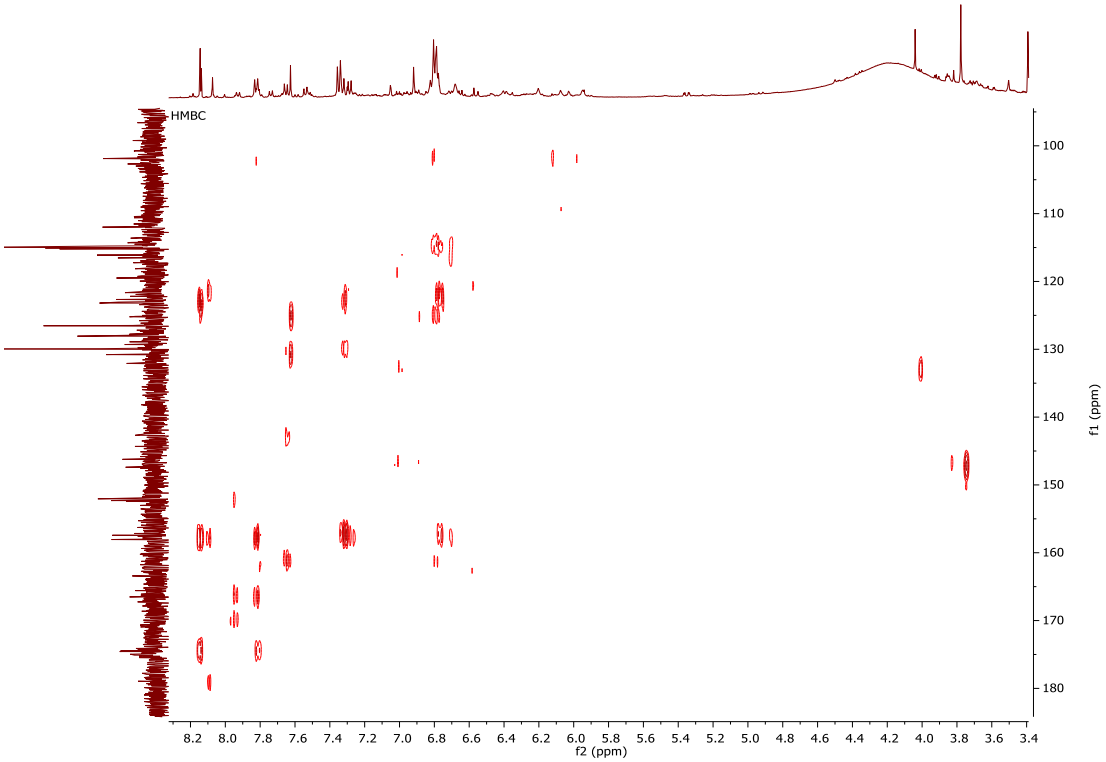

Appendix 26: NMR Spectra for 6,7,4-Trimethoxyisoflavone (235)

Appendix 26a: ^{1}H NMR for Compound 235

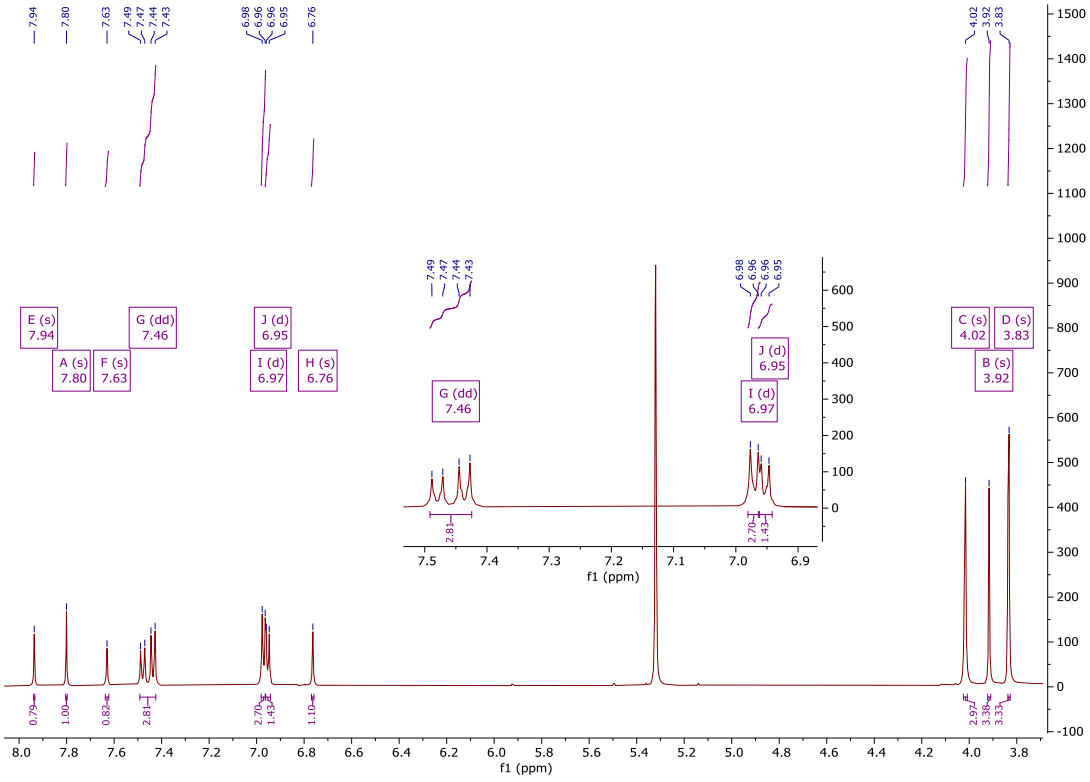

Appendix 26b: ^{13}C NMR for Compound 235

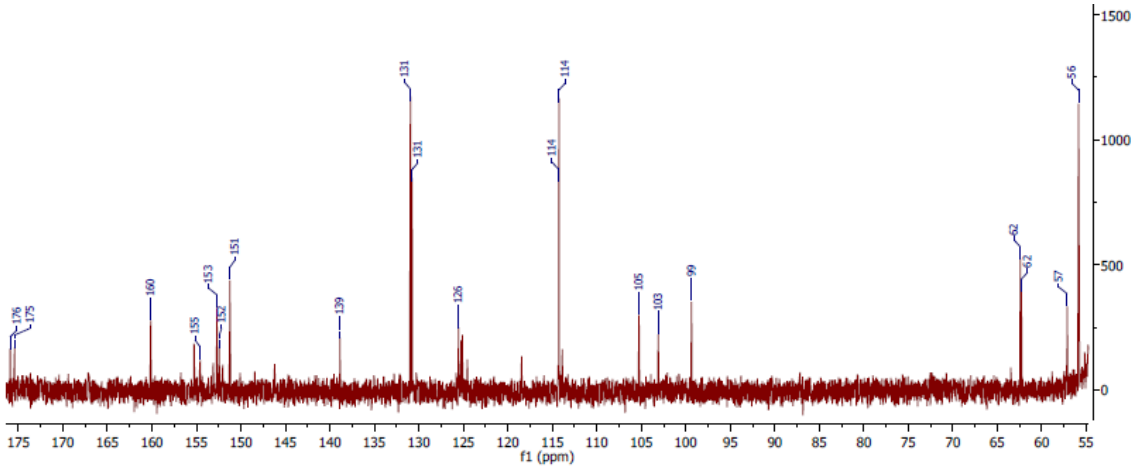

Appendix 26c: H H-Cosy for Compound 235

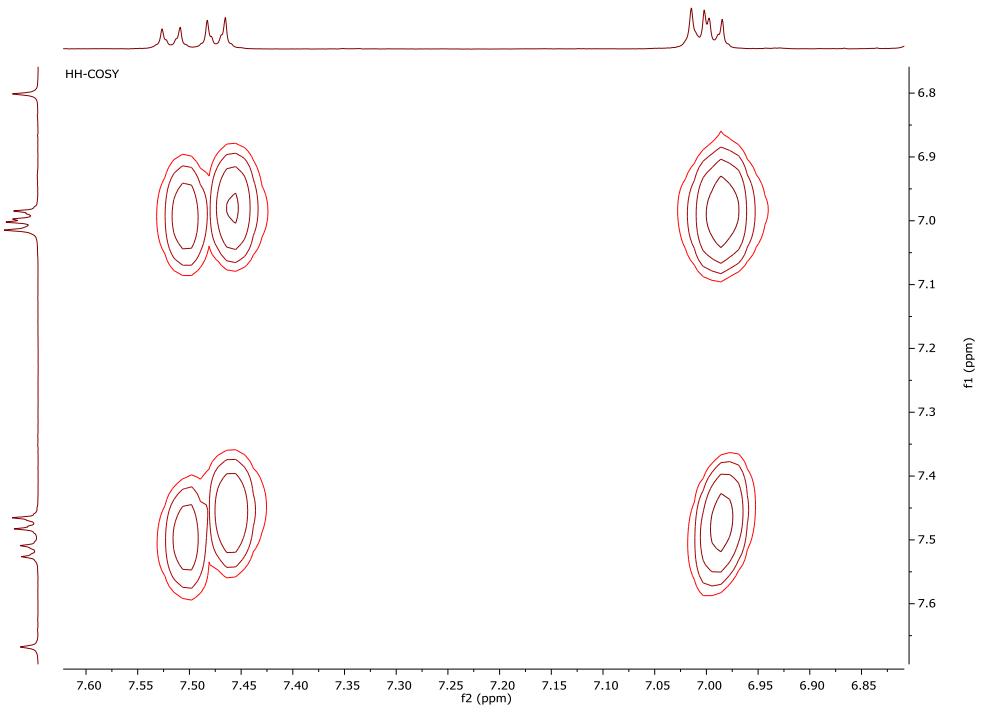

Appendix 26c: HSQC for Compound 235

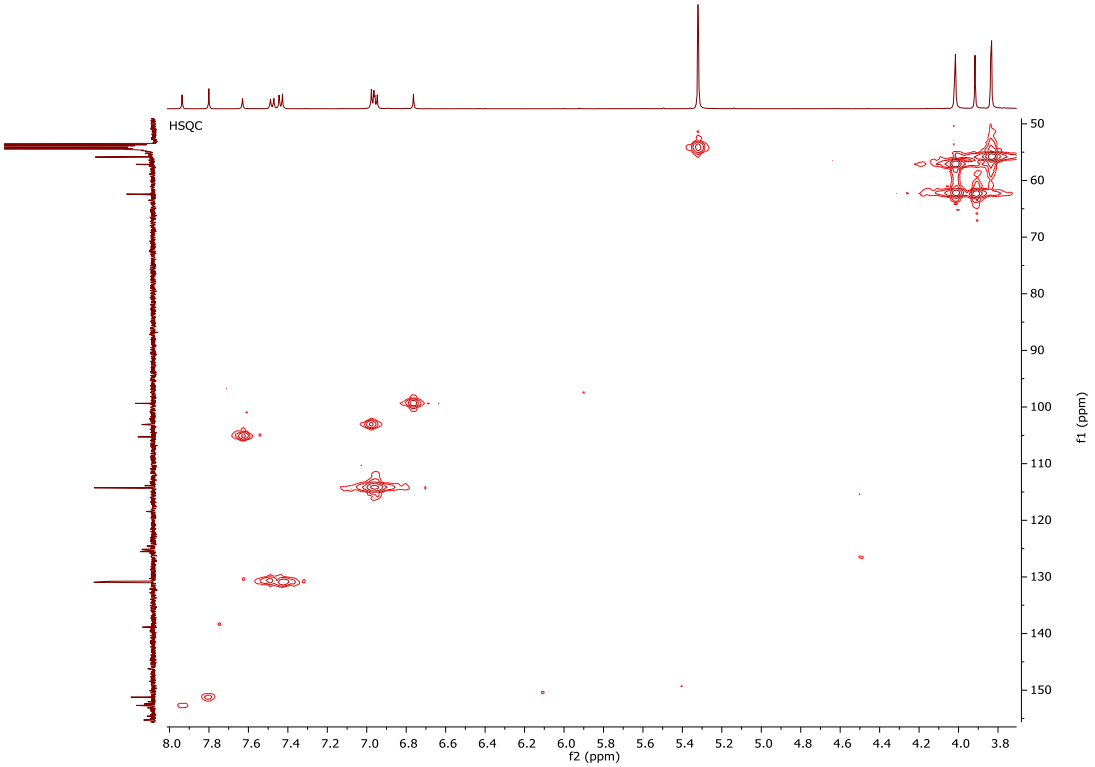

Appendix 26e: HMBC for Compound 235

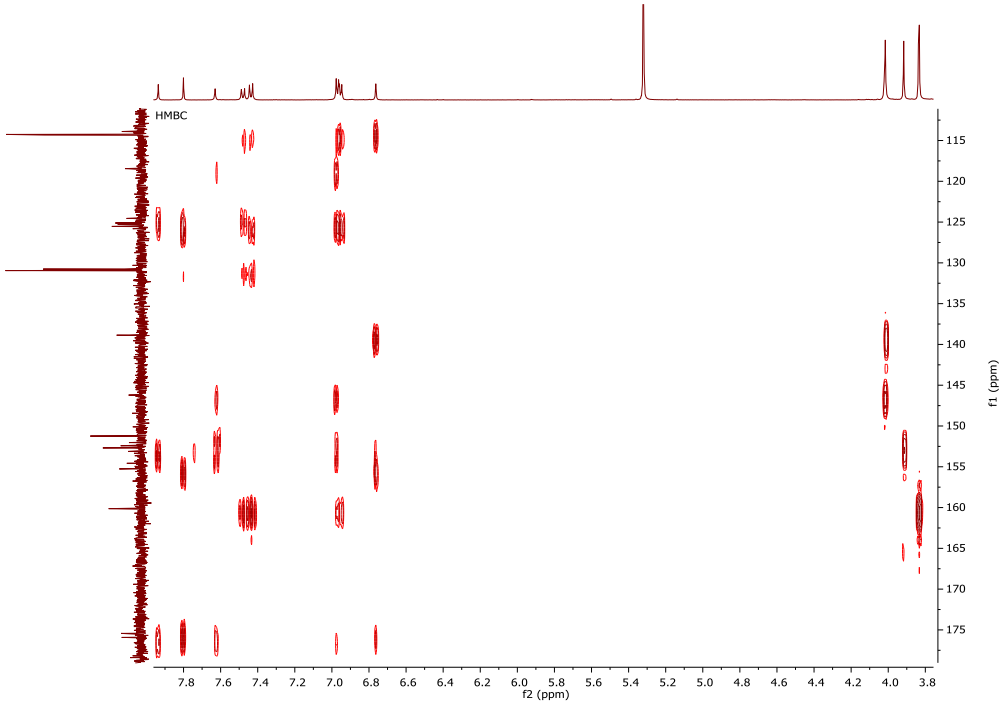

Appendix 27: NMR Spectra for Paraben Acid (236)

Appendix 27a: ^{1}H NMR for Compound 236

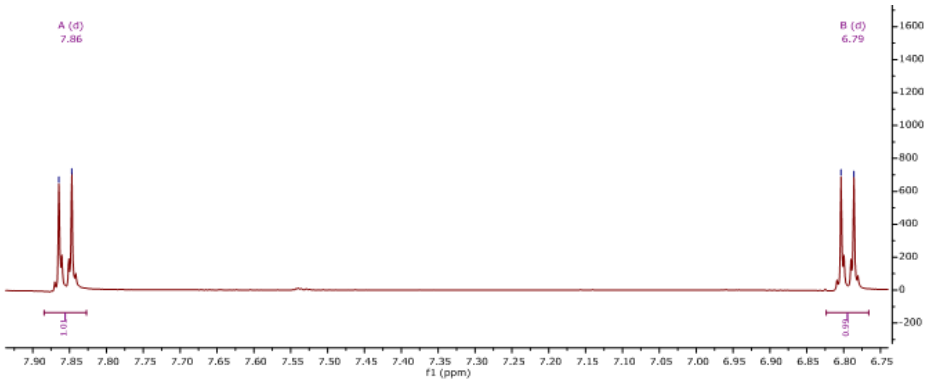

Appendix 27b: ^{13}C NMR for Compound 236

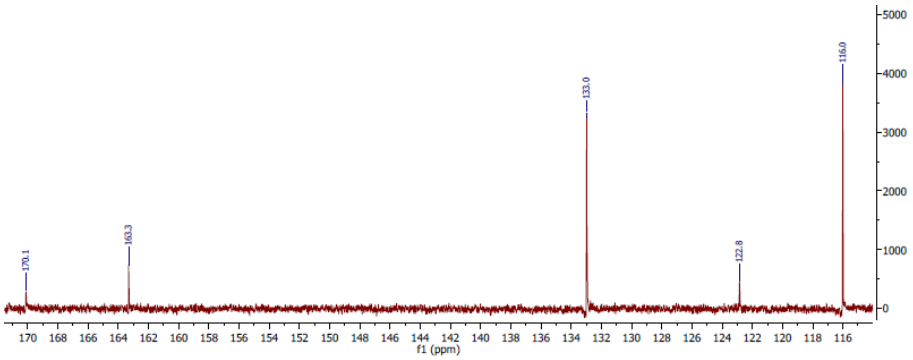

Appendix 27c: H H-Cosy for Compound 236

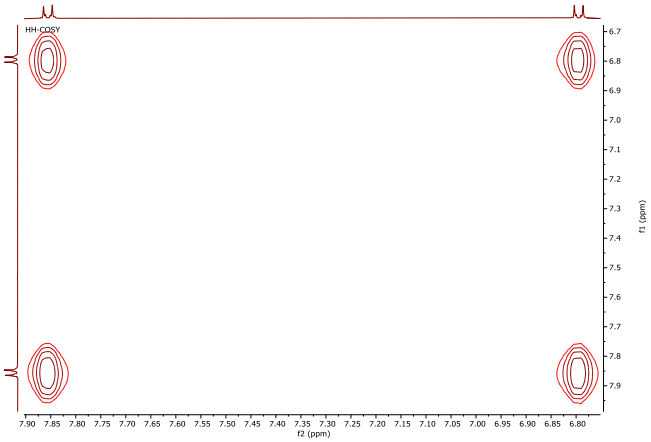

Appendix 27d: HSQC for Compound 236

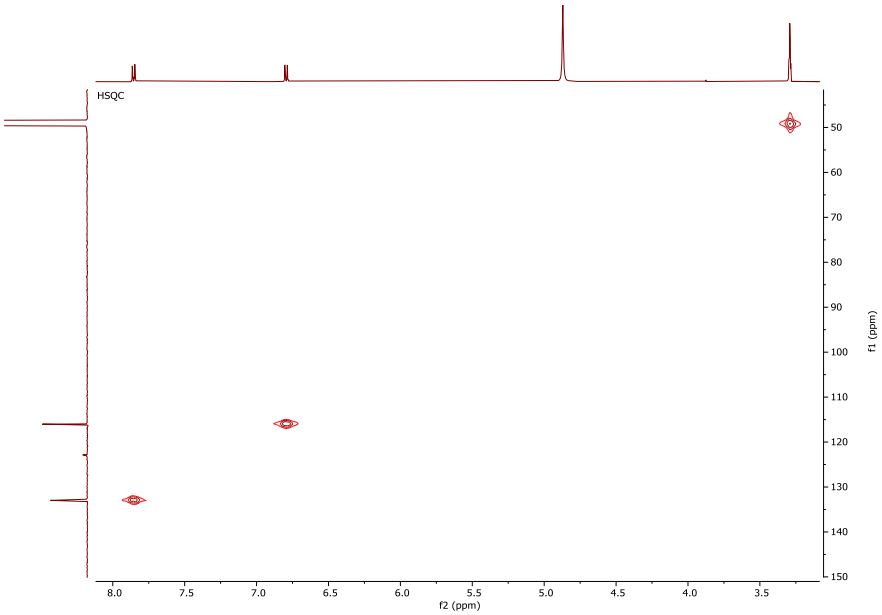

Appendix 27e: HMBC for Compound 236

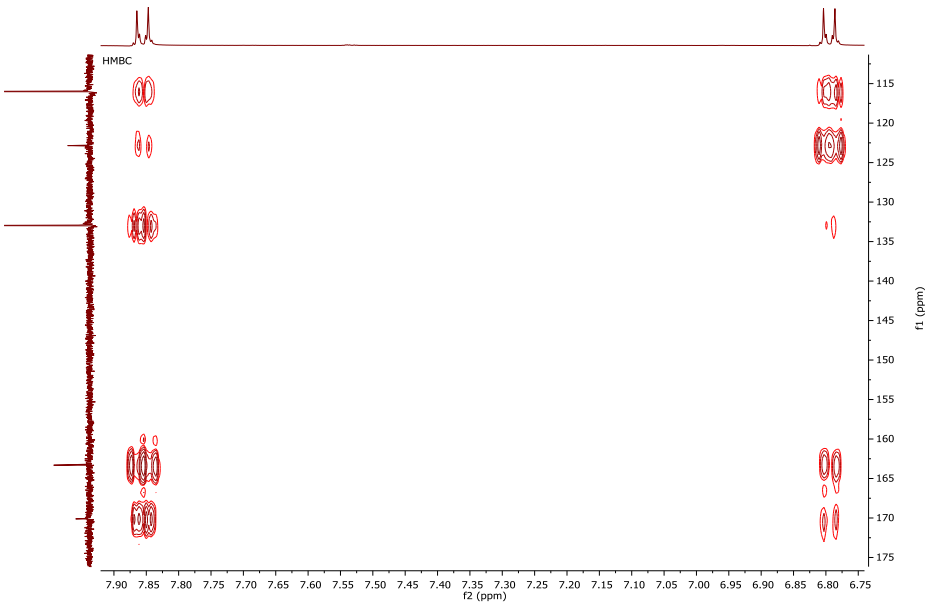

Appendix 28: NMR Spectra for Maackiain (237)

Appendix 28a: ^{1}H NMR for Compound 237

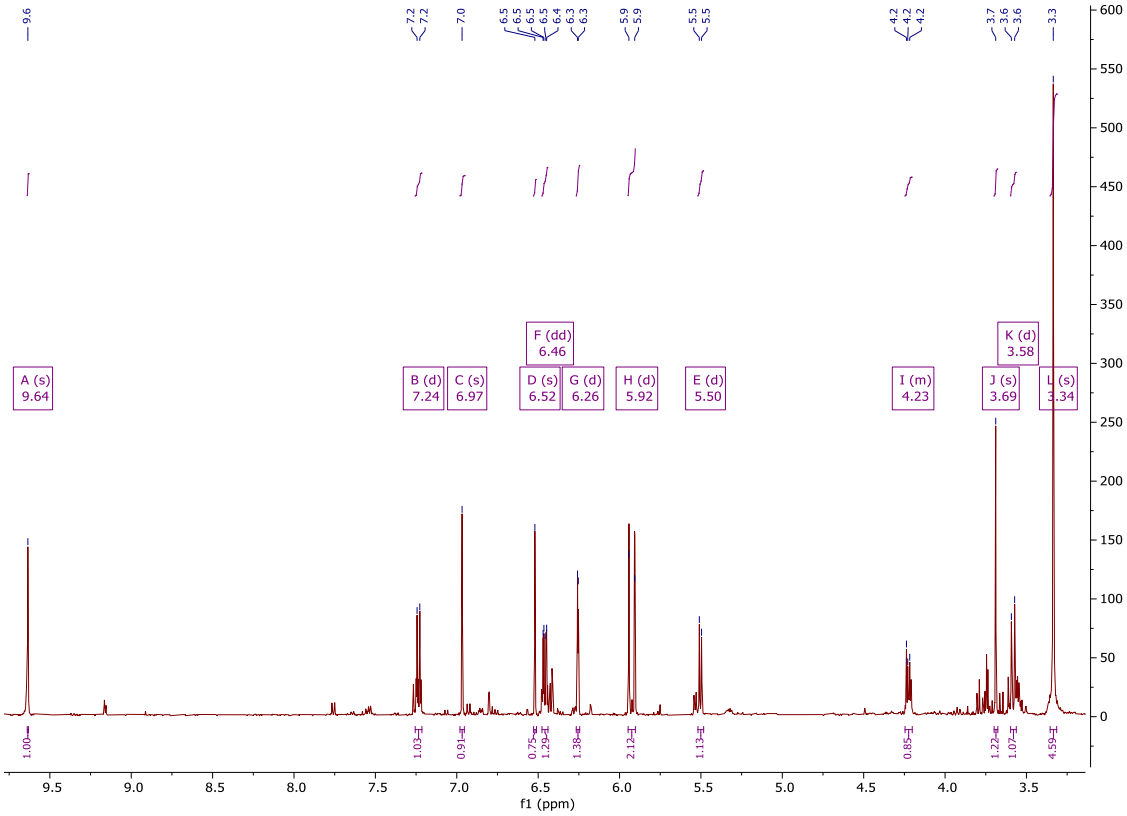

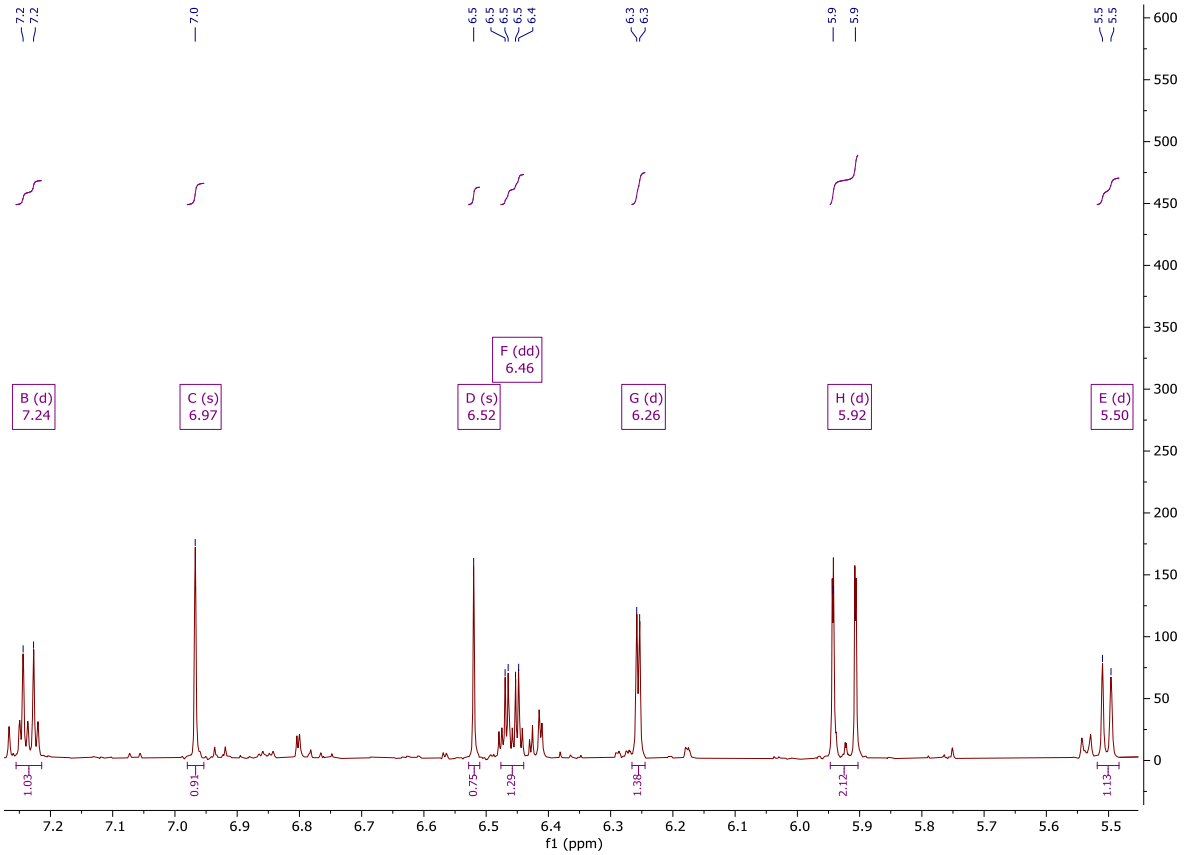

Appendix 28b: ^{13}C NMR for Compound 237

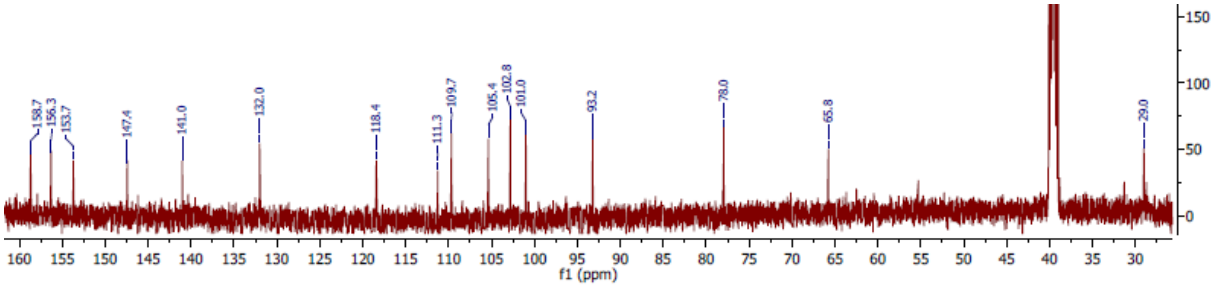

Appendix 28c: H H-Cosy for Compound 237

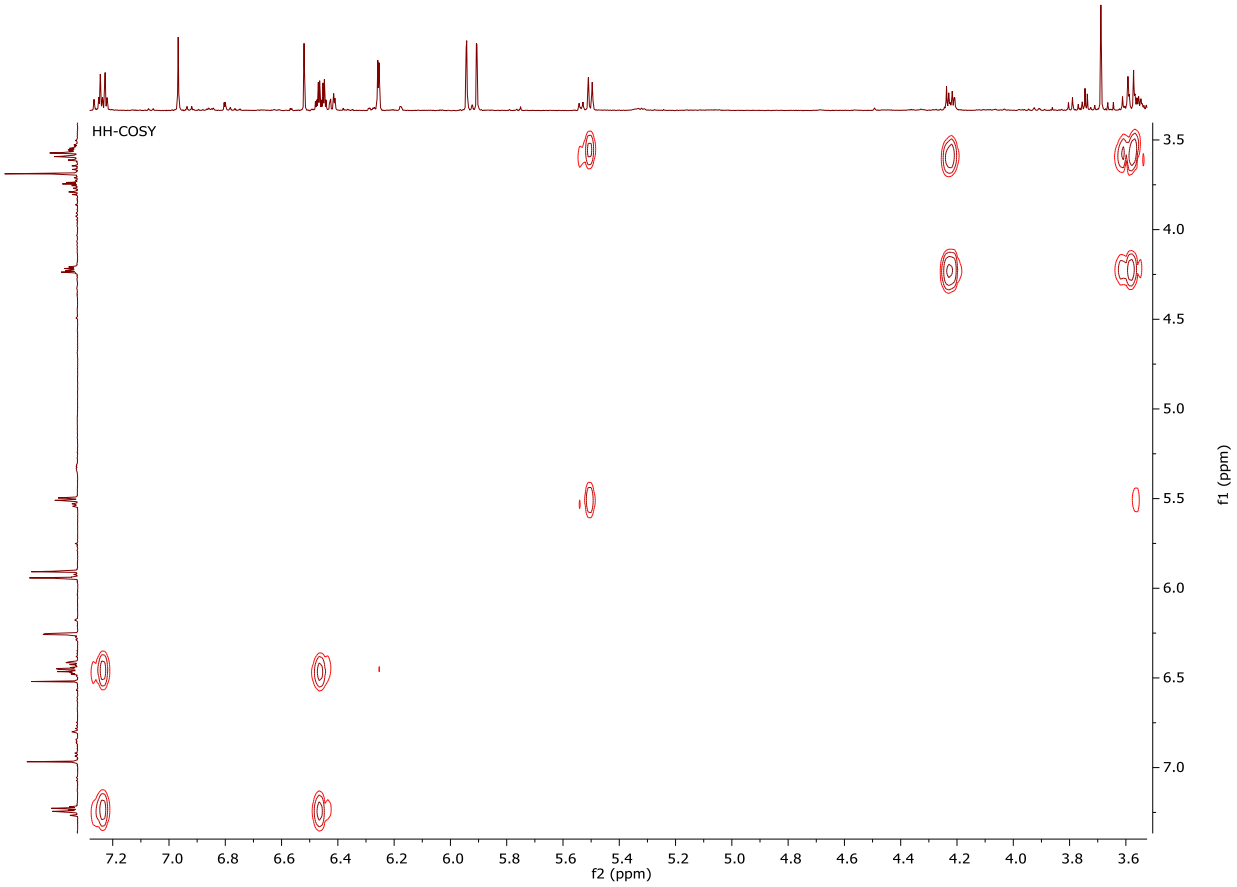

Appendix 28d: HSQC for Compound 237

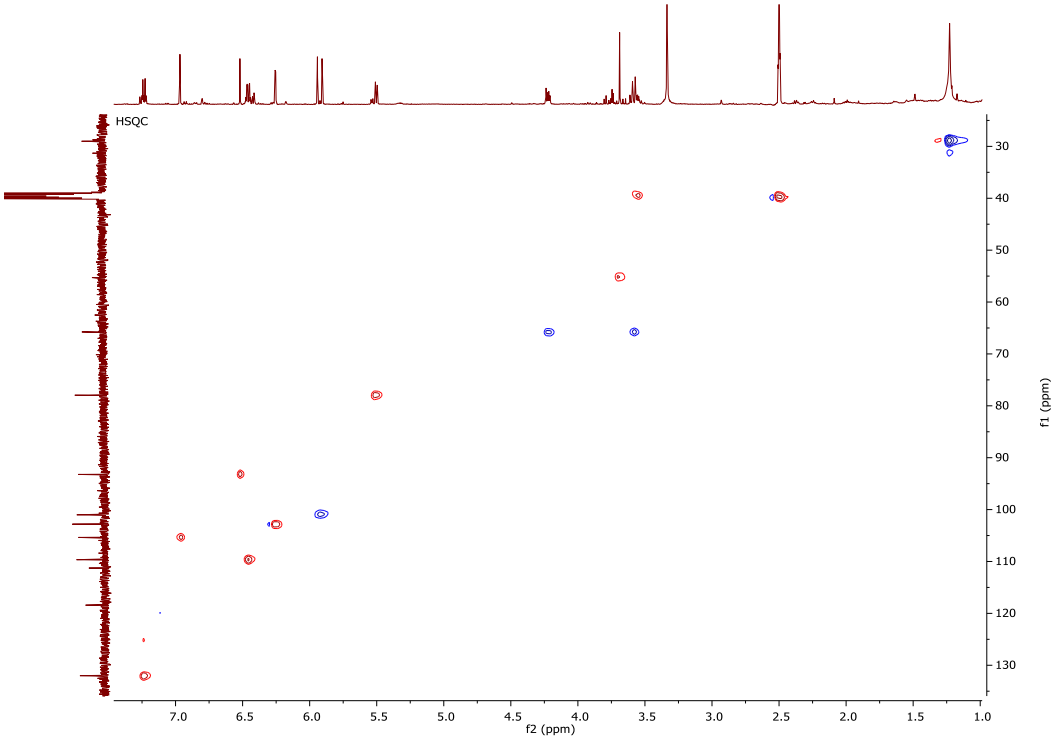

Appendix 28e: HMBC for Compound 237

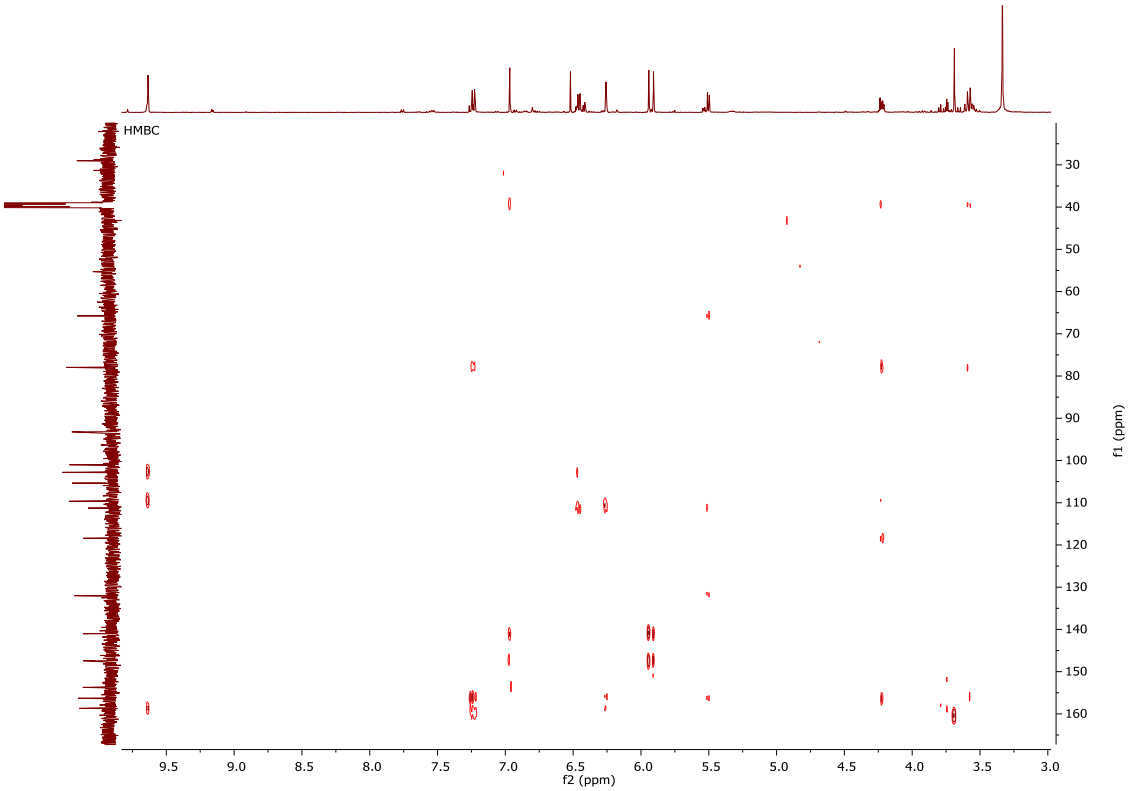

Appendix 29: NMR Spectra for Luteolin (238)

Appendix 29a: ^{1}H NMR for Compound 238

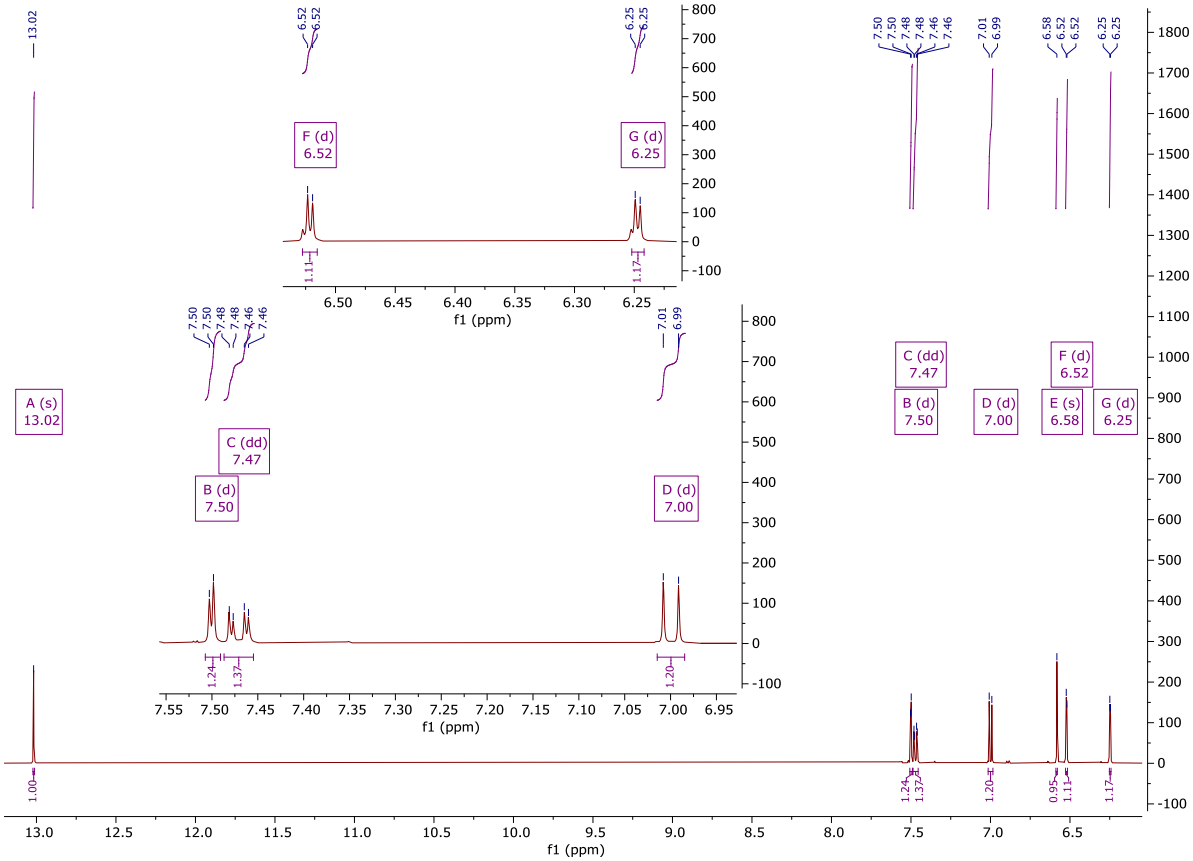

Appendix 29b: ^{13}C NMR for Compound 238

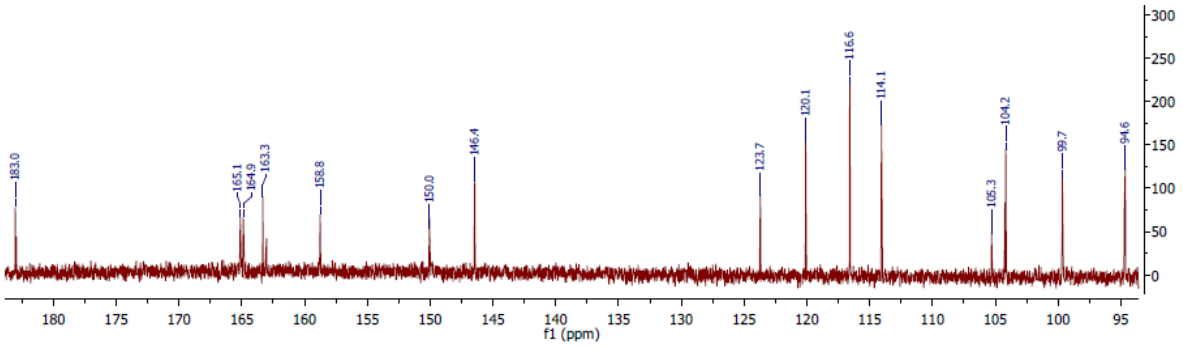

Appendix 29c: H H-Cosy for Compound 238

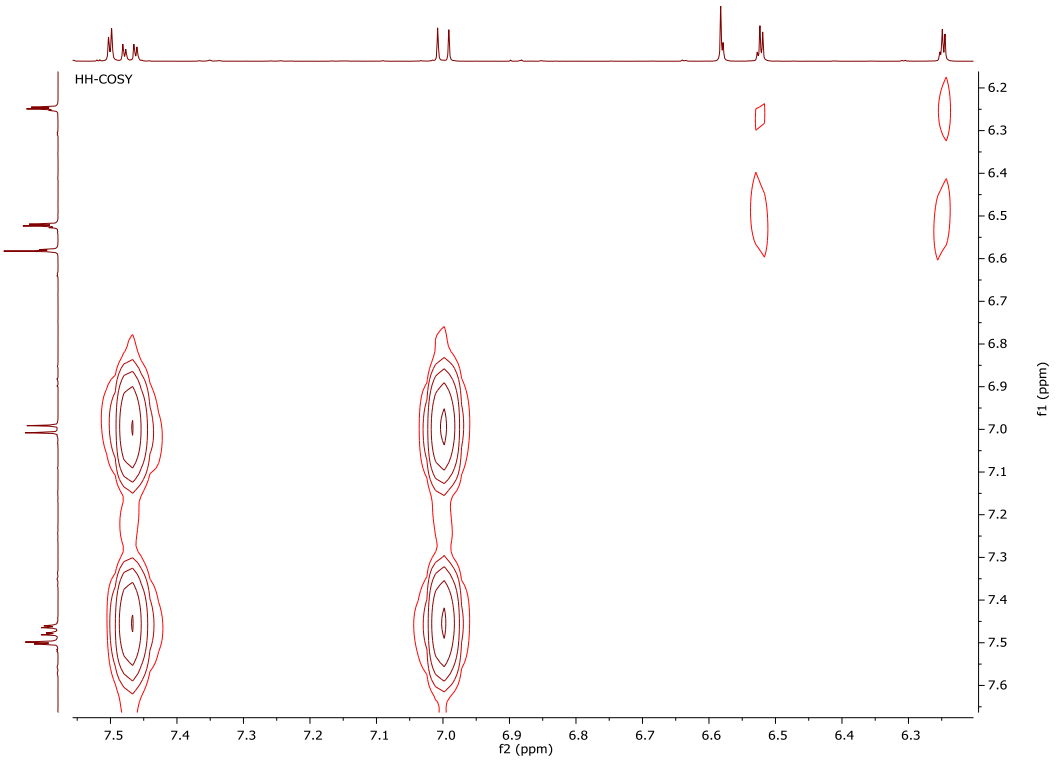

Appendix 29d: HSQC for Compound 238

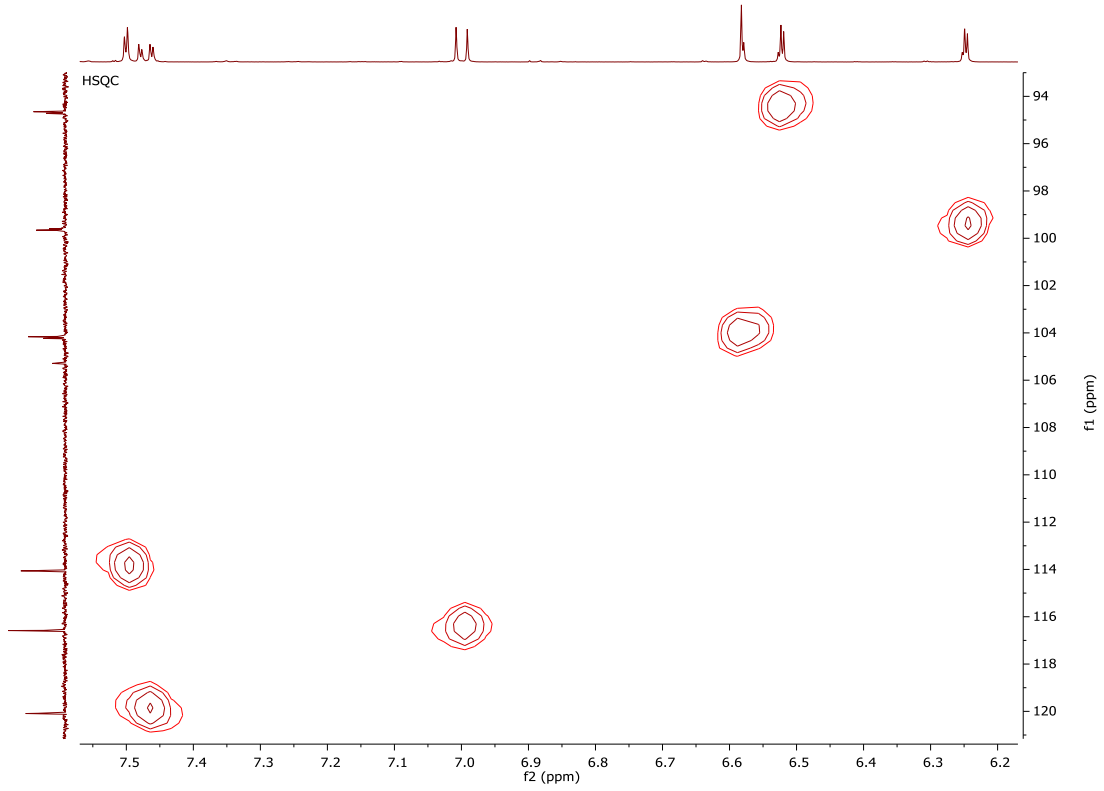

Appendix 29e: HMBC for Compound 238

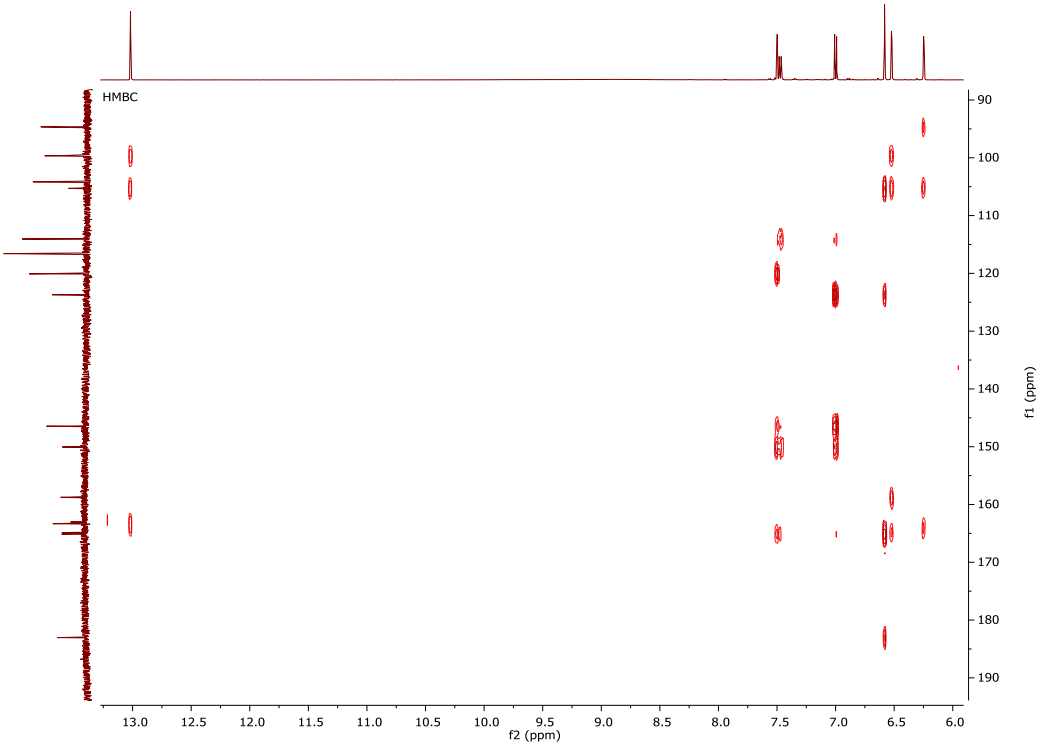

Appendix 30: NMR Spectra for Geneitein (239)

Appendix 30a: ^{1}H NMR for Compound 239

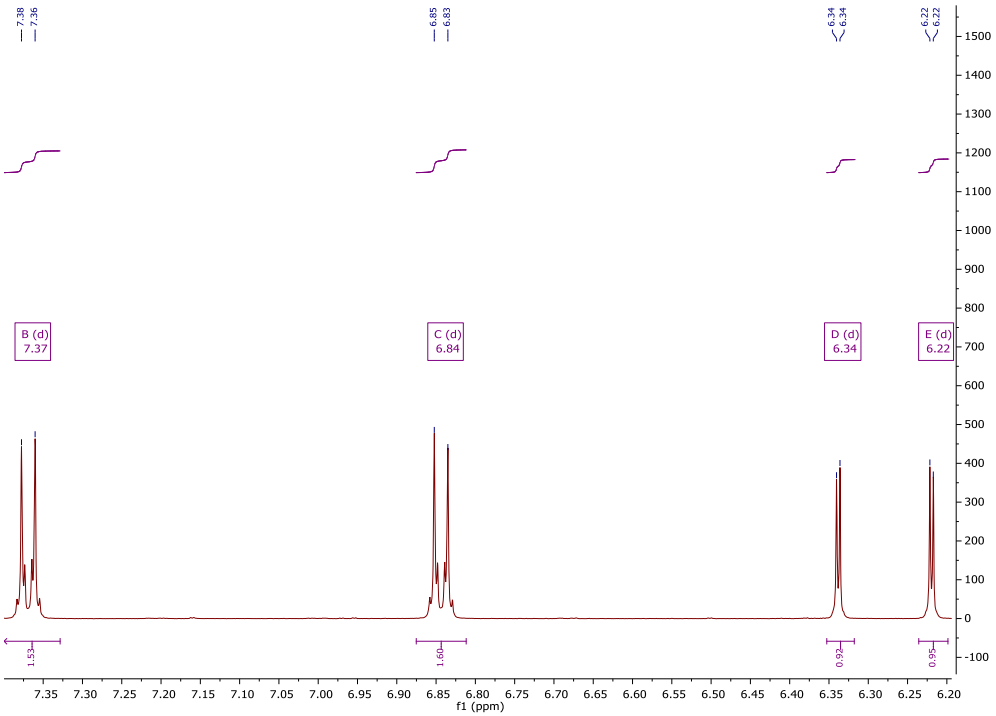

Appendix 30b: ^{13}C NMR for Compound 239

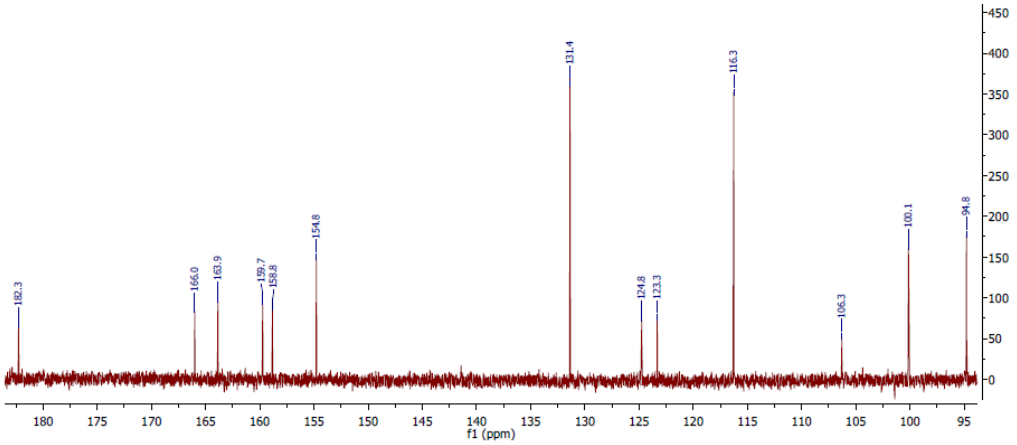

Appendix 30c: H H-Cosy for Compound 239

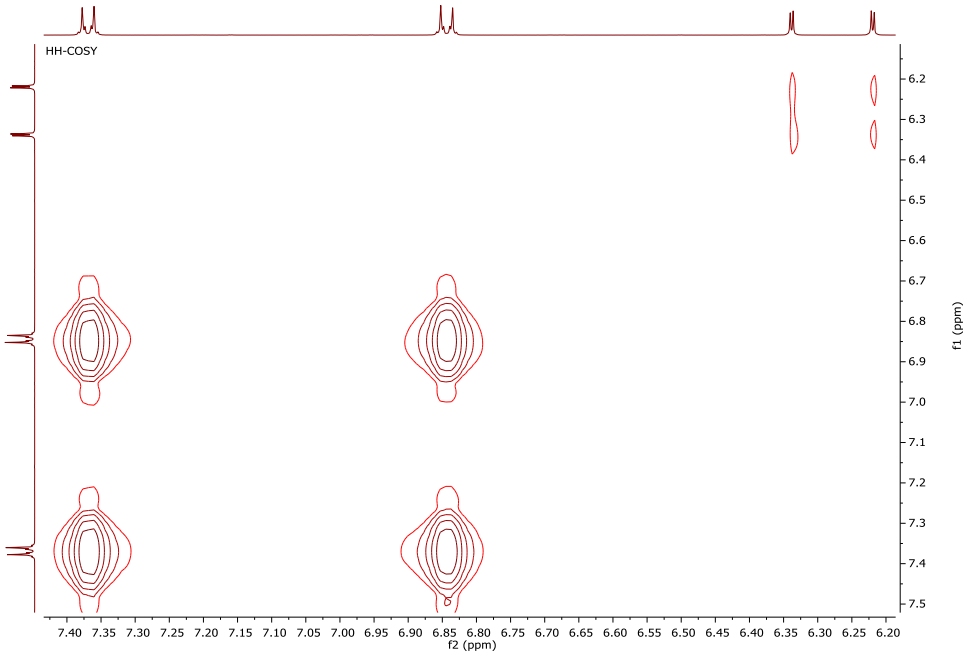

Appendix 30d: HSQC for Compound 239

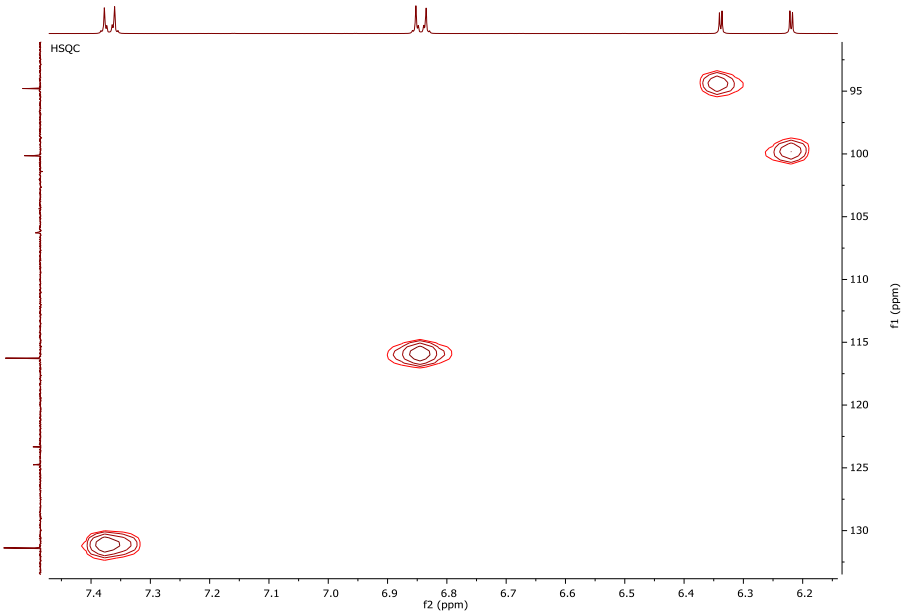

Appendix 30e: HMBC for Compound 239

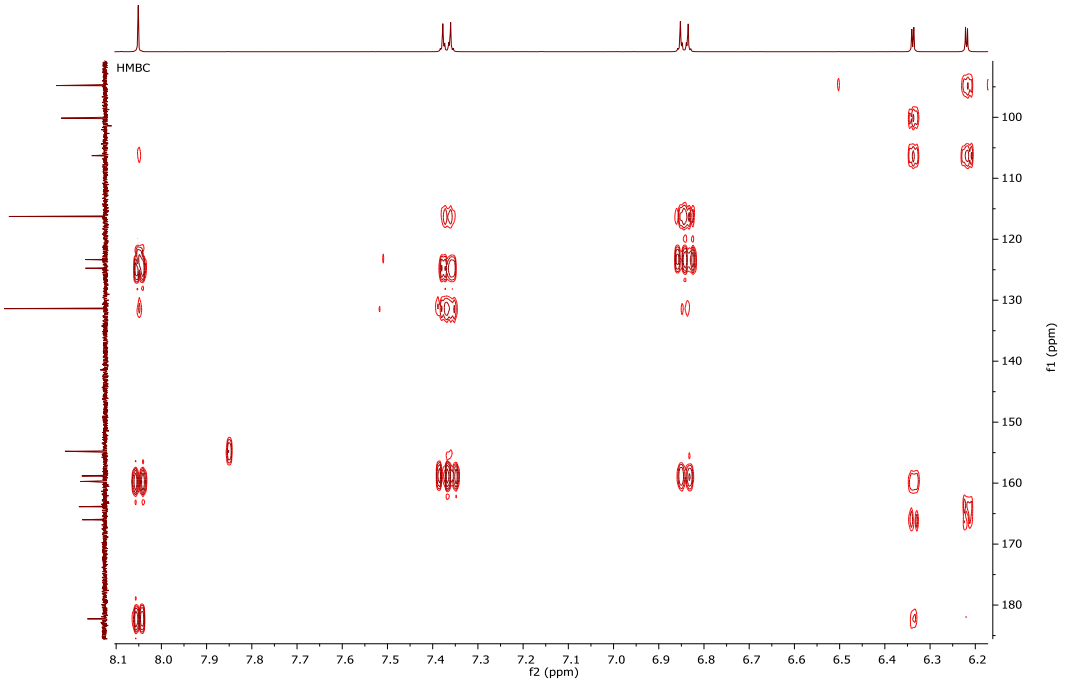

Appendix 31: NMR Spectra for Isoliquiritidenin (240)

Appendix 31a: ^{1}H NMR for Compound 240

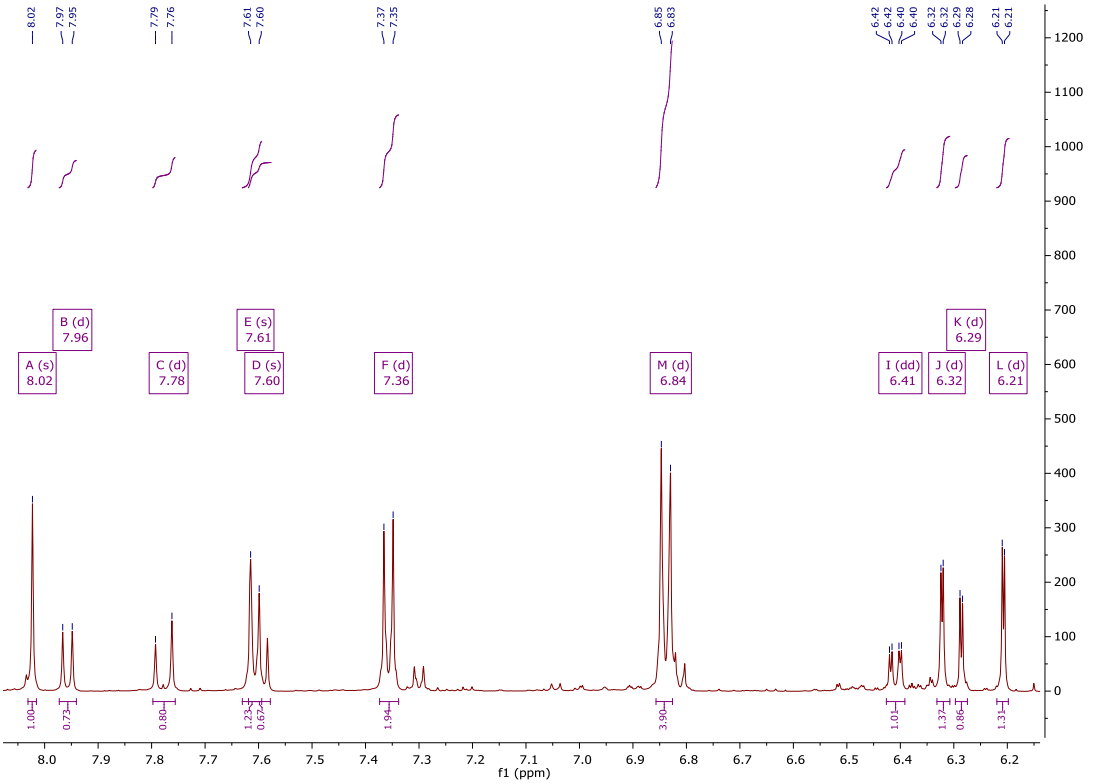

Appendix 31b: ^{13}C NMR for Compound 240

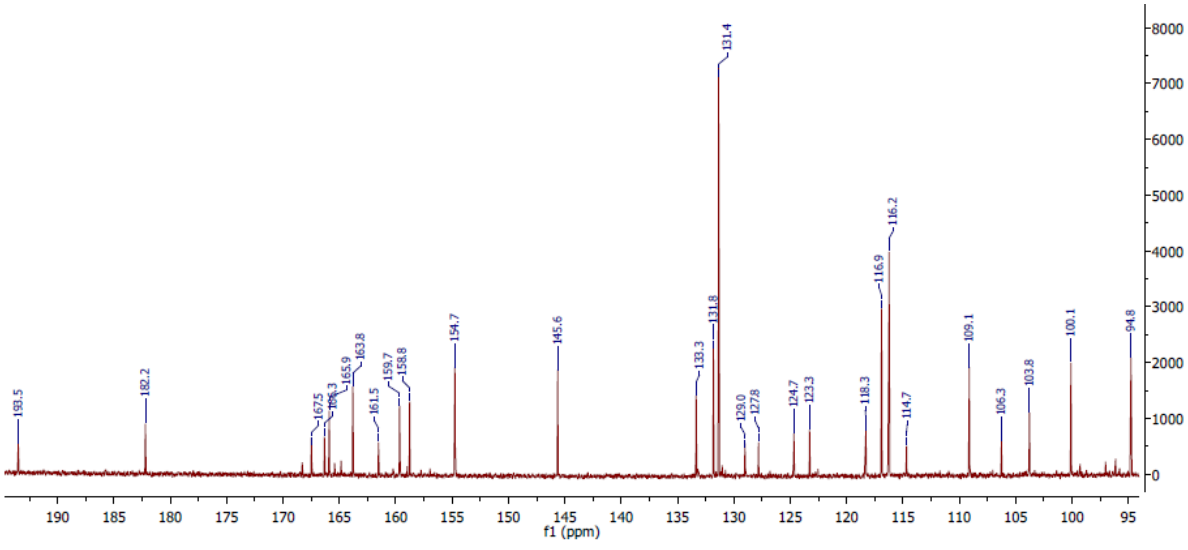

Appendix 31c: H H-Cosy for Compound 240

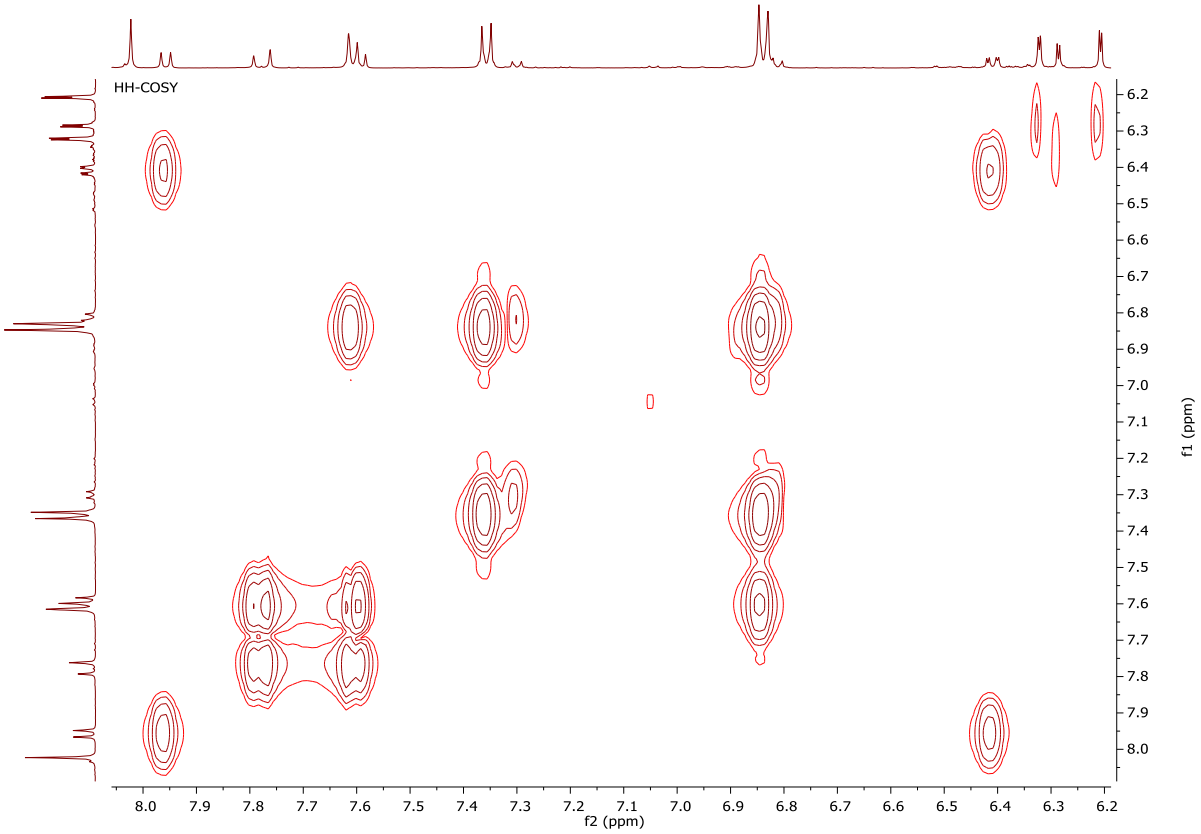

Appendix 31c: HSQC for Compound 240

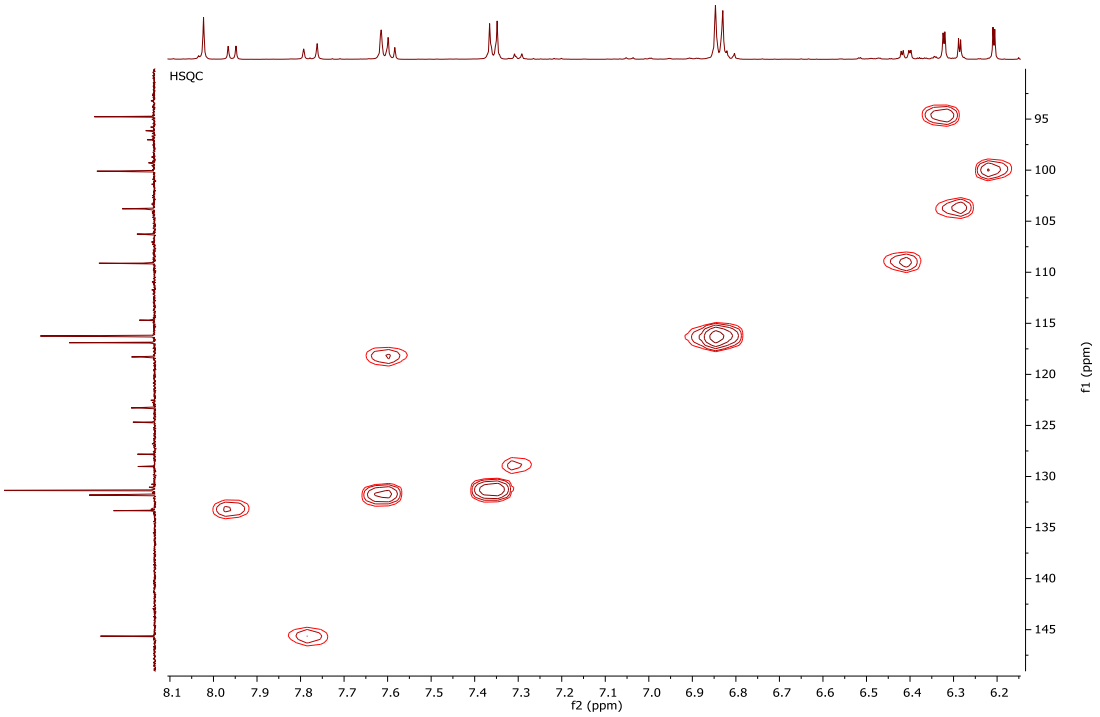

Appendix 31e: HMBC for Compound 240

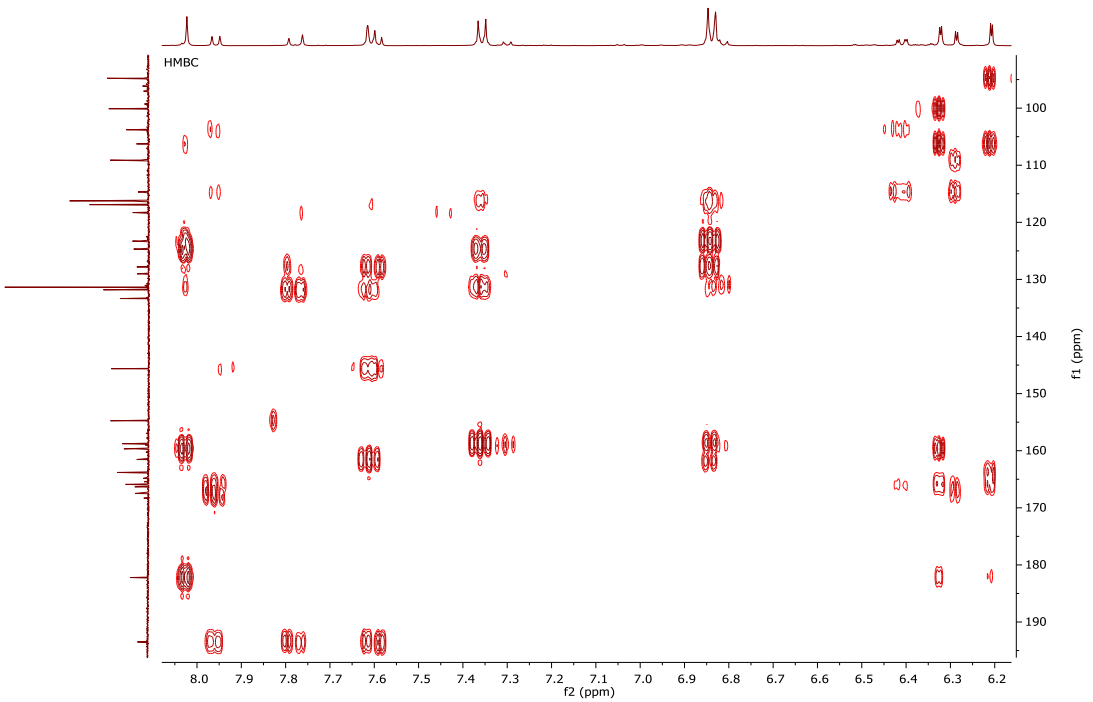

Appendix 32: NMR Spectra for Lascoumestan (241)

Appendix 32a: ^{1}H NMR for Compound 241

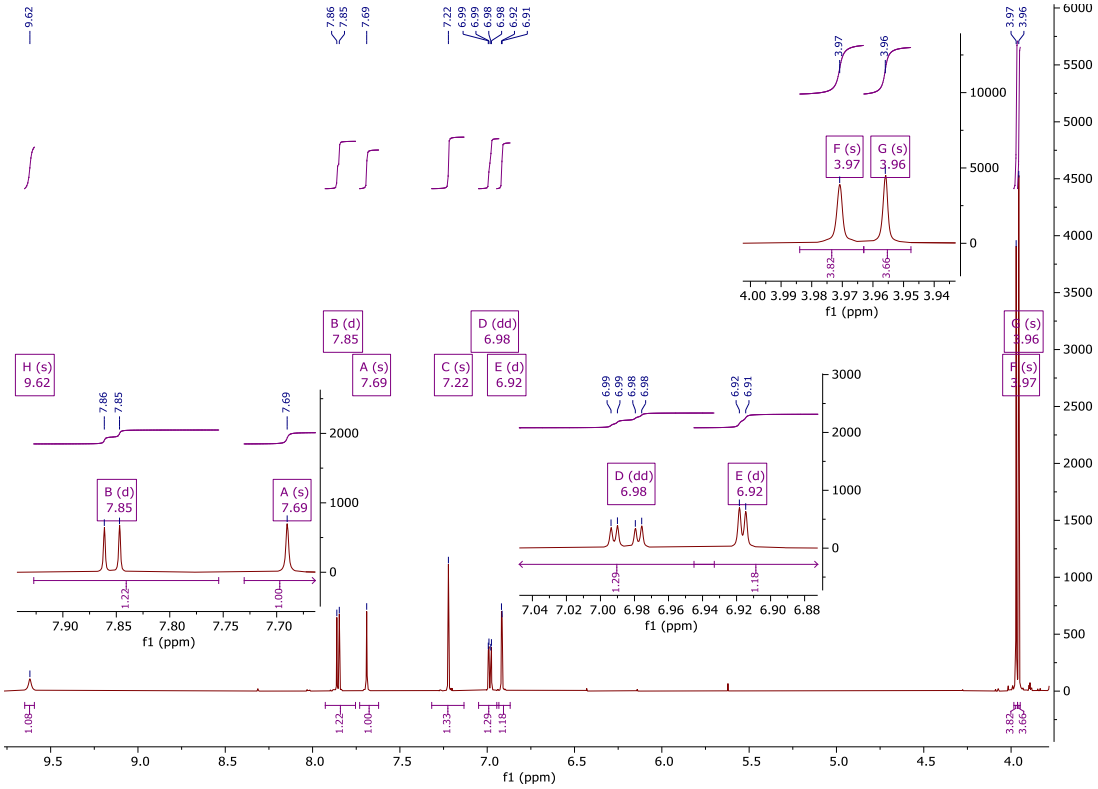

Appendix 32a: ^{1}H NMR for Compound 241 (expansion)

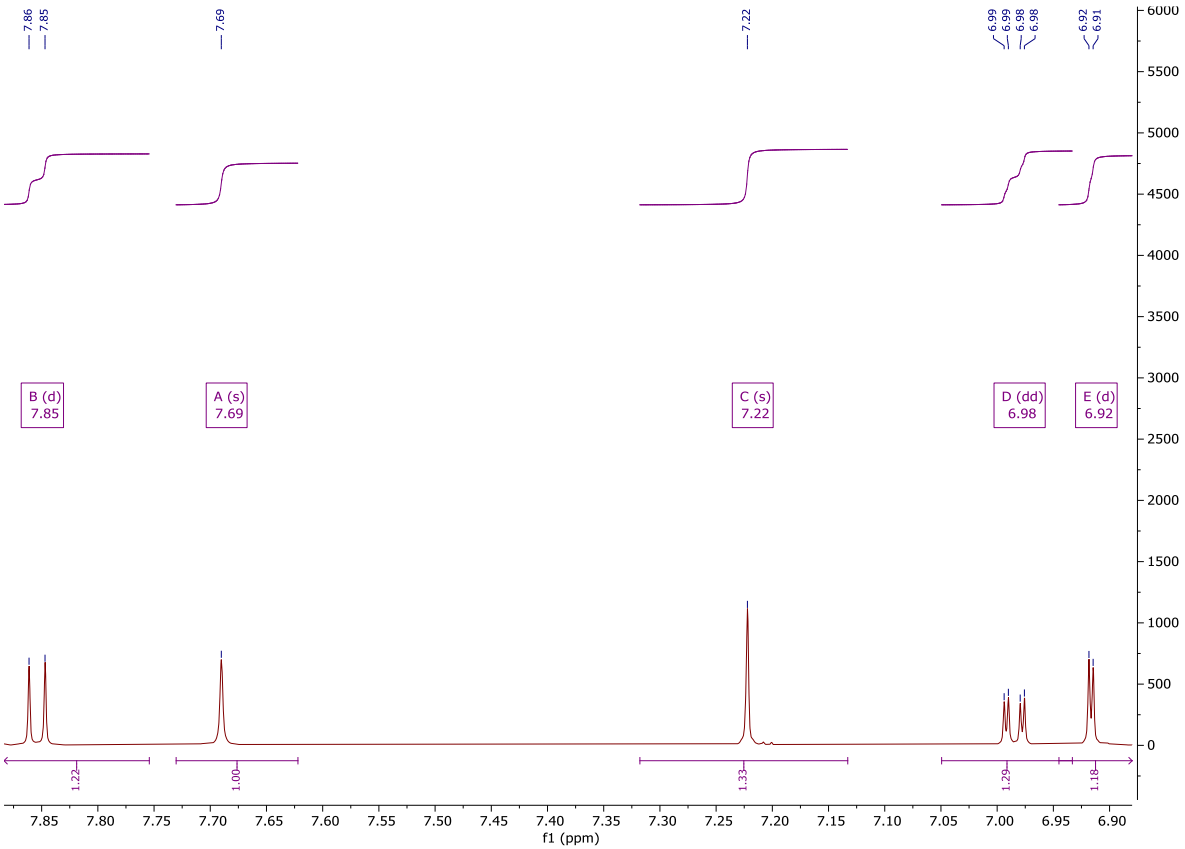

Appendix 32b: ^{13}C NMR for Compound 241

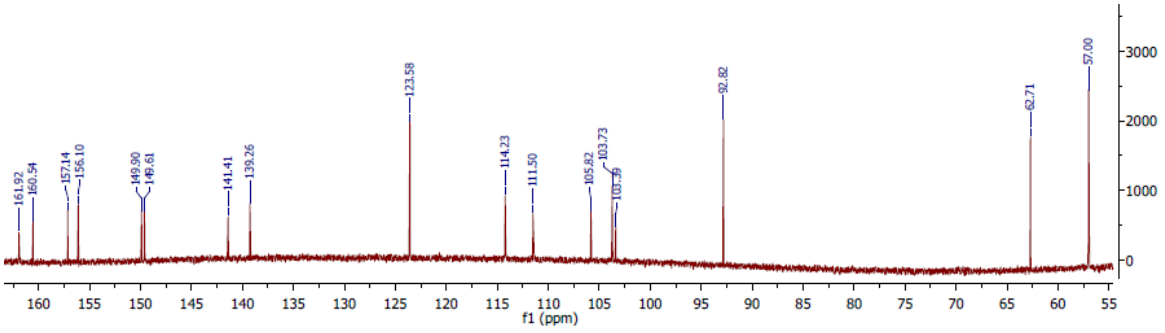

Appendix 32c: H H-Cosy for Compound 241

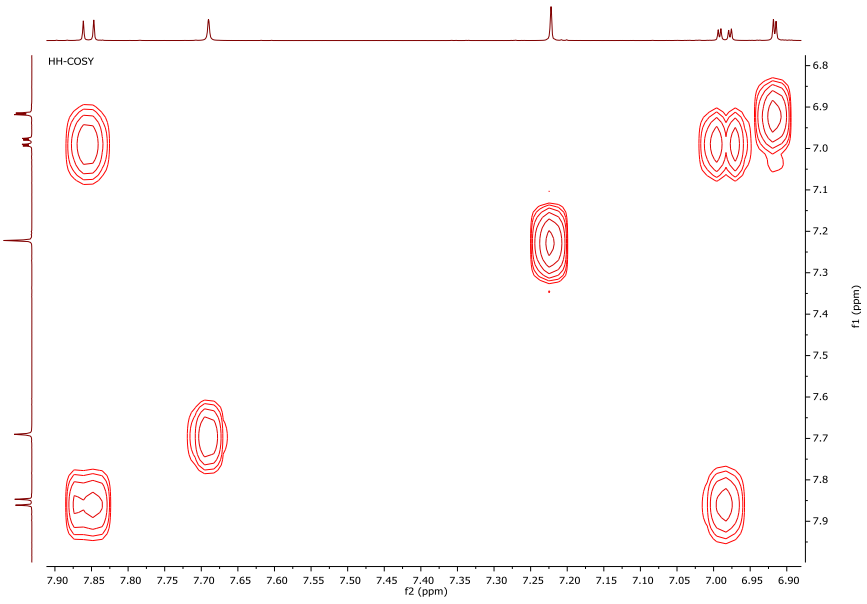

Appendix 32d: HSQC for Compound 241

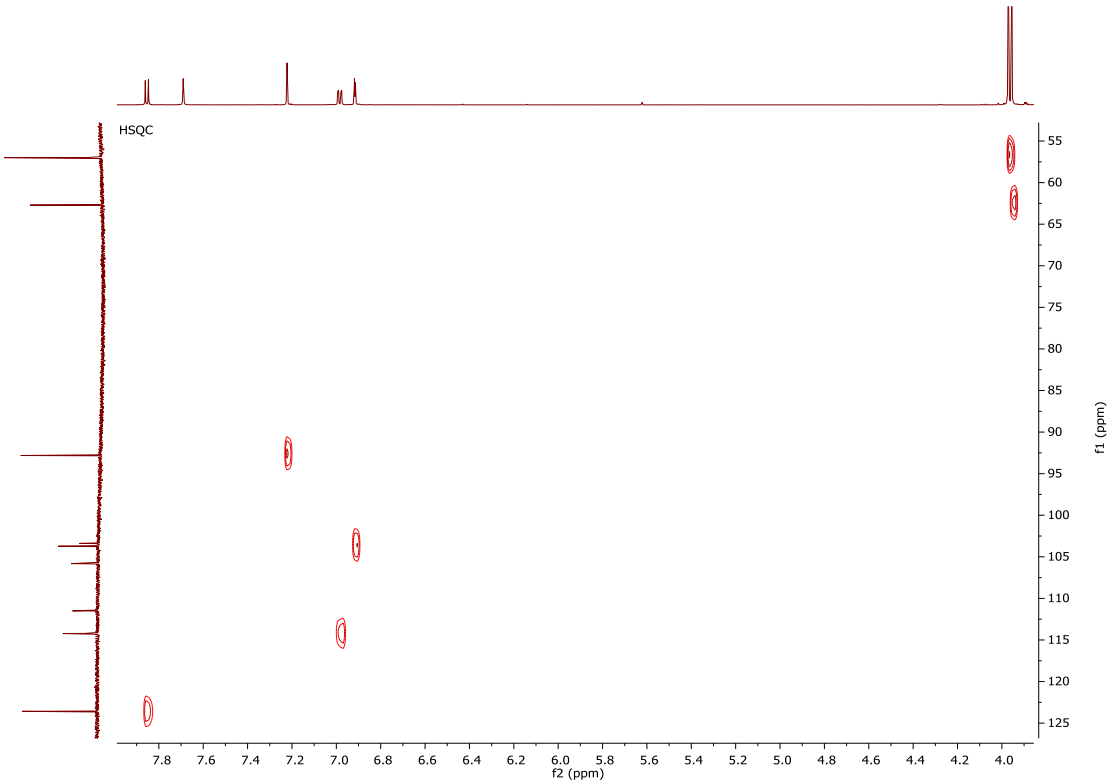

Appendix 32e: HMBC for Compound 241

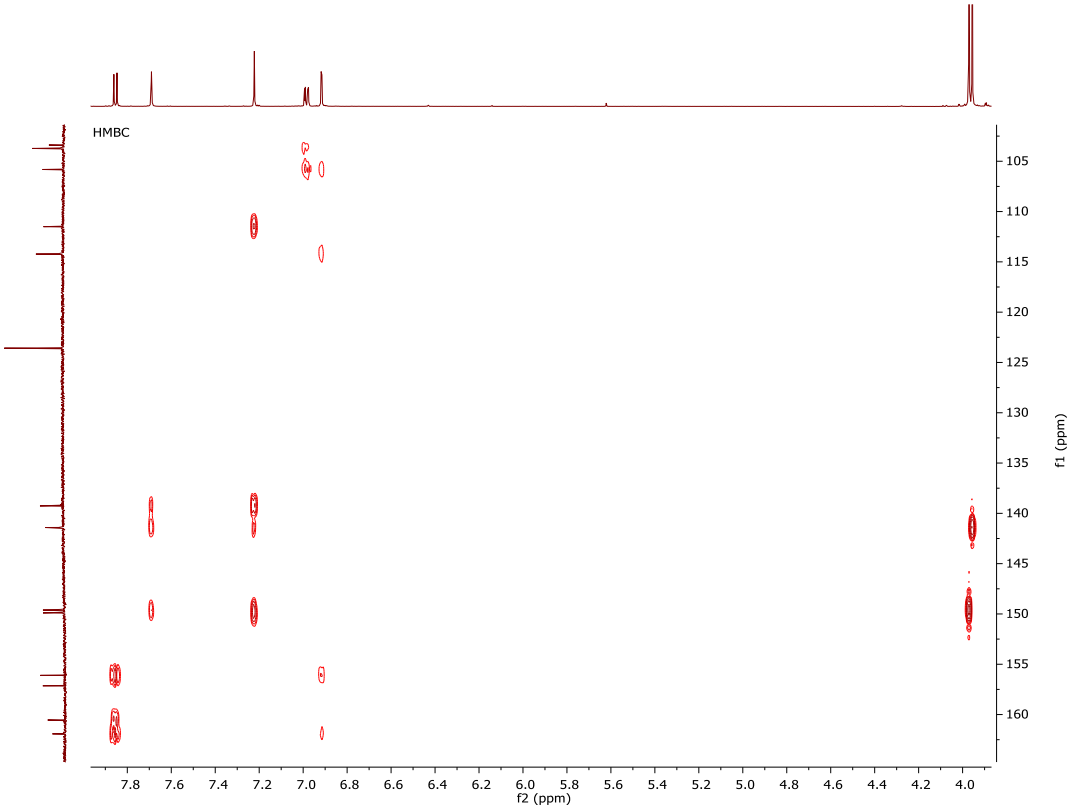

Appendix 32e: HMBC for Compound 241 (expansion)

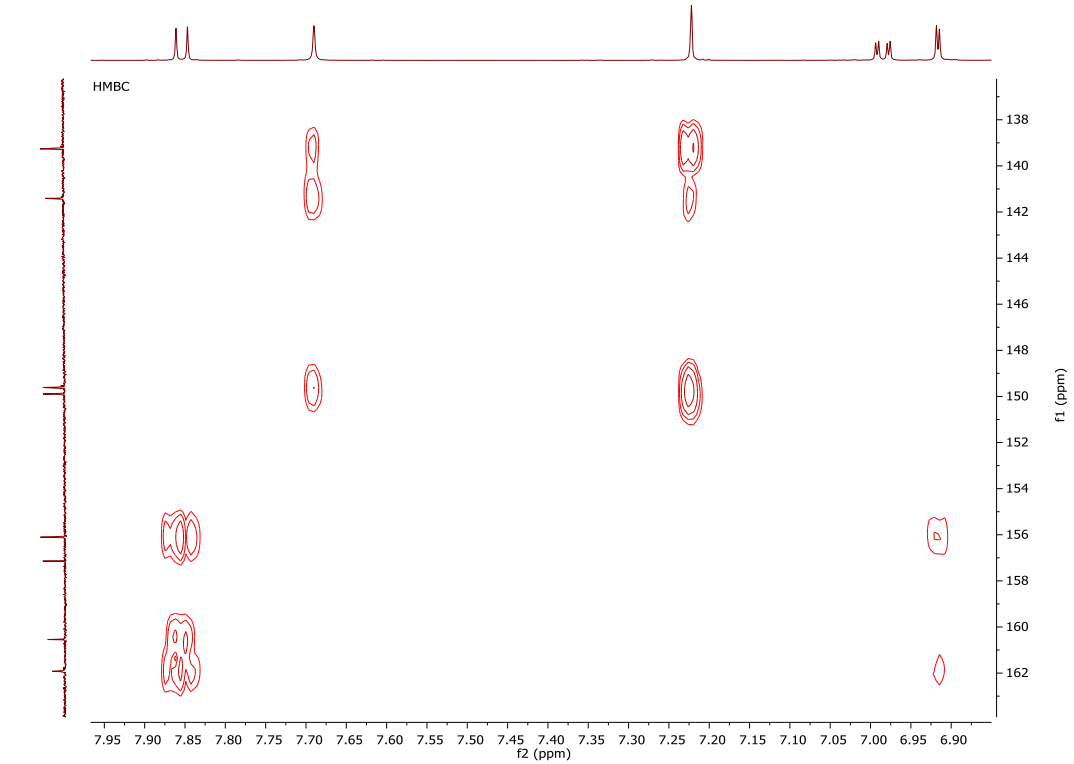

Appendix 32f: UV Spectra for Compound 241

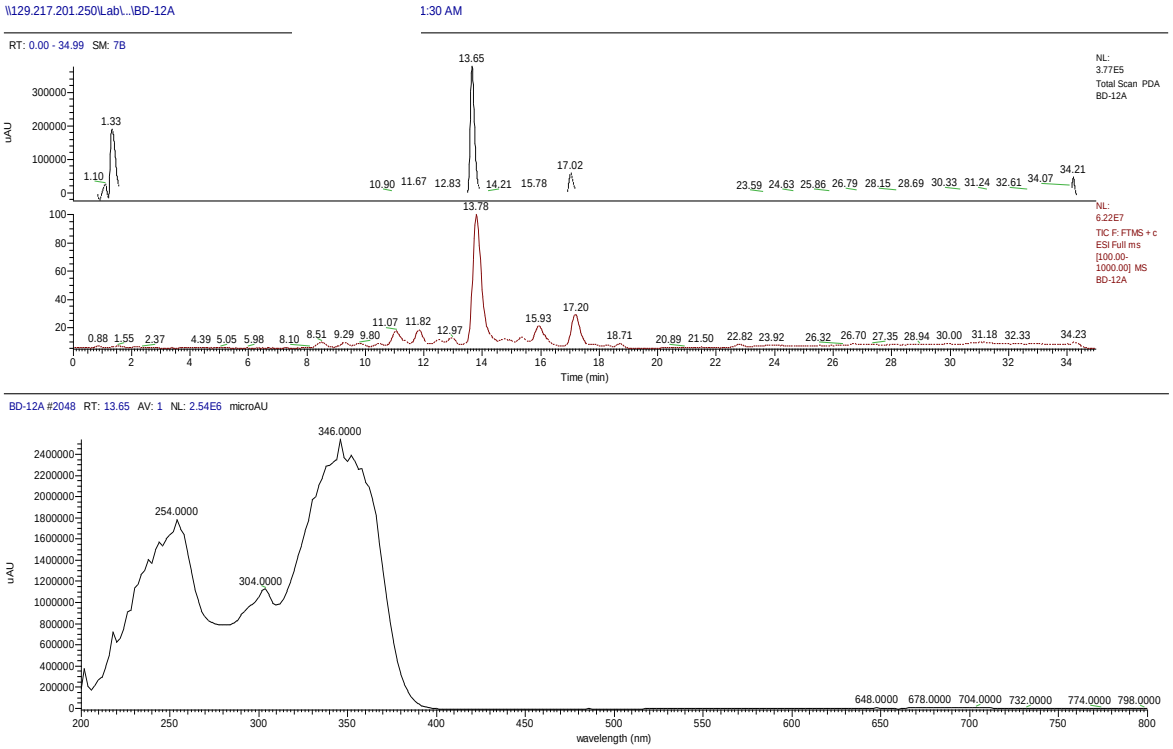

Appendix 32g: IR Spectra for Compound 241

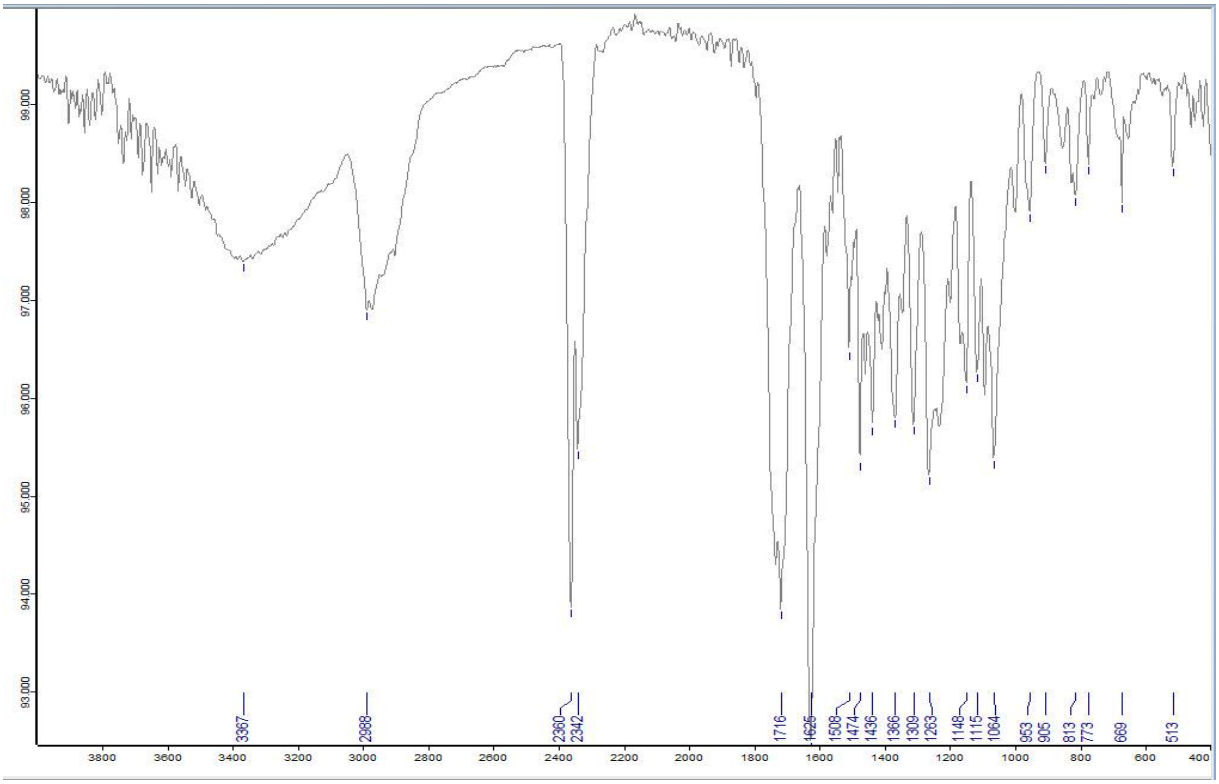

Appendix 32h: Mass Spectra for Compound 241

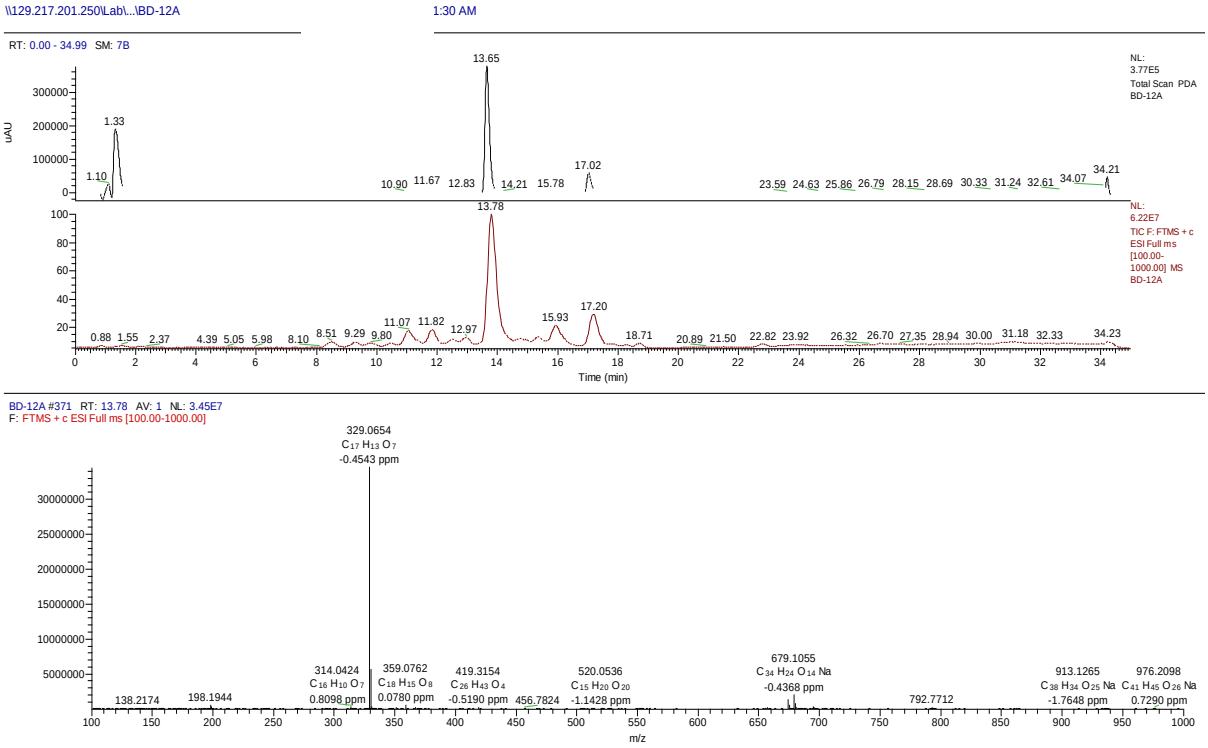

Appendix 33: NMR Spectra of Lascoumaronochromone (242)

Appendix 33a: ^{1}H NMR for Compound 242

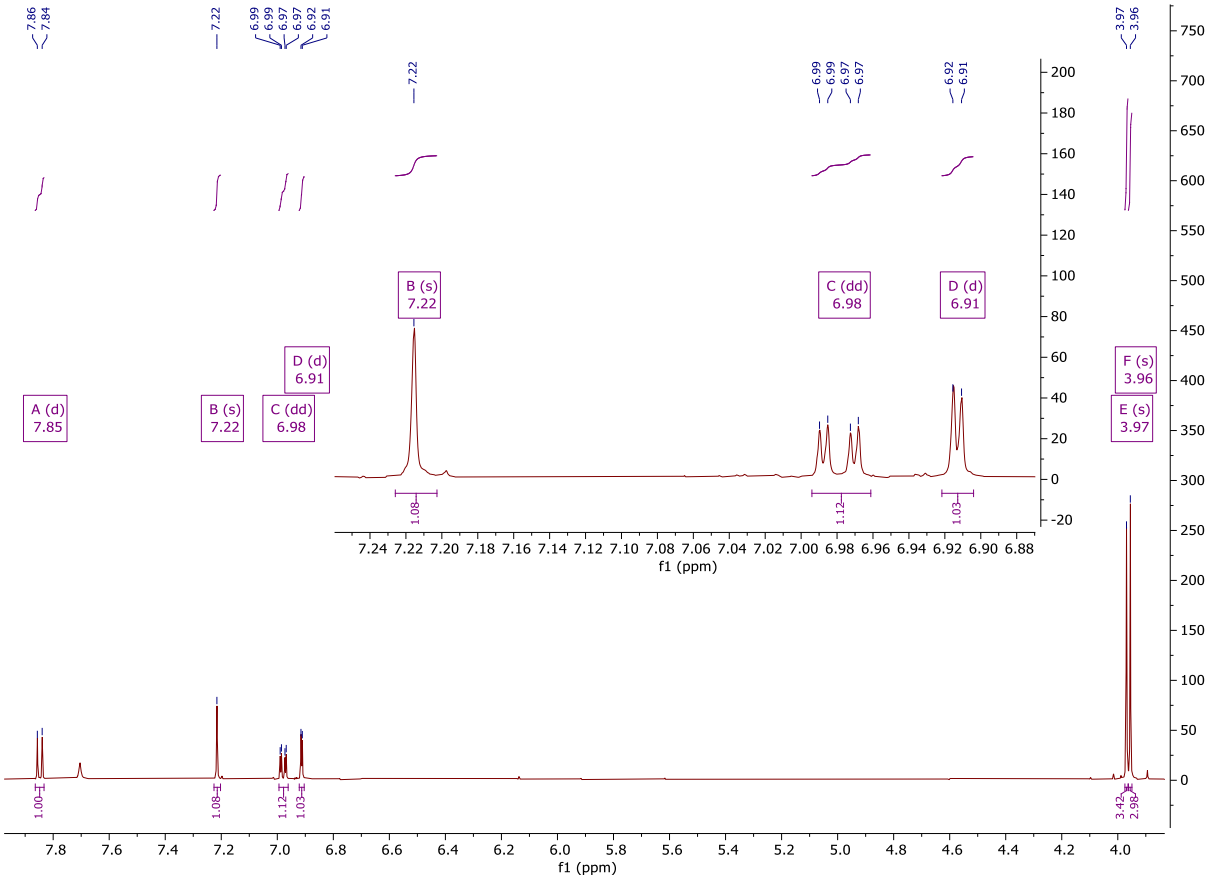

Appendix 33b: ^{13}C NMR for Compound 242

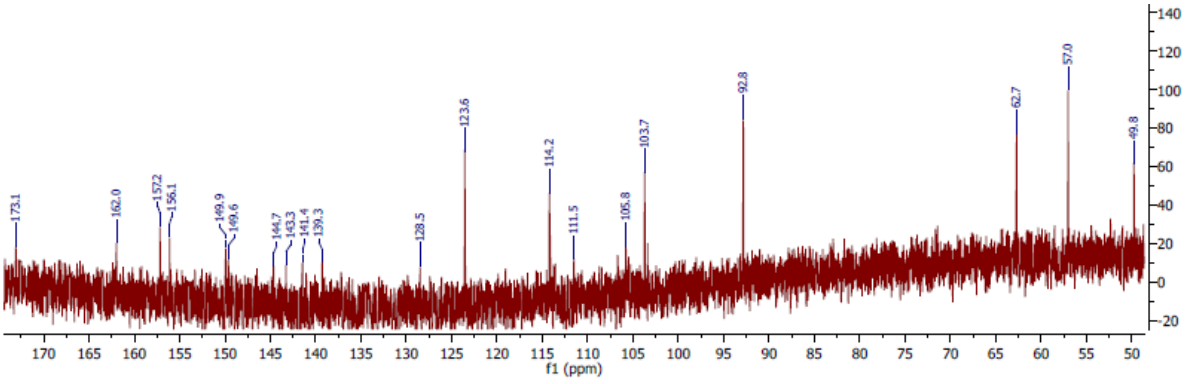

Appendix 33c: H H-Cosy for Compound 242

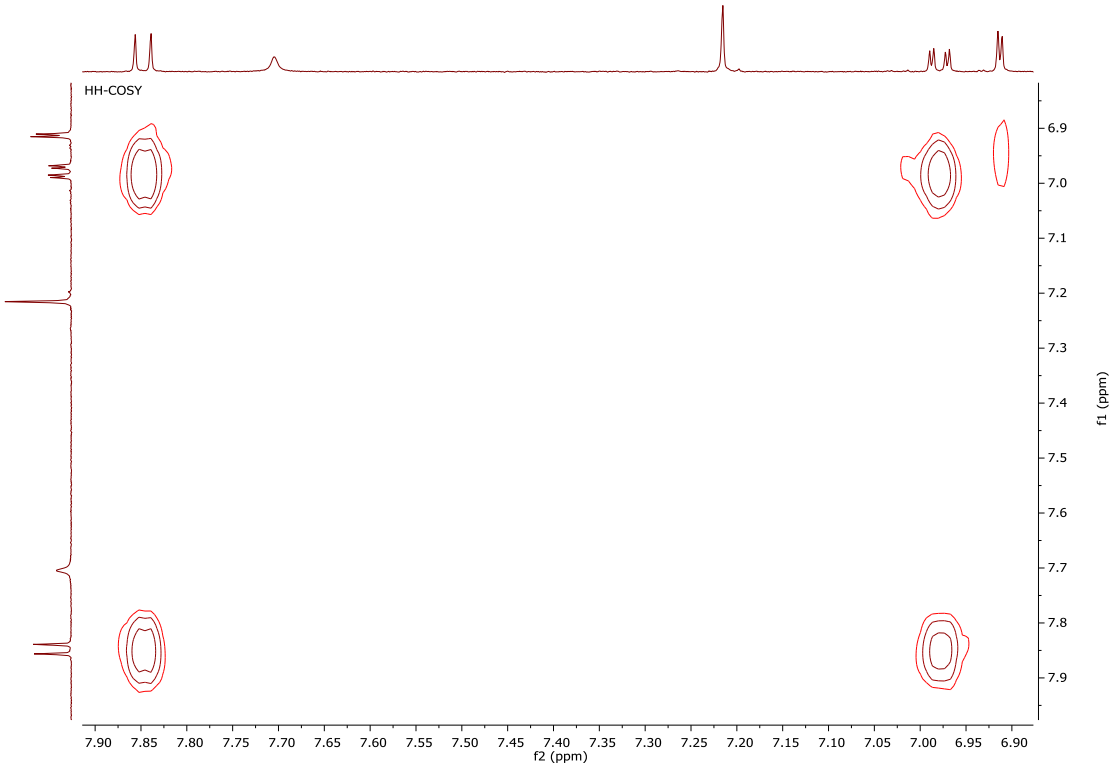

Appendix 33d: HSQC for Compound 242

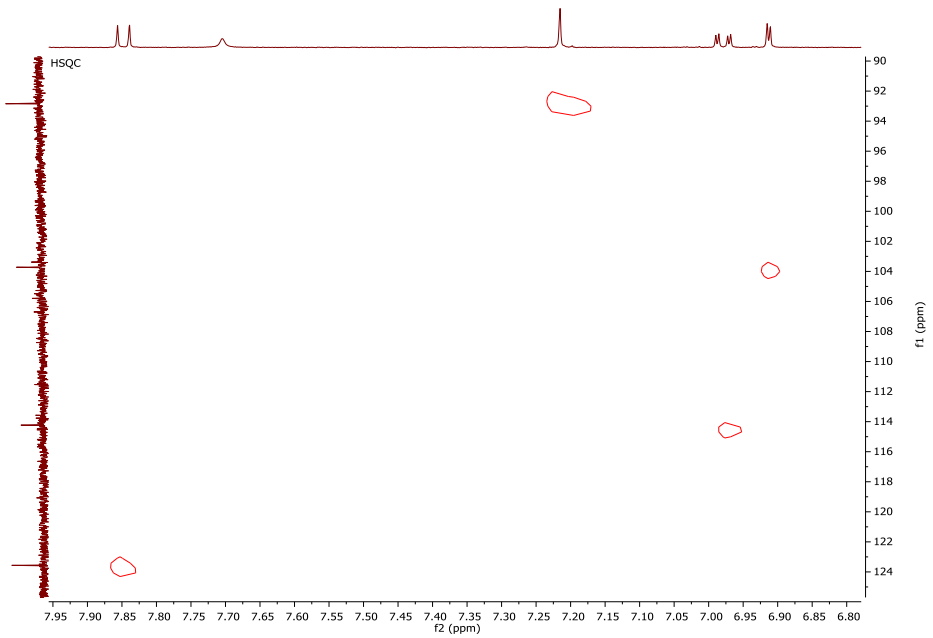

Appendix 33e: HMBC for Compound 242

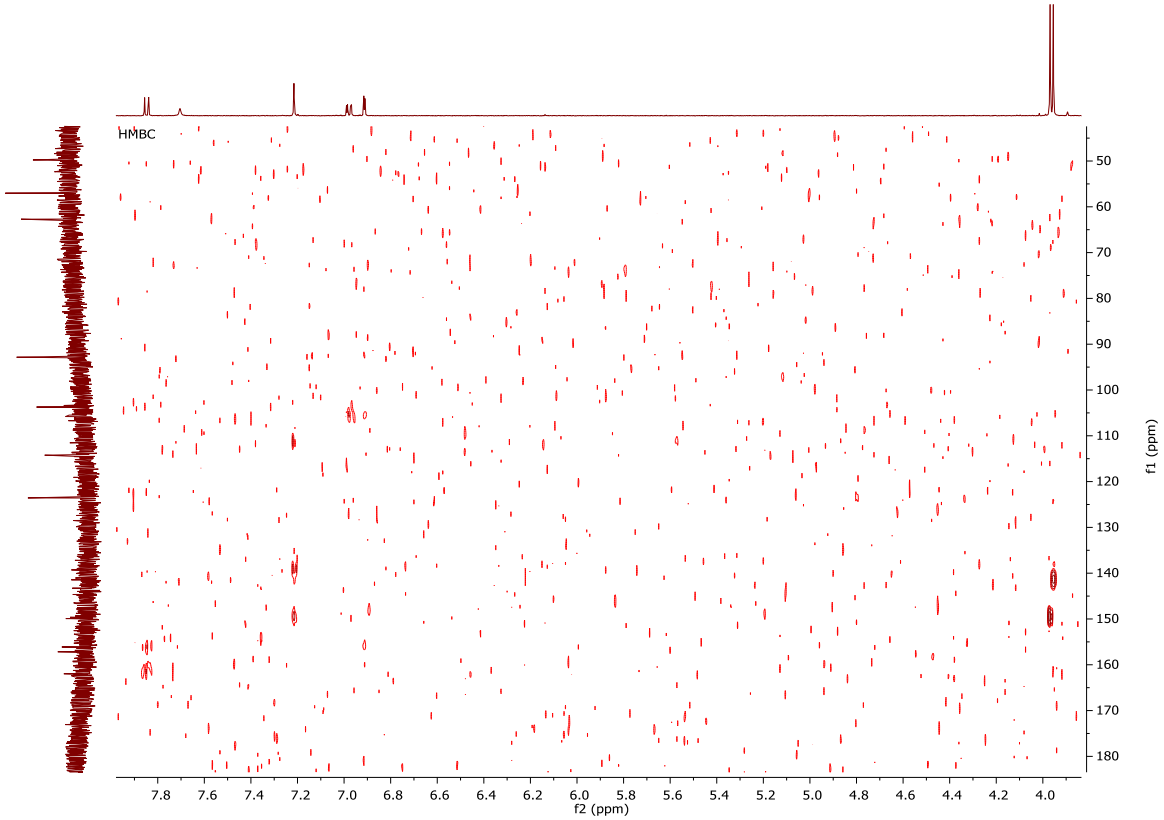

Appendix 33e: HMBC for Compound 242 (expansion)

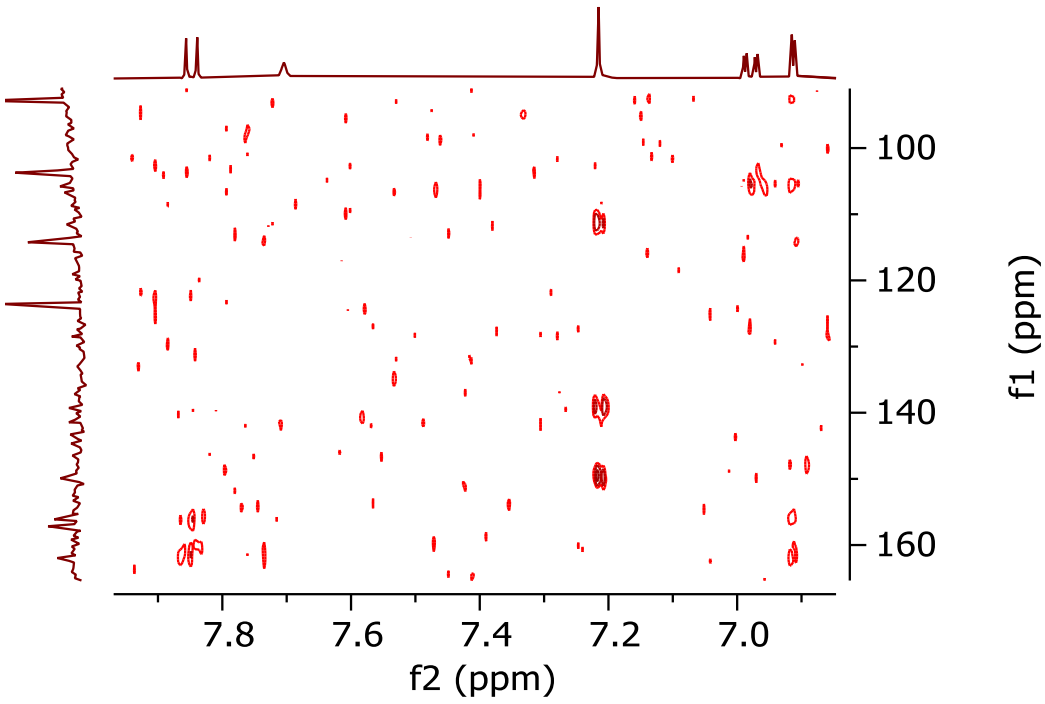

Appendix 33f: Mass Spectra for Compound 242

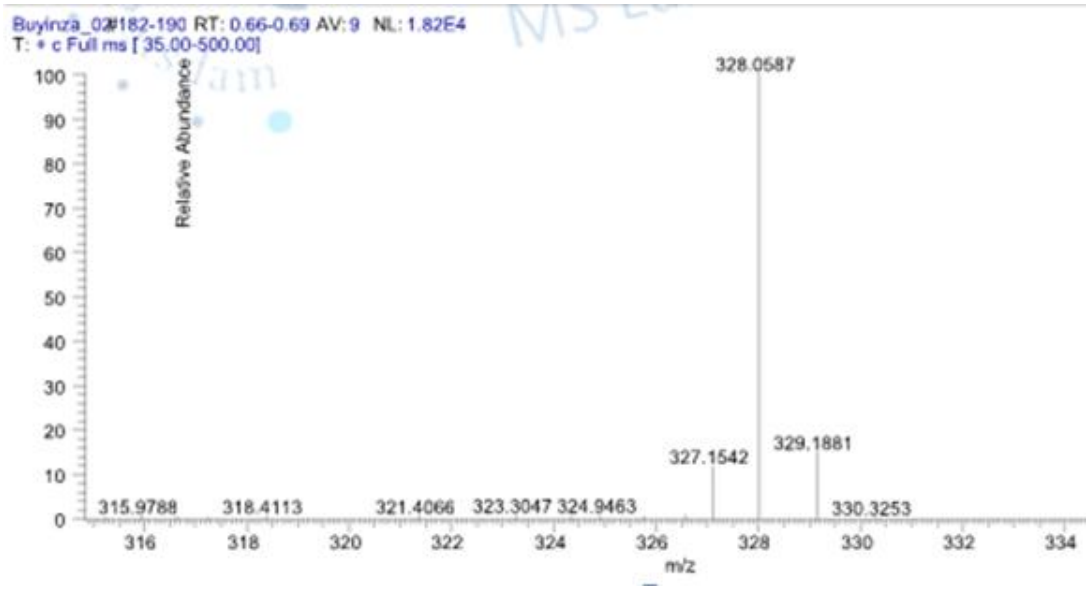

Appendix 34: NMR Spectra for Genistin (243)

Appendix 34a: ^{1}H NMR for Compound 243

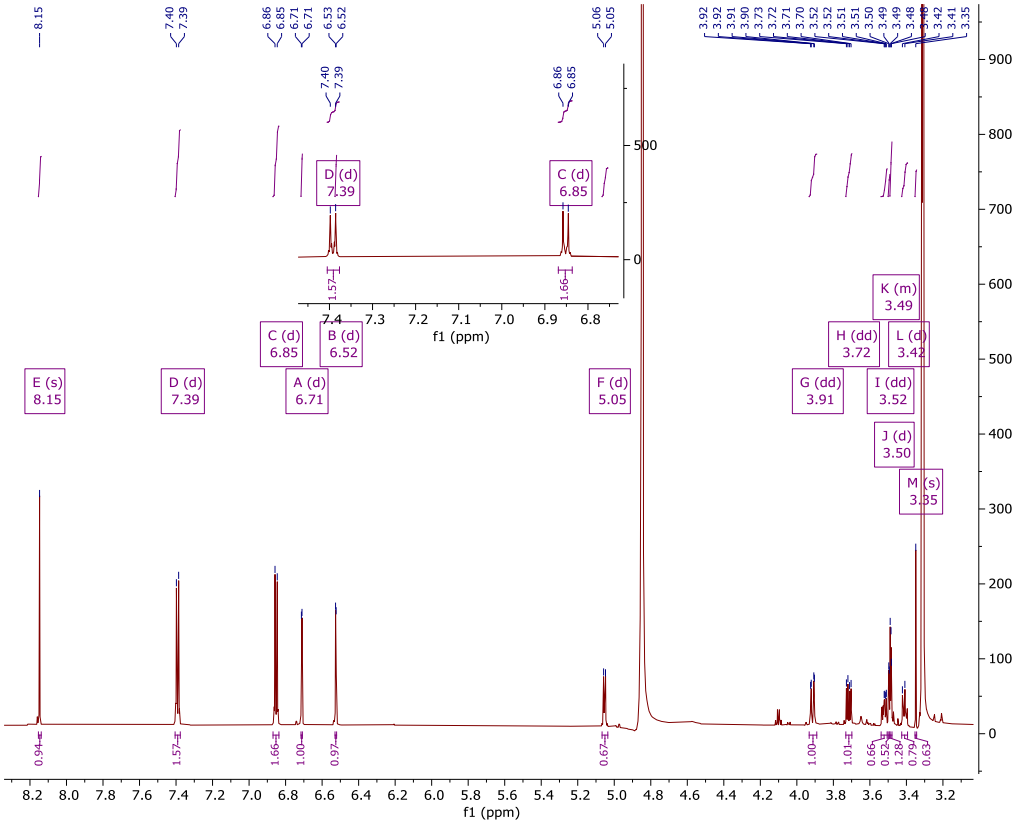

Appendix 34a: ^{1}H NMR for Compound 243 (expansion)

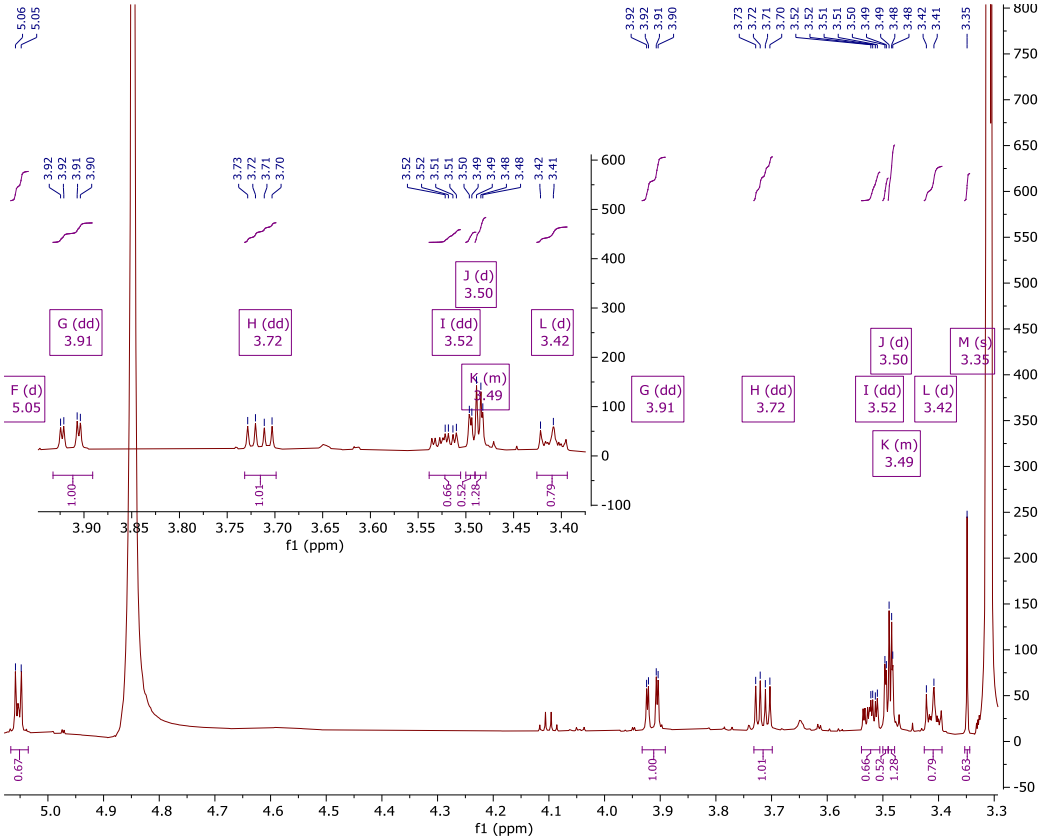

Appendix 34b: ^{13}C NMR for Compound 243

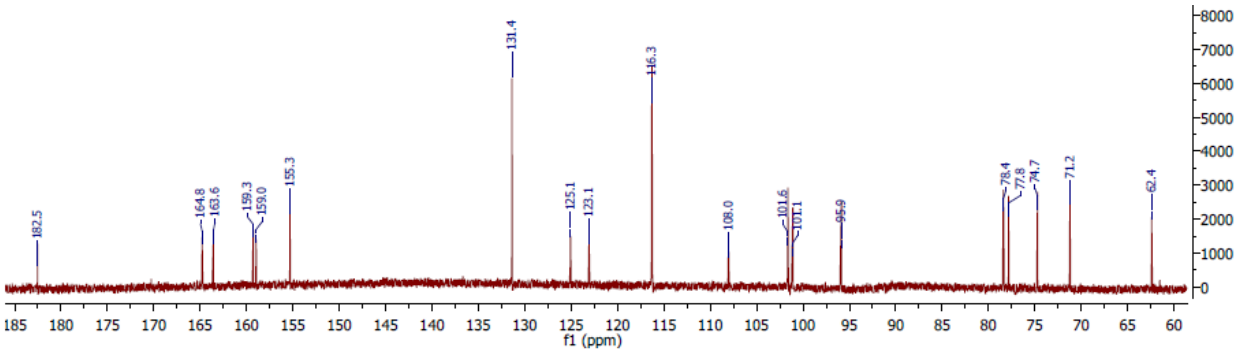

Appendix 34c: H H-Cosy for Compound 243

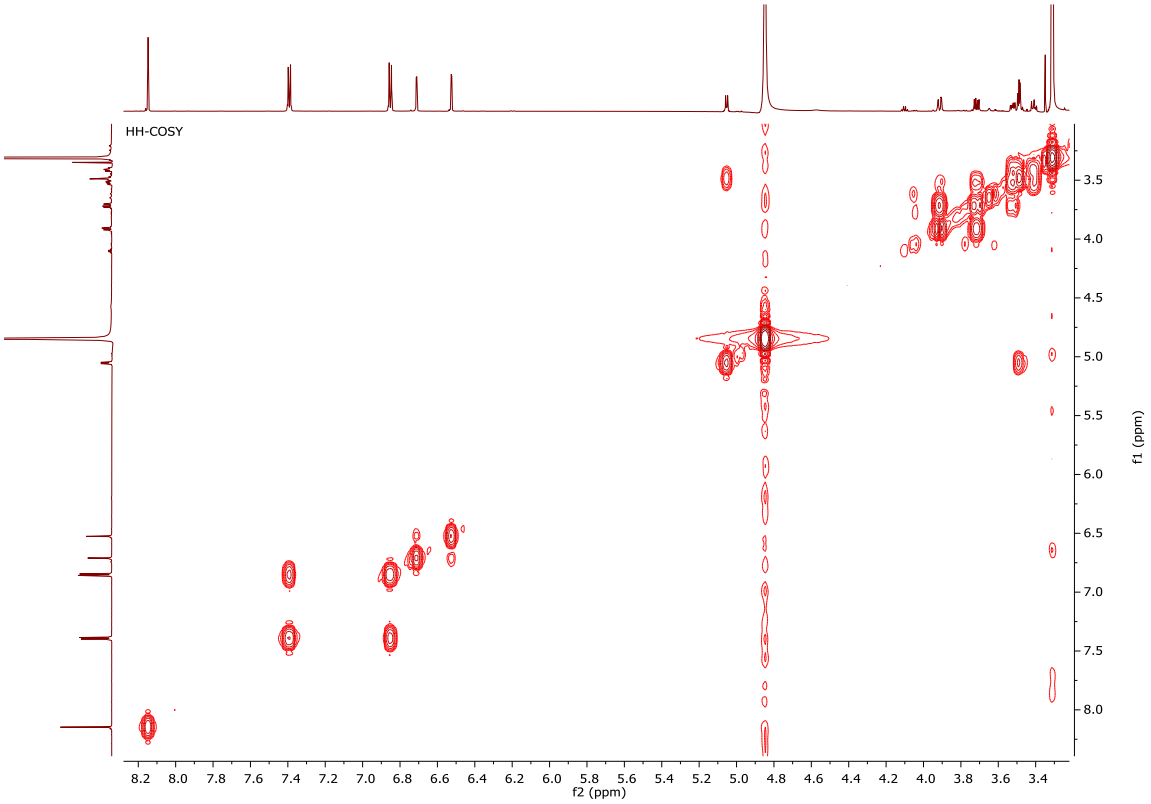

Appendix 34d: HSQC for Compound 243

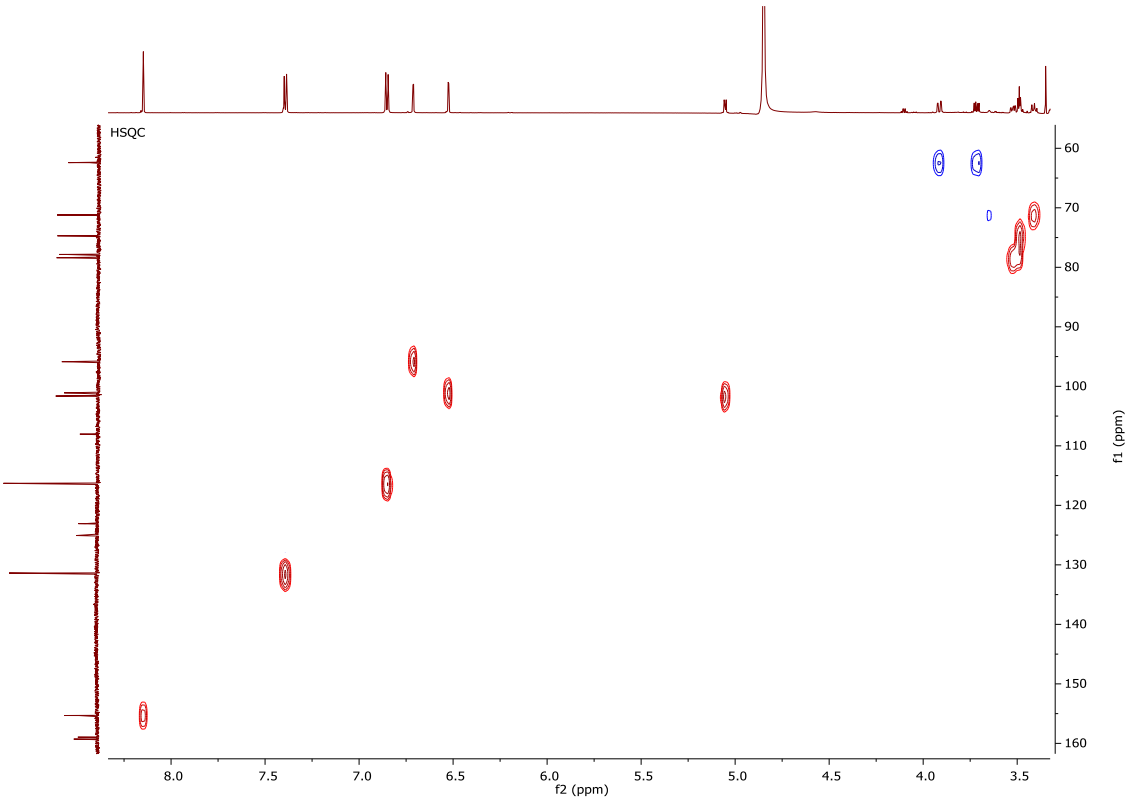

Appendix 34e: HMBC for Compound 243

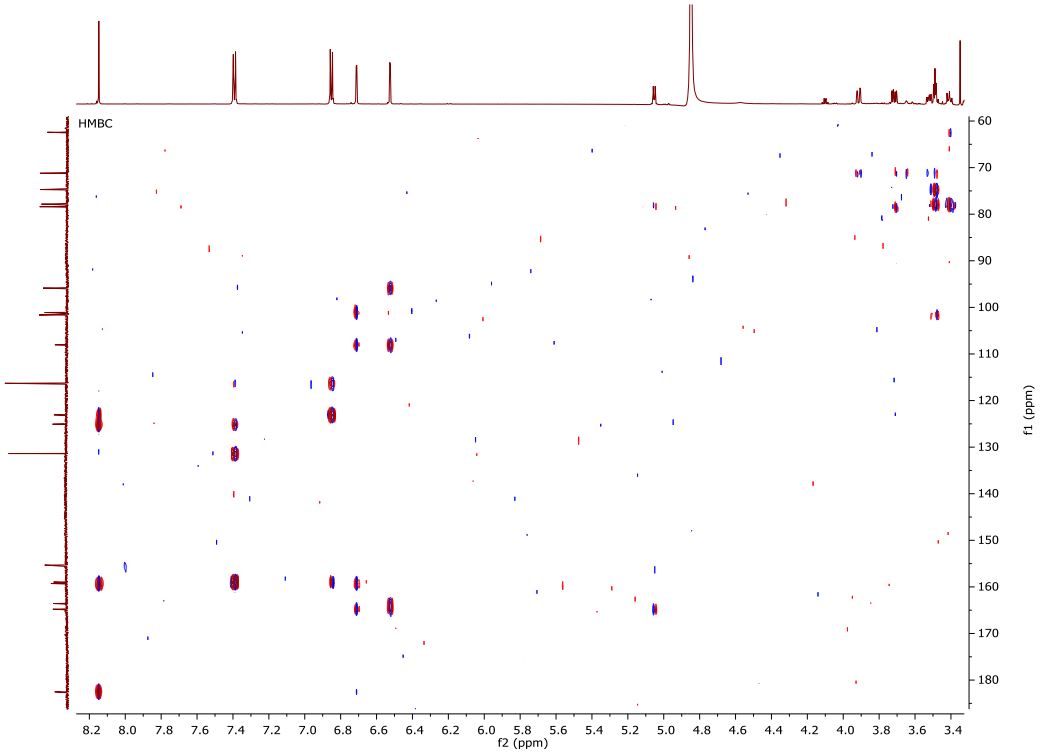

Appendix 34f: UV for Compound 243

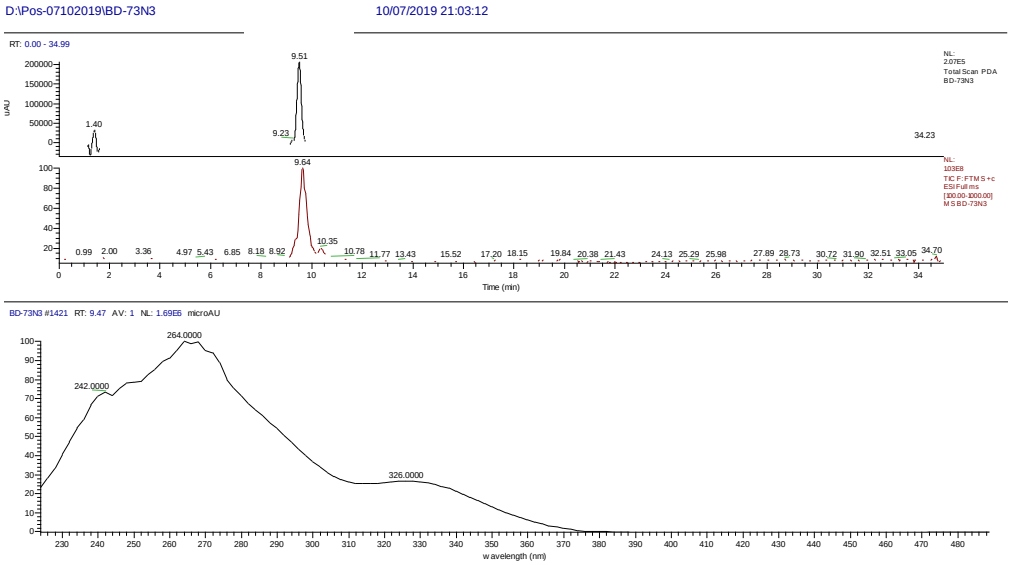

Appendix 34g: Mass Spectra for Compound 243

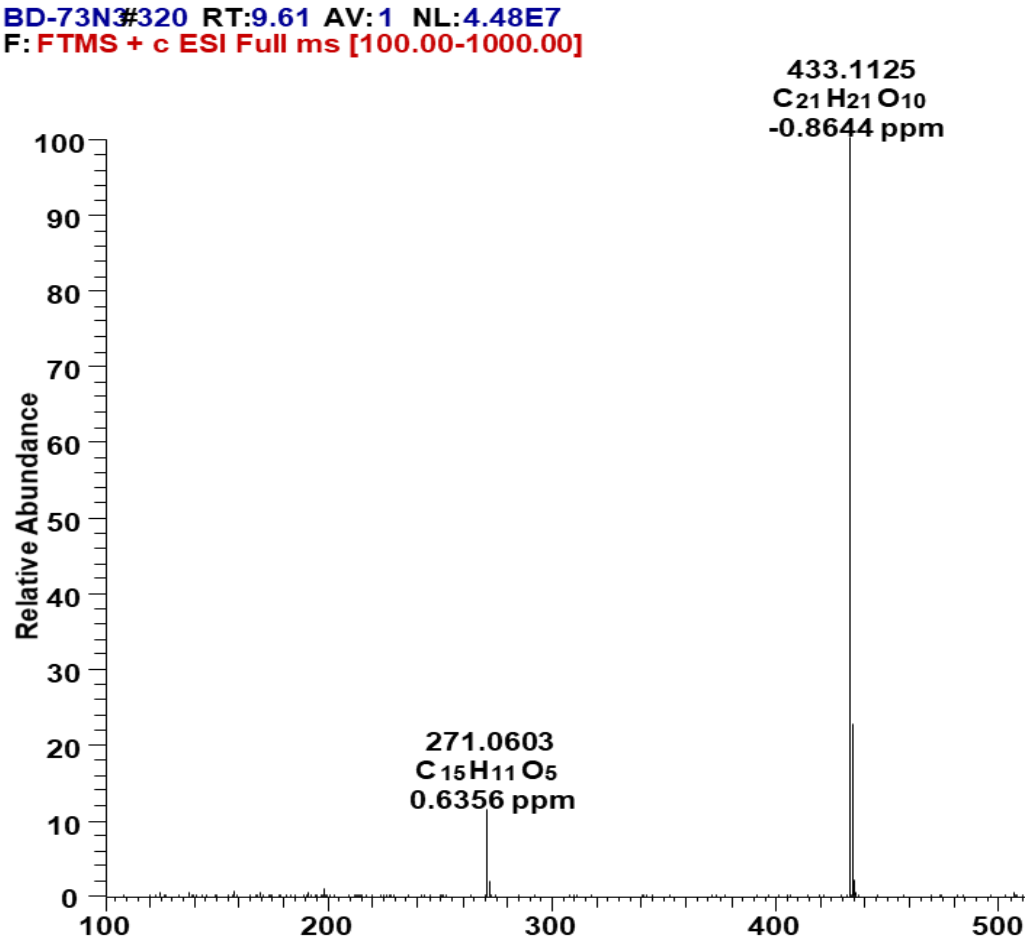

Appendix 35: Publications

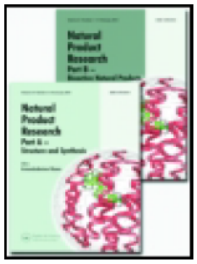

Natural Product Research
Formerly Natural Product Letters

ISSN: 1478-6419 (Print) 1478-6427 (Online) Journal homepage: https://www.tandfonline.com/loi/gnpl20

NATURAL PRODUCT RESEARCH
https://doi.org/10.1080/14786419.2019.1660335

Taylor & Francis
Taylor & Francis Group

SHORT COMMUNICATION

Check for updates

Cytotoxicity of isoflavones from *Millettia dura*

Daniel Buyinza[a,b], Li Jun Yang[c], Solomon Derese[a], Albert Ndakala[a], Paolo Coghi[c], Matthias Heydenreich[d], Vincent Kam Wai Wong[c], Heiko M. Möller[d] and Abiy Yenesew[a]

[a]Department of Chemistry, University of Nairobi, Nairobi, Kenya; [b]Department of Chemistry, Kabale University, Kabale, Uganda; [c]State Key Laboratory of Quality Research in Chinese Medicine, Macau University of Science and Technology, Macau, China; [d]Institut für Chemie, Universität Potsdam, Potsdam, Germany

ABSTRACT

The first phytochemical investigation of the flowers of *Millettia dura* resulted in the isolation of seven isoflavones, a flavonol and a chalcone. Eleven isoflavones and a flavonol isolated from various plant parts from this plant were tested for cytotoxicity against a panel of cell lines, and six of these showed good activity with IC_{50} values of 6-14 μM. Durmillone was the most active with IC_{50} values of 6.6 μM against A549 adenocarcinomic human alveolar basal epithelial cancer cell line with low cytotoxicity against the non-cancerous cell lines BEAS-2B (IC_{50} = 58.4 μM), LO2 hepatocytes (IC_{50} 78.7 μM) and CCD19Lu fibroblasts (IC_{50} >100 μM).

ARTICLE HISTORY
Received 13 June 2019
Accepted 12 August 2019

KEYWORDS
Millettia dura; Leguminosae; isoflavone; cytotoxicity

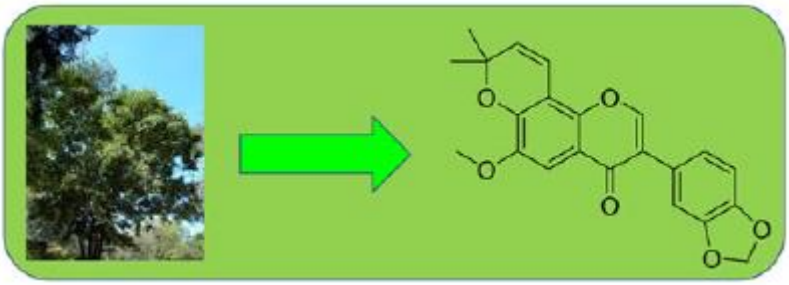

Biochemical Systematics and Ecology 91 (2020) 104053

Contents lists available at ScienceDirect

Biochemical Systematics and Ecology

journal homepage: www.elsevier.com/locate/biochemsyseco

Flavonoids and Isoflavonoids of *Millettia dura* and *Millettia ferruginea*: Phytochemical review and chemotaxonomic values

Daniel Buyinza[a,b], Duncan Mutiso Chalo[c], Solomon Derese[a], Albert Ndakala[a], Abiy Yenesew[a,*]

[a] Department of Chemistry, University of Nairobi, P. O. Box, 30197-00100, Nairobi, Kenya
[b] Department of Chemistry, Kabale University, P. O. Box 317, Kabale, Uganda
[c] School of Biological Sciences University of Nairobi, P. O. Box, 30197-00100, Nairobi, Kenya

ARTICLE INFO

Keywords:
Millettia dura
Millettia ferruginea
Leguminosae
Isoflavone
Rotenoid
Chemotaxonomy

ABSTRACT

The phytochemical information on *Millettia dura* Dunn, *M. ferruginea* (Hochst.) Baker and *M. ferruginea* subsp. *darassana* (Cufod.) J.B. Gillett was reviewed. All the three taxa elaborate mainly isoflavones (33 reported), occurring in the flowers, seeds/seed pods, stem bark and root bark. Out of the 33 isoflavones reported, some 19 (*ca.* 58%) contain prenyl at C-8 or its modification as 2,2-dimethylchromene ring at C-7/C-8, occurring in all the three taxa. Except for three isoflavones isolated from *M. ferruginea* subsp. *darassana*, all the isoflavones of these taxa are 5-deoxygenated. In these taxa, oxygenation at C-6 is a common feature, while isoflavones with C-8 oxygenation are rare, only three reported, and all of these from *M. dura*. There are 7 rotenoids reported from these taxa, and occur almost entirely in the seeds/seedpods of these plants. The major rotenoid with methylenedioxy group at C-2/C-3, millettone and its 12a-hydroxy derivative, millettosine, occur only in *M. dura*, this appears to distinguish *M. dura* from *M. ferruginea*.